NISTIR 8263

Thermophysical Properties of Polyol Ester Lubricants

Thomas J. Bruno
Tara J. Fortin
Marcia L. Huber
Arno Laesecke
Eric W. Lemmon
Elisabeth Mansfield
Mark O. McLinden
Stephanie L. Outcalt
Richard A. Perkins
Kimberly N. Urness
Jason A. Widegren

This publication is available free of charge from:
https://doi.org/10.6028/NIST.IR.8263

National Institute of Standards and Technology
U.S. Department of Commerce

NISTIR 8263

Thermophysical Properties of Polyol Ester Lubricants

Thomas J. Bruno
Tara J. Fortin
Marcia L. Huber
Arno Laesecke
Eric W. Lemmon
Elisabeth Mansfield
Mark O. McLinden
Stephanie L. Outcalt
Richard A. Perkins
Kimberly N. Urness
Jason A. Widegren
Applied Chemicals and Materials Division
Material Measurement Laboratory

This publication is available free of charge from:
https://doi.org/10.6028/NIST.IR.8263

August 2019

U.S. Department of Commerce
Wilbur L. Ross, Jr., Secretary

National Institute of Standards and Technology
Walter Copan, NIST Director and Undersecretary of Commerce for Standards and Technology

National Institute of Standards and Technology Interagency or Internal Report 8263
Natl. Inst. Stand. Technol. Interag. Intern. Rep. 8263, 222 pages (August 2019)

This publication is available free of charge from:
https://doi.org/10.6028/NIST.IR.8263

Abstract

This report summarizes the results of work performed for the Naval Air Warfare Center Aircraft Division by the National Institute of Standards and Technology (NIST), Applied Chemicals and Materials Division on the properties of polyol ester lubricants under interagency agreement number N0042115IP00008. The work includes purity analysis and assessment, decomposition studies, experimental measurements on density, isobaric heat capacity, speed of sound, vapor pressure, viscosity, thermal conductivity, and distillation curve measurements. Models were developed for the thermodynamic properties, viscosity, and thermal conductivity that represent these properties to nearly within their experimental uncertainty for three pure polyol ester base fluids (pentaerythritol tetrapentanoate (POE5), pentaerythritol tetraheptanoate (POE7), pentaerythritol tetrananonanoate (POE9), and a fully qualified lubricant meeting military specification MIL-PRF-23699.

Key words

Correlation, density, equation of state, heat capacity, lubricants, speed of sound, thermal conductivity, thermal decomposition, thermophysical property, vapor pressure, viscosity

Table of Contents

List of Tables

List of Figures

1. Accomplishments and New Findings

We performed an extensive experimental and modeling program on the thermophysical properties of three pure polyol ester fluids, and one fully qualified lubricant that meets military specification MIL-PRF-23699. The three pure fluids were pentaerythritol tetrapentanoate (POE5), pentaerythritol tetraheptanoate (POE7), and pentaerythritol tetranonanoate (POE9). Purity and chemical analysis indicated the MIL-PRF-23699 oil was a complex mixture of pentaerythritol tetraesters. The measured rates of thermal decomposition of the base fluids were comparable within the limits of uncertainty, and MIL-PRF-23699 was more thermally stable than the base fluids.

Thermodynamic property measurements (density, isobaric heat capacity, speed of sound, and vapor pressure) were carried out over a combined temperature range of (263 to 470) K, with pressures up to 63 MPa. These data represent the most comprehensive data set for fluids of this type.

The measured thermodynamic data were used to develop equations of state (EOS) based on Helmholtz energy for the pure fluids POE5, POE7, and POE9, and for the fully qualified lubricant MIL-PRF-23699, which was formulated as a pseudo-pure fluid. The EOS represent the entire fluid surface (liquid, vapor, and supercritical states) despite fluid critical temperatures approximately double the range of the experimental data. The experimental densities were fitted within 0.2 %, speed of sound within 0.1 %, and heat capacity to within 0.3 %. Development of these EOS required new fitting techniques and was possible only because of the accurate and wide-ranging data set.

Transport property measurements (viscosity and thermal conductivity) were measured over a combined temperature range of (275 to 500) K, with pressures up to 138 MPa. These data were used to develop viscosity and thermal conductivity correlations for the four lubricants with deviations comparable to the experimental uncertainties.

Two surrogate mixture models were also developed using the base fluids POE5, POE7, and POE9, however we recommend the use of the pseudo-pure fluid model for the properties of the fully qualified lubricant. Finally, files compatible with the REFPROP computer program (version 10) are provided for the three pure fluids and the fully qualified lubricant. These will allow the modeling of these lubricants, including as a component in mixtures.

2. Purity Analysis of Polyol Ester Base Oils and MIL-PRF-23699 Oil

2.1. Summary

The purity and chemical analysis of the fluids pentaerythritol tetrapentanoate (POE5), pentaerythritol tetraheptanoate (POE7), pentaerythritol tetranonanoate (POE9), and MIL-PRF-23699 were determined by gas chromatography with flame ionization detection (GC-FID) and gas chromatography with mass spectrometry (GC-MS). The base oils POE5, POE7, and POE9 are approximately 96.7 %, 97.3 % and 93.0 % of the title compound, respectively. Generic MIL-PRF-23699 oil is a complex mixture of pentaerythritol tetraesters (details of the analysis are proprietary and are administratively restricted).

2.2. GC-FID and GC-MS Analysis

The pure fluid base oils, with the structure shown in Figure 1, are pentaerythritol-based with the esters pentanoate (POE5), heptanoate (POE7), and nonanoate (POE9). The qualified lubricant is a blend of pentaerythritol polyol esters in the C_5 to C_{10} range (normal and branched alkane), and includes additives to prevent hydrolytic degradation.[1]

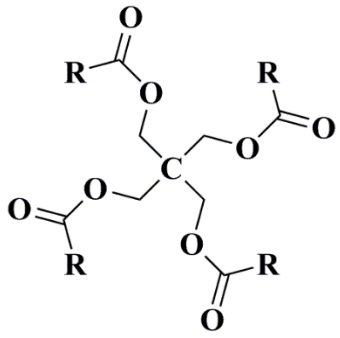

pentaerythritol tetrapentanoate (POE5): R = *n*-C_4H_9
pentaerythritol tetraheptanoate (POE7): R = *n*-C_6H_{13}
pentaerythritol tetranonanoate (POE9): R = *n*-C_8H_{17}

Figure 1: Chemical structure and nomenclature of the pentaerythritol tetraester base oils.

Purity analysis by GC-FID was performed by temperature-programmed chromatographic separation of the diluted sample on a capillary column with a nonpolar stationary phase ((5 % phenyl)-methylpolysiloxane, 320 µm i.d., 0.25 µm thick film). Each sample was diluted to approximately 8 % (by mass) in decane prior to chromatographic analysis. For the pure fluids (POE5, POE7, and POE9), 1 µL of the diluted sample was injected by an autosampler into a split/splitless injector with split ratio of 50:1. The injector temperature was held at 573 K, and the initial head pressure was 66.9 kPa. Flow of the carrier gas through the column was held constant

at 1.6 mL·min^{-1}. The temperature program for separation was: 393 K (for 0.5 min) to 598 K (at 25 K·min^{-1}), held 20 min for POE5 and POE7, and 28 min for POE9. The carrier gas for all GC-FID experiments was research grade nitrogen. Reported purities and expanded uncertainties (k = 2) are based on three replicate injections of a minimum of 5 samples and an estimate for the complete separation and integration of components.

The GC-MS analysis was also performed by temperature-programmed chromatographic separation of the diluted sample on a capillary column with a nonpolar stationary phase ((5 % phenyl)-methylpolysiloxane, 250 µm i.d., 0.25 µm thick film). Approximately 1 µL of the samples used for GC-FID analysis, described above, were injected manually. Chromatographic conditions for the pure fluids were as follows: 573 K inlet temperature, 70:1 injector split ratio, 135.1 kPa initial column head pressure, and 1.5 mL·min^{-1} column flow. The oven temperature program was: 423 K (held for 0.5 min), to 573 K (at a rate of 288 K·min^{-1}, held 7 min) to 593 K (at a rate of 283 K·min^{-1}), held 10 min for POE5 and POE7, and 20 min for POE9. The carrier gas for these separations was ultra-high purity helium.

The percent purity of each base fluid is shown in Table 1. The purity is based upon the uncalibrated area percent of the total FID response of the compound of interest, relative to the impurities. Identifications of the major impurities in the single-component base fluids are included in Table 2, Table 3, and Table 4. The impurities are listed in order of observed chromatographic retention time, relative to the specified fluid, which is an indicator of the size of the species (larger species elute later). The acyl moieties were determined by mass spectral fragmentation patterns.[2] The sizes of the ester groups present on the polyol are indicated; however, the exact structures (linear or branched chains, and number of ester groups) have not been determined. The most significant impurities are polyol tetra-esters with different acyl chain lengths (either larger, smaller, or branched); however, in each sample a small portion is a pentaerythritol (PE) triester, where one of the arms on the polyol is replaced by an unesterified hydroxyl group.

Table 1: GC-FID Analysis of Pentaerythritol Tetraester Base Oils.

Fluid	Formula	CAS No.	Molar Mass	Purity (area %)[a]
POE5	$C_{25}H_{44}O_8$	15834-04-5	472.6	96.7 ± 0.2
POE7	$C_{33}H_{60}O_8$	25811-35-2	584.8	97.3 ± 0.8
POE9	$C_{41}H_{76}O_8$	14450-05-6	697.0	93.0 ± 1.0

[a]Area percent is uncalibrated GC-FID response

Table 2: Major Impurities in POE5 Sample Identified by the Acyl Moieties.

Component	Area %[a]
PE tripentanoate: $(C_4H_9C(O)OCH_2)_3C\text{-}CH_2OH$	0.4
PE with C_4 and C_5 esters	0.2
PE with mixed linear/branched C_5 esters	0.6
PE tetrapentanoate (POE5)	96.7 ± 0.2
PE with C_5 and C_7 esters	1.5
PE with C_5 and C_9 esters	0.2
PE with C_5 esters (structure unknown)	0.4

[a]Area percent is uncalibrated GC-FID response

Table 3: Major Impurities in POE7 Sample Identified by the Acyl Moieties.

Component	Area %[a]
PE triheptanoate: $(C_6H_{13}C(O)OCH_2)_3C\text{-}CH_2OH$	0.1
PE with C_5 and C_7 esters	0.2
PE with C_6 and C_7 esters	1.8
PE tetraheptanoate (POE7)	97.3 ± 0.8
PE with C_7 and C_8 esters	0.2
PE with C_7 esters (structure unknown)	0.3

[a]Area percent is uncalibrated GC-FID response

Table 4: Major Impurities in POE9 Sample Identified by the Acyl Moieties.

Component	Area %[a]
PE trinonanoate: $(C_8H_{17}C(O)OCH_2)_3C\text{-}CH_2OH$	0.2
PE with C_6 and C_9 esters	0.2
PE with C_7 and C_9 esters	0.2
PE with C_8 and C_9 esters	0.3
PE tetranonanoate (POE9)	93.0 ± 1.0
PE with other mixed tetra esters	0.3
PE with C_9 and C_{10} esters	4.9
PE with C_9 and C_{10} esters (larger species)	0.5
PE with larger mixed tetra esters	0.3

[a]Area percent is uncalibrated GC-FID response

3. Thermal Decomposition Kinetics of Polyol Ester Lubricants

3.1. Summary

The global thermal decomposition kinetics of the fluids pentaerythritol tetrapentanoate (POE5), pentaerythritol tetraheptanoate (POE7), pentaerythritol tetranonanoate (POE9), and generic MIL-PRF-23699 were performed in stainless steel ampule reactors at approximately 20.7 MPa and the extent of decomposition determined by gas chromatography with flame ionization detection. The decomposition rates varied from 1.6 (± 0.7) × 10^{-8} s^{-1} at 496 K to 2.3 (± 0.7) × 10^{-4} s^{-1} at 676 K (Tables 5 – 7), with expanded uncertainties given in parentheses. In general, the measured rates of decomposition of the base fluids POE5, POE7, and POE9 (which contained no additives) were comparable within the limits of uncertainty for each fluid measured; in other words, to the resolution of the experimental technique, no fluid was more thermally stable than another. As expected, the qualified lubricant, generic MIL-PRF-23699 (with additives) was more thermally stable than the base fluids. The rates of decomposition for generic MIL-PRF-23699 varied from 1.2 (± 2.7) × 10^{-8} s^{-1} at 497 K to 1.3 (± 0.3) × 10^{-4} s^{-1} at 676 K (Table 8). In general, the addition of anti-wear agents and antioxidants extended the lifetime of the base oils at the conditions tested by approximately a factor of 1.7. Finally, new (unpassivated) stainless steel reactors and alumina surfaces catalyzed the thermal decomposition of the base oils; the decomposition rate of generic MIL-PRF-23699 was impacted less by these factors, due to the inclusion of additives to prevent decomposition by surface reactions.

3.2. Thermal Decomposition Kinetics

The global thermal decomposition kinetics of three polyol ester lubricant base oils and a fully qualified (generic MIL-PRF-23699) formulation were performed in stainless steel ampule reactors to provide a guide for the subsequent property measurements and in-service constraints. The extent of decomposition, as a function of time, was determined by gas chromatography with flame ionization detection (GC-FID). With this information, pseudo-first-order rate constants and Arrhenius parameters were derived. Other techniques used for chemical characterization include gas chromatography with mass spectrometry (GC-MS), nuclear magnetic resonance spectroscopy, and Karl Fischer titration. Presented in this section is a brief description of the measurement procedure and a compilation of the kinetic measurements. The reader is referred to the paper by Urness et al.[3] for more details.

3.2.1. Experimental Details

Tubular stainless steel (316L) ampule reactors with an internal volume of approximately 190 µL were used to test the fluids of interest. The reactors were sealed with a high-pressure valve and

were heated in tight-fitting slots in a thermostated block, as shown in Figure 2. The reactor cell and thermostated block for temperature control are described in more detail elsewhere.[3, 4]

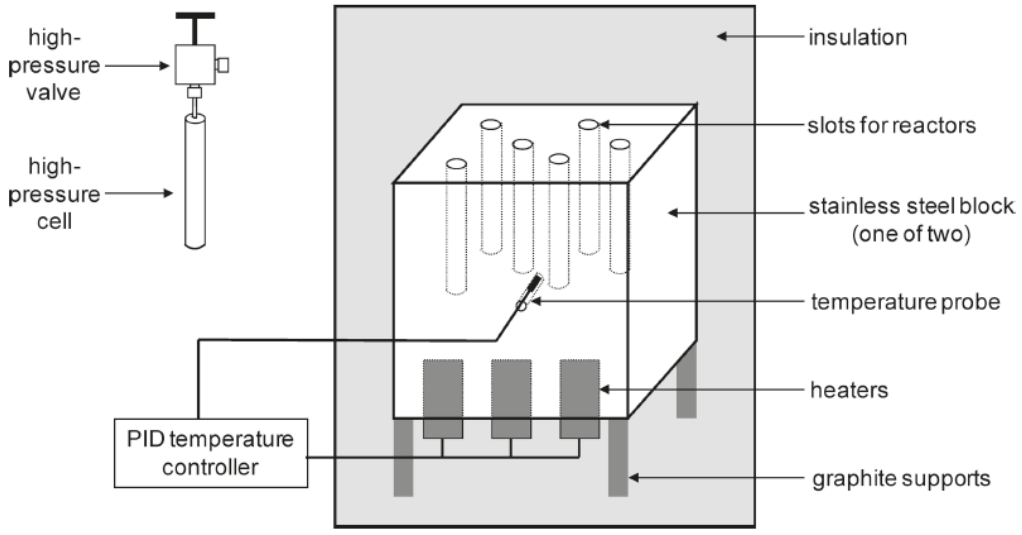

Figure 2: High-pressure cell and thermostat block used for thermal decomposition studies of the polyol ester lubricants.

The cells were loaded with the appropriate amount of fluid to achieve an initial pressure of approximately 20.7 MPa at a given temperature. The fluid mass was estimated with preliminary equations of state developed for POE5 or POE9. The appropriate mass loading of POE7 was the average of the predicted amount of POE5 and POE9. The cells were filled with approximately 150 mg to 180 mg of fluid, depending on the desired reaction temperature, nearly filling the entire cell volume. Prior to heating, the cell was degassed with a single freeze-pump-thaw cycle in liquid nitrogen. The samples were then heated in the temperature range of 498 K to 673 K with reaction times ranging from 10 min to 35 min at 673 K and up to 300 h to 700 h (12 days to 30 days) at 498 K. The reactions were quenched by immersing the cell in a bath of room-temperature water.

3.2.2. Data Analysis

Due to the complexity involved during thermal decomposition, it is necessary to make assumptions to simplify the analysis and determine rate expressions to describe the thermal stability of these fluids. We assume that the reactant of interest, A, thermally decomposes to a set of products and that we can model the overall decomposition with a single, global pseudo-first-order rate constant, k'. Since the product suite contains both hydrocarbons and oxygenated species, quantitative analysis by flame ionization detection (FID) of the product suite is complicated because the detector has a variable response to the amount of oxygen present. To avoid calibrating the FID

response for all possible product species, we monitor the disappearance of the reactant(s), $[A]_t$, relative to the products formed, and compare this to an unheated reference sample, $[A]_0$, to measure the 'unreacted fraction':

$$\ln \frac{[A]_t}{[A]_0} = \ln(\text{unreacted fraction}) = -k't \, . \quad (1)$$

In this equation, k' is the rate constant derived from the slope of the line in a plot of ln(unreacted fraction) vs. reaction time at a particular temperature.

We also assume that analysis of the remaining liquid fraction of the decomposed fluid is representative of the decomposition process. Based on our observations, the extent of decomposition that ensures this is a valid assumption is at most 40 %. Additional decomposition beyond this point results in a significant vapor phase and serves as an indication that the initial set of products is undergoing thermal decomposition. Analysis of samples with more than 40 % of reactant decomposed will also not fall on a straight line with the less-decomposed samples, which serves as an indication of where the pseudo first-order approximation begins to break down.

Finally, the rate constants are measured over a range of temperatures to develop an Arrhenius expression that describes the fluid's thermal stability based on the activation energy, E_a (in $J \cdot mol^{-1}$) and the pre-exponential factor, A (units of s^{-1}):

$$k'(T) = A \exp\left(-\frac{E_a}{RT}\right), \quad (2)$$

where R is the universal gas constant (8.314 $J \cdot mol^{-1} \cdot K^{-1}$) and T is the reaction temperature.

The age of the ampule cell was also shown to be important for test repeatability, indicating that surface reactions can influence the decomposition rates of the polyol esters. This is contrary to previous decomposition studies using the ampule reactors to heat unoxygenated hydrocarbon fuels.[4, 5] Those experiments showed no correlation between cell age and measured decomposition rate. However, heating the pure polyol ester base oils in new, unpassivated cells resulted in decomposition products formed at a faster rate than when an older cell was used under the same conditions. The cells were passivated by several cycles of heating the reactors loaded with the polyol esters followed by cleaning to build up a sufficient surface oxide layer. A more detailed discussion of catalytic decomposition of these polyol esters is presented in Urness et al.[3].

3.3. Results

Linear regressions are used to determine the individual rate constants (k') for the tested fluids. The figures give visual representations of how well the linear fits approximate the data. The data for the base oil POE5 tested at 496 K to 675 K is shown in Figure 3 and Table 5. Results for POE7 tested at 595 K to 675 K are included in Figure 4 and Table 6. Results for POE9 also tested at 595 K to 675 K are summarized in Figure 5 and Table 7. The data for the qualified lubricant at 497 K to 675 K are shown in Figure 6 and Table 8. The derived Arrhenius parameters for the four tested fluids are summarized in Table 9. A detailed discussion of the measured reaction rates, Arrhenius fits, and the formation of reaction products are included in Urness et al.[3].

Table 5: Thermal Decomposition Kinetic Data for POE5.

T /K	+/- /K	1000/T	k' /s^{-1}	ln k'	fit uncert. (95 %) /s^{-1}
495.7	1.0	2.018	1.602×10^{-8}	-17.949	6.92×10^{-9}
520.3	1.0	1.922	3.736×10^{-8}	-17.103	2.12×10^{-8}
596.3	2.0	1.677	2.417×10^{-6}	-12.933	6.74×10^{-7}
599.7	3.2	1.668	3.015×10^{-6}	-12.712	9.09×10^{-7}
599.4	1.8	1.668	3.079×10^{-6}	-12.691	2.09×10^{-6}
621.1	2.4	1.610	1.047×10^{-5}	-11.467	3.28×10^{-6}
624.6	3.4	1.601	1.157×10^{-5}	-11.367	3.33×10^{-6}
624.3	2.0	1.602	9.991×10^{-6}	-11.514	1.94×10^{-6}
648.7	1.6	1.542	4.205×10^{-5}	-10.077	6.52×10^{-6}
649.7	2.6	1.539	5.259×10^{-5}	-9.853	1.04×10^{-5}
649.4	1.8	1.540	5.522×10^{-5}	-9.804	8.43×10^{-6}
670.7	2.0	1.491	1.818×10^{-4}	-8.613	3.70×10^{-5}
675.4	2.6	1.481	2.053×10^{-4}	-8.491	1.02×10^{-4}
675.6	2.0	1.480	2.340×10^{-4}	-8.360	6.91×10^{-5}

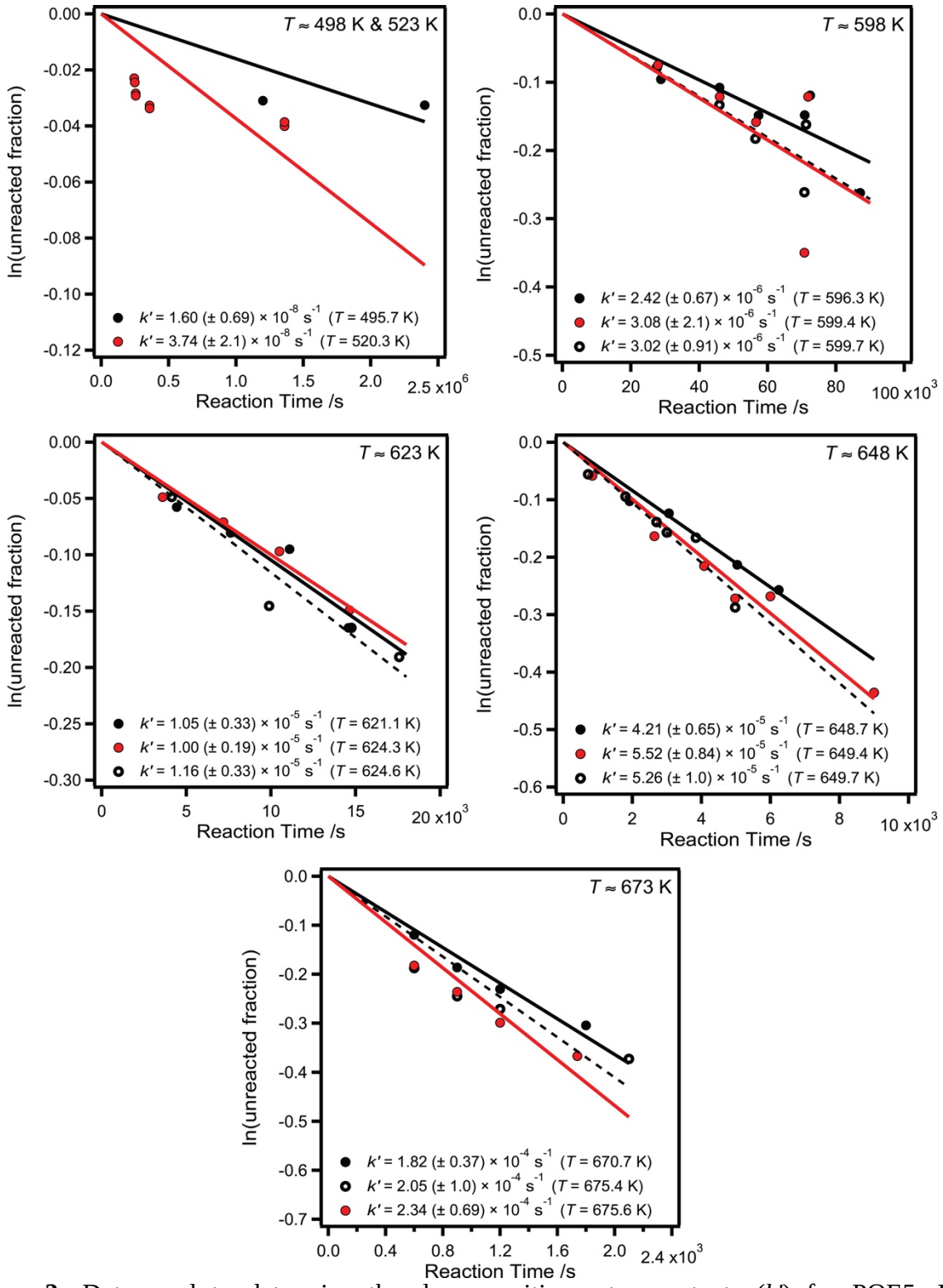

Figure 3: Data used to determine the decomposition rate constants (*k'*) for POE5. Both experimental data (circles) and their corresponding linear fits (solid and dashed lines) are shown.

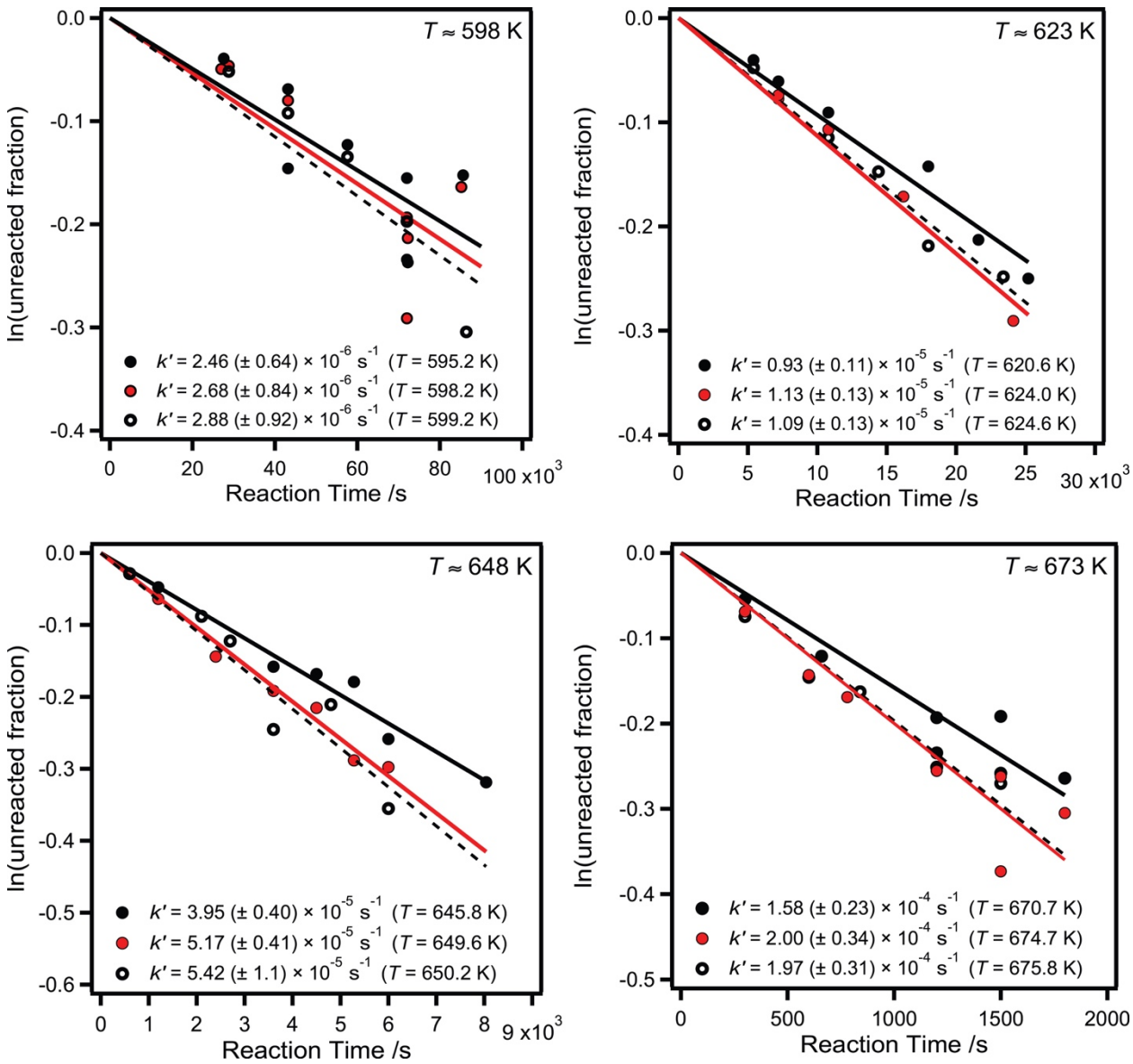

Figure 4: Data used to determine the decomposition rate constants (k') for POE7. Both experimental data (circles) and their corresponding linear fits (solid and dashed lines) are shown.

Table 6: Thermal Decomposition Kinetic Data for POE7.

T /K	+/- /K	1000/T	k' /s^{-1}	ln k'	fit uncert. (95 %) /s^{-1}
595.2	1.7	1.680	2.462×10^{-6}	-12.915	6.41×10^{-7}
599.2	3.5	1.669	2.879×10^{-6}	-12.758	9.16×10^{-7}
598.2	1.7	1.672	2.679×10^{-6}	-12.830	8.42×10^{-7}
620.6	2.2	1.611	9.298×10^{-6}	-11.586	1.09×10^{-6}
624.6	3.5	1.601	1.091×10^{-5}	-11.426	1.26×10^{-6}
624.0	2.2	1.603	1.131×10^{-5}	-11.390	1.34×10^{-6}
645.8	2.1	1.549	3.949×10^{-5}	-10.140	3.98×10^{-6}
650.2	3.9	1.538	5.422×10^{-5}	-9.822	1.14×10^{-5}
649.6	2.1	1.539	5.167×10^{-5}	-9.871	4.07×10^{-6}
670.7	2.4	1.491	1.579×10^{-4}	-8.754	2.28×10^{-5}
675.8	4.5	1.480	1.967×10^{-4}	-8.534	3.13×10^{-5}
674.7	2.3	1.482	2.000×10^{-4}	-8.517	3.42×10^{-5}

Table 7: Thermal Decomposition Kinetic Data for POE9.

T /K	+/- /K	1000/T	k' /s^{-1}	ln k'	fit uncert. (95 %) /s^{-1}
595.2	1.7	1.680	1.910×10^{-6}	-13.168	6.16×10^{-7}
599.2	3.5	1.669	2.364×10^{-6}	-12.955	1.49×10^{-6}
598.2	1.7	1.672	2.155×10^{-6}	-13.048	1.37×10^{-6}
620.6	2.2	1.611	1.002×10^{-5}	-11.511	1.87×10^{-6}
624.6	3.5	1.601	1.157×10^{-5}	-11.367	3.30×10^{-6}
624.0	2.2	1.603	1.207×10^{-5}	-11.325	2.28×10^{-6}
645.8	2.1	1.549	4.337×10^{-5}	-10.046	2.90×10^{-6}
650.2	3.9	1.538	5.175×10^{-5}	-9.869	9.00×10^{-6}
649.6	2.1	1.539	5.254×10^{-5}	-9.854	2.64×10^{-6}
670.7	2.4	1.491	1.921×10^{-4}	-8.558	2.74×10^{-5}
675.8	4.5	1.480	2.547×10^{-4}	-8.276	4.45×10^{-5}
674.7	2.3	1.482	2.449×10^{-4}	-8.315	3.35×10^{-5}

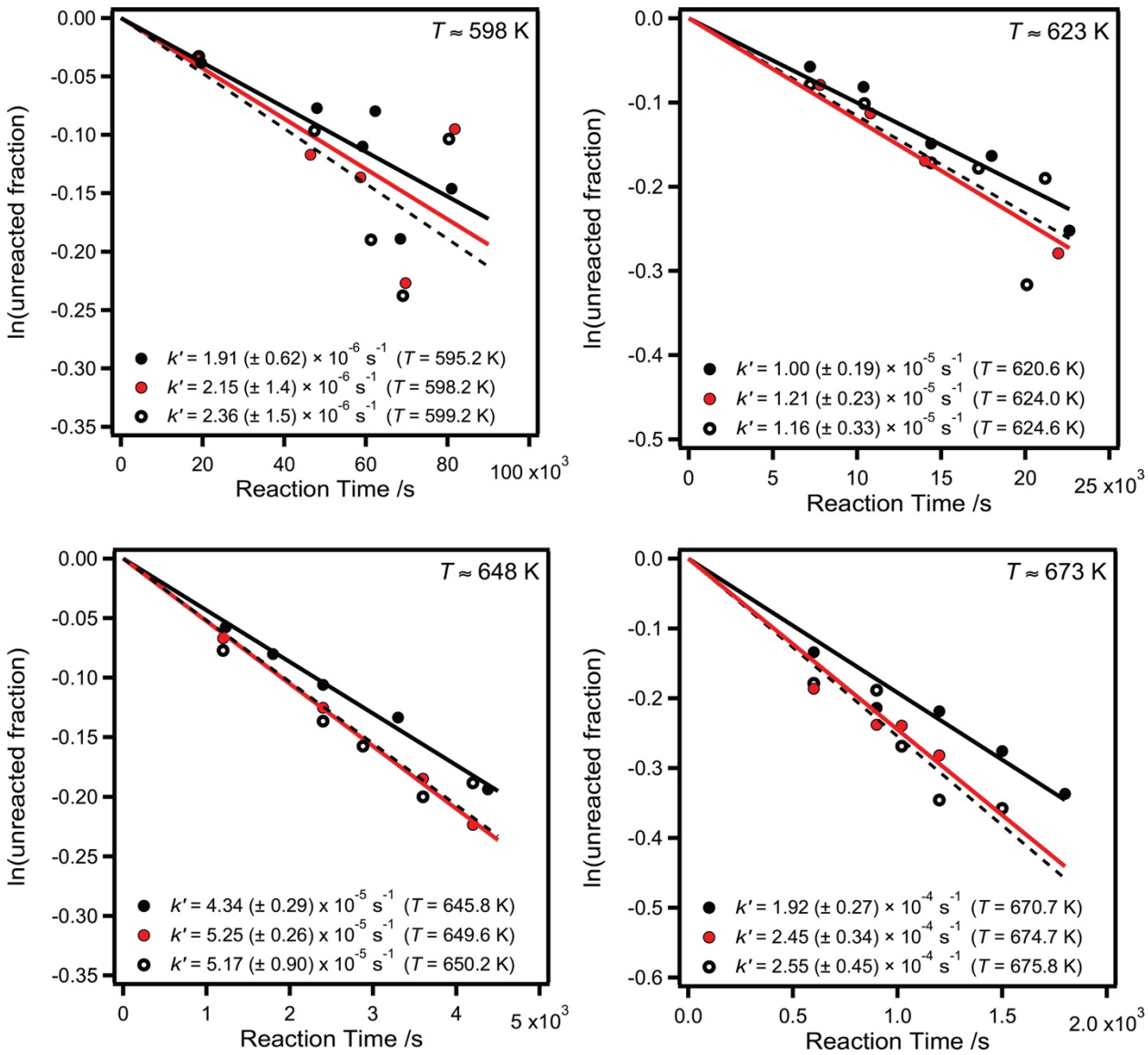

Figure 5: Data used to determine the decomposition rate constants (*k'*) for POE9. Both experimental data (circles) and their corresponding linear fits (solid and dashed lines) are shown.

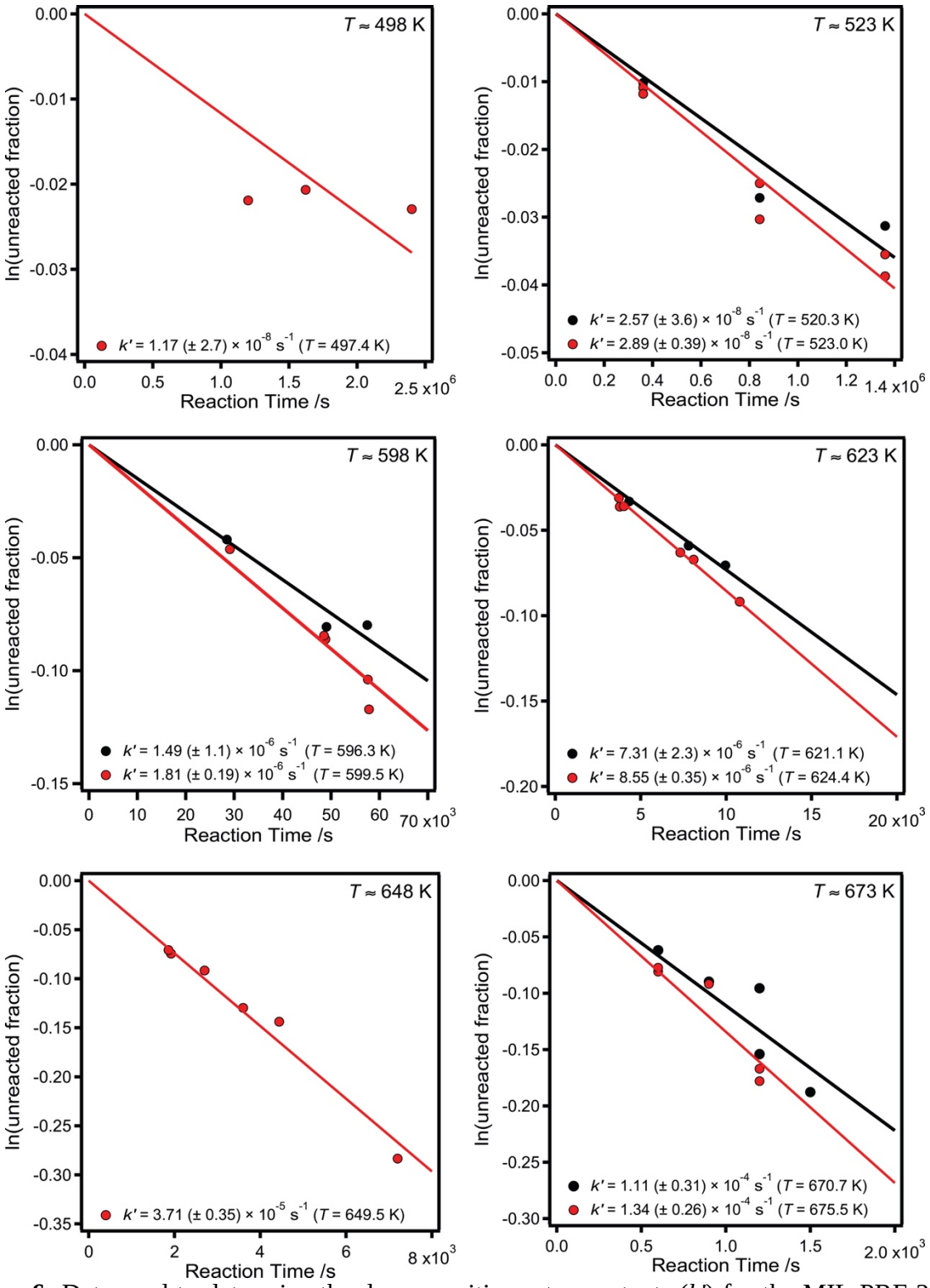

Figure 6: Data used to determine the decomposition rate constants (*k′*) for the MIL-PRF-23699 qualified lubricant. Both experimental data (circles) and their corresponding linear fits (solid and dashed lines) are shown.

Table 8: Thermal Decomposition Kinetic Data for the MIL-PRF-23699 Qualified Lubricant.

T /K	+/- /K	1000/T	k' /s^{-1}	ln k'	fit uncert. (95 %) /s^{-1}
497.4	1.8	2.011	1.168×10^{-8}	-18.266	2.74×10^{-8}
520.3	1.0	1.922	2.568×10^{-8}	-17.477	3.65×10^{-8}
523.0	1.6	1.912	2.894×10^{-8}	-17.358	3.90×10^{-9}
596.3	2.0	1.677	1.493×10^{-6}	-13.415	1.06×10^{-6}
599.5	2.6	1.668	1.807×10^{-6}	-13.224	1.90×10^{-7}
621.1	2.4	1.610	7.313×10^{-6}	-11.826	2.27×10^{-6}
624.4	2.8	1.602	8.546×10^{-6}	-11.670	3.53×10^{-7}
649.5	2.2	1.540	3.707×10^{-5}	-10.203	3.53×10^{-6}
670.7	2.0	1.491	1.110×10^{-4}	-9.106	3.12×10^{-5}
675.5	2.4	1.480	1.342×10^{-4}	-8.916	2.60×10^{-5}

Table 9: Arrhenius Parameters for the Pure Base Oils and the Qualified Lubricant.

fluid	T /K	A /s^{-1}	E_a /kJ·mol^{-1}
POE5	600–675	2.28×10^{8}	158 ± 10
POE7	600–675	5.64×10^{10}	187 ± 6
POE9	500–675	1.41×10^{12}	204 ± 5
MIL-PRF-23699	500–675	2.62×10^{8}	161 ± 7

4. Vapor Pressure

4.1. Summary

The vapor pressures (p_{sat}) of POE5 and *n*-octacosane ($C_{28}H_{58}$, a control compound) were measured by the gas saturation method at temperatures of 353.05 K and 362.93 K. For POE5, the measured p_{sat} was (2.1 ± 0.5) mPa at 353.05 K and (6.7 ± 1.8) mPa at 362.93 K, with reported expanded uncertainties corresponding to a 95 % confidence interval. Temperature gradients within the measurement apparatus were the principal source of uncertainty for these measurements. These values are in good agreement with the one prior report of p_{sat} measurements on POE5.[6] Measurements on lubricant base fluids larger than POE5 were not attempted because their vapor pressures are expected to be below the measurable range of our apparatus.

4.2. Vapor Pressure of POE5

The vapor pressures (p_{sat}) of POE5 and *n*-octacosane ($C_{28}H_{58}$, a control compound) were measured by the gas saturation method [7-15] at temperatures of 353.05 K and 362.93 K. The basis of the gas saturation method is the saturation of an inert carrier gas with vapor from a condensed phase. From measurements of the amount of vapor solute and the amount of carrier gas, one can calculate p_{sat}. An important advantage of this method is that the effect of impurities is relatively small and predictable, which means that samples of limited purity can be measured.

4.2.1. Apparatus Description

The gas saturation apparatus used for this work was developed at NIST and has been described in detail,[16, 17] so only a brief description is presented here. This type of apparatus (called a concatenated gas saturation apparatus) is an advancement on the classical technique in that it allows for various strategies that ensure good data quality. The principal components of the apparatus are a carrier-gas supply system, a series of saturator–adsorber pairs, and a temperature-controlled chamber (Figure 7). The carrier gas-supply system includes a gas cylinder filled with carrier gas, a pressure regulator, an ultra-low-flow mass flow controller, and a Bourdon-tube pressure gauge (located just upstream from the first saturator–adsorber pair). For this work, 18 saturator–adsorber pairs were installed in series. The saturators, which are PTFE tubes filled with glass beads, were located inside a temperature-controlled forced-air chamber. The adsorbers, which are stainless steel tubes filled with porous polymer adsorbent, were located on a manifold above the chamber at room temperature (approximately 294 K). The last adsorber vented to the lab at ambient pressure.

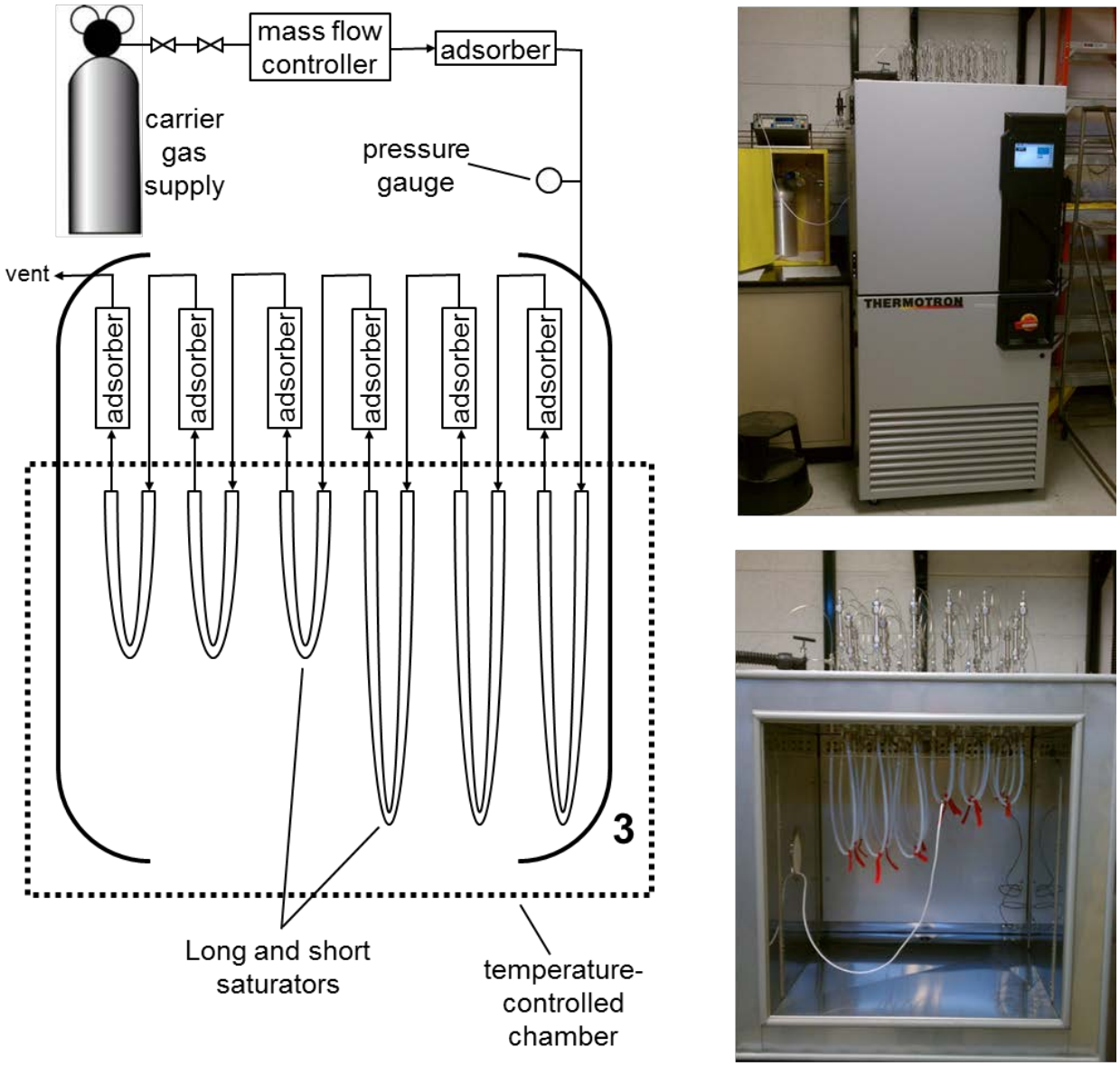

Figure 7: Gas saturation apparatus with 18 saturator-adsorber pairs linked in series. An alternating pattern of long and short saturators was used (three long, three short, three long, etc.). The arrows show the direction of flow for the carrier gas.

4.2.2. Measurements

The use of alternating long (61 cm) and short (33 cm) saturators for each sample compound provides a built-in test for flowrate effects on the measurement of p_{sat}.[11, 17, 18] For these measurements, saturators #2 (long), #5 (short), #8 (long), #11 (short), #14 (long) and #17 (short) were coated with POE5. Saturators #3 (long), #6 (short), #9 (long), #12 (short), #15 (long) and #18 (short) were coated with *n*-octacosane. The other six saturators were left uncoated. The coating procedure consisted of the following steps. First, a 5 % (mass/mass) solution of each sample

compound in hexane was made. The glass beads in each saturator were wetted with ~ 1.5 mL of one of these solutions, and the excess was poured out. Then the solvent was removed by a gentle flow of nitrogen through the adsorber at room temperature for 0.5 h, after which the coated saturators were immediately installed in the temperature-controlled chamber of the apparatus. For the measurements reported herein, no significant difference was observed for the measurements with long or short saturators, which confirms the absence of flowrate effects.

At the beginning of each p_{sat} measurement, the apparatus was flushed with ≥ 310 cm^3 of UHP-grade nitrogen carrier gas at room temperature (the internal void volume of the gas saturation apparatus is approximately 120 cm^3). The intent of this procedure was to remove the small amount of oxygen that is inevitably introduced into the gas saturation apparatus when the adsorbers are removed and reinstalled.[16] Some sample vapor is carried into the adsorbers during the flush but, because of the relatively small flush volume and low flush temperature, this type of measurement error was insignificant. After the flush, the oven temperature was raised to the measurement temperature. Total flow periods ranged from 14 days to 33 days. At the end of that time period, the flow of carrier gas was stopped and the adsorbers were removed for analysis of the trapped vapor. When an adsorber was removed, the lines were immediately capped in order to limit the infiltration of air into the gas saturation apparatus. The flowrate of carrier gas was 3.0 $cm^3 \cdot min^{-1}$.

4.2.3. Instrument Modifications

The p_{sat} measurements on POE5 and *n*-octacosane were at a higher temperature than any previous[16, 17] work in this gas saturation apparatus. At these temperatures, an apparatus modification was necessary in order to obtain accurate measurements of p_{sat}. Specifically, a tight-fitting PTFE sleeve was placed around the end of each adsorber inlet tube (Figure 8). These sleeves had an outer diameter that matched the inner diameter of the saturator tubing. This arrangement insulates the flow of gas from any temperature gradients created by the stainless-steel bulkhead union, which completely penetrates the insulated ceiling of the temperature-controlled chamber. The measured value of p_{sat} for POE5 at 362.93 K increased by about 50 % upon installation of the PTFE sleeves (i.e., the measured p_{sat} was 4.4 ± 1.1 mPa before installing the PTFE sleeves and 6.7 ± 1.8 mPa afterwards). This is a good illustration of the importance of eliminating cold spots at the saturator-adsorber interface.

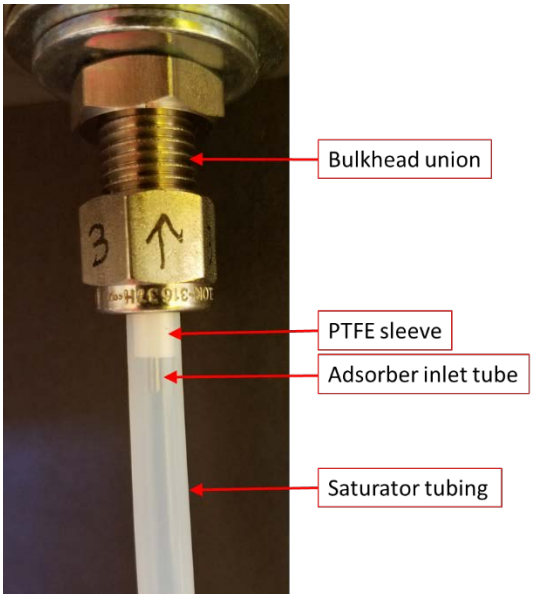

Figure 8: Union between the saturator and adsorber. The PTFE sleeve insulates the carrier gas and vapor solute from the bulkhead union.

4.2.4. Temperature Measurements

The temperature in the temperature-controlled chamber was measured with an ITS-90 calibrated platinum resistance thermometer (PRT). During the course of the p_{sat} measurements, the calibration of the PRT was checked with both a water triple-point cell (T = 273.16 K) and a gallium fixed-point cell (T = 302.9146 K). The temperatures measured by the PRT deviated from the two fixed points by < 0.01 K. At each temperature set-point, the PRT was used to measure the temperature at the bottom/middle of each saturator loop and near the exit end of each saturator. Temperature fluctuations in a specific location in the temperature-controlled chamber were relatively small—the range of measured temperatures typically varied by less than 0.05 K. A larger source of uncertainty comes from temperature gradients in the chamber, which increase in magnitude with temperature settings farther from ambient. For example, the average temperature difference between the middle (loop) and the exit end of a saturator was 0.80 K at a set-point of 353.05 K, and it was 1.02 K at a set-point of 362.93 K. These temperature gradients are the largest source of uncertainty in the p_{sat} measurements.

4.2.5. Mass of Carrier Gas

The mass of carrier gas was determined by the mass flow controller, which has a relative standard uncertainty of 3.2 % for the flow rate used for these measurements. The accuracy of the mass flow controller has been checked repeatedly by mass measurements.[16, 17]

4.2.6. Analysis of Vapor

At the end of the flow period, the vapor collected in each adsorber was prepared for analysis by GC-FID.[17] This was done by elution of each adsorber with hexane into two GC autosampler vials, which already contained ~ 0.3 g of a ~ 0.1 mass % *n*-eicosane solution (in *n*-octane). Then the two eluent fractions, with *n*-eicosane as an internal standard, were analyzed by GC-FID. The relative sensitivity of the FID to *n*-eicosane, POE5, and *n*-octacosane was determined by analyzing known mixtures.

4.3. Calculation of Vapor Pressure

Vapor pressures were calculated from the raw data by a form of the ideal gas law that contains the Poynting correction,

$$p_{sat} = (m \cdot R \cdot T)/(V \cdot M \cdot \Phi), \quad (3)$$

where p_{sat} is the vapor pressure of the sample, m is the recovered mass of sample vapor, R is the gas constant, T is the temperature of the saturator, V is the volume of carrier gas at the temperature and pressure of the saturator, M is the molar mass of sample compound, and Φ is the Poynting correction. Assuming that the condensed phase is incompressible, and knowing that p_{sat} is negligible compared to the experimental pressure (p), then $\Phi = \exp(p \cdot v/R \cdot T)$, where v is the molar volume[19] of the liquid sample. This is a small correction, which lowers all values of apparent p_{sat} by ~ 1 %. The volume of carrier gas, V, was determined from a high-accuracy equation of state for nitrogen[20] as implemented in REFPROP.[21] For these measurements, the effect of the sample vapor on the total vapor volume could be ignored because its mole fraction was very small compared to that of the carrier gas. The pressure in the saturators was taken to be ambient, which is 83.2 kPa (with a standard deviation of 0.6 kPa) on the NIST site in Boulder, Colorado.[17] The values of p_{sat} that were calculated from Eq. 3 were then corrected by dividing by the mole fraction purity of the sample (as determined by GC-FID). The POE5 had a mole fraction purity of 0.967.[3] The *n*-octacosane had a mole fraction purity of 0.995, so this correction is less important for the control compound. These corrected values of p_{sat} are reported in Table 10.

4.4. Uncertainty Calculations

Temperature control is the principal source of uncertainty for these measurements. Considering both temperature gradients and temperature fluctuations, we estimate that the standard uncertainty in temperature is 0.80 K at a setting of 353.05 K and 1.02 K at a setting of 362.93 K. These uncertainties in the measurement temperature result in standard uncertainties (u) of $0.104 \cdot p_{sat}$ and

$0.125 \cdot p_{sat}$ for *n*-octacosane at T = 353 K and 363 K, respectively; for POE5 the uncertainties are $0.096 \cdot p_{sat}$ and $0.114 \cdot p_{sat}$ at T = 353 K and 363 K, respectively. Other significant sources of measurement uncertainty included the following. Uncertainty in the determination of the mass of recovered vapor solute by GC-FID resulted in a standard uncertainty of $u = 0.03 \cdot p_{sat}$. Uncertainty in the determination of the mass of N_2 carrier gas by the mass flow controller resulted in a standard uncertainty of $u = 0.032 \cdot p_{sat}$. Uncertainty in the pressure in the saturators (caused by barometric variability and pressure drop across the apparatus) resulted in a standard uncertainty of $u = 0.024 \cdot p_{sat}$. Impurities in the *n*-octacosane caused a standard uncertainty of $u = 0.005 \cdot p_{sat}$ (based on the initial purity of the *n*-octacosane). Impurities in the POE5 caused a standard uncertainty of $u = 0.033 \cdot p_{sat}$ (based on the initial purity of the POE5). Finally, nonideality of the vapor phase mixture, which is caused by the interaction of the solute vapor with the N_2 carrier gas, caused an estimated standard uncertainty of $u = 0.02 \cdot p_{sat}$.[3, 17] The quadrature sum of the standard uncertainties associated with the measurement of p_{sat} results in combined expanded (k = 2) uncertainties (U_c) of $0.234 \cdot p_{sat}$ and $0.272 \cdot p_{sat}$ for *n*-octacosane at T = 353 K and 363 K, respectively, and $0.230 \cdot p_{sat}$ and $0.261 \cdot p_{sat}$ for POE5 at T = 353 K and 363 K, respectively.

An important advantage of the design of the gas saturation apparatus used for this work is that a control sample can be measured simultaneously with the other sample(s). We have typically employed linear alkanes as the control sample for a variety of reasons.[3, 16, 22, 23] *n*-Octacosane was selected for this work because its p_{sat} curve is very similar to that of POE5 in the temperature range studied; therefore, any systematic errors would have about the same magnitude effect on both. The results of the p_{sat} measurements on *n*-octacosane are shown in Table 10.

Surprisingly, after the first two replicate measurements at 362.93 K, the measured value of p_{sat} drifted lower. At the same time, new peaks started to appear in the chromatograms of vapor trapped by the adsorbers. This is typical behavior for a compound that is decomposing during the p_{sat} measurement,[16] but such decomposition was not expected for *n*-octacosane. Our hypothesis for why the *n*-octacosane started to decompose at these relatively low temperatures is that it contained low levels of olefinic impurities (as evidenced by multiple minor peaks in the ^{1}H NMR spectrum from 4.5 – 6.0 ppm), and olefins are known to initiate autoxidation chemistry under even mild measurement conditions.[16] The observation that the decomposition starts after an induction period is also consistent with autoxidation. In any case, the two initial measurements on *n*-octacosane at 362.93 K both indicated a p_{sat} of 5.0 ± 1.4 mPa. Within the uncertainty of the measurements, this is in agreement with the reference value from the correlation of Lemmon and

Goodwin, which is 6.09 ± 0.30 mPa.[24] This is evidence that, apart from sample decomposition, the measurement method was working properly.

4.5. Results

The results of p_{sat} measurements on POE5 are shown in Table 10. Multiple replicates were performed at 362.93 K with the aim of checking for significant sample decomposition. Unlike *n*-octacosane, the p_{sat} measurements on POE5 showed excellent repeatability and did not drift lower over time. This is evidence that there was no significant decomposition of POE5 during the measurements.[16] Additionally, chromatograms of vapor trapped by the adsorbers remained clear of decomposition product peaks. For these reasons, we believe that all of the measurements on POE5 are valid. The average value for the replicate measurements of p_{sat} at 362.93 K was 6.7 mPa with an expanded uncertainty of 1.8 mPa.

Table 10: The Vapor Pressures (p_{sat}) and Combined Expanded (k = 2) Uncertainties (U_c) for Measurements on POE5 and the Linear Alkane *n*-Octacosane ($C_{28}H_{58}$, Measured as a Control Sample).[a]

Date	T /K	p_{sat}[b] /mPa	U_c /mPa
POE5			
22-Jul-2016	362.93	6.7	1.8
25-Aug-2016	362.93	6.8	1.8
8-Sep-2016	362.93	6.8	1.8
26-Sep-2016	353.05	2.1	0.5
19-Oct-2016	362.93	6.6	1.7
***n*-Octacosane**			
22-Jul-2016	362.93	5.0	1.4
25-Aug-2016	362.93	5.0	1.4
8-Sep-2016	362.93	4.2	[c]
26-Sep-2016	353.05	1.2	[c]
19-Oct-2016	362.93	3.0	[c]

[a]Measurements are listed in chronological order, and measurements with the same date were done simultaneously.
[b]The values of p_{sat} have been corrected for the mole fraction purity of each sample, as described in the text.
[c]Significant decomposition of *n*-octacosane was observed for this measurement.

There is only one prior report of p_{sat} measurements on POE5 in the literature. By use of a gas saturation method that was designed for the measurement of relatively low pressures, Razzouk et

al.[6] collected p_{sat} data for POE5 in the temperature range 334 – 413 K. They also reported a correlation of their data with the Antoine equation. They estimated a measurement uncertainty of $0.05 \cdot p_{sat}$, although the only sources of uncertainty that were considered were the GC-FID analysis, the gas flow rate, and the p_{sat} of *n*-tetracosane (which was used to calibrate the measurement). In any case, by use of the reported Antoine coefficients for POE5,[6] one can calculate a p_{sat} of 2.62 ± 0.13 mPa at 353.05 K and 7.99 ± 0.40 mPa at 362.93 K. These values are within the combined uncertainties of the two measurements. The fact that the two data sets agree lends credence to both.

Measurements on lubricant base fluids larger than POE5 were not attempted because their vapor pressures were expected to be below the measurable range of our apparatus. For example, the p_{sat} curve for POE7 is expected to be about two orders of magnitude lower than for POE5.[6] In principle, it is possible to conduct measurements in our apparatus at higher temperatures and with longer flow periods; however, the large measurement uncertainties at high temperatures and the potential for sample decomposition limit the value and practicality of such measurements.

5. Isobaric Specific Heat Capacity

5.1. Summary

Measured isobaric specific heat capacities and associated expanded uncertainties are reported over the combined temperature range 208 to 503 K; the specific temperature range varied for each fluid and was selected to avoid potential phase transitions. Heat capacities range from an overall low of 1.704 $J \cdot g^{-1} \cdot K^{-1}$ to an overall high of 2.343 $J \cdot g^{-1} \cdot K^{-1}$, with a relative ordering among the four fluids of POE5 < MIL-PRF-23699 < POE7 < POE9 and differences that range from 6.5 % (at 313 K) to 6.8 % (at 408 K). These results are also presented in Fortin.[25]

5.2. Experimental Methods

A commercial differential scanning calorimeter (DSC) (see Figure 9) was used to measure the isobaric specific heat capacity of the four lubricant samples. As the name implies, DSC is a differential technique in which the difference in heat flow between a sample and an inert reference is measured as a function of time and temperature while both are subjected to a controlled environment. More specifically, modulated differential scanning calorimetry (MDSC) was used for the measurements reported herein. The difference between conventional DSC and MDSC lies in the heating profile applied; in DSC, a simple linear profile is utilized, while with our MDSC, a sinusoidal modulation is overlaid on the conventional linear heating ramp. The net effect is equivalent to performing two experiments simultaneously, one experiment at the average linear heating rate and a second at an instantaneous sinusoidal heating rate. In addition, while it is only possible to measure total heat flow with conventional DSC, with MDSC it is possible to separate total heat flow into its two components: one that is a function of the sample's heat capacity and rate of temperature change (the heat capacity or "reversing" component) and one that is a function of the absolute temperature and time (the kinetic or "nonreversing" component). The combined net effect of these two advantages is a simpler, more precise measurement of heat capacity with MDSC compared to conventional DSC. Additional details regarding MDSC theory can be found in Boerio-Goates and Callanan,[26] Reading et al.,[27] Wunderlich et al.,[28] and Höhne et al.,[29] among other references. In this work, measurement runs were performed over a given temperature range using an underlying heating rate of 3 $K \cdot min^{-1}$ and modulated conditions of ±1 K every 120 s. The specific temperature range varied by sample in an effort to avoid phase changes observed during initial exploratory measurement scans. Measurements were made from 233 to 443 K for POE5, from 263 to 428 K for POE7, from 283 to 423 K for POE9, and from 208 to 503 K for MIL-PRF-23699. For all measurements, the measuring cell was continuously purged with a 50 $mL \cdot min^{-1}$ flow of dry nitrogen.

Figure 9: Differential scanning calorimeter.

5.2.1. Instrument Calibration

Determination of accurate heat capacities requires calibration of the instrument baseline, temperature, heat flow, and heat capacity. The instrument baseline was calibrated via two separate measurement runs; in the first the cell was empty and in the second sapphire disks were placed directly on the cell's sample and reference platforms. From these two runs, cell asymmetries were quantified, and the instrument's baseline was adjusted.

Temperature and heat flow were calibrated via measurements of materials with known transition temperatures and heats. A list of some typical calibration substances and recommended transition temperatures can be found in Della Gatta et al.[30] In this work, a combination of adamantane, indium, and tin were used. Indium SRM 2232 and tin SRM 2220 were obtained from the National Institute of Standards and Technology (NIST) and corresponding reference melting temperatures and heats of fusion were obtained from their respective certificates.[31, 32] Adamantane was not available as a certified reference material. The adamantane sample used was obtained from Sigma-Aldrich[†] with a stated purity of > 99 %. Our own analysis by gas chromatography/mass spectrometry indicated a purity of > 99.95 %. The adamantane was used without further purification, and reference values for the temperature and heat of transition for the first order solid-solid transition were taken from Westrum.[33] The applied temperature calibration utilized

[†] In order to describe materials and experimental procedures adequately, it is occasionally necessary to identify commercial products by manufacturers' names or labels. In no instance does such identification imply endorsement by the National Institute of Standards and Technology, nor does it imply that the particular product or equipment is necessarily the best available for the purpose.

measurement results for all three calibrants for the heating rate of interest (3 K·min^{-1}). For the heat flow calibration, we chose to use a single average calibration coefficient calculated using only results from indium and tin measurements.

Heat capacity was calibrated by measuring a material whose heat capacity is known. In this work, sapphire (α-Al_2O_3) was measured under the same experimental conditions as were used for the lubricant samples. The resulting calibration coefficient (K_{cp}) is determined by dividing literature values[30, 34] by measured heat capacities. More specifically, K_{cp} is calculated and applied as a function of temperature; to achieve this, the calibration coefficient is applied to the data during post-processing.

5.2.2. Sample Preparation

All calibration and lubricant samples were encapsulated in hermetically sealed aluminum pans (see Figure 10). Additionally, an empty hermetically sealed pan served as the reference. Five separate pans were prepared for each measured lubricant sample. Sample masses ranged from 8.344 mg to 19.505 mg; multiple masses were measured to check for evidence of mass dependence, which could potentially indicate a significant contribution from the vapor phase. All mass measurements employed a microbalance (see Figure 10) and a double-substitution weighing scheme.[35] There are two main advantages to this process. First, the balance is calibrated over the same limited range as the sample weighings instead of assuming a linear response over the entire balance range, as is the case with most internal balance calibrations. And second, air buoyancy effects are reduced to small differences in volumes of the tare and sample pans and the relatively small effect of standard masses. Air buoyancy is explicitly accounted for via the inclusion of the ambient air density, which is determined from ambient temperature, pressure, and relative humidity measurements and the equation of Picard et al.[36]

Pans were first weighed empty to determine pan weight. They were then filled with sample, sealed closed with a press (see Figure 10), and reweighed to determine sample weight. The sealed pan was then allowed to sit for at least a day, and then it was reweighed to check for any mass loss, which would indicate that the pan was not properly sealed during encapsulation. Finally, pans were reweighed upon completion of the heat capacity measurements to again check for mass loss. A change in mass of > 0.3 % would require data be discarded. No samples had to be discarded as a result of sample loss in this work.

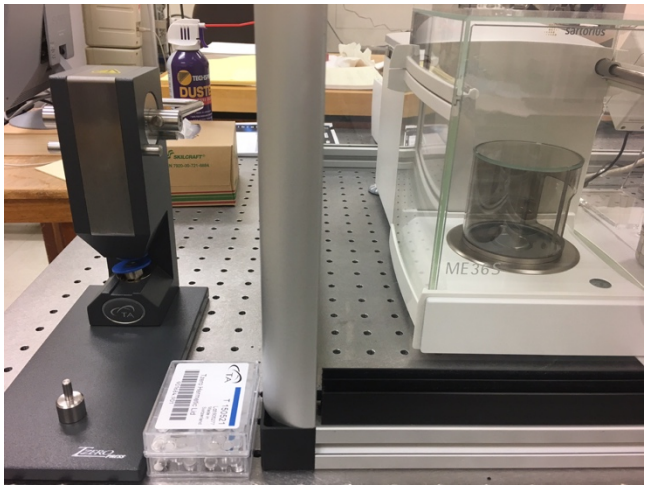

Figure 10: Tools for sample preparation. From left to right: press used to seal sample pans, sample pans and lids, and microbalance used to determine sample mass.

5.2.3. Measurement Procedure

Following the example of and building upon lessons learned during previous work,[37] heat capacity measurements for the four lubricant samples employed the following procedure, executed over two distinct measurement periods. First, the instrument baseline, temperature, and heat flow were calibrated as previously described. Then, prior to the start of sample measurements, the instrument was allowed to warm up and its performance was verified by performing repeat baseline runs, followed by a single indium verification measurement. These checks were repeated approximately every 24 hours if the instrument was set to run multiple samples over several days. For each of the five sample pans prepared for each fluid, two sets of two replicate runs were performed for a total of four replicates with the pan being removed in between. This provided valuable information about the instrument's repeatability and reproducibility, including contributions from pan placement upon the sample platform. Every run of a sample pan was bracketed by a single sapphire calibration run. Since a significant degree of variability was observed among the calibration runs over the course of each measurement period, and the variability appeared to be random in nature, it was determined that the application of an overall average $\bar{K}_{cp}(T)$ would be more representative of the instrument's behavior. A separate average $\bar{K}_{cp}(T)$ was determined and applied for each measurement period; for the first, an average of 80 separate sapphire calibrations was used, while for the second, 20 separate sapphire calibrations went into the average used. Finally, the fifth pan for each sample fluid was measured a second time using a quasi-isothermal method. For this method, rather than ramping the temperature at a constant rate of 3 K·min^{-1}, the temperature was changed in 10 K steps and the sample allowed to

sit at each temperature for a total of 15 minutes to allow for thermal equilibration within the sample. The information obtained from these runs was used in the subsequent uncertainty analysis.

5.3. Results

5.3.1. Measurement Results

Overall averaged heat capacity results ($\bar{\bar{c}}_p$) are plotted as a function of temperature in Figure 11 and are reported in Tables 11 – 14 (Section 5.4) with POE5 in Table 11, POE7 in Table 12, POE9 in Table 13, and MIL-PRF-23699 in Table 14. For clarity, the plotted data in Figure 11 have been limited to a point every 5 K. Additionally, the tabulated data (Tables 11 – 14) represent a subset of the collected measurement data. Although measurement scans were performed over larger temperature ranges than what is shown in the tabulated data, only data from the stable portion of the heat flow curves are presented. Furthermore, although data were collected at > 1 point per second, the data were further reduced to a point every 1 K to make the amount of data presented in the tables more reasonable.

As was previously discussed, for each fluid, five samples were prepared and each of those samples was measured four times for a total of twenty measurement runs per fluid. For a given fluid, replicate measurement results were first averaged for each of the five measured pans/masses and then those averages ($\bar{c}_p$) were compared to check for any evidence of mass dependence. After the first measurement period, some of the fluids showed an apparent mass dependence among the first four pans/masses, while others did not. When present, the observed mass dependence could not be attributed to a contribution from the vapor phase. In an effort to better understand the initial observations, additional measurements were made during a second measurement period using two new sample pans/masses for each fluid, one pan with small masses (< 6 mg) and one pan with larger masses (closer to previously measured masses, ~ 12 – 19 mg). Results for the small masses were determined to be unreliable and have not been included here. Results for the larger masses were consistently higher than earlier measurements and eliminated any previously observed mass dependence. In the absence of an observed mass dependence, results were further averaged to give a single overall average ($\bar{\bar{c}}_p$) as a function of temperature for each measured fluid.

Figure 11 shows that POE9 exhibits the highest heat capacities, ranging from 1.940 $J \cdot g^{-1} \cdot K^{-1}$ at 313.13 K to 2.234 $J \cdot g^{-1} \cdot K^{-1}$ at 412.14 K. POE 5 exhibits the lowest heat capacities, ranging from 1.704 $J \cdot g^{-1} \cdot K^{-1}$ at 263.14 K to 2.143 $J \cdot g^{-1} \cdot K^{-1}$ at 432.15 K. The difference in heat capacity between these two fluids is 6.5 % at 313 K and 6.8 % at 408 K. MIL-PRF-23699, the fully qualified lubricant, has heat capacities that are between those of POE7 and POE5. Because the slope of

MIL-PRF-23699's observed temperature dependence is different from the two lubricant base oils that bracket it, it has heat capacities that are closest to POE5 at lower temperatures (e.g., MIL-PRF-23699 is 0.8 % higher at 273 K) and closest to POE7 at higher temperatures (e.g., MIL-PRF-23699 is 0.9 % lower at 417 K).

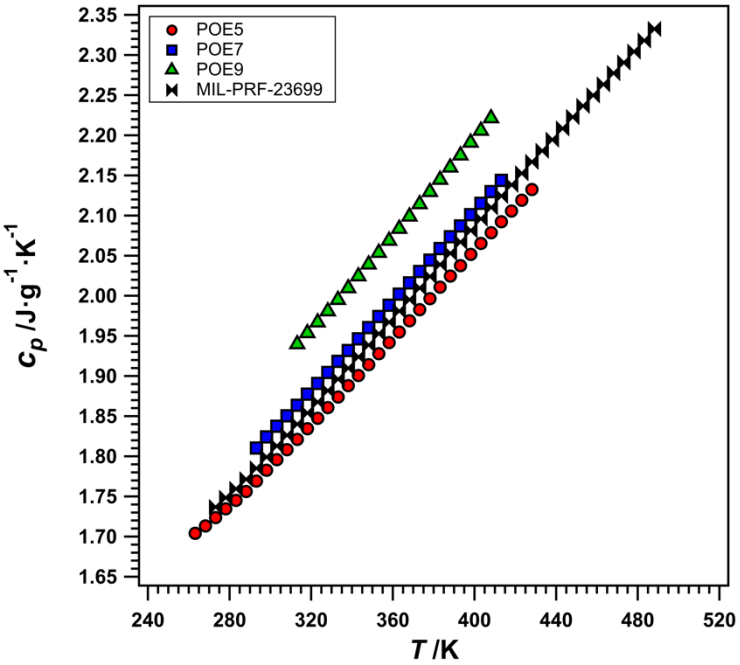

Figure 11: Isobaric specific heat capacity measurements plotted as a function of temperature. Only a subset of data points reported are plotted for clarity.

5.3.2. Uncertainty Estimates

Also included Tables 11 – 14 (Section 5.4) are the associated absolute expanded uncertainty estimates ($U(\bar{\bar{c}}_p)$). The expanded uncertainty is calculated using the expression

$$U(\bar{\bar{c}}_p) = t_{95}(df_{cp}) \cdot u(\bar{\bar{c}}_p)\,, \tag{4}$$

where the coverage factor, $t_{95}(df_{cp})$, is taken from the *t*-distribution for df_{cp} degrees of freedom and a 95 % level of confidence, and $u(\bar{\bar{c}}_p)$ is the combined standard uncertainty for the averaged isobaric specific heat capacity measurements.[38]

The combined standard uncertainty for a single replicate measurement of a single sample mass can be expressed as

$$u(c_p) = \sqrt{\left(\frac{\partial c_p}{\partial K_{cp}}\right)^2 u^2(K_{cp}) + \left(\frac{\partial c_p}{\partial m}\right)^2 u^2(m) + \left(\frac{\partial c_p}{\partial c_{pm}}\right)^2 u^2(c_{pm})}\,, \quad (5)$$

where the first term is the contribution from the uncertainty associated with the heat capacity calibration (K_{cp}), the second term is the contribution from the uncertainty in the sample mass (m), and the last term is the uncertainty associated with the measured heat capacity signal produced by the instrument (c_{pm}). Each of the three standard uncertainty terms ($u(K_{cp})$, $u(m)$, and $u(c_{pm})$) include both random (type A)[38] and systematic (type B)[38] sources of error. For example, $u(K_{cp})$ incorporates the standard deviation for the averaged calibration coefficient ($\bar{K}_{cp}$), as well as contributions from systematic error sources such as temperature alignment and uncertainties associated with the reference values used to calculate K_{cp}. Statistical methods are employed to combine single run standard uncertainties ($u(c_p)$) to calculate the combined standard uncertainty for the average of replicate runs of a single sample mass ($u(\bar{c}_p)$), and to combine standard uncertainties for individual masses ($u(\bar{c}_p)$) to calculate the overall combined standard uncertainty for a given fluid ($u(\bar{\bar{c}}_p)$). The statistical methods used for this last calculation depend on the specific circumstances. In this work, the observed between-mass variances were often significantly larger than the observed within-mass variances. Under these circumstances, it is preferable to determine the variance of the overall average of the group means,[38] which is calculated using the expression

$$u(\bar{\bar{c}}_p) = \frac{s_{\bar{\bar{c}}p}}{n_{\bar{\bar{c}}p}}\,, \quad (6)$$

where $s_{\bar{\bar{c}}p}$ is the standard deviation for the overall average specific heat capacity ($\bar{\bar{c}}_p$) and $n_{\bar{\bar{c}}p}$ is the number of averaged masses ($n_{\bar{\bar{c}}p}$ = 5 in this work). The degrees of freedom to use when determining the appropriate coverage factor for calculating expanded uncertainties (Eq. 4) are equal to $n_{\bar{\bar{c}}p}$ – 1. Corresponding coverage factors ($t_{95}(df_{cp})$) have not been included in Tables 11 – 14 since, in this work, all coverage factors are equivalent (t_{95} = 2.776). Overall, expanded uncertainties range between 0.036 J·g^{-1}·K^{-1} and 0.065 J·g^{-1}·K^{-1} (1.61 % to 2.93 %).

5.4. Data Tables

Table 11: Measured Isobaric Heat Capacities for POE5.

T /K	$\bar{\bar{c}}_p$ /J·g^{-1}·K^{-1}	$U(\bar{\bar{c}}_p)$ /J·g^{-1}·K^{-1}	T /K	$\bar{\bar{c}}_p$ /J·g^{-1}·K^{-1}	$U(\bar{\bar{c}}_p)$ /J·g^{-1}·K^{-1}	T /K	$\bar{\bar{c}}_p$ /J·g^{-1}·K^{-1}	$U(\bar{\bar{c}}_p)$ /J·g^{-1}·K^{-1}
263.14	1.704	0.040	293.14	1.769	0.039	323.14	1.848	0.037
264.15	1.706	0.040	294.15	1.772	0.039	324.15	1.850	0.037
265.15	1.708	0.040	295.14	1.775	0.039	325.14	1.853	0.037
266.14	1.710	0.040	296.15	1.777	0.039	326.15	1.855	0.037
267.14	1.712	0.040	297.14	1.780	0.038	327.15	1.858	0.037
268.15	1.713	0.040	298.14	1.783	0.038	328.15	1.861	0.037
269.14	1.715	0.040	299.15	1.785	0.038	329.14	1.863	0.037
270.14	1.717	0.040	300.14	1.788	0.038	330.15	1.866	0.037
271.15	1.719	0.040	301.15	1.791	0.038	331.15	1.869	0.037
272.14	1.721	0.040	302.14	1.793	0.038	332.14	1.871	0.037
273.14	1.724	0.040	303.15	1.796	0.038	333.14	1.874	0.037
274.14	1.726	0.040	304.15	1.799	0.038	334.15	1.877	0.037
275.15	1.728	0.039	305.14	1.801	0.038	335.14	1.880	0.037
276.14	1.730	0.039	306.15	1.803	0.038	336.14	1.883	0.037
277.14	1.733	0.039	307.15	1.806	0.038	337.14	1.886	0.037
278.15	1.735	0.039	308.14	1.808	0.038	338.14	1.888	0.037
279.15	1.737	0.039	309.14	1.811	0.038	339.15	1.891	0.037
280.15	1.739	0.039	310.15	1.814	0.038	340.14	1.894	0.037
281.14	1.741	0.039	311.15	1.816	0.038	341.14	1.896	0.037
282.15	1.743	0.039	312.14	1.819	0.038	342.15	1.898	0.038
283.15	1.745	0.038	313.15	1.821	0.037	343.14	1.901	0.037
284.15	1.747	0.038	314.14	1.824	0.037	344.15	1.903	0.037
285.15	1.750	0.038	315.15	1.827	0.037	345.15	1.906	0.037
286.14	1.752	0.038	316.14	1.829	0.037	346.15	1.909	0.037
287.14	1.754	0.038	317.15	1.832	0.037	347.14	1.911	0.037
288.15	1.756	0.038	318.15	1.834	0.037	348.14	1.914	0.037
289.15	1.759	0.039	319.14	1.837	0.037	349.15	1.917	0.037
290.14	1.761	0.039	320.15	1.840	0.037	350.14	1.920	0.037
291.14	1.764	0.039	321.15	1.842	0.037	351.14	1.922	0.037
292.14	1.767	0.039	322.14	1.845	0.037	352.14	1.925	0.037

Table 11, continued.

T /K	$\bar{\bar{c}}_p$ /J·g^{-1}·K^{-1}	$U(\bar{\bar{c}}_p)$ /J·g^{-1}·K^{-1}	T /K	$\bar{\bar{c}}_p$ /J·g^{-1}·K^{-1}	$U(\bar{\bar{c}}_p)$ /J·g^{-1}·K^{-1}	T /K	$\bar{\bar{c}}_p$ /J·g^{-1}·K^{-1}	$U(\bar{\bar{c}}_p)$ /J·g^{-1}·K^{-1}
353.14	1.928	0.037	380.14	2.002	0.038	407.14	2.076	0.039
354.15	1.931	0.037	381.15	2.005	0.038	408.14	2.079	0.039
355.14	1.933	0.037	382.14	2.008	0.038	409.14	2.081	0.039
356.15	1.936	0.037	383.14	2.011	0.038	410.15	2.084	0.039
357.15	1.939	0.037	384.14	2.014	0.038	411.15	2.087	0.039
358.14	1.942	0.037	385.15	2.016	0.038	412.14	2.090	0.039
359.15	1.944	0.037	386.14	2.019	0.038	413.15	2.092	0.039
360.15	1.947	0.037	387.14	2.022	0.038	414.15	2.095	0.039
361.14	1.950	0.037	388.15	2.025	0.038	415.15	2.098	0.039
362.15	1.952	0.037	389.15	2.027	0.038	416.14	2.101	0.039
363.15	1.955	0.037	390.14	2.030	0.038	417.15	2.103	0.040
364.14	1.958	0.037	391.15	2.033	0.038	418.15	2.106	0.040
365.14	1.961	0.037	392.15	2.035	0.038	419.15	2.108	0.040
366.15	1.963	0.037	393.15	2.038	0.039	420.14	2.111	0.040
367.14	1.966	0.037	394.15	2.040	0.039	421.15	2.114	0.040
368.14	1.969	0.037	395.15	2.043	0.039	422.15	2.116	0.040
369.14	1.972	0.037	396.14	2.046	0.039	423.15	2.119	0.040
370.14	1.975	0.037	397.14	2.049	0.039	424.14	2.122	0.040
371.15	1.977	0.037	398.14	2.052	0.039	425.15	2.125	0.040
372.14	1.980	0.037	399.14	2.055	0.039	426.15	2.127	0.041
373.14	1.983	0.037	400.15	2.057	0.039	427.14	2.130	0.041
374.15	1.986	0.037	401.14	2.060	0.039	428.15	2.133	0.041
375.14	1.988	0.038	402.14	2.063	0.039	429.15	2.135	0.041
376.14	1.991	0.038	403.15	2.065	0.039	430.14	2.138	0.041
377.14	1.994	0.038	404.15	2.068	0.039	431.15	2.140	0.041
378.15	1.997	0.038	405.14	2.071	0.039	432.15	2.143	0.041
379.15	1.999	0.038	406.15	2.073	0.039			

Table 12: Measured Isobaric Heat Capacities for POE7.

T /K	$\bar{\bar{c}}_p$ /J·g^{-1}·K^{-1}	$U(\bar{\bar{c}}_p)$ /J·g^{-1}·K^{-1}	T /K	$\bar{\bar{c}}_p$ /J·g^{-1}·K^{-1}	$U(\bar{\bar{c}}_p)$ /J·g^{-1}·K^{-1}	T /K	$\bar{\bar{c}}_p$ /J·g^{-1}·K^{-1}	$U(\bar{\bar{c}}_p)$ /J·g^{-1}·K^{-1}	T /K	$\bar{\bar{c}}_p$ /J·g^{-1}·K^{-1}	$U(\bar{\bar{c}}_p)$ /J·g^{-1}·K^{-1}
293.14	1.811	0.053	325.14	1.896	0.050	357.14	1.985	0.048	389.14	2.076	0.048
294.14	1.813	0.053	326.14	1.899	0.050	358.14	1.988	0.048	390.14	2.079	0.048
295.14	1.816	0.053	327.14	1.902	0.050	359.14	1.991	0.048	391.14	2.082	0.048
296.14	1.819	0.053	328.14	1.905	0.050	360.14	1.994	0.048	392.14	2.085	0.048
297.14	1.822	0.053	329.14	1.908	0.050	361.14	1.997	0.048	393.14	2.087	0.048
298.14	1.824	0.053	330.14	1.910	0.050	362.14	1.999	0.048	394.14	2.090	0.048
299.14	1.827	0.053	331.14	1.913	0.050	363.14	2.002	0.048	395.14	2.093	0.048
300.14	1.830	0.053	332.14	1.916	0.050	364.14	2.005	0.048	396.14	2.095	0.048
301.14	1.832	0.053	333.14	1.918	0.050	365.14	2.008	0.048	397.14	2.098	0.048
302.14	1.835	0.053	334.13	1.921	0.050	366.14	2.011	0.048	398.14	2.101	0.048
303.14	1.838	0.052	335.14	1.924	0.050	367.14	2.013	0.048	399.14	2.104	0.048
304.14	1.840	0.052	336.14	1.927	0.050	368.14	2.016	0.048	400.14	2.107	0.048
305.14	1.843	0.052	337.14	1.929	0.049	369.14	2.019	0.048	401.14	2.110	0.048
306.14	1.845	0.052	338.14	1.932	0.049	370.14	2.022	0.048	402.14	2.113	0.048
307.14	1.848	0.052	339.14	1.935	0.049	371.14	2.025	0.048	403.14	2.115	0.048
308.14	1.851	0.052	340.14	1.938	0.049	372.14	2.027	0.048	404.14	2.118	0.048
309.14	1.853	0.052	341.13	1.940	0.048	373.14	2.030	0.048	405.14	2.121	0.048
310.14	1.856	0.052	342.14	1.943	0.048	374.14	2.033	0.048	406.14	2.124	0.048
311.14	1.858	0.052	343.14	1.946	0.048	375.14	2.036	0.048	407.14	2.127	0.048
312.14	1.861	0.051	344.14	1.949	0.048	376.14	2.039	0.048	408.14	2.130	0.048
313.14	1.864	0.051	345.13	1.952	0.048	377.14	2.042	0.048	409.14	2.133	0.048
314.14	1.867	0.051	346.14	1.955	0.049	378.14	2.045	0.048	410.14	2.135	0.048
315.14	1.869	0.051	347.14	1.958	0.049	379.14	2.048	0.048	411.14	2.138	0.048
316.14	1.872	0.051	348.14	1.960	0.048	380.14	2.050	0.048	412.13	2.141	0.049
317.14	1.875	0.051	349.14	1.963	0.049	381.14	2.053	0.048	413.14	2.144	0.049
318.14	1.878	0.050	350.14	1.966	0.049	382.14	2.056	0.048	414.13	2.147	0.049
319.14	1.880	0.050	351.14	1.969	0.049	383.14	2.059	0.048	415.14	2.150	0.049
320.14	1.883	0.050	352.14	1.972	0.049	384.14	2.062	0.048	416.14	2.152	0.049
321.14	1.886	0.050	353.14	1.974	0.049	385.14	2.065	0.048	417.14	2.155	0.049
322.13	1.888	0.050	354.14	1.977	0.049	386.14	2.068	0.048			
323.14	1.891	0.050	355.14	1.980	0.048	387.14	2.071	0.048			
324.14	1.894	0.050	356.14	1.983	0.048	388.14	2.074	0.048			

Table 13: Measured Isobaric Heat Capacities for POE9.

T /K	$\bar{\bar{c}}_p$ /J·g^{-1}·K^{-1}	$U(\bar{\bar{c}}_p)$ /J·g^{-1}·K^{-1}	T /K	$\bar{\bar{c}}_p$ /J·g^{-1}·K^{-1}	$U(\bar{\bar{c}}_p)$ /J·g^{-1}·K^{-1}	T /K	$\bar{\bar{c}}_p$ /J·g^{-1}·K^{-1}	$U(\bar{\bar{c}}_p)$ /J·g^{-1}·K^{-1}
313.13	1.940	0.037	347.13	2.036	0.038	381.13	2.139	0.037
314.13	1.943	0.037	348.13	2.039	0.037	382.13	2.142	0.037
315.14	1.945	0.037	349.13	2.042	0.037	383.13	2.145	0.036
316.13	1.948	0.037	350.14	2.045	0.037	384.13	2.148	0.036
317.14	1.951	0.038	351.13	2.048	0.037	385.13	2.151	0.036
318.13	1.954	0.037	352.13	2.051	0.037	386.13	2.154	0.036
319.13	1.956	0.037	353.14	2.054	0.037	387.13	2.157	0.036
320.14	1.959	0.037	354.13	2.057	0.037	388.13	2.160	0.036
321.13	1.962	0.037	355.14	2.060	0.037	389.13	2.163	0.037
322.13	1.964	0.037	356.13	2.063	0.037	390.13	2.166	0.037
323.14	1.967	0.037	357.13	2.066	0.037	391.13	2.169	0.037
324.13	1.970	0.038	358.13	2.069	0.037	392.13	2.172	0.037
325.13	1.972	0.038	359.13	2.072	0.037	393.13	2.175	0.037
326.13	1.975	0.038	360.13	2.075	0.037	394.13	2.178	0.037
327.13	1.978	0.038	361.13	2.078	0.037	395.14	2.181	0.037
328.14	1.981	0.037	362.13	2.081	0.037	396.13	2.185	0.037
329.14	1.984	0.038	363.13	2.084	0.037	397.13	2.188	0.037
330.13	1.986	0.037	364.13	2.087	0.037	398.13	2.191	0.037
331.13	1.989	0.037	365.13	2.090	0.037	399.13	2.194	0.037
332.13	1.992	0.037	366.13	2.093	0.037	400.13	2.197	0.037
333.13	1.995	0.037	367.13	2.096	0.037	401.13	2.200	0.037
334.13	1.998	0.037	368.13	2.099	0.037	402.14	2.203	0.036
335.13	2.001	0.037	369.13	2.102	0.037	403.13	2.206	0.036
336.14	2.004	0.037	370.13	2.105	0.037	404.14	2.209	0.036
337.13	2.007	0.038	371.13	2.108	0.037	405.13	2.212	0.036
338.13	2.010	0.038	372.13	2.111	0.037	406.13	2.215	0.036
339.13	2.013	0.038	373.13	2.114	0.037	407.13	2.218	0.036
340.13	2.016	0.038	374.14	2.117	0.038	408.13	2.221	0.036
341.14	2.018	0.038	375.14	2.120	0.038	409.13	2.225	0.036
342.14	2.021	0.038	376.13	2.123	0.037	410.14	2.228	0.036
343.13	2.024	0.038	377.13	2.126	0.037	411.13	2.230	0.036
344.13	2.027	0.038	378.13	2.129	0.037	412.14	2.234	0.036
345.14	2.030	0.038	379.13	2.132	0.037			
346.13	2.033	0.038	380.14	2.135	0.037			

Table 14: Measured Isobaric Heat Capacities for MIL-PRF-23699.

T /K	$\bar{\bar{c}}_p$ /J·g^{-1}·K^{-1}	$U(\bar{\bar{c}}_p)$ /J·g^{-1}·K^{-1}	T /K	$\bar{\bar{c}}_p$ /J·g^{-1}·K^{-1}	$U(\bar{\bar{c}}_p)$ /J·g^{-1}·K^{-1}	T /K	$\bar{\bar{c}}_p$ /J·g^{-1}·K^{-1}	$U(\bar{\bar{c}}_p)$ /J·g^{-1}·K^{-1}
273.15	1.737	0.048	312.15	1.837	0.048	351.15	1.947	0.050
274.15	1.739	0.048	313.15	1.840	0.048	352.15	1.950	0.050
275.15	1.742	0.048	314.15	1.843	0.048	353.15	1.953	0.050
276.15	1.744	0.047	315.15	1.846	0.048	354.15	1.956	0.050
277.16	1.746	0.047	316.15	1.849	0.048	355.15	1.959	0.050
278.15	1.749	0.047	317.15	1.851	0.048	356.15	1.961	0.050
279.15	1.751	0.047	318.15	1.854	0.048	357.15	1.964	0.050
280.15	1.753	0.047	319.15	1.857	0.048	358.15	1.967	0.050
281.15	1.755	0.047	320.15	1.860	0.048	359.15	1.970	0.050
282.15	1.757	0.047	321.15	1.862	0.048	360.15	1.973	0.050
283.15	1.760	0.047	322.15	1.865	0.048	361.15	1.976	0.050
284.15	1.762	0.047	323.15	1.868	0.048	362.15	1.978	0.050
285.15	1.764	0.047	324.15	1.870	0.048	363.15	1.981	0.050
286.15	1.767	0.047	325.15	1.873	0.048	364.15	1.984	0.050
287.15	1.769	0.047	326.15	1.876	0.048	365.15	1.987	0.050
288.15	1.771	0.047	327.15	1.879	0.048	366.15	1.990	0.050
289.15	1.774	0.048	328.15	1.882	0.048	367.15	1.992	0.050
290.15	1.777	0.048	329.15	1.885	0.048	368.15	1.995	0.050
291.15	1.779	0.048	330.15	1.888	0.048	369.15	1.998	0.050
292.15	1.782	0.048	331.15	1.891	0.048	370.15	2.001	0.050
293.15	1.785	0.048	332.15	1.893	0.048	371.15	2.004	0.050
294.15	1.788	0.048	333.15	1.896	0.048	372.15	2.007	0.050
295.15	1.791	0.048	334.15	1.899	0.048	373.15	2.010	0.050
296.15	1.794	0.048	335.15	1.902	0.048	374.15	2.013	0.050
297.15	1.797	0.048	336.15	1.904	0.048	375.15	2.015	0.050
298.15	1.799	0.048	337.15	1.907	0.048	376.15	2.018	0.050
299.15	1.802	0.048	338.15	1.910	0.048	377.15	2.021	0.050
300.15	1.805	0.048	339.15	1.913	0.049	378.15	2.024	0.051
301.15	1.808	0.048	340.15	1.916	0.049	379.15	2.027	0.051
302.15	1.810	0.048	341.15	1.918	0.049	380.15	2.030	0.051
303.15	1.813	0.048	342.15	1.921	0.049	381.15	2.033	0.051
304.15	1.816	0.048	343.15	1.924	0.049	382.15	2.036	0.051
305.15	1.818	0.048	344.15	1.927	0.049	383.15	2.039	0.051
306.15	1.821	0.048	345.15	1.930	0.049	384.15	2.042	0.051
307.15	1.824	0.048	346.15	1.933	0.049	385.15	2.045	0.051
308.15	1.826	0.048	347.15	1.936	0.049	386.15	2.048	0.052
309.15	1.829	0.048	348.15	1.939	0.049	387.15	2.050	0.052
310.15	1.832	0.048	349.15	1.941	0.050	388.15	2.053	0.052
311.15	1.835	0.048	350.15	1.944	0.050	389.15	2.056	0.052

Table 14, continued.

T /K	$\bar{\bar{c}}_p$ /J·g^{-1}·K^{-1}	$U(\bar{\bar{c}}_p)$ /J·g^{-1}·K^{-1}	T /K	$\bar{\bar{c}}_p$ /J·g^{-1}·K^{-1}	$U(\bar{\bar{c}}_p)$ /J·g^{-1}·K^{-1}	T /K	$\bar{\bar{c}}_p$ /J·g^{-1}·K^{-1}	$U(\bar{\bar{c}}_p)$ /J·g^{-1}·K^{-1}
390.15	2.059	0.052	425.15	2.158	0.056	460.14	2.255	0.061
391.15	2.062	0.052	426.15	2.161	0.056	461.15	2.258	0.061
392.15	2.064	0.052	427.15	2.164	0.057	462.15	2.261	0.061
393.15	2.067	0.052	428.15	2.167	0.057	463.15	2.264	0.061
394.15	2.070	0.052	429.15	2.170	0.057	464.15	2.266	0.062
395.15	2.073	0.053	430.15	2.172	0.057	465.15	2.269	0.062
396.15	2.076	0.053	431.15	2.175	0.057	466.15	2.272	0.062
397.15	2.079	0.053	432.15	2.178	0.057	467.15	2.275	0.062
398.15	2.082	0.053	433.15	2.181	0.058	468.15	2.278	0.062
399.15	2.085	0.053	434.15	2.184	0.058	469.15	2.280	0.062
400.15	2.087	0.054	435.15	2.186	0.058	470.15	2.283	0.062
401.16	2.090	0.054	436.15	2.189	0.058	471.15	2.286	0.062
402.16	2.093	0.054	437.15	2.192	0.058	472.15	2.288	0.062
403.15	2.096	0.054	438.15	2.195	0.058	473.15	2.291	0.062
404.15	2.099	0.054	439.15	2.197	0.058	474.15	2.294	0.062
405.15	2.102	0.054	440.15	2.200	0.058	475.15	2.296	0.062
406.15	2.105	0.054	441.15	2.203	0.058	476.15	2.299	0.062
407.15	2.107	0.054	442.15	2.206	0.059	477.15	2.302	0.062
408.15	2.110	0.054	443.15	2.209	0.059	478.15	2.304	0.063
409.15	2.113	0.054	444.15	2.212	0.059	479.15	2.307	0.063
410.15	2.116	0.055	445.15	2.214	0.059	480.15	2.310	0.063
411.15	2.119	0.055	446.15	2.217	0.059	481.15	2.313	0.064
412.15	2.122	0.055	447.15	2.220	0.059	482.15	2.315	0.064
413.15	2.125	0.055	448.15	2.223	0.059	483.15	2.318	0.063
414.15	2.127	0.055	449.15	2.226	0.059	484.15	2.321	0.063
415.15	2.130	0.055	450.15	2.228	0.059	485.15	2.324	0.063
416.16	2.133	0.055	451.15	2.231	0.060	486.15	2.327	0.063
417.15	2.136	0.056	452.15	2.234	0.060	487.15	2.330	0.063
418.15	2.138	0.056	453.15	2.237	0.060	488.15	2.333	0.064
419.15	2.141	0.056	454.15	2.239	0.060	489.15	2.335	0.064
420.15	2.144	0.056	455.15	2.242	0.060	490.15	2.338	0.064
421.15	2.147	0.056	456.15	2.245	0.061	491.15	2.341	0.065
422.15	2.150	0.056	457.15	2.247	0.061	492.15	2.343	0.064
423.15	2.153	0.056	458.15	2.250	0.061			
424.15	2.156	0.056	459.15	2.253	0.061			

6. Speed of Sound

6.1. Summary

The speed of sound of the POE lubricants was measured over wide ranges of temperature and pressure in a dual-path, pulse-echo-type instrument. These measurements, together with the density and heat capacity measurements, provided the data necessary for fitting equations of state (EOS) for each of the POEs. The reason for the measurement of speed of sound may not be obvious. The speed of sound is closely related to heat capacity, which is important for any type of thermal calculation. Speed of sound data gives information on the change of heat capacity with pressure, but c_p at a reference pressure is required; thus, the combination of c_p data from the DSC measurements and the speed of sound over a wide range of pressure is very valuable for EOS fitting.

6.2. Principle of the Measurement

The speed of sound of the POE lubricants was measured over wide ranges of temperature and pressure in a dual-path, pulse-echo-type instrument. In this technique, a piezoelectric transducer is located within a sample volume of the test fluid. It is excited with a sinusoidal burst, near the crystal resonance frequency, from an arbitrary function generator, thus emitting ultrasonic pulses from each face of the crystal, which travel through the fluid sample, reflect off planar surfaces at each end of the sample volume, and return to the transducer, which also serves as the detector. The difference in the arrival times of the echo signals gives the speed of sound by

$$w = \frac{2(L_2 - L_1)}{\Delta t} \quad , \tag{7}$$

where w is the speed of sound, L_1 and L_2 are the path lengths, and Δt is the time difference. The differential nature of this technique cancels end effects and improves the accuracy.

6.3. Experimental Method

6.3.1. Instrument Description

A quartz crystal with a diameter of 24 mm, thickness of 0.36 mm, and resonant frequency of 8.000 MHz served as the ultrasonic transducer. The quartz crystal is “X-cut,” which means that its thickness expands and contracts when a voltage is applied to electrodes on opposite faces of the crystal. It was excited with a 10-cycle sinusoidal burst from an arbitrary function generator. The fluid path lengths on the opposite faces of the crystal were 30 mm and 12 mm (ratio of 2.5:1); these separations of the crystal and the reflectors were provided by tubular spacers fabricated of a

machinable ceramic. A high-speed switch connected the crystal to the function generator during the input sinusoidal burst and then, after a delay of 6 μs, switched the crystal to the input of a three-stage amplifier (5× per stage for a total of 125×), which then fed into a digital storage oscilloscope. The echo signals were recorded for off-line analysis.

The measuring cell holding the crystal and fluid sample was contained in a pressure vessel rated to 93 MPa. This, in turn, was held in a thermostated oil bath operating from 228 K to 423 K. A photo of the oil bath and associated fluid-handling manifold is shown as Figure 12. A photo of the instruments (which are located in the adjacent room) is shown as Figure 13. A schematic of the measuring cell is shown in Figure 14.

Figure 12: Dual-path, pulse-echo, speed of sound instrument showing the thermostat (which contains the measuring cell) and the fluid manifold and pressure transducer; a vacuum system for evacuating the measuring cell is to the left of the thermostat.

The temperature of the oil bath was measured with a long-stem 25-ohm standard platinum resistance thermometer (SPRT); the temperature-sensing portion of the SPRT was located immediately adjacent to the pressure vessel, as indicated in Figure 14. The resistance of the SPRT was ratioed to a standard resistor (which was held in a thermostated enclosure) with an AC resistance bridge. The SPRT, standard resistor, and resistance bridge were calibrated as a system over the range of 234.316 K to 429.749 K with fixed-point cells (mercury triple point, water triple point, and indium freezing point). The standard uncertainty in the SPRT/resistor/bridge system was estimated as 3 mK. The short-term (minute-to-minute) variations in the oil-bath temperature were 2 mK or less. No long-term (hour-to-hour) variation was observed. The temperature gradients in the oil bath were less than 2.5 mK over the region of the pressure vessel. The combined standard

uncertainty in the temperature measurement, including the effects of the SPRT, standard resistor, resistance bridge, calibration standards, stability of the oil bath, and temperature gradients in the oil bath was 4 mK.

Figure 13: Instrument rack for the pulse-echo speed of sound instrument.

The pressure was measured with a vibrating-quartz-crystal pressure transducer with a maximum pressure of 138 MPa. The transducer was held at room temperature. The transducer was calibrated by the manufacturer with piston gages; this calibration included a temperature-compensation term. The zero of the transducer was checked regularly (while the system was evacuated between samples) and readings were corrected for any drift in the zero. The standard uncertainty in pressure was 0.007 MPa.

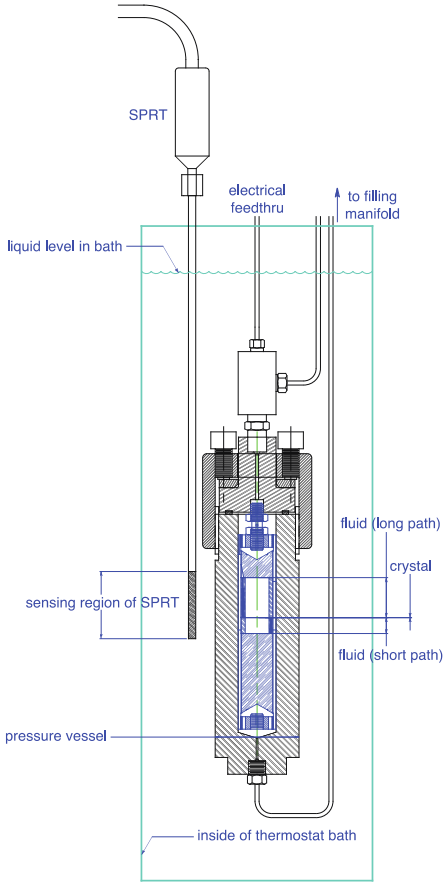

Figure 14: Schematic diagram of the measuring cell inside the pressure vessel.

6.3.2. Measurement Sequence

The fluid sample was loaded into a manual piston-type pump and degassed by pulling a vacuum on the head space of the pump. The sample was then pushed into the measuring cell (which had been evacuated), the pump was valved off, the oil bath was set to the first set-point temperature, and the experimental run was begun.

The entire experiment was controlled by a PC running a custom control program written in Visual Basic 6. At each (T, p) state point multiple echo signals were recorded and analyzed. The pressure of the fluid sample, as well as the temperature of the oil bath, were scanned every 30 s. The approach to equilibrium conditions was determined by monitoring three quantities: (1) the difference of the average temperature computed over the previous eight scans compared to the set-point temperature; (2) the standard deviation of the previous eight temperature scans; (3) the rate of change of pressure with time, computed with a linear fit of the previous eight pressure readings.

When all three of these were within preset tolerances a “converged” flag was set in the control program, and measurements commenced following an additional equilibration time of 20 minutes. A single measurement set comprised recording three echo signals and the four temperature and pressure readings made at the start and end of the set and between the recording of the echoes. Four such sets, spaced 10 minutes apart, were recorded before moving to the next (T, p) state point. These raw data were analyzed with a separate program to generate the (T, p, w) data points.

When measurements at the first temperature were completed, the temperature was increased by an increment of 10 K; since the cell was completely filled with liquid, the increase in temperature also increased the pressure. Measurements continued along this pseudo isochore (line of constant density) until either the desired maximum temperature or maximum pressure was reached. The bath was then cooled to a temperature 20 K above the initial temperature of the isochore, and the total quantity of sample in the measuring cell was reduced by opening the valve to the pump and backing out the pump piston to achieve a starting pressure for the next isochore of less than 1 MPa. The next isochore then commenced. This process was repeated to cover the liquid surface of the POE, within the operating limits of the pulse-echo instrument.

6.4. Calibration of Path-Length Difference and Measurement Uncertainties

The difference of the path lengths in the measuring cell, i.e., ($L_2 - L_1$) in Eq. 7, was calibrated as a function of temperature and pressure with measurements on propane over the temperature range of 260 K to 420 K, with pressures to 56 MPa.

The propane speed of sound, as calculated with the equation of state (EOS) of Lemmon et al.[39], was taken as the known quantity in the calibration. The EOS, in turn, represents the high-accuracy propane measurements of Meier and Kabelac[40] with an average absolute deviation of 0.012 %. The RMS deviation of the calibration equation from the measurements was 0.010 %. Combining, in quadrature, the deviation of the EOS from the data of Meier and Kabelac[40] with the deviation of the path-length calibration equation from the present measurements yields an estimated combined standard uncertainty of 0.016 % in our speed of sound measurements. This represents a conservative estimate of the uncertainty since it is likely that a portion of the difference between the path-length calibration and the present data is due to systematic deviations between the EOS and the data of Meier and Kabelac.[40]

When reporting the uncertainties in experimental data it is customary to combine the effects of the state-point uncertainty (i.e., the effects of the uncertainties in temperature, pressure, and composition) with those in the uncertainty of the primary measurand (i.e., the speed of sound):

$$U_c(w) = 2 \times 100 \times \left\{ u^2(w) + \left[\frac{\partial w}{\partial T}\right]^2 u^2(T) + \left[\frac{\partial w}{\partial p}\right]^2 u^2(p) \right\}^{\frac{1}{2}} / w \ , \qquad (8)$$

where the $u(x)$ are the standard ($k = 1$) uncertainties in the different measurands (temperature, pressure, and speed of sound), the derivatives of the speed of sound with temperature and pressure are computed with an equation of state. The coverage factor of 2 corresponds to a 95 % confidence interval, and the factor of 100 converts the relative deviation to a percentage deviation. The $U_c(w)$ is the relative, combined, expanded ($k = 2$) uncertainty in the speed of sound; it averaged 0.035 % for the present measurements.

As discussed in Section 2, the purity of the POE base-stocks ranged from 93 % to 97 %, and the effect of the impurities on the speed of sound could not be determined. Thus, the present measurements and their uncertainties must be considered as representative of the particular batches of POE base-stocks actually measured, rather than the corresponding pure fluids. Similarly, since the MIL-PRF-23699 lubricant is a complex mixture, those measurements apply only to that particular blend.

6.5. Results

The measurements carried out on the POE base-stocks and the general MIL-PRF-23699 lubricant are depicted in Figure 15. The measured data, as well as the relative, combined, expanded ($k = 2$) uncertainty in the speed of sound for each point, are reported in Table 15 through Table 18. As indicated above, the data in these tables are the averages of four sets of three replicates each.

The minimum temperature for the measurements was dictated by the fluid itself; these fluids are quite viscous at low temperatures, and this resulted in large damping of the ultrasonic signal. Thus, there was a minimum temperature (which varied from 283 K to 298 K for the different fluids) below which measurements were not possible. The maximum temperature was the upper limit of the temperature bath, 423 K.

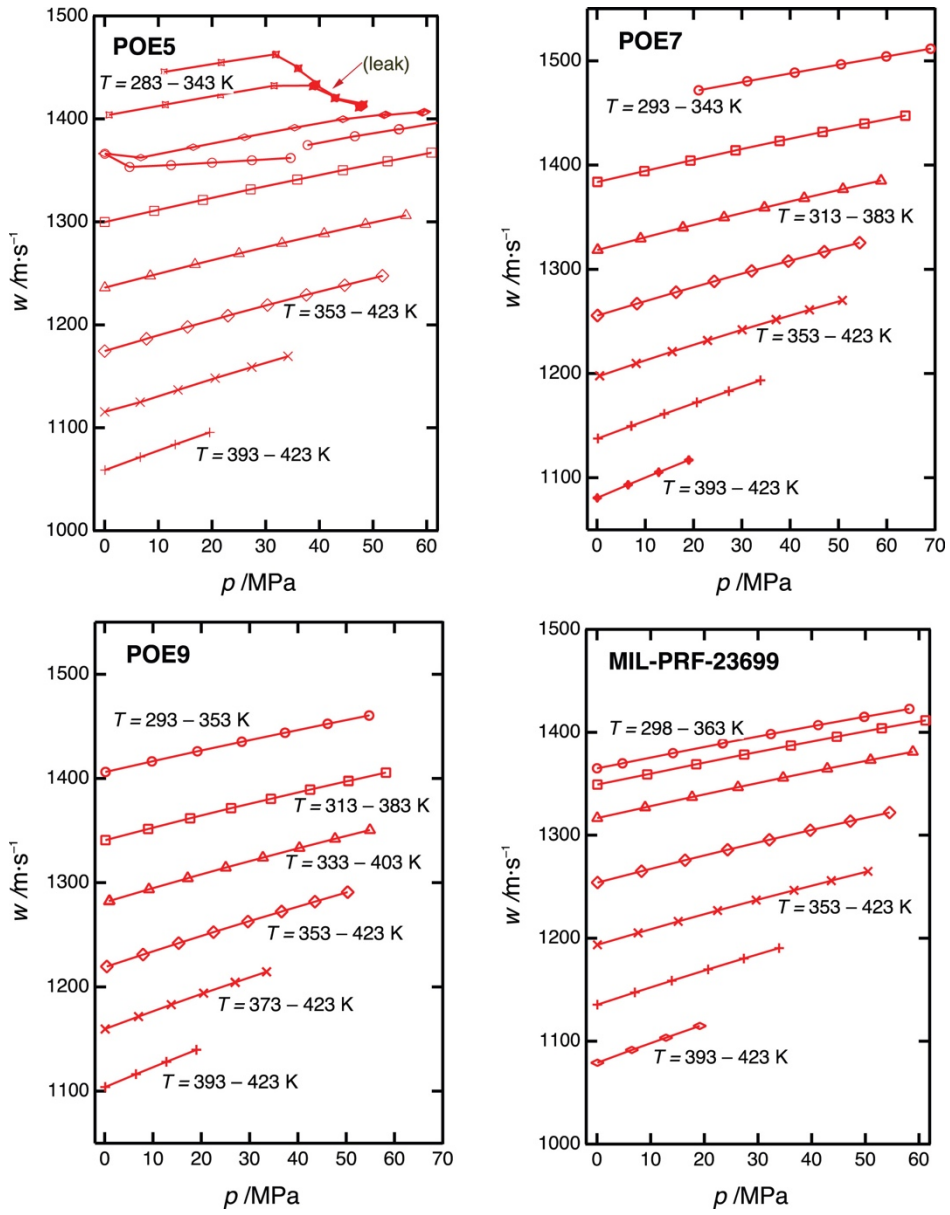

Figure 15: Measurements of the speed of sound for the POE lubricants; the lines connect the points along the various isochores.

6.6. Data Tables

Table 15: Measured Temperature *T*, Pressure *p*, Speed of Sound *w*, and Relative Combined, Expanded (*k* = 2) State Point Uncertainty in the Speed of Sound U_c for POE5; Average Values for the Four Sets of Three Replicate Measurements at Each (*T*, *p*) State Point are Given. The Different Isochores Are Separated by Blank Lines.

T /K	*P* /MPa	*w* /m·s^{-1}	U_c /%	*T* /K	*P* /MPa	*w* /m·s^{-1}	U_c /%
293.132	0.0181	1365.476	0.0336	373.195	-0.0012	1114.547	0.0363
303.139	4.6281	1352.481	0.0336	383.204	6.6170	1123.916	0.0356
313.156	12.3615	1354.345	0.0334	393.214	13.6633	1135.933	0.0350
323.159	19.9948	1356.712	0.0332	403.227	20.5941	1147.366	0.0346
333.162	27.4316	1359.075	0.0331	413.244	27.4179	1158.290	0.0342
343.150	34.6454	1361.348	0.0329	423.268	34.1569	1168.884	0.0339
343.149	37.8186	1373.896	0.0328	393.212	0.0598	1058.043	0.0373
353.181	46.6117	1382.536	0.0327	403.225	6.6308	1070.679	0.0364
363.190	54.8395	1389.436	0.0326	413.243	13.1395	1083.017	0.0357
373.203	62.9956	1396.435	0.0324	423.268	19.5660	1094.871	0.0352
313.151	0.0116	1298.964	0.0341	293.132	0.0220	1365.564	0.0336
323.158	9.2331	1309.912	0.0337	303.139	6.7167	1361.617	0.0335
333.160	18.2892	1320.514	0.0334	313.155	16.5015	1371.845	0.0332
343.150	27.2037	1330.844	0.0331	323.159	26.0576	1381.541	0.0329
353.178	35.8680	1340.310	0.0330				
363.190	44.3935	1349.543	0.0328	333.161	35.3991	1390.771	0.0328
373.203	52.7121	1358.259	0.0327	343.150	44.4116	1399.142	0.0326
383.211	60.8812	1366.682	0.0325	353.179	52.2295	1403.441	0.0329
				363.189	59.3763	1405.913	0.0329
333.161	0.0235	1235.110	0.0347				
343.147	8.4892	1246.653	0.0342	283.156	0.8291	1403.250	0.0334
353.177	16.8423	1257.782	0.0338	293.136	11.3041	1413.168	0.0332
363.189	25.0229	1268.384	0.0335	303.143	21.5828	1422.759	0.0329
373.203	33.0341	1278.414	0.0333	313.159	31.5667	1431.637	0.0327
383.211	40.8868	1287.980	0.0331	323.162	38.8582	1431.089	0.0330
393.219	48.5825	1297.095	0.0329	333.164	42.9600	1419.635	0.0330
403.230	56.1271	1305.814	0.0328	343.151	47.7591	1411.782	0.0329
353.174	-0.0041	1173.564	0.0354	283.156	11.0513	1445.017	0.0330
363.187	7.7667	1185.506	0.0348	293.138	21.7276	1454.206	0.0328
373.200	15.4369	1197.063	0.0344	303.142	31.9038	1462.040	0.0329
383.209	22.9599	1208.040	0.0340	313.160	36.0455	1448.525	0.0329
393.218	30.3350	1218.414	0.0337	323.163	39.3803	1433.108	0.0328
403.230	37.5838	1228.346	0.0335	333.165	43.0477	1419.990	0.0328
413.246	44.7169	1237.920	0.0333	343.152	48.1996	1413.426	0.0329
423.268	51.7545	1247.224	0.0331	343.152	47.7037	1411.590	0.0327
				343.153	47.3341	1410.221	0.0327

Table 16: Measured Temperature *T*, Pressure *p*, Speed of Sound *w*, and Relative Combined, Expanded (*k* = 2) State Point Uncertainty in the Speed of Sound U_c for POE7; Average Values for the Four Sets of Three Replicate Measurements at Each (*T*, *p*) State Point are Given. The Different Isochores Are Separated by Blank Lines.

T /K	*P* /MPa	*w* /m·s^{-1}	U_c /%	*T* /K	*P* /MPa	*w* /m·s^{-1}	U_c /%
283.155	10.7533	1461.887	0.0329	353.171	0.5680	1196.837	0.0352
293.135	21.0581	1471.087	0.0327	363.184	8.1298	1208.707	0.0347
303.142	31.1244	1479.814	0.0326	373.199	15.5794	1220.118	0.0342
313.158	40.9369	1488.077	0.0324	383.207	22.8906	1230.966	0.0339
323.161	50.5395	1496.098	0.0323	393.217	30.0552	1241.250	0.0336
333.163	59.9084	1503.747	0.0322	403.229	37.0907	1251.098	0.0334
343.151	69.0824	1511.182	0.0322	413.244	43.9979	1260.560	0.0332
				423.267	50.8041	1269.768	0.0330
293.133	0.1014	1383.068	0.0336				
303.139	9.8016	1393.456	0.0332	373.193	0.2097	1136.740	0.0361
313.158	19.3432	1403.608	0.0330	383.203	7.1101	1148.769	0.0354
323.161	28.7051	1413.383	0.0328	393.212	13.9457	1160.488	0.0349
333.163	37.8083	1422.467	0.0327	403.226	20.6757	1171.670	0.0344
343.150	46.6989	1431.130	0.0325	413.243	27.3110	1182.451	0.0341
353.180	55.3789	1439.184	0.0324	423.267	33.8513	1192.864	0.0338
363.190	63.8466	1446.854	0.0323				
				393.212	0.0595	1079.740	0.0371
313.152	0.1386	1317.694	0.0340	403.225	6.4499	1092.408	0.0363
323.158	9.0420	1328.609	0.0336	413.242	12.7709	1104.602	0.0356
333.160	17.7932	1339.162	0.0334	423.265	19.0114	1116.304	0.0351
343.149	26.3088	1349.000	0.0331				
353.179	34.6727	1358.365	0.0329				
363.190	42.9057	1367.550	0.0328				
373.203	50.9466	1376.285	0.0326				
383.211	58.8016	1384.559	0.0325				
333.158	0.1071	1254.690	0.0346				
343.145	8.2742	1266.043	0.0341				
353.176	16.3619	1277.106	0.0338				
363.188	24.2793	1287.619	0.0335				
373.202	32.0324	1297.604	0.0332				
383.210	39.6262	1307.147	0.0331				
393.218	47.0703	1316.239	0.0329				
403.228	54.3619	1324.926	0.0328				

Table 17: Measured Temperature *T*, Pressure *p*, Speed of Sound *w*, and Relative Combined, Expanded (*k* = 2) State Point Uncertainty in the Speed of Sound U_c for POE9; Average Values for the Four Sets of Three Replicate Measurements at Each (*T*, *p*) State Point are Given. The Different Isochores Are Separated by Blank Lines.

T /K	*P* /MPa	*w* /m·s^{-1}	U_c /%	*T* /K	*P* /MPa	*w* /m·s^{-1}	U_c /%
293.133	0.1710	1405.453	0.0335	353.170	0.4437	1218.551	0.0351
303.138	9.7687	1415.509	0.0332	363.183	7.9422	1230.084	0.0346
313.155	19.1881	1425.255	0.0330	373.197	15.3050	1241.121	0.0343
323.159	28.3704	1434.416	0.0328	383.206	22.5374	1251.709	0.0338
333.161	37.3299	1443.121	0.0326	393.213	29.6497	1261.885	0.0336
343.149	46.1568	1451.746	0.0325	403.227	36.6317	1271.643	0.0333
353.178	54.7552	1459.767	0.0324	413.243	43.5317	1281.214	0.0331
				423.267	50.3031	1290.412	0.0330
313.151	0.1498	1339.892	0.0340				
323.156	9.0089	1350.639	0.0337	373.193	0.0919	1158.622	0.0359
333.160	17.6835	1360.935	0.0333	383.204	6.9885	1170.615	0.0353
343.149	26.1628	1370.704	0.0331	393.213	13.7831	1182.159	0.0348
353.178	34.4059	1379.683	0.0329	403.225	20.4689	1193.196	0.0343
363.189	42.5199	1388.502	0.0327	413.241	27.0109	1203.621	0.0340
373.202	50.4624	1396.960	0.0326	423.266	33.5078	1213.914	0.0337
383.209	58.2317	1405.082	0.0325				
				393.209	0.1092	1103.001	0.0368
333.158	1.0101	1281.574	0.0344	403.223	6.4763	1115.404	0.0361
343.144	9.1619	1292.665	0.0340	413.240	12.7660	1127.381	0.0354
353.175	17.1956	1303.384	0.0336	423.265	18.9870	1138.977	0.0349
363.188	25.0554	1313.568	0.0334				
373.201	32.7592	1323.282	0.0332				
383.209	40.2988	1332.563	0.0330				
393.217	47.6836	1341.455	0.0328				
403.228	54.9122	1349.960	0.0327				

Table 18: Measured Temperature *T*, Pressure *p*, Speed of Sound *w*, and Relative Combined, Expanded (*k* = 2) State Point Uncertainty in the Speed of Sound U_c for MIL-PRF-23699; Average Values for the Four Sets of Three Replicate Measurements at Each (*T*, *p*) State Point are Given. The Different Isochores Are Separated by Blank Lines.

T /K	*P* /MPa	*w* /m·s^{-1}	U_c /%	*T* /K	*P* /MPa	*w* /m·s^{-1}	U_c /%
298.164	0.0204	1364.191	0.0337	353.172	0.0875	1192.607	0.0353
303.141	4.7472	1369.078	0.0336	363.185	7.6660	1204.184	0.0347
313.157	14.1680	1378.989	0.0333	373.199	15.1458	1215.418	0.0343
323.162	23.4335	1388.665	0.0331	383.208	22.4756	1226.067	0.0339
333.164	32.3985	1397.558	0.0329	393.217	29.6654	1236.215	0.0336
343.152	41.2161	1406.251	0.0327	403.229	36.7231	1245.936	0.0334
353.181	49.8133	1414.365	0.0325	413.245	43.6624	1255.313	0.0332
363.190	58.2269	1422.186	0.0324	423.267	50.5006	1264.450	0.0330
303.137	0.0914	1348.400	0.0338	373.193	0.0908	1134.449	0.0361
313.155	9.3595	1358.215	0.0335	383.202	7.0672	1146.398	0.0355
323.159	18.4941	1368.108	0.0332	393.214	13.9420	1157.927	0.0349
333.162	27.4283	1377.554	0.0330	403.226	20.7130	1168.982	0.0345
343.150	36.1299	1386.451	0.0328	413.243	27.3789	1179.592	0.0341
353.179	44.6903	1395.024	0.0327	423.268	33.9478	1189.828	0.0338
363.191	53.0624	1403.284	0.0325				
373.203	61.2328	1411.107	0.0324	393.213	0.0816	1078.164	0.0371
				403.226	6.5066	1090.583	0.0362
313.151	0.0590	1315.825	0.0341	413.243	12.8606	1102.565	0.0356
323.158	8.9728	1326.154	0.0337	423.267	19.1386	1114.092	0.0351
333.161	17.7144	1336.232	0.0334				
343.149	26.2779	1345.893	0.0331				
353.179	34.6986	1355.166	0.0329				
363.190	42.9250	1363.991	0.0328				
373.204	50.9851	1372.464	0.0326				
383.211	58.8677	1380.595	0.0325				
333.158	0.4482	1254.829	0.0346				
333.158	0.1071	1253.110	0.0346				
343.148	8.3103	1264.178	0.0341				
353.177	16.4139	1274.888	0.0338				
363.189	24.3485	1285.088	0.0335				
373.203	32.1269	1294.812	0.0333				
383.210	39.7524	1304.125	0.0331				
393.219	47.2227	1313.050	0.0329				
403.229	54.5226	1321.542	0.0328				

7. Compressed-Liquid Density

7.1. Summary

The compressed-liquid densities of the fluids pentaerythritol tetrapentanoate (POE5), pentaerythritol tetraheptanoate (POE7), pentaerythritol tetranonanoate (POE9), and a fully qualified lubricant (MIL-PRF-23699) have been measured within a temperature range of 270 K to 470 K at pressures from 0.5 MPa to 50 MPa with a vibrating-tube densimeter. The high freezing points of all but the POE5 sample resulted in the pressure range of the measurements at lower isotherms (270 K and 290 K) being reduced to avoid solidifying the sample. The compressed-liquid densities of the lubricants studied ranged from 829 $kg \cdot m^{-3}$ to 1063 $kg \cdot m^{-3}$. The densities of the four fluids had a fair amount of overlap (~ 100 $kg \cdot m^{-3}$) with the densities of POE5 > MIL-PRF-23699 > POE7 > POE9 for similar state points. These results are also presented in Outcalt.[41]

7.2. Experimental Methods

The apparatus used to measure compressed-liquid densities over the temperature range of 270 K to 470 K and to pressures of 50 MPa is described in Outcalt and McLinden.[42] A schematic of the apparatus is illustrated in Figure 16. The heart of the apparatus is a commercial vibrating-tube densimeter; however, several physical and procedural improvements have been implemented beyond that of the commercial instrument operated in a stand-alone mode. The densimeter is housed in a specially designed two-stage thermostat for improved temperature control. The uncertainty in the temperature is 0.03 K with stability of 5 mK during an isothermal measurement. Pressures are measured with an oscillating quartz crystal pressure transducer with an uncertainty of 5 kPa.

The densimeter apparatus has been designed, and software has been written so that the operation and data acquisition are fully automated. Electronically actuated pneumatic valves and a programmable syringe pump are used to move from one pressure to the next and/or flush fresh sample through the system. Operation of the densimeter in this manner allows for measurements to be made 24 hours a day.

Upon receipt, samples were transferred to 300 mL stainless steel cylinders. Closed cylinders were connected to a vacuum system and then submerged in liquid nitrogen to freeze the contained sample. Once the sample was frozen, the vapor space was evacuated. Once evacuated, the container was sealed, and the sample was heated to facilitate driving air that may have been

entrained in the liquid, into the vapor space. This procedure was repeated three times for each sample.

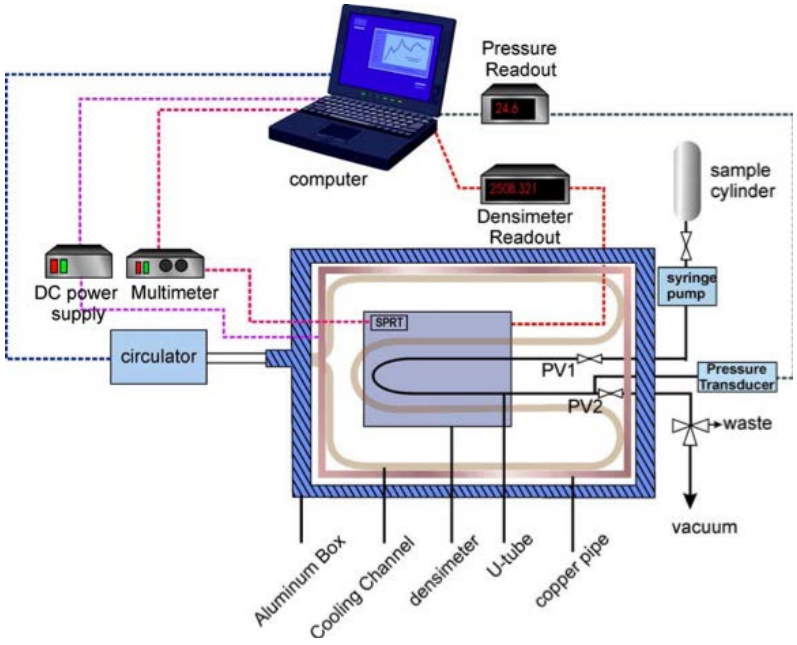

Figure 16: Schematic of the compressed-liquid density apparatus.

7.3. Determination of Uncertainty

In previous work, toluene (SRM 211d) and 99.999 % propane had been used as calibration fluids. Due to the higher density ranges of the fluids studied in this work, toluene (SRM 211d) and HPLC-grade water were used as calibration fluids. The toluene and water samples underwent the same degassing procedure described above. Toluene was measured at 142 state points from 270 K to 470 K at pressures from 0.5 MPa to 50 MPa, and water was measured at 104 points from 290 K to 470 K at pressures from 2 MPa to 45 MPa. Additionally, the period of oscillation of the U-tube was measured under vacuum from 270 K to 470 K in 20 K increments. The NIST database REFPROP[21, 43, 44] was used to predict the densities of the water and toluene. The calibration data were combined and correlated with the equation of May et al.[45] The correlation represents the toluene and water data to average absolute deviations (AADs) of 0.13 $kg \cdot m^{-3}$ and 0.18 $kg \cdot m^{-3}$, respectively.

The uncertainty in densities predicted by the equation of state for water increases from less than 0.003 % at temperatures below 423 K to 0.05 % at temperatures above that in the temperature and pressure range of this work. The overall combined expanded uncertainty (k = 2, 95 % confidence level) in densities presented here was calculated with the root sum of squares method (as described

in the Guide to the Expression of Uncertainty in Measurement[38]) to be 0.71 kg·m^{-3} to 1.24 kg·m^{-3}. The range of the uncertainty is a result of the range of uncertainty in the equation of state of water. The uncertainty encompasses the uncertainties in the temperature measurement, pressure measurement, equations of state for water and toluene, and the repeatability of the measurements of the lubricant samples.

7.4. Results

The compressed-liquid densities of the fluids POE5, POE7, POE9, and MIL-PRF-23699 were measured over the temperature range of 270 K to 470 K at pressures from 0.5 MPa to 50 MPa. The high freezing points of all but the POE5 sample resulted in the pressure range of the measurements at lower isotherms (270 K and 290 K) being reduced to avoid solidifying the samples. Additionally, there were no measurements of the POE9 sample at 270 K for the same reason. Measurement results are depicted in Figure 17 and reported in Table 19 to Table 22. The compressed-liquid densities of the lubricants studied range from 829 kg·m^{-3} to 1063 kg·m^{-3}, with a relative order between the four fluids of POE9 < POE7 < MIL-PRF-23699 < POE5.

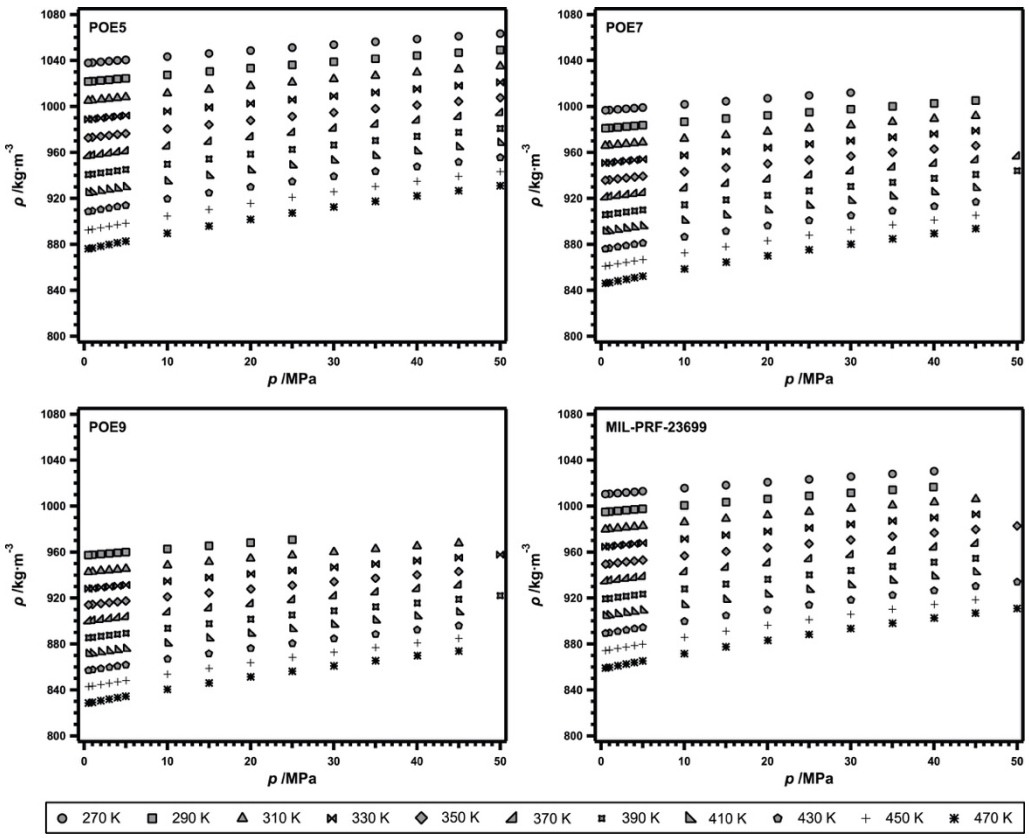

Figure 17: Compressed-liquid density data as a function of pressure measured along isotherms at temperatures from 270 K to 470 K.

7.5. Data Tables

Table 19: Compressed-Liquid Densities of POE5.

270 K		290 K		310 K		330 K		350 K		370 K	
p /MPa	ρ /kg·m^{-3}	p /MPa	ρ /kg·m^{-3}	p /MPa	ρ /kg·m^{-3}	p /MPa	ρ /kg·m^{-3}	p /MPa	ρ /kg·m^{-3}	p /MPa	ρ /kg·m^{-3}
50.01	1063.3	49.99	1049.2	50.02	1035.0	50.02	1020.9	50.01	1007.5	50.0	994.0
45.02	1061.0	45.04	1046.7	45.04	1032.3	45.03	1018.0	45.03	1004.3	45.0	990.7
40.01	1058.6	40.04	1044.2	40.01	1029.6	40.02	1015.1	40.00	1001.1	40.0	987.4
35.00	1056.2	35.02	1041.5	35.01	1026.7	35.01	1012.1	35.03	998.0	35.0	984.0
30.01	1053.7	30.01	1038.8	30.01	1023.8	30.01	1009.0	30.02	994.6	30.0	980.5
25.02	1051.2	25.02	1036.1	25.01	1020.9	25.01	1005.8	25.02	991.2	25.0	976.8
20.02	1048.6	20.03	1033.3	20.01	1017.8	20.01	1002.5	20.04	987.7	19.9	973.0
15.02	1046.0	15.05	1030.4	15.02	1014.7	15.02	999.2	15.02	984.1	15.0	969.0
10.05	1043.3	10.04	1027.4	10.00	1011.4	10.03	995.7	10.04	980.3	10.0	965.0
5.01	1040.4	5.03	1024.4	5.05	1008.1	5.04	992.1	5.04	976.4	5.02	960.7
4.04	1039.9	4.00	1023.8	4.01	1007.4	4.02	991.3	4.01	975.6	4.01	959.8
3.01	1039.3	3.04	1023.1	3.02	1006.7	3.03	990.6	3.02	974.7	3.05	958.9
2.01	1038.7	2.03	1022.5	2.05	1006.0	2.01	989.8	2.00	973.9	2.02	958.0
1.01	1038.1	1.02	1021.9	1.02	1005.3	1.01	989.1	1.02	973.1	1.01	957.0
0.53	1037.8	0.51	1021.6	0.53	1005.0	0.50	988.7	0.52	972.6	0.51	956.6
390 K		**410 K**		**430 K**		**450 K**		**470 K**			
p /MPa	ρ /kg·m^{-3}	p /MPa	ρ /kg·m^{-3}	p /MPa	ρ /kg·m^{-3}	p /MPa	ρ /kg·m^{-3}	p /MPa	ρ /kg·m^{-3}		
49.99	980.8	50.01	968.1	50.00	955.5	50.05	943.2	50.03	931.0		
45.02	977.4	45.02	964.4	45.01	951.6	45.01	939.1	45.01	926.6		
40.03	973.9	40.04	960.7	40.04	947.6	40.01	934.8	40.04	922.1		
35.02	970.2	35.01	956.7	35.03	943.5	35.01	930.3	35.02	917.4		
30.04	966.4	30.03	952.7	30.01	939.1	30.03	925.7	30.01	912.4		
25.01	962.5	25.05	948.5	25.02	934.6	25.02	920.8	25.01	907.2		
20.01	958.4	20.01	944.1	20.03	929.8	20.00	915.6	20.01	901.6		
15.03	954.2	15.01	939.4	15.03	924.8	15.01	910.2	15.02	895.8		
10.05	949.7	10.01	934.6	10.01	919.5	10.02	904.5	10.01	889.5		
5.02	945.0	5.03	929.5	5.04	913.9	5.04	898.3	5.02	882.7		
4.02	944.0	4.01	928.3	4.03	912.8	4.01	897.0	4.01	881.3		
3.02	943.0	3.01	927.3	3.01	911.5	3.01	895.7	3.01	879.8		
2.03	942.1	2.03	926.2	2.01	910.3	2.01	894.4	2.02	878.3		
1.03	941.1	1.04	925.1	1.03	909.1	1.03	893.0	1.03	876.8		
0.54	940.6	0.51	924.5	0.52	908.5	0.53	892.4	0.54	876.1		

Table 20: Compressed-Liquid Densities of POE7.

270 K		290 K		310 K		330 K		350 K		370 K	
p /MPa	ρ /kg·m^{-3}	p /MPa	ρ /kg·m^{-3}	p /MPa	ρ /kg·m^{-3}	p /MPa	ρ /kg·m^{-3}	p /MPa	ρ /kg·m^{-3}	p /MPa	ρ /kg·m^{-3}
		50.01	1007.5	50.03	994.4	50.03	981.5	50.02	968.8	50.0	956.2
		45.01	1005.1	45.02	991.8	45.01	978.8	45.02	965.9	45.0	953.1
		40.01	1002.6	40.03	989.2	39.99	976.0	40.02	962.9	40.0	949.9
		35.03	1000.1	35.02	986.5	35.01	973.1	35.02	959.9	35.0	946.7
29.99	1011.9	30.02	997.5	30.02	983.7	29.99	970.1	30.03	956.7	30.0	943.3
25.01	1009.5	25.03	994.9	25.01	980.9	25.06	967.2	25.01	953.4	25.0	939.8
20.01	1007.0	20.01	992.2	20.01	978.0	20.04	964.0	20.03	950.1	20.0	936.2
15.01	1004.4	15.01	989.4	15.01	975.0	15.02	960.8	15.02	946.6	15.0	932.5
10.04	1001.8	10.01	986.6	10.01	971.9	9.99	957.4	10.02	943.0	10.0	928.5
5.01	999.0	5.02	983.7	5.01	968.7	5.02	954.0	5.03	939.2	5.03	924.4
4.00	998.5	4.01	983.1	4.02	968.1	4.00	953.3	4.06	938.5	4.02	923.6
3.01	997.9	3.06	982.5	3.01	967.4	3.02	952.6	3.03	937.7	3.04	922.7
2.02	997.4	2.02	981.9	2.03	966.8	2.03	951.9	2.01	936.9	2.03	921.9
1.02	996.8	1.02	981.2	1.01	966.1	1.04	951.1	1.02	936.1	1.03	921.0
0.54	996.6	0.55	980.9	0.51	965.8	0.53	950.8	0.52	935.7	0.53	920.6
390 K		**410 K**		**430 K**		**450 K**		**470 K**			
p /MPa	ρ /kg·m^{-3}	p /MPa	ρ /kg·m^{-3}	p /MPa	ρ /kg·m^{-3}	p /MPa	ρ /kg·m^{-3}	p /MPa	ρ /kg·m^{-3}		
50.00	944.0	50.03	932.2	50.00	920.5	50.04	909.1	50.02	897.7		
45.03	940.7	45.02	928.7	45.03	916.8	45.03	905.2	45.02	893.6		
40.03	937.4	40.01	925.1	40.03	913.0	40.03	901.1	40.02	889.3		
35.03	933.9	35.02	921.4	35.01	909.1	35.03	896.9	35.04	884.8		
30.02	930.3	30.03	917.6	30.03	905.0	30.04	892.5	30.04	880.1		
25.01	926.5	25.01	913.5	25.01	900.7	25.02	887.9	25.01	875.2		
20.01	922.6	20.03	909.4	20.01	896.2	20.01	883.1	20.03	870.0		
15.03	918.6	15.02	905.0	15.02	891.4	14.99	877.9	15.05	864.5		
10.03	914.4	10.02	900.4	10.02	886.4	10.04	872.5	10.03	858.6		
5.02	909.9	5.04	895.5	5.03	881.1	5.05	866.7	5.02	852.2		
4.04	909.0	4.01	894.5	4.02	880.0	4.01	865.5	4.02	850.9		
3.03	908.1	3.03	893.5	3.01	878.9	3.02	864.3	3.05	849.5		
2.03	907.1	2.02	892.4	2.02	877.8	2.01	863.0	2.04	848.1		
1.01	906.1	1.01	891.4	1.01	876.6	1.03	861.7	1.05	846.7		
0.52	905.7	0.53	890.9	0.52	876.0	0.53	861.1	0.52	846.0		

Table 21: Compressed-Liquid Densities of POE9.

290 K		310 K		330 K		350 K		370 K		390 K	
p /MPa	ρ /kg·m^{-3}	p /MPa	ρ /kg·m^{-3}	p /MPa	ρ /kg·m^{-3}	p /MPa	ρ /kg·m^{-3}	p /MPa	ρ /kg·m^{-3}	p /MPa	ρ /kg·m^{-3}
		50.02	970.2	49.99	957.7	50.08	945.8	50.01	933.7	49.99	922.0
		45.01	967.7	45.01	955.1	45.00	943.0	45.02	930.8	45.01	918.8
		40.01	965.1	40.00	952.4	40.00	940.1	40.01	927.7	40.02	915.6
		35.01	962.6	35.02	949.6	35.01	937.2	35.03	924.6	35.03	912.3
		30.02	959.9	30.04	946.8	30.03	934.1	30.02	921.3	30.03	908.8
25.01	970.7	25.00	957.2	25.02	943.9	25.01	931.0	25.01	918.0	24.99	905.2
20.00	968.1	20.00	954.4	20.05	940.9	20.04	927.8	20.02	914.5	20.03	901.5
15.00	965.4	15.02	951.5	15.02	937.8	15.01	924.4	15.03	910.9	15.02	897.6
10.01	962.7	10.02	948.5	10.01	934.6	10.01	921.0	10.03	907.2	10.05	893.6
5.01	959.9	5.03	945.5	5.03	931.3	5.01	917.4	5.03	903.2	5.03	889.3
4.04	959.3	4.01	944.8	4.03	930.6	4.02	916.6	4.00	902.4	4.01	888.4
3.05	958.7	3.01	944.2	3.04	929.9	3.02	915.9	3.03	901.6	3.03	887.5
2.04	958.2	2.02	943.6	2.04	929.2	2.02	915.1	2.02	900.8	2.04	886.6
1.02	957.6	1.03	942.9	1.02	928.5	1.02	914.4	1.04	899.9	1.03	885.7
0.51	957.3	0.51	942.6	0.52	928.1	0.53	914.0	0.53	899.5	0.53	885.3

410 K		430 K		450 K		470 K	
p /MPa	ρ /kg·m^{-3}	p /MPa	ρ /kg·m^{-3}	p /MPa	ρ /kg·m^{-3}	p /MPa	ρ /kg·m^{-3}
50.03	910.6	50.02	899.4	50.02	888.5	50.01	877.7
45.02	907.3	45.02	895.9	45.02	884.8	45.02	873.8
40.01	903.8	40.02	892.3	40.04	880.9	40.04	869.7
35.02	900.3	35.02	888.5	35.01	876.9	35.02	865.4
30.00	896.6	30.01	884.6	30.02	872.7	30.01	860.9
25.01	892.8	25.02	880.5	25.04	868.3	25.02	856.2
20.02	888.8	20.02	876.2	20.00	863.7	20.03	851.3
15.01	884.6	15.00	871.6	15.02	858.8	15.02	846.0
10.00	880.2	10.03	866.9	10.02	853.6	10.01	840.4
5.02	875.5	5.01	861.8	5.04	848.2	5.00	834.4
4.02	874.5	4.01	860.8	4.04	847.0	4.03	833.2
3.03	873.6	3.04	859.7	3.01	845.8	3.01	831.9
2.01	872.6	2.02	858.6	2.02	844.6	2.01	830.6
1.02	871.6	1.04	857.6	1.02	843.4	1.01	829.2
0.52	871.1	0.51	857.0	0.54	842.9	0.53	828.6

Table 22: Compressed-Liquid Densities of MIL-PRF-23699.

270 K		290 K		310 K		330 K		350 K		370 K	
p /MPa	ρ /kg·m^{-3}	p /MPa	ρ /kg·m^{-3}	p /MPa	ρ /kg·m^{-3}	p /MPa	ρ /kg·m^{-3}	p /MPa	ρ /kg·m^{-3}	p /MPa	ρ /kg·m^{-3}
				50.01	1008.6	50.00	995.5	49.99	982.7	50.04	970.1
				45.03	1006.0	45.04	992.8	45.01	979.7	45.01	967.0
40.02	1030.3	39.94	1016.6	40.04	1003.3	40.01	989.9	40.04	976.7	40.03	963.8
35.01	1028.0	35.02	1014.1	35.02	1000.6	35.02	987.0	35.02	973.6	35.03	960.5
30.03	1025.6	30.04	1011.5	30.04	997.8	30.01	984.1	30.00	970.5	30.01	957.1
25.01	1023.2	25.01	1008.9	25.01	995.0	25.01	981.0	25.01	967.2	25.01	953.6
20.01	1020.7	20.01	1006.2	20.01	992.0	20.02	977.9	20.01	963.8	20.02	950.0
15.01	1018.2	15.03	1003.4	15.02	989.0	15.01	974.7	15.03	960.4	15.01	946.2
10.03	1015.6	10.01	1000.6	10.02	985.9	10.04	971.4	10.03	956.7	10.02	942.3
5.01	1012.9	5.00	997.6	5.03	982.7	5.01	967.9	5.03	952.9	5.02	938.2
4.04	1012.3	4.01	997.0	4.02	982.0	4.02	967.2	4.01	952.1	4.00	937.3
3.01	1011.8	3.02	996.4	3.01	981.4	3.01	966.4	3.03	951.4	3.02	936.5
2.01	1011.2	2.03	995.8	2.01	980.7	2.02	965.7	2.02	950.6	2.01	935.6
1.03	1010.7	1.03	995.2	1.04	980.1	1.03	965.0	1.03	949.8	1.02	934.7
0.52	1010.4	0.52	994.9	0.53	979.7	0.53	964.6	0.55	949.4	0.52	934.3
390 K		**410 K**		**430 K**		**450 K**		**470 K**			
p /MPa	ρ /kg·m^{-3}	p /MPa	ρ /kg·m^{-3}	p /MPa	ρ /kg·m^{-3}	p /MPa	ρ /kg·m^{-3}	p /MPa	ρ /kg·m^{-3}		
50.02	957.7	50.01	945.7	50.00	933.9	50.02	922.4	49.99	910.9		
45.01	954.5	45.02	942.2	45.01	930.3	44.99	918.4	44.99	906.8		
40.01	951.1	40.03	938.6	40.02	926.4	40.06	914.4	40.03	902.5		
35.03	947.5	35.02	934.9	35.03	922.5	35.01	910.2	35.02	898.0		
30.03	943.9	30.01	931.0	30.03	918.3	30.01	905.7	30.01	893.3		
25.03	940.1	25.02	927.0	25.00	914.0	25.00	901.1	25.00	888.3		
20.03	936.2	20.02	922.8	20.00	909.5	20.03	896.3	20.04	883.1		
15.01	932.1	15.01	918.3	15.02	904.7	15.02	891.1	15.01	877.5		
10.03	927.9	10.01	913.7	10.02	899.7	10.03	885.7	10.01	871.6		
5.02	923.4	5.03	908.9	5.02	894.4	5.00	879.8	5.01	865.2		
4.01	922.5	4.00	907.8	4.04	893.3	4.03	878.6	4.01	863.8		
3.01	921.5	3.04	906.8	3.03	892.1	3.01	877.3	3.03	862.5		
2.04	920.6	2.01	905.8	2.02	891.0	2.01	876.1	2.04	861.1		
1.03	919.6	1.01	904.7	1.02	889.8	1.02	874.8	1.03	859.7		
0.53	919.2	0.53	904.2	0.53	889.3	0.53	874.2	0.54	859.0		

8. Ambient-Pressure Density and Speed of Sound

8.1. Summary

Measured densities and speeds of sound, calculated adiabatic compressibilities, and all associated expanded uncertainties are reported over the combined temperature range 278 K to 343 K and at ambient pressure (~ 83 kPa). Densities range from an overall low of 918.32 $kg \cdot m^{-3}$ to an overall high of 1030.29 $kg \cdot m^{-3}$, with a relative order between the four fluids of POE9 < POE7 < MIL-PRF-23699 < POE5 and differences that range from 6.5 % (at 343.15 K) to 6.7 % (at 283.15 K). Sound speeds range from an overall low of 1205.2 $m \cdot s^{-1}$ to an overall high of 1438.9 $m \cdot s^{-1}$, with a relative order of POE5 < MIL-PRF-23699 < POE7 < POE9 and differences that range from 3.4 % (at 343.15 K) to 2.8 % (at 283.15 K). Adiabatic compressibilities range from an overall low of 482.9 TPa^{-1} to an overall high of 709.4 TPa^{-1}, with POE7 exhibiting the highest overall values and POE5 and MIL-PRF-23699 exhibiting the lowest values, depending on temperature. Overall differences in adiabatic compressibilities range from 1.2 % at 343.15 K to 1.6 % at 283.15 K. These results are also presented in Fortin.[25]

8.2. Experimental Methods

A commercial density (ρ) and sound speed (w) analyzer (see Figure 18) was used to simultaneously measure these two properties over the combined temperature range 278 K to 343 K and at ambient pressure (~ 83 kPa in Boulder, CO). The instrument contains two measurement cells in series: a sound speed cell that measures the propagation time of ~ 3 MHz sound waves through a liquid-filled cavity and a density cell that utilizes a vibrating-tube densimeter constructed of borosilicate glass. Both cells are housed in a thermostated copper block whose temperature is controlled between 278 K and 343 K with a combination of thermoelectric Peltier elements and an integrated Pt-100 resistance thermometer. Measurements of air and water performed at 293 K, 313 K, and 333 K are required to adjust the apparatus constants in the instrument's working equations for both sound speed and density; this is referred to as an adjustment procedure. Additionally, calibration measurements are performed to verify the instrument's performance before and after sample measurements. These involve measuring water and toluene standard reference material (SRM) 211d every 5 K from 343 K to 278 K. Additional details about the density and sound speed analyzer can be found in Laesecke et al.,[46] Fortin,[47] and Fortin et al.[48]

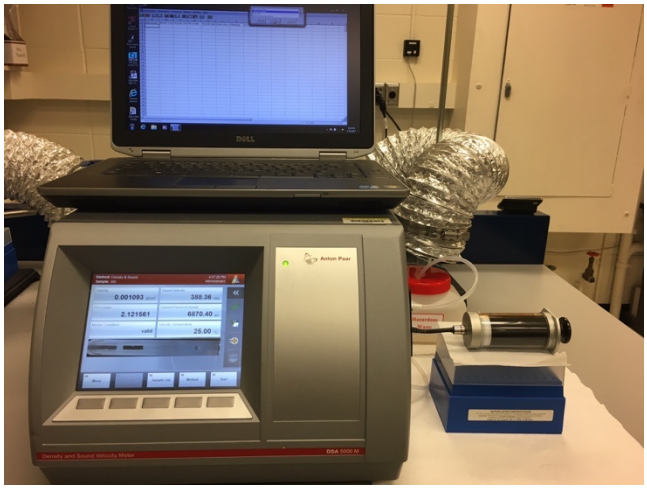

Figure 18: Density and sound speed analyzer.

Prior to measurements, each sample was degassed via repeat “freeze-pump-thaw” cycles. The sample was transferred to a glass bulb and the bulb was then attached to a vacuum system (see Figure 19). The first part of the cycle (the “freeze”) is achieved by submerging the bulb in a Dewar of liquid nitrogen for several minutes. The vapor space over the still frozen sample is then evacuated by opening the bulb to the vacuum line (the “pump”). Once evacuated, the bulb is heated to facilitate driving any remaining dissolved impurities into the vapor space (the “thaw”). This cycle was repeated a minimum of five times to ensure complete removal of dissolved gases.

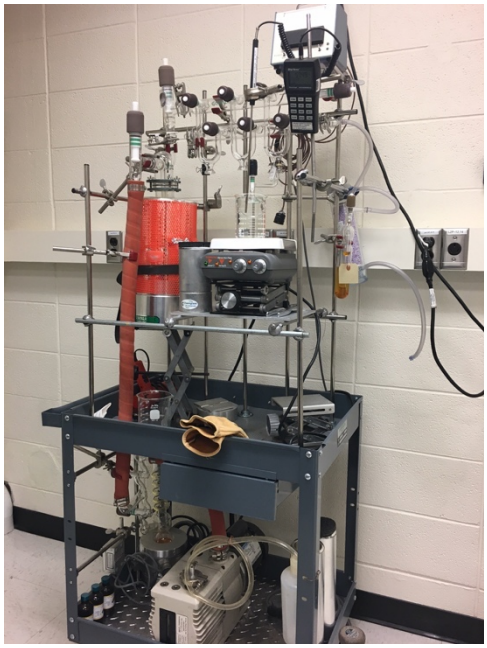

Figure 19: Vacuum system for degassing samples.

Freshly degassed sample was then drawn up into a gas-tight 50 mL glass syringe, which remained attached to the instrument inlet for the duration of the measurements of a given sample (see Figure 18). Approximately 3 mL of sample was injected into the instrument (enough to fill both cells) and measurements were made via programmed scans between the maximum and minimum temperature in 5 K decrements. For all samples, the maximum temperature was 343 K, and for all but POE9, the minimum temperature was 278 K. POE9 could only be measured to 283 K; below that, the sample solidified. Five to seven measurement scans were performed for each of the four samples with a fresh aliquot of sample fluid injected into the instrument prior to the start of each scan. In between samples, the measurement cells were thoroughly cleaned and dried. Additionally, since these samples proved difficult to clean out of the instrument, the first run of each new sample was discarded during analysis to minimize any chances of cross-contamination between samples.

8.3. Results and Uncertainty Analysis

Measurement results are presented in Table 23 and Table 24 for density ($\bar{\rho}$) and speed of sound ($\bar{w}$), respectively. The tabulated values represent the average of three to six replicate measurement scans, depending on the sample. Also included in the tables are the associated absolute and relative expanded uncertainty estimates ($U(\bar{\rho})$ and $U(\bar{w})$). Using density as an example, the expanded uncertainty is calculated using the expression

$$U(\bar{\rho}) = t_{95}\left(df_{\rho}\right) \cdot u(\bar{\rho}) \ , \tag{9}$$

where the coverage factor, $t_{95}\left(df_{\rho}\right)$, is taken from the *t*-distribution for df_{ρ} degrees of freedom and a 95 % level of confidence, and $u(\bar{\rho})$ is the combined standard uncertainty for the averaged density measurements.[38] The combined standard uncertainty for density and speed of sound include contributions for the standard deviation of replicate temperature scans, instrument resolution, instrument calibration, as well as the uncertainty in measured temperature and pressure. Additional details concerning the uncertainty analysis calculations can be found in Fortin et al.[48] For the density data (Table 23), reported absolute expanded uncertainties (1.65 to 1.66 kg·m^{-3}) correspond to relative expanded uncertainties of 0.12 % to 0.18 %. For the sound speed data (Table 24), reported absolute expanded uncertainties (1.7 m·s^{-1}) correspond to relative expanded uncertainties of 0.1 % to 0.2 %.

To facilitate comparisons among the four samples, the averaged densities shown in Table 23 are plotted as a function of temperature in Figure 20. POE5 exhibits the highest densities, ranging from 977.88 kg·m^{-3} at 343.15 K to 1030.29 kg·m^{-3} at 278.15 K. POE9 exhibits the lowest densities,

ranging from 918.32 kg·m^{-3} at 343.15 K to 961.49 kg·m^{-3} at 283.15 K. The difference in density between these two fluids is 6.5 % at 343.15 K and 6.7 % at 283 K. MIL-PRF-23699, the fully qualified lubricant, exhibits densities most similar to POE7. MIL-PRF-23699 has densities ranging from 954.42 to 1003.53 kg·m^{-3}, while POE7 has densities ranging from 940.20 to 989.09 kg·m^{-3}, a difference of approximately 1.5 %.

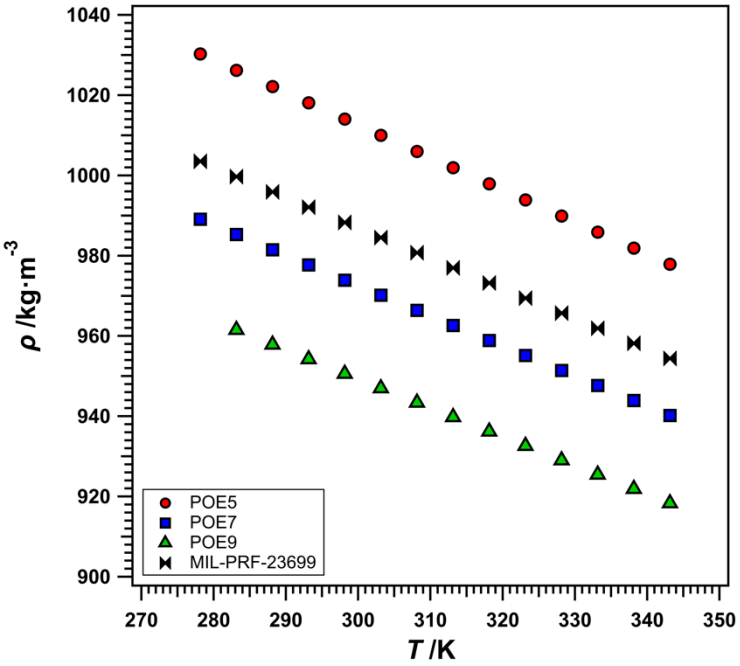

Figure 20: Ambient-pressure density measurements plotted as a function of temperature.

The averaged speeds of sound shown in Table 24 are plotted as a function of temperature in Figure 21. The trend in sound speeds is the opposite of that observed for density. POE9 exhibits the highest sound speeds, ranging from 1246.4 m·s^{-1} at 343.15 K to 1438.9 m·s^{-1} at 283.15 K, while POE5 exhibits the lowest, ranging from 1205.2 to 1400.3 m·s^{-1} over the same temperature range. The corresponding difference in sound speeds for these two fluids ranges from 3.4 % at 343.15 K to 2.8 % at 283.15 K. Similar to density, MIL-PRF-23699 exhibits sound speeds that are most similar to POE 7 with differences that range from 0.1 % to 0.2 % at 343.15 K and 278.15 K, respectively.

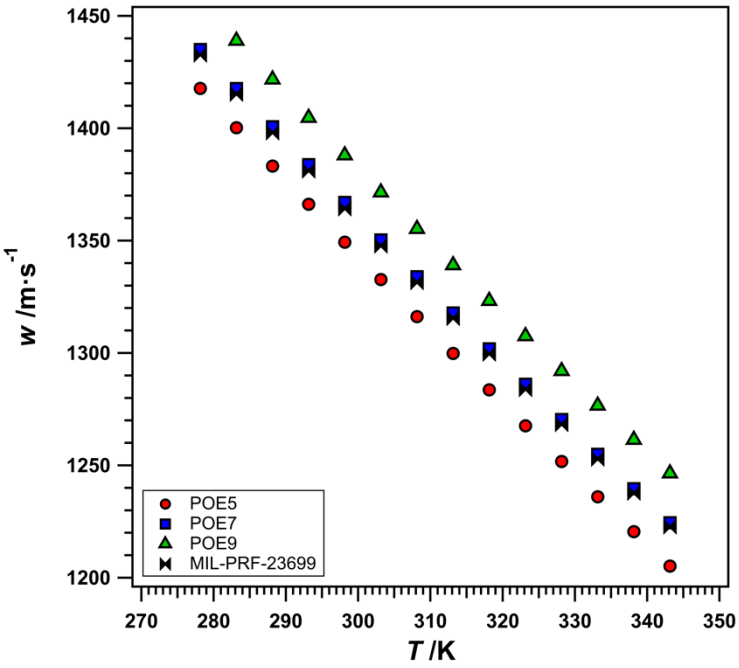

Figure 21: Ambient-pressure speed of sound measurements plotted as a function of temperature.

In addition to densities and speeds of sound, averaged adiabatic compressibilities ($\bar{\kappa}_s$) were calculated from measured quantities via the relation

$$\kappa_s = \frac{1}{\rho \cdot w^2} \ , \tag{10}$$

where ρ is density, w is speed of sound, and the subscript s indicates "at constant entropy." Results for all four fluids are reported in Table 25 and shown plotted as a function of temperature in Figure 22. Also included in Table 25 are corresponding absolute and relative expanded uncertainties ($U(\bar{\kappa}_s)$). Since adiabatic compressibility is a calculated quantity, its uncertainty is derived from the propagation of uncertainties for the two measured quantities. Reported absolute expanded uncertainties, ranging from 1.0 to 1.6 TPa^{-1}, correspond to relative expanded uncertainties of 0.2 %.

The observed trend in adiabatic compressibility (Figure 22) is less straightforward than that observed for either density or speed of sound. Here, POE7 exhibits the highest values, ranging from 709.4 TPa^{-1} at 343.15 K to 491.0 TPa^{-1} at 278.15 K. However, the fluid with the lowest values changes with temperature. At 343.15 K, MIL-PRF-23699 exhibits the lowest adiabatic compressibility (700.8 TPa^{-1}), while at 278.15 K, POE5 is the lowest (482.9 TPa^{-1}). Additionally,

the overall differences are significantly smaller than what was observed for the other properties, ranging from 1.2 % at 343.15 K to 1.6 % at 283.15 K. Finally, at 343.15 K, the adiabatic compressibility of MIL-PRF-23699 is essentially equivalent to that of POE9, differing by just 0.03 %, while at the low end of the temperature range MIL-PRF-23699 is most similar to POE5, with a difference of 0.5 % at 278.15 K.

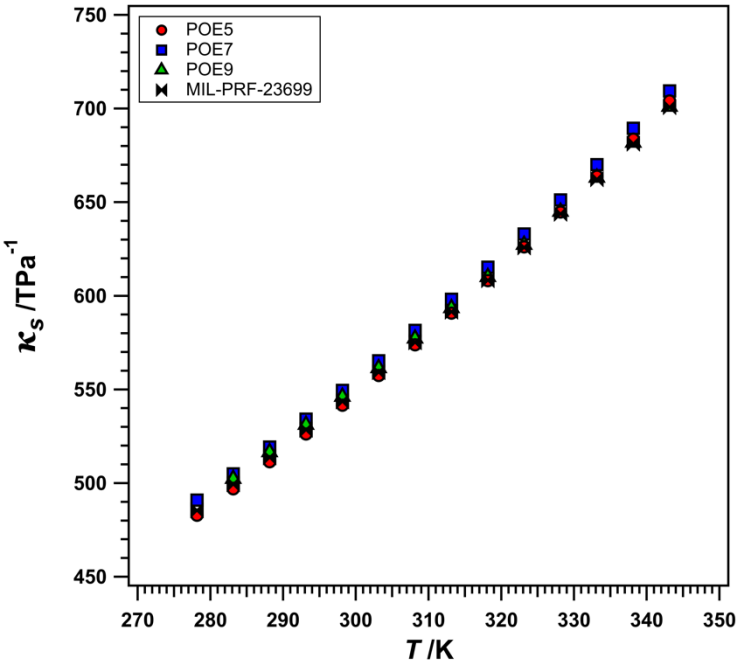

Figure 22: Calculated ambient-pressure adiabatic compressibilities plotted as a function of temperature.

8.4. Data Tables

Table 23: Measured Densities for Four Lubricant Samples at Ambient Pressure (~ 83 kPa).

	POE5				POE7			
T /K	$\overline{\rho}$ /kg·m^{-3}	t_{95}	$U(\overline{\rho})$ /kg·m^{-3}	$U(\overline{\rho})$ /%	$\overline{\rho}$ /kg·m^{-3}	t_{95}	$U(\overline{\rho})$ /kg·m^{-3}	$U(\overline{\rho})$ /%
343.15	977.88	2.041	1.66	0.17	940.20	2.042	1.65	0.14
338.15	981.88	2.041	1.66	0.17	943.92	2.042	1.65	0.14
333.15	985.88	2.041	1.66	0.17	947.66	2.042	1.65	0.13
328.15	989.89	2.041	1.66	0.17	951.39	2.042	1.65	0.13
323.15	993.90	2.041	1.66	0.17	955.13	2.042	1.65	0.13
318.15	997.92	2.041	1.66	0.17	958.87	2.042	1.65	0.13
313.15	1001.94	2.041	1.66	0.17	962.62	2.042	1.65	0.13
308.15	1005.97	2.041	1.66	0.16	966.38	2.042	1.65	0.13
303.15	1010.00	2.041	1.66	0.16	970.14	2.042	1.65	0.13
298.15	1014.04	2.041	1.65	0.16	973.91	2.042	1.65	0.12
293.15	1018.08	2.041	1.65	0.16	977.69	2.041	1.65	0.12
288.15	1022.14	2.041	1.65	0.16	981.48	2.041	1.65	0.12
283.15	1026.21	2.041	1.65	0.16	985.27	2.041	1.65	0.12
278.15	1030.29	2.041	1.65	0.16	989.09	2.041	1.65	0.12
	POE9				**MIL-PRF-23699**			
T /K	$\overline{\rho}$ /kg·m^{-3}	t_{95}	$U(\overline{\rho})$ /kg·m^{-3}	$U(\overline{\rho})$ /%	$\overline{\rho}$ /kg·m^{-3}	t_{95}	$U(\overline{\rho})$ /kg·m^{-3}	$U(\overline{\rho})$ /%
343.15	918.32	2.042	1.65	0.18	954.42	2.042	1.65	0.17
338.15	921.88	2.042	1.65	0.18	958.17	2.042	1.65	0.17
333.15	925.45	2.042	1.65	0.18	961.92	2.042	1.65	0.17
328.15	929.02	2.042	1.65	0.18	965.68	2.042	1.65	0.17
323.15	932.60	2.042	1.65	0.18	969.44	2.042	1.65	0.17
318.15	936.18	2.042	1.65	0.18	973.20	2.042	1.65	0.17
313.15	939.77	2.042	1.65	0.18	976.97	2.042	1.65	0.17
308.15	943.37	2.042	1.65	0.18	980.74	2.042	1.65	0.17
303.15	946.97	2.042	1.65	0.17	984.52	2.042	1.65	0.17
298.15	950.58	2.042	1.65	0.17	988.30	2.042	1.65	0.17
293.15	954.20	2.042	1.65	0.17	992.09	2.042	1.65	0.17
288.15	957.85	2.042	1.65	0.17	995.89	2.042	1.65	0.17
283.15	961.49	2.042	1.65	0.17	999.71	2.042	1.65	0.17
278.15					1003.53	2.042	1.65	0.16

Table 24: Measured Speeds of Sound for Four Lubricants at Ambient Pressure (~ 83 kPa).

	POE5				POE7			
T /K	$\bar{w}$ /m·s^{-1}	t_{95}	$U(\bar{w})$ /m·s^{-1}	$U(\bar{w})$ /%	$\bar{w}$ /m·s^{-1}	t_{95}	$U(\bar{w})$ /m·s^{-1}	$U(\bar{w})$ /%
343.15	1205.2	2.034	1.7	0.1	1224.5	2.034	1.7	0.2
338.15	1220.5	2.034	1.7	0.1	1239.6	2.034	1.7	0.2
333.15	1236.1	2.034	1.7	0.1	1254.9	2.034	1.7	0.2
328.15	1251.8	2.034	1.7	0.1	1270.4	2.034	1.7	0.2
323.15	1267.6	2.034	1.7	0.1	1286.1	2.033	1.7	0.2
318.15	1283.6	2.034	1.7	0.1	1301.9	2.033	1.7	0.2
313.15	1299.8	2.033	1.7	0.1	1317.8	2.033	1.7	0.2
308.15	1316.2	2.033	1.7	0.1	1333.9	2.033	1.7	0.2
303.15	1332.7	2.033	1.7	0.1	1350.3	2.033	1.7	0.2
298.15	1349.3	2.033	1.7	0.1	1367.0	2.032	1.7	0.2
293.15	1366.2	2.033	1.7	0.1	1383.8	2.031	1.7	0.2
288.15	1383.2	2.033	1.7	0.1	1400.7	2.029	1.7	0.2
283.15	1400.3	2.033	1.7	0.1	1417.7	2.029	1.7	0.2
278.15	1417.7	2.033	1.7	0.1	1435.0	2.028	1.7	0.2
	POE9				**MIL-PRF-23699**			
T /K	$\bar{w}$ /m·s^{-1}	t_{95}	$U(\bar{w})$ /m·s^{-1}	$U(\bar{w})$ /%	$\bar{w}$ /m·s^{-1}	t_{95}	$U(\bar{w})$ /m·s^{-1}	$U(\bar{w})$ /%
343.15	1246.4	2.034	1.7	0.1	1222.8	2.033	1.7	0.1
338.15	1261.4	2.034	1.7	0.1	1237.7	2.033	1.7	0.1
333.15	1276.6	2.034	1.7	0.1	1252.9	2.032	1.7	0.1
328.15	1292.0	2.034	1.7	0.1	1268.3	2.032	1.7	0.1
323.15	1307.5	2.033	1.7	0.1	1283.9	2.031	1.7	0.1
318.15	1323.2	2.033	1.7	0.1	1299.6	2.031	1.7	0.1
313.15	1339.1	2.033	1.7	0.1	1315.5	2.031	1.7	0.1
308.15	1355.2	2.033	1.7	0.1	1331.5	2.030	1.7	0.1
303.15	1371.5	2.033	1.7	0.1	1347.7	2.029	1.7	0.1
298.15	1387.9	2.032	1.7	0.1	1364.3	2.030	1.7	0.1
293.15	1404.7	2.032	1.7	0.1	1381.1	2.030	1.7	0.1
288.15	1421.7	2.032	1.7	0.1	1398.1	2.031	1.7	0.1
283.15	1438.9	2.031	1.7	0.1	1415.3	2.031	1.7	0.1
278.15					1432.7	2.031	1.7	0.1

Table 25: Calculated Adiabatic Compressibilities for Four Lubricants at Ambient Pressure (~ 83 kPa)

	POE5			POE7		
T /K	$\overline{\kappa}_s$ /TPa^{-1}	$U(\overline{\kappa}_s)$ /TPa^{-1}	$U(\overline{\kappa}_s)$ /%	$\overline{\kappa}_s$ /TPa^{-1}	$U(\overline{\kappa}_s)$ /TPa^{-1}	$U(\overline{\kappa}_s)$ /%
343.15	704.1	1.5	0.2	709.4	1.6	0.2
338.15	683.7	1.5	0.2	689.5	1.5	0.2
333.15	663.9	1.4	0.2	670.1	1.5	0.2
328.15	644.7	1.4	0.2	651.2	1.4	0.2
323.15	626.1	1.3	0.2	633.0	1.4	0.2
318.15	608.2	1.3	0.2	615.3	1.3	0.2
313.15	590.7	1.2	0.2	598.2	1.3	0.2
308.15	573.8	1.2	0.2	581.5	1.2	0.2
303.15	557.5	1.2	0.2	565.3	1.2	0.2
298.15	541.6	1.1	0.2	549.5	1.2	0.2
293.15	526.3	1.1	0.2	534.2	1.1	0.2
288.15	511.4	1.0	0.2	519.3	1.1	0.2
283.15	497.0	1.0	0.2	505.0	1.0	0.2
278.15	482.9	1.0	0.2	491.0	1.0	0.2
	POE9			**MIL-PRF-23699**		
T /K	$\overline{\kappa}_s$ /TPa^{-1}	$U(\overline{\kappa}_s)$ /TPa^{-1}	$U(\overline{\kappa}_s)$ /%	$\overline{\kappa}_s$ /TPa^{-1}	$U(\overline{\kappa}_s)$ /TPa^{-1}	$U(\overline{\kappa}_s)$ /%
343.15	701.0	1.6	0.2	700.8	1.6	0.2
338.15	681.8	1.5	0.2	681.2	1.5	0.2
333.15	663.1	1.5	0.2	662.2	1.4	0.2
328.15	644.9	1.4	0.2	643.8	1.4	0.2
323.15	627.2	1.4	0.2	625.8	1.4	0.2
318.15	610.1	1.3	0.2	608.4	1.3	0.2
313.15	593.4	1.3	0.2	591.5	1.3	0.2
308.15	577.2	1.2	0.2	575.2	1.2	0.2
303.15	561.4	1.2	0.2	559.2	1.2	0.2
298.15	546.1	1.2	0.2	543.6	1.1	0.2
293.15	531.1	1.1	0.2	528.5	1.1	0.2
288.15	516.5	1.1	0.2	513.7	1.1	0.2
283.15	502.3	1.0	0.2	499.4	1.0	0.2
278.15				485.5	1.0	0.2

9. Thermal Conductivity

9.1. Summary

The thermal conductivity of the liquid phase of three POE base oils and the fully qualified lubricant was measured over the temperature range of 300 K to 500 K at pressures up to 69 MPa in a transient hot-wire apparatus. These measurements provided the data necessary for development of models for the thermal conductivity of POE lubricants.

9.2. Instrument Description

The thermal conductivity was measured with a high-temperature apparatus that allows isothermal control of the temperature of the hot-wire cell in a specially designed furnace. The experiment control electronics are shown in Figure 23 (left). The temperature control furnace, valve manifold, and piston pump are shown in Figure 23 (right). In the present measurements, the fluid was contained in the cylindrical bore of a microreactor, shown in Figure 24, with an inner diameter of 8 mm, which is concentric with the hot wire of 12.7 μm diameter that is 11.429 cm long and located along the central axis of the bore.

Figure 23: (left) Transient hot-wire measurement electronics including: control computer, Wheatstone bridge containing hot-wires, power supplies, multimeters, multiplexer, and lock-in amplifier (for AC hot-wire experiments). (right) Temperature and pressure control system including: DC powered furnace, pressure manifold, piston pump, pressure transducer, and platinum resistance thermometers.

The hot wire has two lead wires at each end to allow separate current and sense leads for four-wire resistance measurements. The lead wires pass through a four-wire high-pressure seal with compressed Teflon sealant. The microreactor with a volume of 5 mL is located within an aluminum isothermal cylinder, also shown in Figure 24, with thermowells for platinum resistance sensors for control of temperature and measurement of temperature gradients, and for an SPRT to measure the initial cell temperature, T_i, with an expanded uncertainty of $U(T_i) = 0.005$ K. The measurement cell/isothermal cylinder is in turn located within a cylindrical isothermal enclosure of aluminum with a wall thickness of 13 mm, which is placed in the furnace that is controlled by the system computer at the desired temperature. An air gap between the cell/isothermal cylinder and the isothermal enclosure further reduces temperature gradients in the measurement cell. Pressures, p, are determined with a pressure transducer with an expanded uncertainty of $U(p) = 7$ kPa. All reported uncertainties are for a coverage factor of $k = 2$, an approximately 95 % confidence interval.

Figure 24: Transient hot-wire cell components including aluminum isothermal block, 5 mL microreactor, wire pressure feedthrough, and alumina hot-wire support and electrical insulation components.

9.3. Measurement Principle

Hot wires with a small diameter and large length-to-diameter ratio are used to approximate a transient line source as closely as possible as described many years ago by Healy et al.[49] Deviations from the transient line-source model are treated as corrections to the experimental temperature rise. In this approach, the ideal temperature rise, ΔT_{id}, is given by

$$\Delta T_{id} = \frac{q}{4\pi\lambda}\left[\ln(t) + \ln\left(\frac{4a}{r_0^{\,2} C}\right)\right] = \Delta T_{w} + \sum_{i=1}^{10} \delta T_i \,, \tag{11}$$

where q is the power applied per unit length, λ is the thermal conductivity of the fluid, t is the elapsed time from the onset of heating, $a = \lambda/(\rho c_p)$ is the thermal diffusivity of the fluid, ρ is the density of the fluid, c_p is the isobaric specific heat capacity of the fluid, r_0 is the radius of the hot wire, C = 1.781... is the exponential of Euler's constant. The ideal temperature rise is equivalent to the measured temperature rise of the wire, ΔT_w, summed with the corrections, δT_i, that account for deviations from ideal line-source conduction.[49] The form of Eq. 11 is that of a line, where the thermal conductivity can be found from the slope and the thermal diffusivity can be found from the intercept. A line is fit to ΔT_{id} versus ln(t) data over a time interval, typically from 0.1 s to 1.0 s, with the thermal conductivity obtained from the slope of this fitted line. The thermal diffusivity from the intercept of this fitted line typically has an order of magnitude higher uncertainty and was not considered in this work. Assuming the thermal conductivity increases linearly with temperature for a small temperature rise, the experimental temperature, T, associated with the thermal conductivity is the average wire temperature over the time interval that was fit.

The largest correction for both gas and liquid measurements accounts for the finite dimensions and heat capacity of the hot wire. This correction for finite wire dimensions is most significant at short experiment times. The single-wire cell requires correction for finite diameter and length (axial conduction) during data analysis based on the two-dimensional transient analytical solution of Woodfield et al.[50] The end time for the fit interval was selected so the transient temperature gradient in the fluid did not penetrate to the cavity wall and fluid convection was not significant. An experiment duration of 1 s was considered optimal for all measurements.

Heat transfer by thermal radiation between media at two different temperatures T_1 and T_2 is proportional to (T_1^4 - T_2^4). When T_1 and T_2 are nearly the same (small temperature rise) this is approximately T^3 (T_1 - T_2) so in the present hot-wire experiments the thermal radiation correction increases in proportion to T^3 and remains relatively small at temperatures up to 500 K. The transparent fluid correction[49] was applied for the present measurements in both the gas and liquid phases. This correction is best for gas measurements, but even for higher density liquid measurements, where there is more absorption and emission of thermal radiation, this correction is considered reasonable at these temperatures.

9.4. Measurement Process

Measurements were started with a clean and evacuated hot-wire cell and pressure system. Pressure was controlled with a variable-volume piston pump. The pump was nearly filled with new sample

such that the vapor headspace was at the top of the pump at the pump outlet. The pump was then connected to the pressure system and the entire system, including the pump, was evacuated to degas the sample in the pump. The vacuum was disconnected, and the degassed sample was then injected into the measurement system, which was at the desired temperature. Measurements were made along isotherms, starting at the lowest pressure and increasing pressure to 69 MPa for a total of eight to nine pressures per isotherm. At each pressure, transient hot-wire measurements were made at five different power levels (yielding five different experimental temperatures and temperature rises) with two experiments of one second duration per power level. Thus, ten measurements were made at each initial temperature and pressure.

Each isotherm required 1 day to complete. Seven isotherms at temperatures of 300, 333, 367, 400, 433, 467, and 500 K were completed for each fluid. The liquid in the measurement cell was removed by pressurizing with carbon dioxide gas at the top of the measurement cell and withdrawing sample from the bottom of the cell through the pressure system manifold. The remaining liquid in the pump was also discharged through the pressure system manifold. The cell and pump were cleaned with multiple fills and discharges of liquid toluene. Between each fill and discharge of toluene solvent the system was filled with supercritical carbon dioxide that was discharged before the cell was evacuated. The pump was disassembled and cleaned between each sample. The final cleaning step was a fill of the entire pressure system, including the cleaned pump and hot-wire cell, with supercritical carbon dioxide. The discharge from this fill/soak was examined for residual liquid oil that might have been retained. Cleaning was continued until the carbon dioxide discharge contained no observable oil residue.

9.4.1. Catalytic Alumina Support/ Insulator Problem

Measurements were initially made with one of our typical single-wire cells with alumina components to support the hot wire and provide electrical insulation. The high-pressure wire feedthrough had a soapstone sealant. Measurements were made on the POE9 sample, with repeatability issues at temperatures above 400 K. The problems became more pronounced with the POE7 sample. Chemical analysis of sample removed from the hot-wire apparatus after these issues were observed indicated decomposition. Subsequent testing of POE samples over ground alumina indicated catalytic activity, supporting our observations of decomposition producing changes in measured thermal conductivity. Macor machinable ceramic was then tested with no catalytic activity indicated. The cell used in all the measurements reported here used Macor, glass capillary, and Teflon for wire support and electrical insulation (i.e., the tests with POE9 and POE7 were repeated). There was no indication of decomposition during the measurements reported here.

9.5. Results and Uncertainties

The measured thermal conductivity is shown as a function of pressure for each of the isotherms in Figure 25 through Figure 28. The measured thermal conductivity data are given in Appendix A in Tables A1 through A4. The measured thermal conductivity data are reported at nominal isotherm temperatures, T_i, of 300, 333, 367, 400, 433, 467, and 500 K with pressures, p, up to 69 MPa. Since five different applied power levels were each measured twice, there are up to ten measurements reported for each fluid and each initial temperature and pressure.

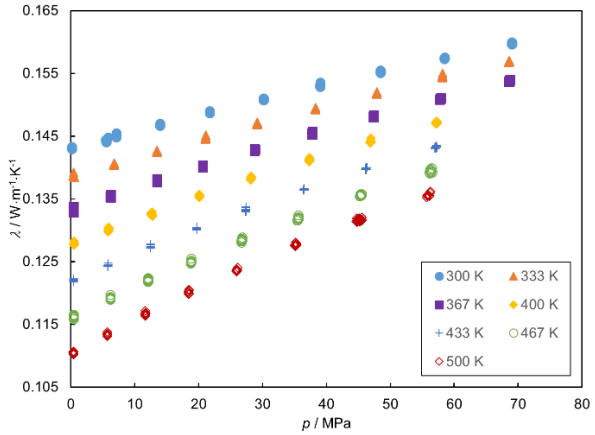

Figure 25: Thermal conductivity data for POE5 as a function of pressure measured along isotherms at temperatures from 300 K to 500 K.

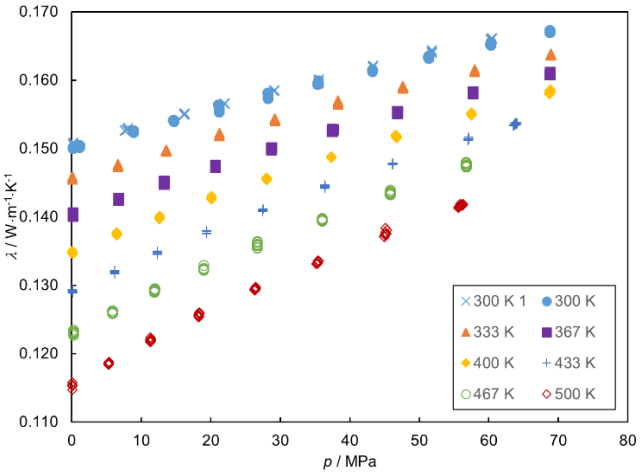

Figure 26: Thermal conductivity data for POE7 as a function of pressure measured along isotherms at temperatures from 300 K to 500 K.

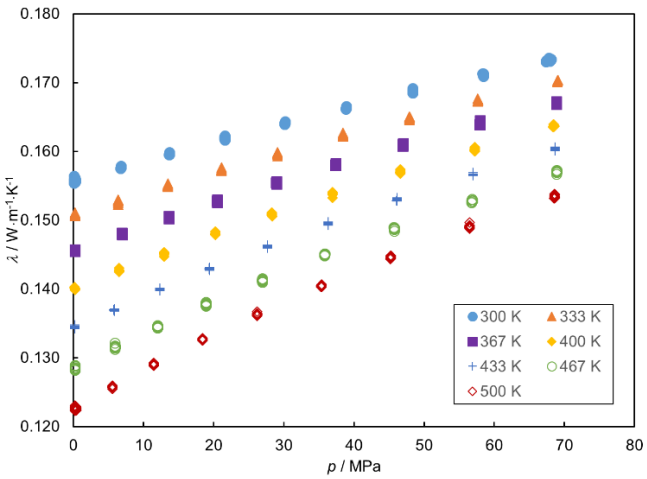

Figure 27: Thermal conductivity data for POE9 as a function of pressure measured along isotherms at temperatures from 300 K to 500 K.

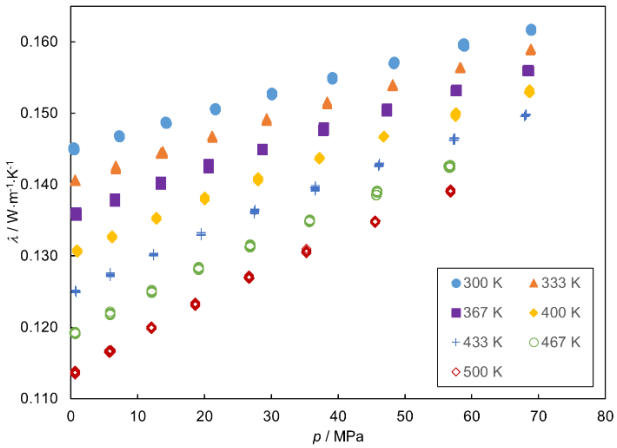

Figure 28: Thermal conductivity data for MIL-PRF-23699 lubricant as a function of pressure measured along isotherms at temperatures from 300 K to 500 K.

Measurements were removed from analysis when deviation plots of the temperature rise as a function of ln(t) indicated convection occurred during a measurement. The measured thermal conductivity, λ, is associated with the experimental temperature, T, and p. The experiment temperature rise is reflected in the difference between T and T_i. The expanded uncertainty for T is comparable to that of T_i, and $U(T)$ = 0.005 K. The expanded relative uncertainty for the reported thermal conductivity data is $U(\lambda)$ = 0.5 %. A parameter STAT was also calculated; it is the expanded relative uncertainty in the slope of the line fit to ΔT_{id} data as a function of ln(t) in Eq. 11 to get the experimental thermal conductivity. This parameter was 0.002 or less for all of the measurements reported here, which is much less than the expanded uncertainty. All expanded uncertainties are for a coverage factor of k = 2, an approximately 95 % confidence interval.

The measurement sequence for the POE samples reported here was POE7, POE5, MIL-PRF-23699, and POE9. POE7 was measured first since it was still in the pump after the alumina catalysis problem was identified and it was decided that the new hot-wire cell without alumina was required for these measurements. The first assembly of the new cell failed at the highest pressure of the initial 300 K isotherm when the lead wires slipped in the Teflon wire sealant. Mechanical support from an additional Teflon tube between the cell and the sealant was added in the second assembly that eliminated this problem. Thus, there are two independent measurements of the POE7 sample reported at 300 K from each assembly. Agreement between these two independent assemblies is within the expanded uncertainty of $U(\lambda) = 0.5$ %. The data from both assemblies are shown in Figure 26 (indicated as "300 K" and "300 K 1" in the figure legend).

At any given temperature, the thermal conductivity of the POE samples generally increases in the order of POE5, MIL-PRF-23699, POE7, and POE9. The corrections in Eq. 11 require estimates for the thermophysical properties of the measured liquid. These property estimates were based on preliminary values, but this adds only slightly to $U(\lambda)$ since the corrections are small for liquid samples.

10. Viscosity

10.1. Summary

Viscosities of the four lubricants were measured with a commercial oscillating-piston viscometer that was modified at NIST with regard to thermal insulation, calibration, sample charging and pressurization, as well as automation and data acquisition. The instrument uses a variant of the falling body technique except that the motion of the sensing body is not unidirectional and driven by gravity but alternating and driven by electromagnetic induction from two magnetic coils. Measurements on the four lubricants were carried out over temperature ranges of 275 K to 430 K for POE5, 280 K to 450 K for POE7, 290 K to 450 K for POE9, and 290 K to 450 K for MIL-PRF-23699; in all cases the maximum pressure was ~ 137 MPa. Measurements on squalane over a similar temperature and pressure range were required for calibration purposes. These results are also presented in Laesecke et al.[51]

10.2. Experimental

The experimental setup is shown in Figure 29. The tubular cell containing the sample and a viscosity-sensing cylinder is rated to 137 MPa. The cell can be thermostated between 270 K and 450 K with polydimethylsiloxane heat transfer liquid and a small laboratory circulator. For the samples in this project, three sensing cylinders were used in the viscosity ranges 1 mPa·s to 20 mPa·s, 2.5 mPa·s to 50 mPa·s, and 5 mPa·s to 100 mPa·s. Since these sensors had not been used at NIST previously, they had to be calibrated. Squalane ($C_{30}H_{64}$) was chosen as reference liquid because its viscosity had been characterized recently in an international effort. The calibration required viscosity measurements of squalane with all three sensors in addition to the lubricant measurements. Mylona et al.[52] published two reference correlations for the viscosity of squalane, one formulated in terms of temperature and density and one in terms of temperature and pressure. Schmidt et al.[53] published a third reference correlation in terms of temperature and pressure and an additional viscosity data set that was measured at Imperial College (IC), London (UK) with a vibrating wire viscometer in the temperature range from 338.2 K to 473 K with pressures up to 200 MPa. This data set is the only one that overlaps with the temperature and pressure range of the viscometer used at NIST; it is therefore essential for the calibration of the three sensors. Unfortunately, it was found that none of the three reference correlations represents the IC data set within its estimated uncertainty of 2 %. The combined range of deviations extends from -7.8 % to +7.4 %. If these correlations were used for calibrations, significant systematic errors would be propagated through other measurements. To avoid this, a new correlation of the

IC data set had to be developed in this project which does represent these data within their quoted uncertainty of 2 %.

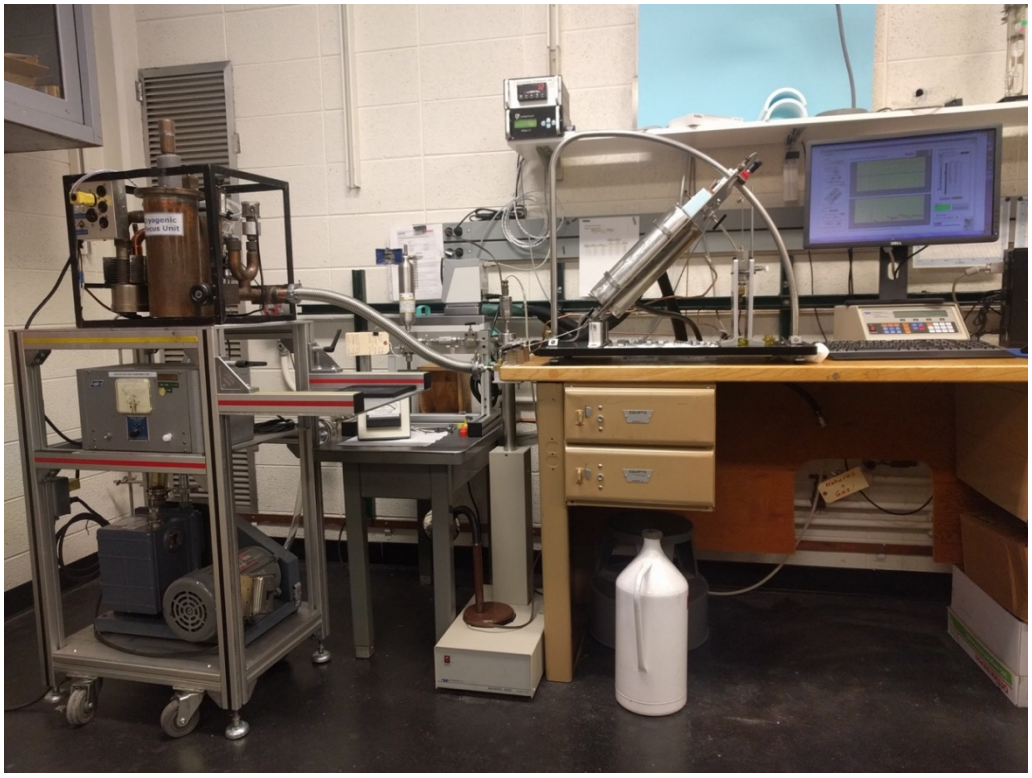

Figure 29: View of the oscillating-piston viscometer (above the bench drawers) with the vacuum system, sample cylinder, circulator, and syringe pump from left to right.

The temperature of the sample liquid in the viscometer was measured with a 100 Ω platinum resistance temperature detector (RTD) that was calibrated and mounted on the outside of the pressure vessel by the manufacturer. The RTD is in a sealed space and cannot be removed from the pressure vessel to check its calibration. The manufacturer-quoted uncertainty of the temperature measurement is 0.1 K. This uncertainty component contributes at most an uncertainty of 0.47 % to the viscosity measurements of POE9 at 290 K and 4.8 MPa where the maximum gradient $(\partial\eta/\partial T)_p$ occurs. The pressure in the viscometer was generated with a high-pressure syringe pump rated to 137 MPa with a maximum sample volume of 65 mL. Pressure was measured with a transducer rated to 207 MPa with a full-scale uncertainty of 0.05 %, or 0.104 MPa. Prior to this project, the transducer calibration was checked with a primary pressure balance at 55.2 MPa, 41.4 MPa, 27.6 MPa, and 13.8 MPa, and the highest deviation was 0.024 MPa at the lowest calibration pressure. This uncertainty component contributes negligibly to the present measurements because the gradients $(\partial\eta/\partial p)_T$ are rather small for compressed liquids.

The sample liquids were loaded into stainless steel cylinders and degassed by repeated freezing with liquid nitrogen-vacuum pumping-and thawing cycles. The sample cylinder was then mounted on the inlet of the viscometer manifold and the manifold was evacuated. The piston of the syringe pump was cycled during the vacuum pumping to remove residues on the walls of the syringe pump cylinder. With the syringe pump piston at the top position, the vacuum system was valved off and the sample cylinder valve opened. Sample liquid was drawn into the syringe pump cylinder until its volume of 65 mL was filled. After closing the sample cylinder valve, the valve between the syringe pump and the high-pressure cell was opened and sample was pumped into the viscometer manifold until it began to drain from the outlet of the manifold. Then, pumping was stopped, the outlet valve closed, and the measurement of an isotherm commenced with the customized LabVIEW software by programming the circulator to the desired temperature, setting the appropriate equilibration time, as well as the desired pressures and the measurement duration, at each pressure.

Figure 30: Front panel of the custom LabVIEW virtual instrument developed in this project to automate the oscillating-piston viscometer with its associated circulator and syringe pump. Shown are the cell temperature (red) and the viscosity (blue) in the top plot, and the cell pressure (thin red) in the bottom plot for measurements of POE5 along the 320 K isotherm.

In the beginning of the project, viscosity data acquisition and scheduling were performed with software from the viscometer manufacturer. This was supplemented by a custom-developed LabVIEW utility that was adapted from the automated vibrating-tube densimeter (described in Section 7) to control and schedule the pressures to be generated by the high-pressure syringe pump (see Figure 30). This automation code was completed in November 2016 and accelerated the viscometer throughput by a factor of three. Due to its agility, it provides much more transparency of the internal viscometer state to the user. For instance, the presence of sample liquid or solvent in the viscometer cell is now indicated when the RTD registers a corresponding temperature change.

The viscosity measurements were carried out in the sequence POE9, squalane, POE7, squalane, POE5, MIL-PRF-23699, squalane with extensive rinsing of the viscometer between each sample. The solvent was a mixture of hexane isomers. During the rinsing, the high-pressure cell was thermostated to 308 K. The volume of rinsing solvent was at least 300 mL which provided for 4.6 fillings of the cylinder of the high-pressure syringe pump. The internal volume of the high-pressure cell was approximately 8 mL and that of the remaining parts of the viscometer manifold approximately 5 mL. Thus, the solvent volume was sufficient to rinse the viscometer volume several times over.

The MIL-PRF-23699 sample was measured last because prior measurements in the other instruments revealed that it was difficult to remove. During the viscosity measurements, it was observed that the MIL-PRF-23699 sample diffused through PTFE tape seals on the top and the bottom of the sample cylinder as these showed the brown color of the sample liquid after a few days. In addition, it was observed after the measurements of the MIL-PRF-23699 sample, that the hexane solvent was not miscible with that sample. Therefore, the viscometer was rinsed in addition with dodecane and then again with hexane. Despite this more extensive rinsing with two solvents, the following repeat squalane calibration measurements at 360 K and 370 K using the 5 mPa·s to 100 mPa·s sensing piston were invalid. Therefore, it was not possible to report calibrated viscosity data from measurements with this piston at these two temperatures. When results are reported at these two temperatures, they were obtained with one of the other two pistons.

10.3. Results

A total of 715 viscosity data points were measured with all three sensing pistons for the calibration liquid squalane from 277 K to 450 K with pressures to 137 MPa. Calibration functions in terms of pressure were obtained at each measured temperature by referencing the measured viscosities to

those calculated from the VFT correlation of Mylona et al.[52] at temperatures below 340 K, and the correlation of the IC data set that was developed in this work at temperatures above 340 K. The VFT correlation of Mylona et al.[52] represents the experimental data of other laboratories within ±3 % and the correlation of the IC data set represents these data within their quoted uncertainty of 2 %. The calibration functions were subsequently applied in the analysis of the measured lubricant viscosities.

The viscosity measurement results for the lubricants are plotted as a function of pressure in Figures 31 through 34 and are reported in Tables B1 through B4 in Appendix B. The tabulated data are presented in the order they were measured with respect to temperature. A total of 269 data points are reported for POE5 in Table B1. The lowest temperature of these data is 275 K. A total of 286 data points are reported for POE7 in Table B2. The lowest temperature of these data is 280 K. A total of 161 data points are reported in Table B3 for POE9. Due to solidification of the sample, the lowest temperature of these measurements was limited to 290 K. A total of 214 data points are reported for the MIL-PRF-23699 sample in Table B4. The lowest temperature of these data is 290 K. POE9 has the highest viscosity because it is the largest and most complex molecule with strong interlocking possibilities of the nonanoate side chains. As the length of these side chains decreases from POE9 to POE7 and POE5, so decreases the viscosity of the compounds. The viscosity of the MIL-PRF-23699 sample is close to that of POE9.

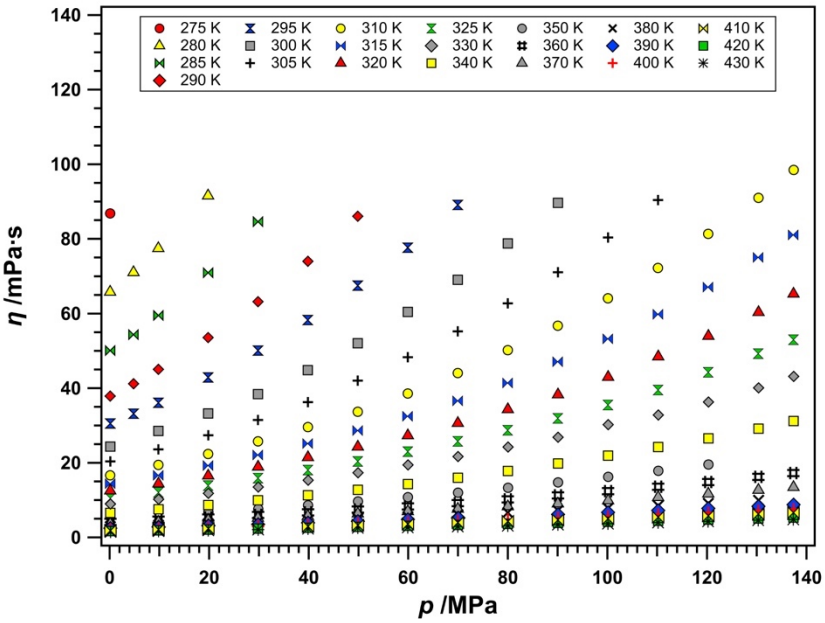

Figure 31: Viscosity data for POE5 as a function of pressure measured along isotherms at temperatures from 275 K to 430 K.

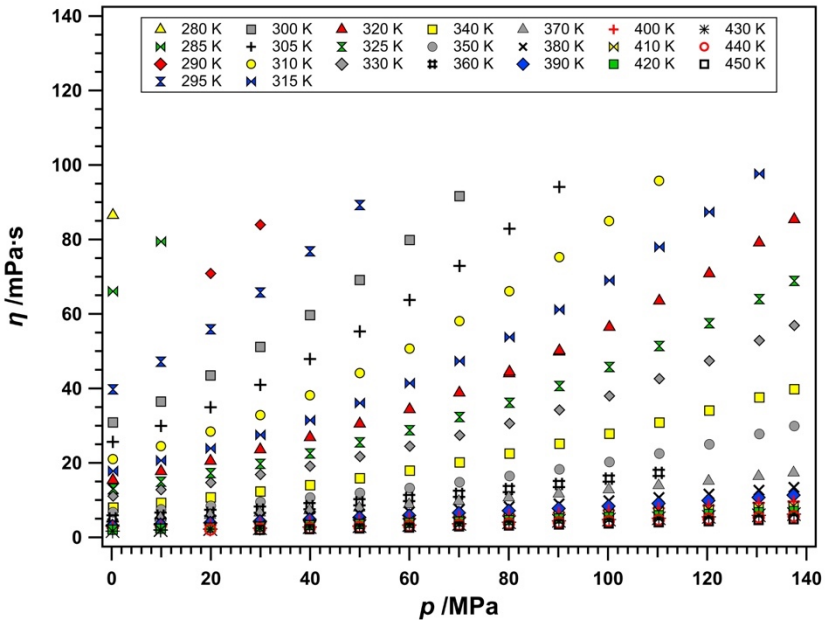

Figure 32: Viscosity data for POE7 as a function of pressure measured along isotherms at temperatures from 280 K to 450 K.

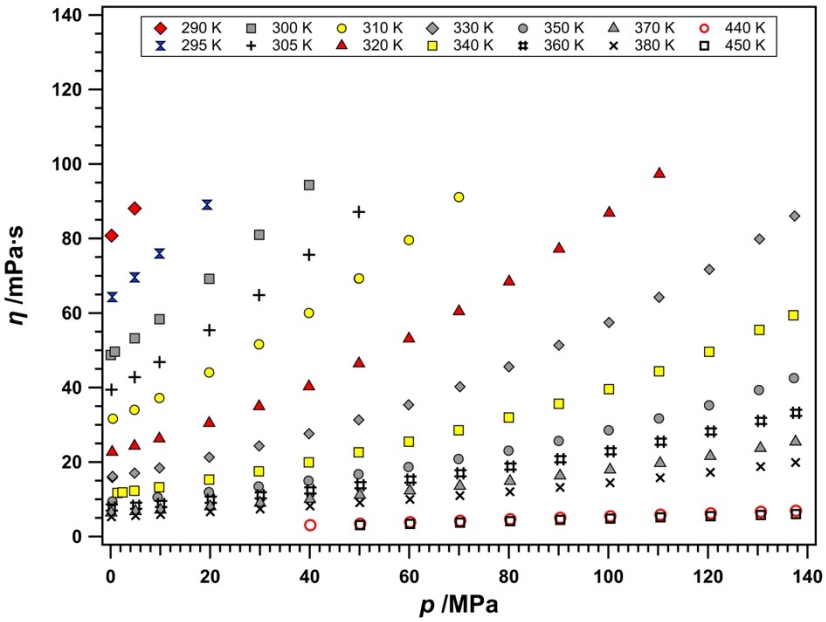

Figure 33: Viscosity data for POE9 as a function of pressure measured along isotherms at temperatures from 290 K to 450 K.

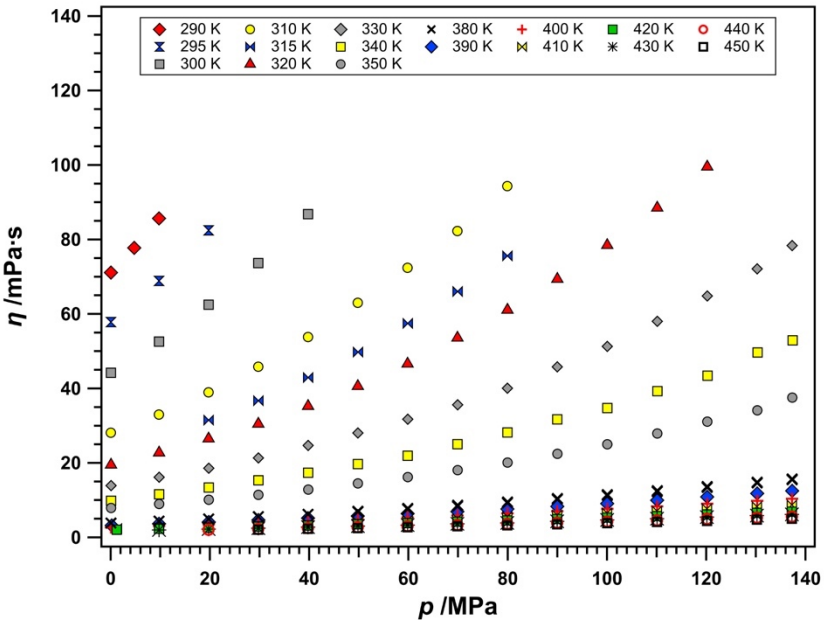

Figure 34: Viscosity data for MIL-PRF-23699 as a function of pressure measured along isotherms at temperatures from 290 K to 450 K.

While the calibration with squalane ensures the mutual consistency of the measurements with the three sensing pistons within ±3 % below 340 K and 2 % above 340 K, it is difficult to assess the total uncertainty of the viscosity measurements with this instrument rigorously. This would require an in-depth analysis of the fluid mechanics and secondary flows around the alternating sensing pistons as was done for falling body viscometers by Schaschke et al.[54] Next, it would be necessary to derive the working equation that relates the period of the piston alternation to the viscosity of the sample taking into account the effect of thermal expansion and of sample compression on the viscometer tube and the sensing pistons. Absent such analysis, and based on our experience with falling body viscometers,[55, 56] the expanded uncertainty of the present measurements is estimated conservatively from 5 % at atmospheric pressure to 10 % at the maximum pressure of 137 MPa.

11. Advanced Distillation Curve of MIL-PRF-23699

11.1. Summary

The advanced distillation curve methodology was applied at atmospheric pressure, in a noble gas environment, to a sample of MIL-PRF-23699 to establish an initial boiling temperature. Due to decomposition of the heated fluid, the distillation was carried out to only 10 % distillate volume fraction. In this fraction, some of the additives were observed, in addition to decomposition products such as carboxylic acids; no polyol ester base oils were observed. No initial boiling temperature is defined under the conditions tested, because the fluid was not thermally stable.

11.2. Advanced Distillation Curve Applied to MIL-PRF-23699

The Advanced Distillation Curve[57, 58] was applied at atmospheric pressure to a sample of a qualified aviation turbine engine lubricant (MIL-PRF-23699). Since the boiling range of this fluid was predicted to be very high (boiling point reported by the manufacturer was 672 K at 3.98 kPa), the main objective was to establish an initial boiling temperature.

11.2.1. Experimental Method

A round bottom flask was filled with 200 mL of the fluid by volumetric pipette. Due to the viscous nature of the fluid, a small amount of sample was lost to the walls of the pipette. To reduce oxidative reactions, argon was bubbled through the fluid for approximately 10 minutes prior to heating. A flow of argon was also maintained on top of the fluid throughout heating to keep the environment free of oxygen; the flow was low enough to prevent cooling and displacement of the heated fluid. Two temperatures were recorded throughout the measurement, one in the fluid (kettle temperature, T_k) and one in the vapor phase (head temperature, T_h).

11.3. Results

The liquid mixture was heated to and maintained at 573 K for 30 minutes; no change in the fluid was observed. Further heating of the fluid in the kettle (T_k) to 620 K caused the colorless/faintly yellow fluid to become red (T_h = 328 K). The fluid continued to darken with increased heating, becoming an opaque brown fluid. The first bubble in the fluid was observed at a kettle temperature (T_k) of 622 K (T_h = 333 K). A sustained boil was observed at T_k = 639 K and T_h = 361 K and the first drop of fluid was collected at T_k = 649 K and T_h = 399 K. The fluid temperature was maintained between 643 K and 653 K for approximately 30 minutes; the head temperature (T_h) remained consistent between 400 K and 401 K. The 10 % volume fraction was collected at T_k = 656 K and T_h = 419 K.

Samples of the first drop, 10 % volume fraction, and the remaining kettle fractions were diluted in hexane and analyzed by GC-MS. The first drop contained predominately species associated with the thermal decomposition of the fluid. Species included carboxylic acids, in addition to methyl esters of the acids, the corresponding aldehyde, alkanes, and larger species. The composition of the 10 % fraction was similar to the composition of the 1st drop. As expected, the 10 % fraction contained a larger portion of species with higher boiling points than the first drop fraction. The remaining fluid in the kettle, although a very dark brown color, still contained primarily unreacted polyol esters, antioxidants, and anti-wear agents. Additional details of the analysis are proprietary and are administratively restricted.

12. Modeling

12.1. Summary

Equations of state were developed for the pure fluids POE5, POE7, and POE9, and for the fully qualified lubricant (MIL-PRF-23699, formulated as a pseudo-pure fluid). The equations are formulated in terms of Helmholtz energy with independent variables of temperature and density. Equations expressed in terms of the Helmholtz energy have the advantage that properties are simple derivatives of this fundamental property, including those that cannot be measured, such as entropy. The experimental data measured as part of this project were used in a regression procedure to determine the coefficients of the equations of state. All densities measured in this work, including those measured in the atmospheric-pressure densimeter and those measured in the high-pressure densimeter, were fitted to within 0.2 %, speed of sound to within ~ 0.1 %, and the isobaric heat capacity to within ~ 0.3 %. All equations extrapolate in a physically reasonable manner.

Viscosity models were developed for the pure fluids POE5, POE7, and POE9, and for the fully qualified lubricant (formulated as a pseudo-pure fluid). These correlations represent the viscosity of the liquid phase at pressures up to 140 MPa to within 5 to 10 %, which is the estimated uncertainty of the experimental data. Similarly, correlations for the thermal conductivity of the pure fluids POE5, POE7, and POE9, and for the fully qualified lubricant (formulated as a pseudo-pure fluid) were developed that represent the thermal conductivity of the liquid phase at pressures up to 70 MPa to within 0.4 % to 0.7 % depending on the fluid. The estimated uncertainty of the experimental data is 0.5 %. Two surrogate mixture models were developed using the base fluids POE5, POE7, and POE9. One focused on viscosity, and the other on thermodynamic properties. Neither were capable of representing the experimental data to within or near the experimental uncertainty, and we recommend the use of the pseudo-pure fluid model for the properties of the fully qualified lubricant.

12.2. Equations of State

Equations of state are tools to calculate the thermodynamic properties of pure fluids and mixtures, and have often been expressed as a function of pressure with independent variables of temperature and density. Modern-day equations of state now use the Helmholtz energy (also with independent variables of temperature and density) to enable the calculation of all thermodynamic properties. Equations expressed in terms of the Helmholtz energy have the advantage that properties are simple derivatives of this fundamental property, including those that cannot be measured, such as entropy. Equations expressed in terms of pressure require integration to calculate caloric properties (such as enthalpies and sound speeds) and are thus no longer used for high-accuracy applications.

Through density (ρ) derivatives of the Helmholtz energy, one can obtain properties such as pressure (p), and its isothermal derivatives, such as $dp/d\rho$. At zero density, these properties are generally zero or simple values of temperature (T) (for example, $dp/d\rho = RT$ at $p = 0$, where R is the gas constant). Non-ideal gas properties ($p > 0$) require a "real-gas" contribution (i.e., departure from ideal-gas behavior), which accounts for the interaction between molecules.

Unlike pressure and its derivatives, caloric properties require derivatives with respect to temperature, and this adds an additional complication. The calculation of caloric properties includes, in addition to the real-gas contribution, an ideal-gas contribution at zero pressure, which is represented by an equation that describes the isobaric heat capacity at zero pressure. This property can be obtained in a number of ways, through either experimental methods, or, for simple molecules, through simulation or group-contribution methods. When no such data or methods are available, the development of equations of state can become substantially more difficult, but is possible with current techniques as explained further below.

One of the most important properties in the development of equations of state is the critical temperature because of its use as a reducing parameter. This value is generally known for most fluids, especially for those where the critical temperature is less than ~ 450 K. At higher temperatures, fluids typically decompose below the critical temperature, but measurements that require the fluid to be at high temperatures for a small amount of time can obtain close estimates of the critical point. For the oils studied in this work, the critical temperatures are well beyond the decomposition limit, and no direct measurement is possible. Other methods are available that can be used for the estimation of the critical point properties, but the uncertainties in the calculated values are often much larger than that required to develop an equation of state. This work is one of the first to attempt to fit an equation of state where the critical temperature was only known within ~ 100 K.

The critical density is also used as a reducing parameter in an equation of state. Because of the high uncertainty in the measurement of the density at the critical point, its value is almost always fitted simultaneously with the other parameters, and then compared to measured values to ensure it lies within the uncertainties from other sources. If the critical temperature were known, then an estimated value of the critical density could be obtained simply by the ratio of T/T_c. For example, at a reduced value of $0.5 \times T_c$, the critical density would be about one-third the value of the densities in the liquid phase. At about $0.3 \times T_c$, the critical density is about one-fourth the value of the liquid-

phase densities. Thus, for example, for POE5 an estimated value of the critical density could be obtained as 0.25 to 0.33 of the liquid-phase values. From the final equation of state for POE5, the value of the liquid-phase density at 300 K ($0.34\times T_c$) showed it to be around $0.36\times\rho_c$.

The unknown value of the critical density was bound to the even more elusive value of the critical temperature. No previous work had ever demonstrated if the critical temperature could be determined for fluids where the temperatures of the measured properties are only a fraction of the critical temperature. This was initially thought to not be possible because only densities, heat capacities, and speeds of sound were being fitted. Through months of fitting, the sensitivity of the critical temperature in a high-accuracy equation of state became apparent, where "high-accuracy" in this work refers to the limited region where the measurements are available. Fitting each of the oils and the mixture showed that the critical temperature could only be varied within about 10 to 20 degrees while still maintaining low uncertainties in the measured data.

Recently, one of the key factors in the development of equations of state has become the rectilinear diameter. This value is the average of the liquid and vapor densities at saturation. Through significant practical experience, this property has been key to obtaining correct vapor-phase values when no measurements are available in that phase. The rectilinear diameter, in effect, mirrors the properties of the liquid phase onto those in the vapor phase and helps ensure the saturation dome and corresponding vapor properties are at least representative of the true fluid properties. Other constraints placed on the equation of state during its development contribute to the correct behavior in this phase, as explained in Section 12.2.3. These constraints involve properties, such as the phase identification parameter (PIP) and Gruneisen parameter, that are generally unfamiliar to all except those that fit equations.

The importance of correct vapor-phase properties comes into play when developing the ideal-gas heat capacity equation discussed earlier, and that is needed to obtain the ideal-gas part of the equation of state for caloric properties such as heat capacities, speeds of sound, enthalpies, and entropies. The ideal-gas heat capacities are related to the liquid-phase heat capacities by the contribution from the heat capacity in the vapor phase and from the second derivative of the vapor pressure curve with respect to temperature. Neither the vapor-phase properties nor vapor pressures at ambient conditions or higher are known; but with the techniques discussed above, the vapor-phase properties can be at least qualitatively represented by the current state-of-the-art fitting in equations of state, and the vapor pressure can be extrapolated to higher temperatures to some degree based on the values available at very low pressures.

The ability to make an equation with so many unknown properties that are generally required in fitting, which can then represent those properties with some degree of accuracy in regions far outside that of the available measurements, is made possible through very high accuracy data for density, speed of sound, and heat capacity in the liquid phase, along with the vapor pressure data at very low pressure. The key, however, to this success stems from not only the types and temperature ranges of the data, but more importantly from the high-pressure range of the data. If data had only been measured at saturation, the determination of the critical point would not have been possible. The high-pressure data enabled the ability to control the slope and curvature of the Helmholtz energy equation in the liquid phase; however, with the extensive temperature-pressure grid of data measured in this work, the derivatives of this fundamental thermodynamic property are fixed, and an entire surface can be extended far beyond the limits of the data. Because the surface is fixed due to the range and accuracy of the data, when done carefully, the surface can be extended to the critical point, and then into the vapor phase with state-of-the-art fitting techniques.

12.2.1. Functional Form of the Equation of State

Equations of state based on the Helmholtz energy are commonly expressed in a dimensionless form with dimensionless independent variables of density $\delta = \rho/\rho_c$ and reciprocal temperature $\tau = T_c / T$. The critical point properties are given in Table 26. The form of this equation is

$$\frac{a(\rho,T)}{RT} = \alpha(\delta,\tau) = \alpha^0(\delta,\tau) + \alpha^r(\delta,\tau) \ . \tag{12}$$

The Helmholtz energy of the ideal gas is given by

$$a^0 = h^0 - RT - Ts^0 \ . \tag{13}$$

The ideal-gas enthalpy and entropy are given by

$$h^0 = h_0^0 + \int_{T_0}^{T} c_p^0 \mathrm{d}T \quad \text{and} \tag{14}$$

$$s^0 = s_0^0 + \int_{T_0}^{T} \frac{c_p^0}{T} \mathrm{d}T - R\ln\left(\frac{\rho T}{\rho_0 T_0}\right) , \tag{15}$$

where c_p^0 is the ideal-gas heat capacity. The subscript 0 for density and temperature indicate ideal gas properties, where ρ_0 is the ideal-gas density at T_0 and p_0 [$\rho_0 = p_0/(T_0R)$], and T_0 and p_0 are arbitrary reference states. Combining these equations results in the following equations for the dimensional and dimensionless Helmholtz energies of the ideal gas,

$$a^0 = h_0^0 + \int_{T_0}^{T} c_p^0 \mathrm{d}T - RT - T\left[s_0^0 + \int_{T_0}^{T} \frac{c_p^0}{T} \mathrm{d}T - R\ln\left(\frac{\rho T}{\rho_0 T_0}\right)\right] \text{ and} \tag{16}$$

$$\alpha^0 = \frac{h_0^0 \tau}{RT_c} - \frac{s_0^0}{R} - 1 + \ln\frac{\delta\tau_0}{\delta_0\tau} - \frac{\tau}{R}\int_{\tau_0}^{\tau}\frac{c_p^0}{\tau^2}\,\mathrm{d}\tau + \frac{1}{R}\int_{\tau_0}^{\tau}\frac{c_p^0}{\tau}\mathrm{d}\tau\,, \tag{17}$$

where $\delta_0 = \rho_0 / \rho_c$ and $\tau_0 = T_c / T_0$.

Table 26: Molar Mass and Critical Point Parameters.

Substance	M /g·mol^{-1}	T_c /K	p_c /MPa	ρ_c /mol·dm^{-3}
POE5	472.612	890.0	1.27	0.556
POE7	584.835	940.0	1.03	0.412
POE9	697.051	970.0	0.885	0.316
MIL-PRF-23699	557.6	930.0	1.08	0.439

Models for the calculation of real fluid properties of fluids are abundant, requiring any number of terms depending on the complexity of the method. Fitting methods are often used to determine the coefficients of a particular model, being fitted to experimental data for the fluid and constrained by various criteria explained in some detail here and in more detail in other work, such as that of Span and Wagner[59], Lemmon and Jacobsen[60], and Lemmon et al.[39]

The equation used to describe the ideal-gas heat capacities used for the oils is given by

$$\frac{c_p^0}{R} = \nu_0 + \sum_{i=1}^{2} \nu_i \left(\frac{u_i}{T}\right)^2 \frac{\exp(u_i/T)}{[\exp(u_i/T)-1]^2}\,, \tag{18}$$

where the parameters are given in Table 27. This is the Planck-Einstein functional form; it was used so that the shape of the ideal-gas heat capacity versus temperature would be similar to that derived from statistical mechanical models.

Table 27: Coefficients of the Ideal-Gas Heat Capacity Equation.

	POE5	POE7	POE9	MIL-PRF-23699
v_0	30.0	55.0	75.0	50.0
v_1	850.0	1100.0	1000.0	1000.0
v_2	2000.0	3000.0	2700.0	2000.0
u_1	69.0	109.0	93.0	78.0
u_2	98.0	240.5	360.0	105.0

The real-gas contribution comes from the equation of state given further below. The parameters in this equation were fitted by minimizing the deviations between the experimental data measured in this work and the calculations from the equation. The fitting program is described by Lemmon and Jacobsen [60] and Lemmon et al.[39] In effect, each data point that is fitted is given a weight that is multiplied by the square of the deviation between the experimental point and the calculated value. The sum of these squared values multiplied by a weighting value, assigned by the one doing the fit, is then calculated. Additionally, a number of constraints are applied to ensure that the equation extrapolates well to very low temperatures and to high temperatures and pressures as explained in Section 12.2.3. This is necessary to use the developed EOS in mixture modeling where the equations used in the mixture often require calculations from the pure-fluid equation of state that are beyond the limits of the experimental data (in particular, below the triple point of the pure fluid). This is the modern practice in fitting equations of state and is done in all high-accuracy equations as described in multiple documents available in the literature.

The final functional form was determined through months of fitting POE5, POE7, and POE9 separately, but with each receiving about two weeks of fitting at a time. The approach used to develop the final equations of state was to develop a single equation that used the same exponents on density, temperature, and the parameters for the Gaussian terms (explained below), and to allow only the coefficients of the equation for each oil to change. This required several weeks of fitting one of the three pure fluids, and then the functional form consisting of all coefficients, exponents, parameters, and so on would be transferred to a different oil and the process would continue. Each transfer generally resulted in failure of the fit for the next oil in reproducing the experimental data based on fitting new coefficients only. In these situations, the exponents and other parameters were again fitted, and the process continued. After many iterations, a set of parameters began to emerge that would transfer easily from one fluid to the next.

The final set of parameters was developed during the fitting of POE7. After substituting these parameters into the fit for POE5, a new set of coefficients was fitted within an extremely short

amount of time (compared to the work that was required up to this point), and this set of parameters was deemed adequate for these two fluids.

However, when applied to POE9, the situation was a bit different. The sample that was used to measure the properties of POE9 had nearly double the amount of impurities than in the samples delivered for POE5 and POE7. This resulted in twice the uncertainty in the molar mass of the substance. Densities and heat capacities were measured on a mass basis, and thus the density needs to be divided by the molar mass to obtain molar densities, and the heat capacities must be multiplied by the molar mass to obtain the molar properties required in fitting. The thermodynamic equation used to calculate the speed of sound from the Helmholtz energy is a function of the square root of the molar mass. Because of the lack of the true molar mass, our current program used to fit equations of state required modification to fit mass density and heat capacity while allowing the molar mass to change.

Ironically, due to this complication and the unknown values of the critical temperature and critical density, an optimum set of values for these three properties and the coefficients could not produce an equation that both represented the liquid-phase measurements and the vapor pressures. The substance delivered to NIST and labeled as POE9 is really a mixture of this substance and a number of other substances (as indicated in Table 4), and fitting this mixture to a pure fluid equation of state is yet another cause of the inability to fit it with the same uncertainties in vapor pressure as those for POE5 and POE7. The final equation was developed with much lower weights on the vapor pressures to obtain deviations in the other properties that were still generally within the uncertainties in those measurements. The average deviations in the measurements are larger (especially for vapor pressure) than is the case for those for POE5 and POE7. The deviations are discussed in the next section.

The functional form for the final equations of state for all three oils and the pseudo-pure fluid model for MIL-PRF-23699 is given below:

$$\begin{aligned}\alpha^{\mathrm{r}}(\delta,\tau) = &\sum N_k \delta^{d_k} \tau^{t_k} + \sum N_k \delta^{d_k} \tau^{t_k} \exp\left(-\delta^{l_k}\right) \\ &+ \sum N_k \delta^{d_k} \tau^{t_k} \exp\left(-\eta_k (\delta - \varepsilon_k)^2 - \beta_k (\tau - \gamma_k)^2\right)\end{aligned} . \quad (19)$$

The first summation is a simple polynomial expression in terms of temperature and density, the second summation is composed of polynomial-exponential terms, and the third summation contains Gaussian bell-shaped terms (see Span and Wagner[59]). The exponents on temperature and density and the parameters inside the Gaussian terms are identical for all fluids and are given in Table 28. The coefficients N_k for each fluid are given in Table 29.

Table 28: Parameters of the Equation of State.

k	t_k	d_k	l_k	η_k	β_k	γ_k	ε_k
1	1.0	5					
2	0.08	1					
3	1.2	1					
4	1.162	2					
5	0.54	3					
6	1.08	2	1				
7	1.56	3	1				
8	1.78	3	1				
9	1.42	4	1				
10	1.62	5	1				
11	2.0	1		1.0	0.36	1.57	1.7
12	1.0	2		1.31	0.35	1.45	0.55
13	1.0	4		0.46	0.55	1.63	0.95
14	1.0	3		20.0	1000.0	1.09	0.91

Table 29: Coefficients (N_k) of the Equation of State.

k	POE5	POE7	POE9	MIL-PRF-23699
1	0.0106971	0.00996664	0.00811	0.00990044
2	1.510321	1.801441	1.446665	1.633544
3	–2.596894	–2.872737	–2.303871	–2.6606
4	–2.311273	–2.347331	–2.320483	–2.328001
5	0.3332414	0.3403607	0.336244	0.3281252
6	2.500028	2.550799	2.383751	2.4664585
7	7.527764	7.625433	8.210469	7.657825
8	–5.405529	–5.44993	–6.200227	–5.569829
9	0.94954	0.8612612	0.813201	0.914727
10	0.3303842	0.3734221	0.377317	0.3668741
11	–0.0234605	–0.00711446	0.0023328	–0.007457
12	0.0156448	0.02289254	0.0217847	0.028916
13	–0.0092188	–0.00893703	–0.009014	–0.0103879
14	–0.5415831	–0.75359521	–1.54251	–0.645008

12.2.2. Experimental Data and Comparisons to the Equation of State

The accuracy of the equation of state can be determined by statistical comparisons of calculated property values to experimental data. These statistics are based on the percent deviation in any property, *X*, defined as

$$\Delta X = 100\left(\frac{X_{\text{data}} - X_{\text{calc}}}{X_{\text{data}}}\right) . \tag{20}$$

With this definition, the average absolute deviation is defined as

$$\text{AAD} = \frac{1}{n}\sum_{i=1}^{n}\left|\Delta X_i\right| , \tag{21}$$

where *n* is the number of data points. Table 30 lists the AAD values between the experimental data and those calculated from the equation of state. Comparisons given in the following paragraphs use the average absolute deviations given by Eq. 21 unless otherwise stated (such as the maximum value). Discussions of maximum errors or of systematic offsets use the absolute values of the deviations, unless otherwise noted. In the plots, data points with excessive deviations are shown at the outer limits to indicate where these outliers were measured.

Table 30: Summary of Experimental Data.

Apparatus	No. of points	T /K	p /MPa	ρ /mol·dm^{-3}	AAD /%
POE5					
Density					
High-pressure densimeter	165	270-470	0.5-50	1.85-2.25	0.06
Atmospheric-pressure densimeter	14	278-343	0.083	2.07-2.18	0.048
Speed of Sound					
Atmospheric-pressure instrument	14	278-343	0.083		0.027
High-pressure pulse-echo	68	283-423	0.001-63		0.052
Heat Capacity					
DSC	170	263-432	0.083		0.097
Vapor pressure					
Gas saturation & literature	10	334-413			11.7
POE7					
Density					
High-pressure densimeter	161	270-470	0.511-50	1.45-1.73	0.063
Atmospheric-pressure densimeter	14	278-343	0.083	1.61-1.69	0.053
Speed of Sound					
Atmospheric-pressure instrument	14	278-343	0.083		0.077
High-pressure pulse-echo	49	283-423	0.059-69.1		0.081
Heat Capacity					
DSC	125	293-417	0.083		0.088
Vapor pressure					
Literature	4	374-433			4.4
POE9					
Density					
High-pressure densimeter	145	290-470	0.506-50.1	1.19-1.39	0.051
Atmospheric-pressure densimeter	13	283-343	0.083	1.32-1.38	0.073
Speed of Sound					
Atmospheric-pressure instrument	13	283-343	0.083		0.053
High-pressure pulse-echo	41	293-423	0.092-58.2		0.052
Heat Capacity					
DSC	100	313-412	0.083		0.267
Vapor pressure					
Literature	5	395-476			

Table 30, continued.

Apparatus	No. of points	T /K	p /MPa	ρ /mol·dm^{-3}	AAD /%
MIL-PRF-23699					
Density					
High-pressure densimeter	161	270-470	0.518-50	1.54-1.85	0.074
Atmospheric-pressure densimeter	14	278-343	0.083	1.71-1.8	0.068
Speed of Sound					
Atmospheric-pressure instrument	14	278-343	0.083		0.04
High-pressure pulse-echo	51	298-423	0.02-61.2		0.053
Heat Capacity					
DSC	220	273-492	0.083		0.171

All densities measured in this work, including those measured in the atmospheric-pressure densimeter and those measured in the high-pressure densimeter, were fitted to within 0.2 % as shown in Figures 35 – 38. The average absolute deviations for each set of measurements and for each of the four fluids is between 0.05 % and 0.07 %. The bias in the deviations between the equations of state and the density measurements for POE5 and POE7 are mostly negligible, whereas those for POE9 are –0.03 % and –0.07 % for the two data sets. This bias is caused by the higher impurities in the sample and the difficulty of fitting the equation as explained in section 12.2.2.

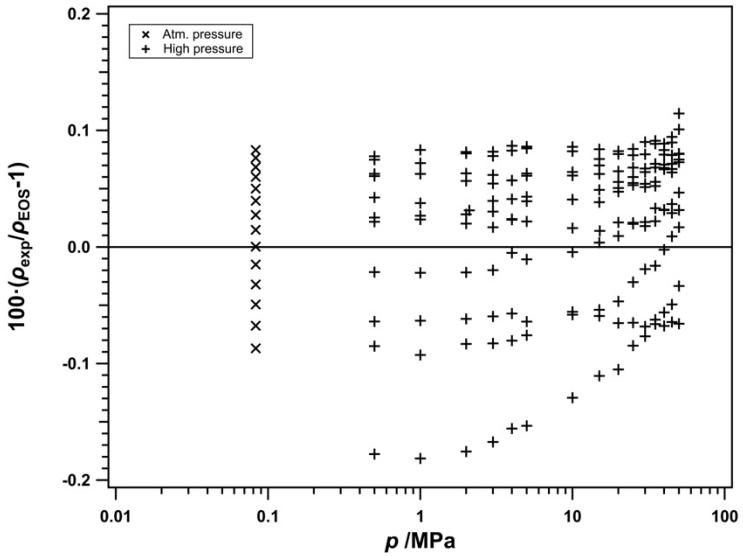

Figure 35: Comparisons of densities calculated with the equation of state to experimental data for POE5 as a function of pressure.

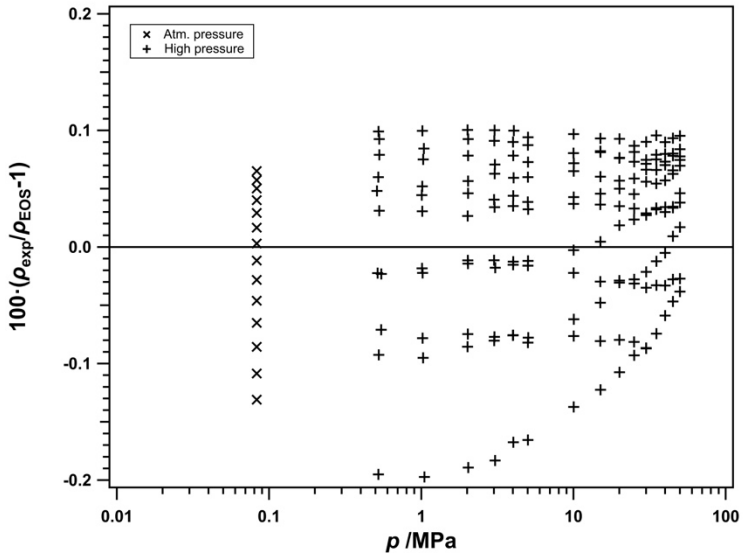

Figure 36: Comparisons of densities calculated with the equation of state to experimental data for POE7 as a function of pressure.

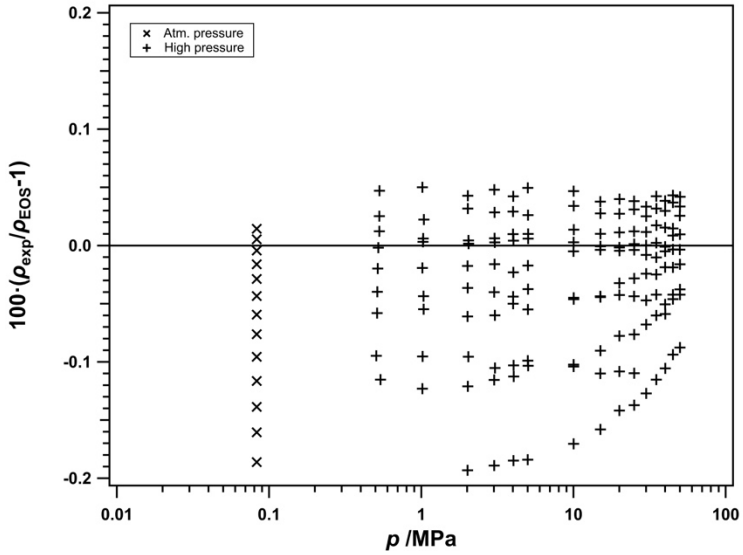

Figure 37: Comparisons of densities calculated with the equation of state to experimental data for POE9 as a function of pressure.

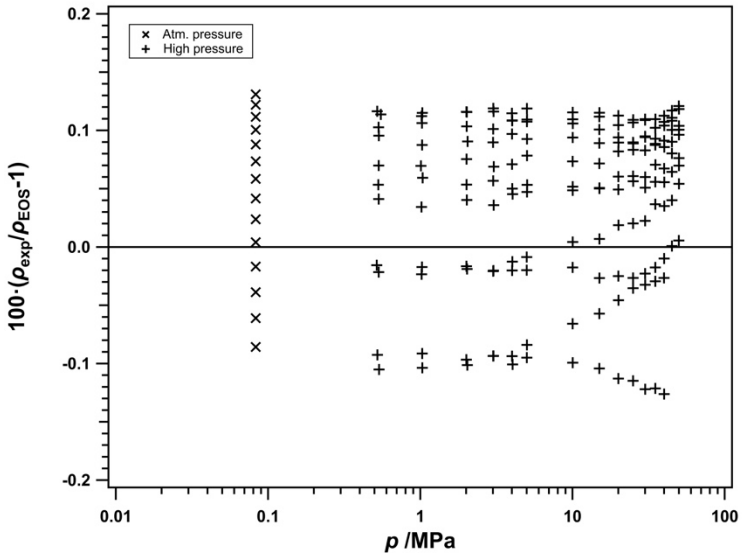

Figure 38: Comparisons of densities calculated with the equation of state to experimental data for MIL-PRF-23699 as a function of pressure.

Deviations between the equation of state and the measurements for the speed of sound given in this work are nearly identical for all four fluids. As shown in Figures 39 to 42, deviations generally range from +0.1 % to –0.4 %. Most of the data lie between ±0.1 %, except 3 to 6 points for each fluid. The average absolute deviations range between 0.05 % for POE5, POE9, and MIL-PRF-23699 to 0.08 % for POE7. The equations of state represent both sets of measurements (those taken at atmospheric pressure and those taken at high pressure) with nearly equal distributions (excluding the few outliers below –0.1 %).

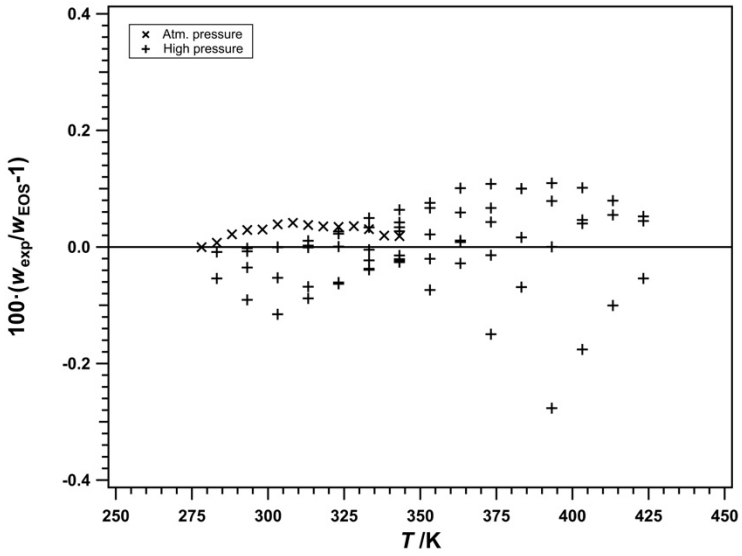

Figure 39: Comparisons of speeds of sound calculated with the equation of state to experimental data for POE5 as a function of temperature.

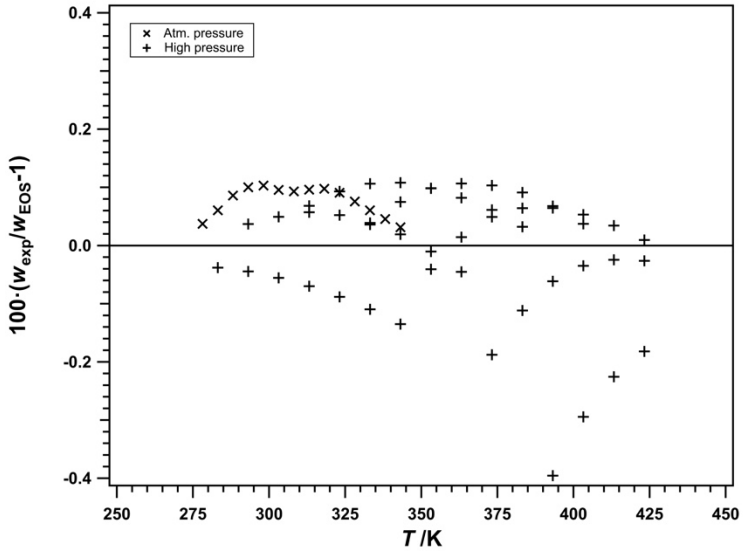

Figure 40: Comparisons of speeds of sound calculated with the equation of state to experimental data for POE7 as a function of temperature.

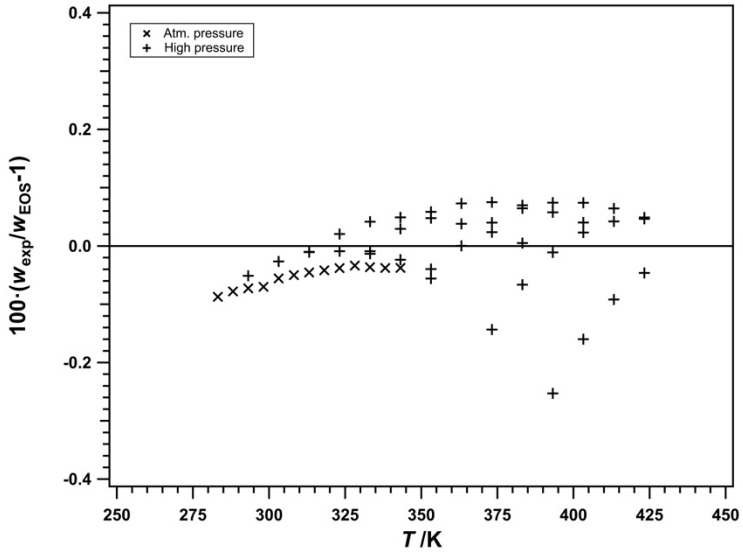

Figure 41: Comparisons of speeds of sound calculated with the equation of state to experimental data for POE9 as a function of temperature.

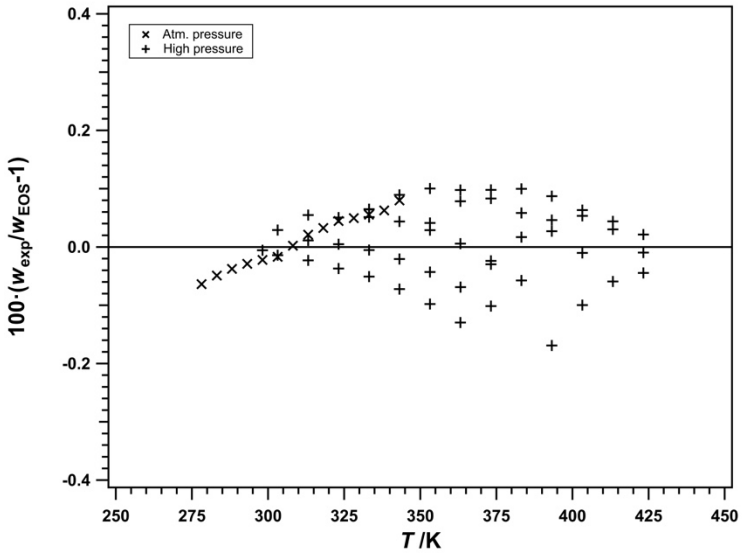

Figure 42: Comparisons of speeds of sound calculated with the equation of state to experimental data for MIL-PRF-23699 as a function of temperature.

The equations of state represent the isobaric heat capacity data within 0.3 % for POE5, POE7, and MIL-PRF-23699 as shown in Figure 43. The average absolute deviations are less than 0.1 % for POE5 and POE7, and 0.17 % for MIL-PRF-23699. For POE9, the largest deviation is –0.85 % and the AAD is 0.27 %. As with the other properties, POE9 shows larger errors as explained elsewhere.

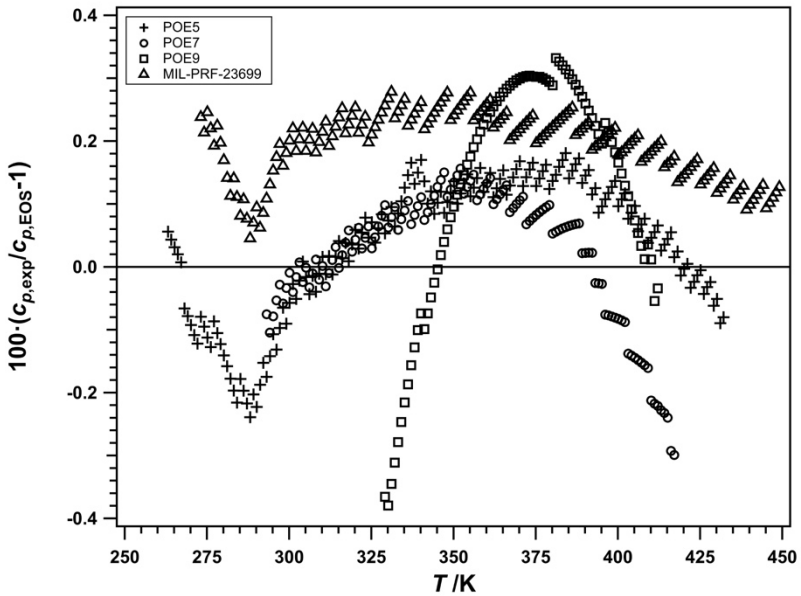

Figure 43: Comparisons of isobaric heat capacities calculated with the equations of state for POE5, POE7, POE9, and MIL-PRF-23699 to experimental data as a function of temperature.

The vapor pressures were by far the most difficult property to accurately model while keeping all other data within their uncertainties. However, without these data it would not have been possible to obtain the critical temperatures with the "low" uncertainty that we believe we have achieved. The values at the critical point (temperature and density) were extremely sensitive to the vapor pressures, and fitting these at the same time as all other measurements to a functional form that was required to maintain smooth behavior to lower extremes than previously done with any other fluid presented many new challenges. The use of one functional form where only the coefficients changed between the four fluids but the temperature exponents and Gaussian bell-shaped parameters were identical for each fluid contributed in both positive and negative ways. The vapor pressures for POE5 and POE7 benefitted from the same functional form. The equations for these fluids represent the vapor pressures generally within 3 %, except one point with a deviation of 10 % that could not be fitted without damaging the representation of all other points. The situation with POE9 is quite different due to the much higher impurities. The rigid functional form could not be forced to fit these data to within the same deviations and comparing with data on a percent deviation basis gives a false impression, especially since the lowest pressure is less than 1 mPa (a factor of one billionth of the critical pressure). Five points are available for POE9.[6] At 476 K, the vapor pressure measurement is 0.17 Pa, and the calculated value is 0.94 Pa. At 395 K, the measured value is 0.05 mPa and the calculated value is 0.39 mPa. These calculated values are still within the uncertainty of the measured values.

12.2.3. Extrapolation Behavior

The extrapolation behavior of equations of state has become an extremely important part of fitting equations of state over the last 15 years. Each of the approximately 50 publications on equations of state in that time frame show this behavior to demonstrate that the equation has been fitted correctly. The current criteria for each equation to be accepted as final includes some of the following:

1) All properties must extrapolate to near 0 K without extreme changes, and must be very smooth and follow the correct path to around 50 to 100 K. Most equations start to deviate from the desired path below these temperatures, but each new generation of equations continues to improve at lower temperatures as better starting functional forms become available. An example for POE5 is shown in Figure 44 for the Phase Identification Parameter, or PIP.

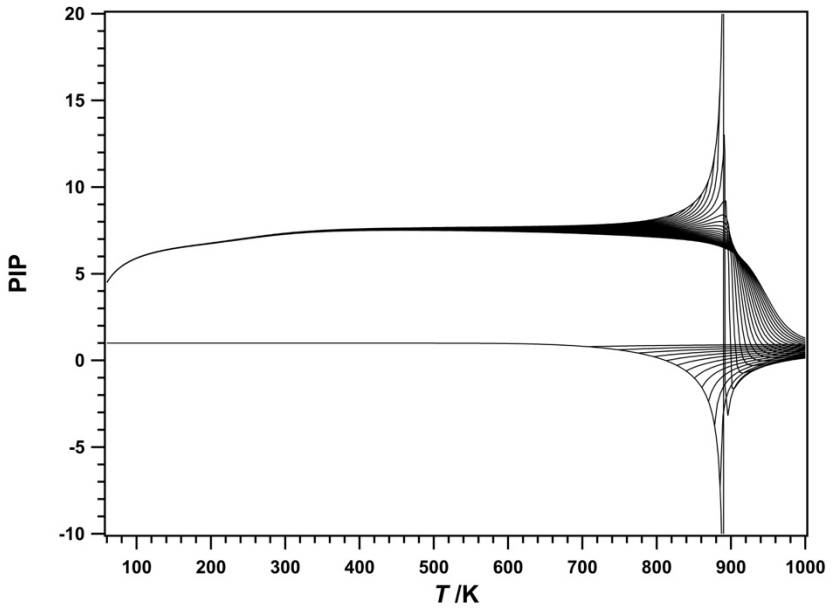

Figure 44: Phase Identification Parameter (PIP) versus temperature diagram showing isobars and saturation curves from 0 to 3 MPa in steps of 0.1 MPa for POE5.

2) All properties must extrapolate to infinite temperature, pressure, and density. This is verified continuously while fitting with the use of pressure-density plots showing isotherms over a large range of temperatures. The isotherms should converge at extremely high pressures, but not cross. Plots of the correct behavior are shown in the R-125 publication of Lemmon and Jacobsen[60]. This is demonstrated in Figure 45 for POE7.

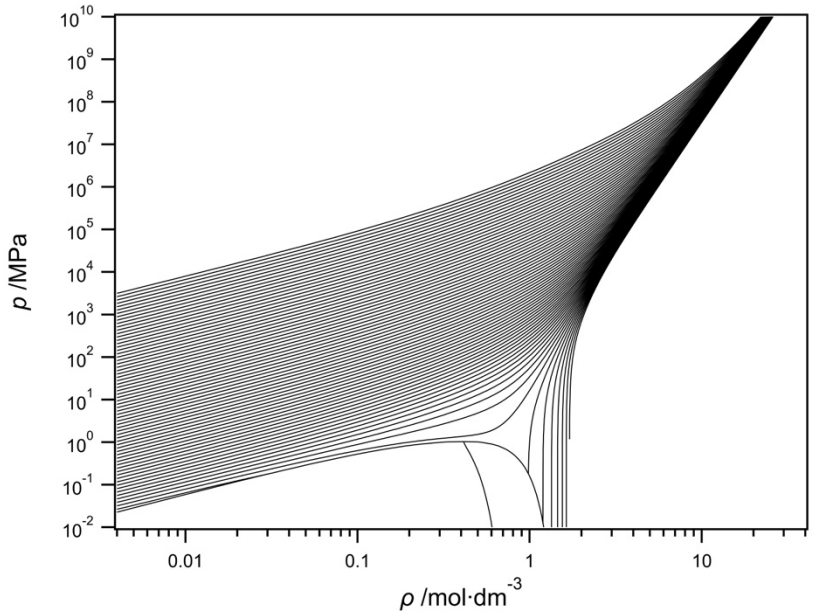

Figure 45: Isothermal behavior of the POE7 equation of state at extreme conditions of temperature (up to 10^{12} K) and pressure (up to 10^{10} MPa).

3) The rectilinear diameter (the average of the saturated liquid and vapor densities) must be linear in the critical region down to about one-half of the critical temperature. Below that, the line bends slightly to allow the liquid-phase density to increase at low temperatures. Figure 46 shows this for POE9.

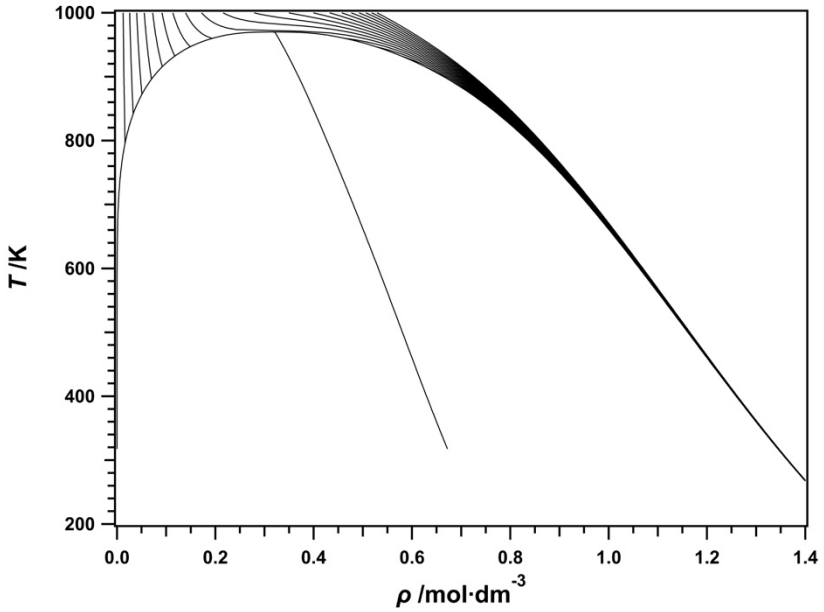

Figure 46: Temperature versus density diagram showing the saturation boundaries, the rectilinear diameter (the average of the saturation densities), and isobars up to 2 MPa for POE9.

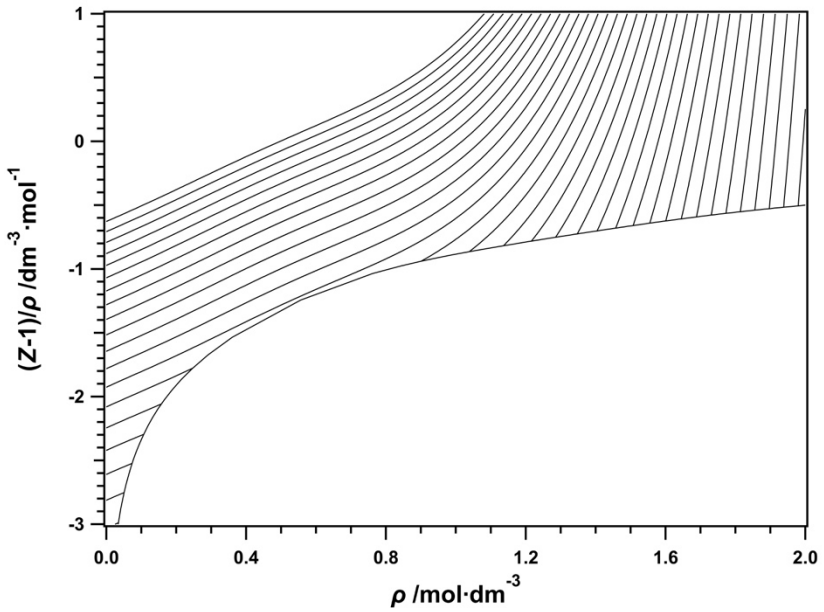

Figure 47: Calculations of $(Z-1)/\rho$ along isotherms versus density for POE5; isotherms are shown from temperatures of 400 K to 1200 K in steps of 25 K.

4) The slopes of isotherms in the vapor phase for the property $(Z - 1)/\rho$, where Z is the compressibility factor and ρ is the density, should have little or no curvature, except for highly associating fluids such as water. Figure 47 shows this for POE5. This is extremely important for fluids that have no data in the vapor phase, as is case for the oils fitted in this work.

5) The first partial derivative of pressure with respect to density at constant temperature for the critical isotherm absolutely must never be negative, and the second derivative must be negative in the vapor phase and positive in the liquid phase, with the transition exactly at the critical point. If these criteria are not met, the equation will generally have two critical points (the critical point is the point where these two derivatives are both equal to zero).

6) The derivatives of the residual isochoric heat capacity (c_v) with respect to saturation temperature for both the liquid and vapor phases should be positive near the critical point. In the vapor phase, this should be true everywhere except for highly associating fluids. During fitting, the 3rd and 4th derivatives are also forced to be positive very close to the critical point to ensure proper critical region behavior.

7) For most fluids, the slope of isochores in both vapor, liquid, and critical states with respect to temperature should be negative (it is unclear if this criterion is also correct for associating fluids). Figure 48 shows this and the c_v criteria above for POE5.

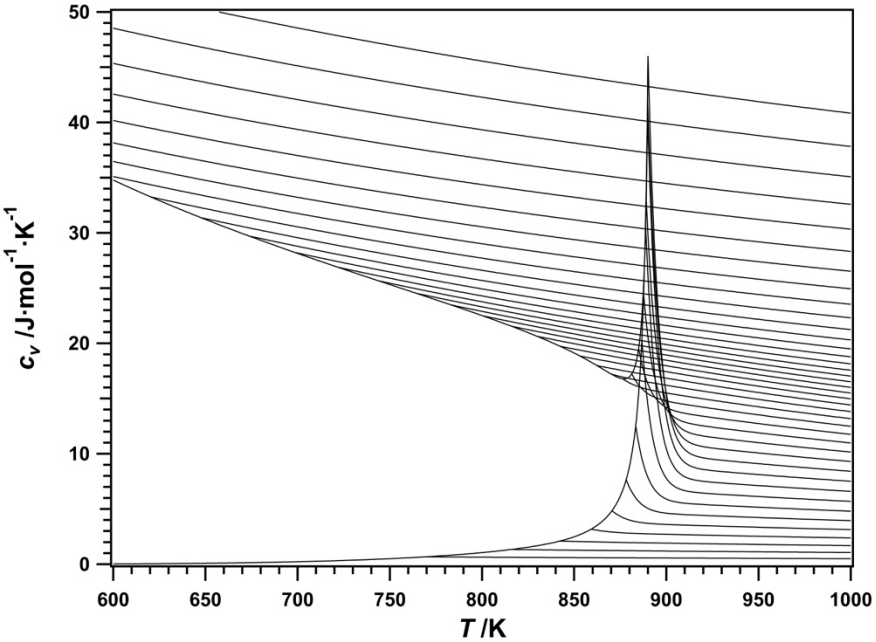

Figure 48: Residual isochoric heat capacity versus temperature diagram for POE5; lines of constant density up to 2 mol·dm^{-3} are shown.

8) The second, third, and fourth virial coefficients must conform to the same behavior as manifested in calculations from molecular simulations. The behavior of these virial coefficients from the equation of state for POE7 is shown in Figure 49; the curves shown are typical of those from statistical thermodynamic models.

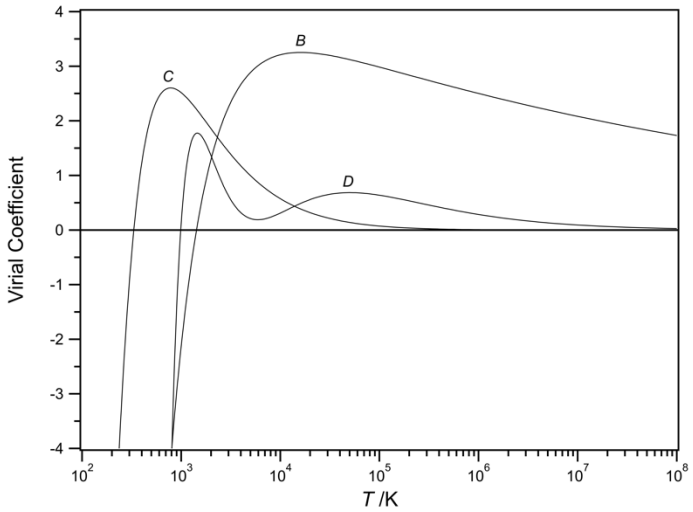

Figure 49: Calculated values of the second virial coefficient B ($dm^3 \cdot mol^{-1}$), third virial coefficient C ($dm^3 \cdot mol^{-1}$)^2, and fourth virial coefficient D ($dm^3 \cdot mol^{-1}$)^3 for POE7.

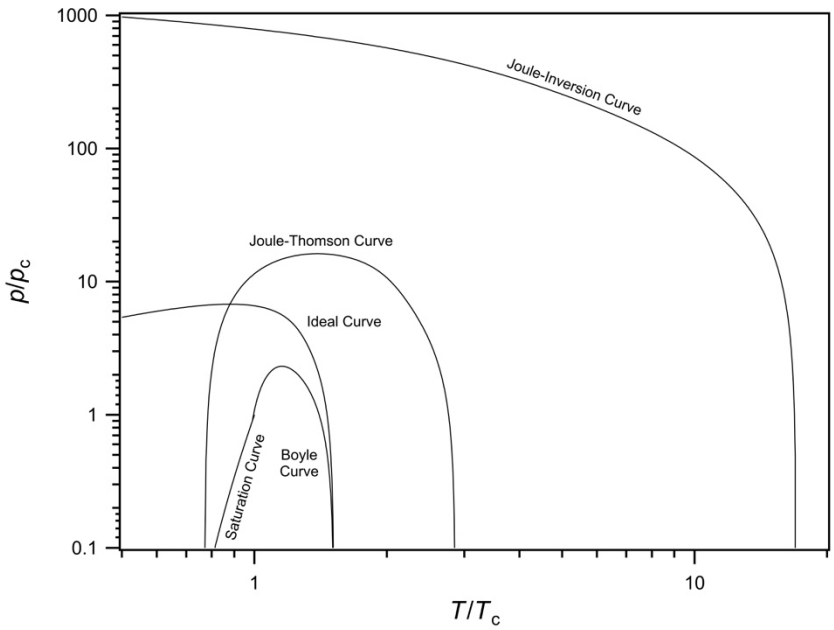

Figure 50: Characteristic (ideal) curves of the equation of state for POE9 as a function of temperature and pressure.

9) The ideal curves, as described in other publications on equations of state, must be smooth and appear similar to that shown in the R-125 publication.[60] The curves shown in Figure 50 for POE9 do not fully meet these criteria but are sufficiently correct for the application of the oils fitted in this work.

There are numerous other criteria that must be fulfilled before an equation can be considered "finished", but these are not documented here. The nine above are the most important, and the equations here meet all of the other criteria.

12.2.4. Estimated Uncertainties of Calculated Properties

The expanded uncertainty of calculated values in the liquid phase for the oils that were measured in this work is 0.2 % in density and speed of sound between 260 K and 450 K with pressures to 70 MPa. For speed of sound, the uncertainty may increase to 0.3 % above 380 K. Outside of these ranges, the uncertainties will slowly increase as a function of the distance from the upper or lower bounds given above. The amount of the increase is unknown but will be gradual (based on experience in fitting other equations where the extrapolation behavior of the equation is correct). For these fluids, the values could be as small as 0.4 % at 220 K (assuming the oil is still fluid) or, for density, at temperatures up to 600 K. The uncertainties in the critical region and vapor phase are unknown, but not expected to exceed 1 % for density at temperatures up to 600 K in the vapor phase. The uncertainty in vapor-phase speed of sound is unknown due to the lack of information pertaining to the ideal-gas isobaric heat capacity.

The uncertainties in heat capacities in the liquid phase are 0.5 % from 250 K to 450 K, except for POE9 where the uncertainty increases to 1 % or more below 330 K. The uncertainties for vapor pressures are difficult to quantify due to the extremely low vapor pressures below 500 K. An approximate value would be one order of magnitude; for example, at a temperature where the calculated value of the vapor pressure is 1 Pa, the true value could be between 0.1 Pa to 10 Pa. For vapor pressures above 0.1 MPa, the same may be true, but it is estimated that the uncertainties would be less than 50 %. For example, the equation for POE5 calculates a temperature at 0.1 MPa of 707 K, but the true value may lie between 671 K (where the vapor pressure is 0.05 MPa) and 730 K (where the vapor pressure is 0.15 MPa).

12.2.5. Calculated Values

As an aid in code implementation, calculated values of properties from the equation of state are given in Table 31. The number of digits displayed does not indicate the accuracy in the values but are given for validation of computer code.

Table 31: Calculated Values of Properties for Algorithm Verification.

	T /K	ρ /mol·dm^{-3}	p /MPa	c_v /J·mol^{-1}·K^{-1}	c_p /J·mol^{-1}·K^{-1}	w /m·s^{-1}
POE5	300.0	2.24	86.7515	710.515	845.862	1658.37
	890.0	0.555	1.26998	1362.9	52007400.0	32.6999
	800.0	0.079	0.422597	1260.95	1283.6	93.9009
	500.0	0.0	0.0	942.314	950.628	94.2014
POE7	300.0	1.74	87.1105	906.79	1073.18	1683.26
	940.0	0.41	1.03	2229.74	8161290.0	25.6542
	800.0	0.027	0.160361	1919.11	1933.27	94.9921
	500.0	0.0	0.0	1243.0	1251.32	84.5927
POE9	300.0	1.43	95.8767	1151.98	1352.93	1733.14
	970.0	0.32	0.884998	3064.23	9291810.0	18.8048
	800.0	0.017	0.104378	2546.39	2558.4	90.0762
	500.0	0.0	0.0	1572.95	1581.26	77.4309
MIL-PRF-23699	300.0	1.8	28.5227	841.412	1003.51	1478.92
	930.0	0.44	1.08	1652.07	36093600.0	28.9772
	800.0	0.036	0.209763	1509.9	1525.29	95.3025
	500.0	0.0	0.0	1142.46	1150.77	86.6593

12.3. Viscosity Modeling

12.3.1. Methodology

There are a wide variety of models that can be used to represent the viscosity of a pure fluid. In this project, the primary concern was to represent the liquid-phase viscosity over a wide range of pressures including up to relatively high pressures of 140 MPa. Since the final goal is to provide a model that can be incorporated into REFPROP[21], the model must also be able to represent the viscosity of the gas and supercritical phases, even though experimental data is not available in these regions. Thus we have chosen a hybrid approach[61] that represents the viscosity as a sum of terms;

Error! Bookmark not defined.

$$\eta(\rho_r, T_r) = \eta_0(T_r) + \Delta\eta(\rho_r, T_r) + \Delta\eta_c(\rho_r, T_r), \quad (22)$$

where ρ_r and T_r are reduced density and temperature given by $\rho_r = \rho/\rho_c$ and $T_r = T/T_c$, the subscript c denotes critical values, and the first term, $\eta_0(T)$, is the contribution to the viscosity in the dilute-gas limit. The critical enhancement term, $\Delta\eta_c(\rho,T)$, arises from the long-range density fluctuations that occur in a fluid near its critical point, which contribute to divergence of the viscosity at the critical point. Finally, the term $\Delta\eta(\rho,T)$, the residual term, represents the contribution of all other

effects to the viscosity of the fluid at elevated densities including many-body collisions, molecular-velocity correlations, and collisional transfer. In this work, we will use the estimation method of Chung et al.[62] for the zero-density term, we will neglect the critical enhancement term, and use an empirical model for the residual contribution. The critical enhancement for viscosity contributes only very near to the critical point, and we will not discuss it further here.

As mentioned above, the dilute-gas viscosity is calculated with the model of Chung et al.[62]:

$$\eta_0(T) = 4.0785\sqrt{MT}\,\frac{F_c}{V_c^{2/3}\,\Omega_\eta^*}\ , \tag{23}$$

Where Ω_η^* is the viscosity collision integral, F_c is the higher order correction factor (neglecting the contribution from the dipole moment and association effects), given as

$$\begin{aligned}\Omega_\eta^* &= 1.16145T^{*-0.14874} + 0.52487\exp(-0.77320T^*) + 2.16178\exp(-2.43787T^*) \\ &- 6.435x10^{-4}T^{*0.14874}\sin(18.0323T^{*-0.76830} - 7.27371)\end{aligned} \tag{24}$$

and

$$F_c = 1 - 0.2756\omega\ , \tag{25}$$

where $T^* = T/\varepsilon$, is the reduced temperature and ε (K) is the energy scaling parameter. This parameter was obtained with the method of Chung et al.[62] according to

$$\varepsilon/k = T_c/1.2593, \tag{26}$$

where V_c is the critical volume in $cm^3 \cdot mol^{-1}$, T_c is in K, and M is the molar mass of the fluid in $g \cdot mol^{-1}$, ω is the dimensionless acentric factor, and the viscosity is in μPa·s.

The residual viscosity term, $\Delta\eta(\rho_r,T_r)$, represents the contribution of all other effects to the viscosity of the fluid at elevated densities including many-body collisions, molecular-velocity correlations, and collisional transfer. Because there is little theoretical guidance concerning this term, we develop an empirical model based on our experimentally obtained data. The procedure adopted during this analysis uses symbolic regression software[63] to fit the experimental data to the residual viscosity. Symbolic regression is a type of genetic programming that allows the

exploration of arbitrary functional forms to regress data. The functional form is obtained by use of a set of operators, parameters, and variables as building blocks. We first adopt a form suggested by the hard sphere model of Assael et al.[64] and pull out a factor ($\rho_r^{2/3}T_r^{1/2}$), such that $\Delta\eta(\rho_r,T_r) = (\rho_r^{2/3}T_r^{1/2})F(\rho_r,T_r)$. We have used this approach successfully for a variety of fluids, including alkanes[65] and refrigerants[66], and most recently, ammonia[67]. Since we are interested in the viscosity of highly viscous fluids at high pressures, we adopt a scaled variable $\Gamma = \rho_r^{\gamma}/T_r$, also referred to as thermodynamic scaling, suggested by the works of Bair and Casalini.[68] Scaling in this variable has been suggested as a way to obtain good extrapolation to high pressures. The power γ is determined by plotting the residual viscosity $(\eta-\eta_0)/(\rho_r^{2/3}T_r^{1/2})$ vs ρ_r^{γ}/T_r and finding the value of γ that causes the data to collapse into a single line. Symbolic regression is then used to find the function $\Delta\eta(\rho_r,T_r) = (\rho_r^{2/3}T_r^{1/2})F(\rho_r,T_r)$. In the present work, we restricted the operators to the set (+,−,×,/) and the operands (constant, T_r, ρ_r and ρ_r^{γ}/T_r), with γ fixed as described previously. All densities are obtained from the equations of state described earlier in this report. The functional form for each fluid will be determined by the symbolic regression algorithm based on the available data and will not be the same for each fluid.

12.3.2. Results

12.3.2.1. POE5

The equation of state for POE5 discussed in Section 12.2 has the following values for critical temperature and density, that we adopt here as well: T_c = 890.0 K, ρ_c = 0.556 mol·L^{-1}. The molar mass is 472.612 g·mol^{-1} and the acentric factor is 0.89. Using Eqs. 25 – 26 leads to ε/k = 706.7418 K and F_c = 0.75472. The density scaling factor was found to be γ = 3.58. The equation for residual viscosity obtained from symbolic regression was

$$\Delta\eta(\rho_r,T_r) = (a_1\Gamma + a_2\Gamma^2 + a_3\Gamma^6 + a_4\Gamma^{13})\sqrt{T_r}\rho_r^{2/3}, \quad (27)$$

where $\Gamma = \rho_r^{3.58}/T_r$, a_1 = 1.4307113, a_2 = 0.019090959, a_3 = 4.0904180×10^{-12} and a_4 = 1.3888478×10^{-30}. Eqs. 22 – 26 combined with Eq. 27 are then used to calculate the viscosity. Comparisons with our experimental data in Section 10 resulted in an average absolute deviation of 1.8 %, a bias of 0.13 %, and an uncertainty at the 95 % level of 4.7 %. This is consistent with the experimental uncertainty estimated to be 5 % at the lowest pressures rising to 10 % at the highest pressure nearing 140 MPa. Deviation plots as a function of temperature, pressure and density are shown in Figures 51 – 53. As shown in Figure 52, we did not observe any trends in the deviations as a function of pressure.

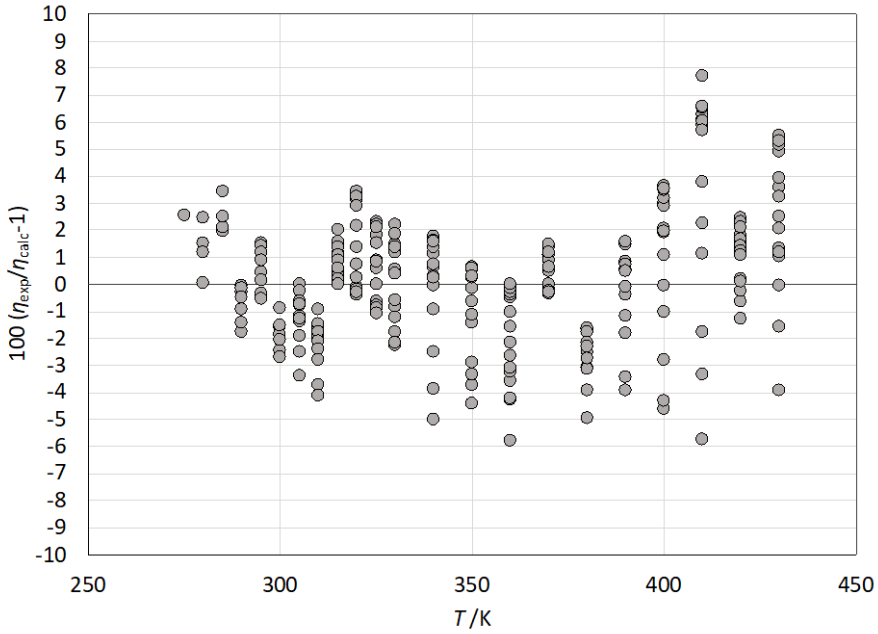

Figure 51: Percentage deviations in viscosity for POE5 as a function of temperature.

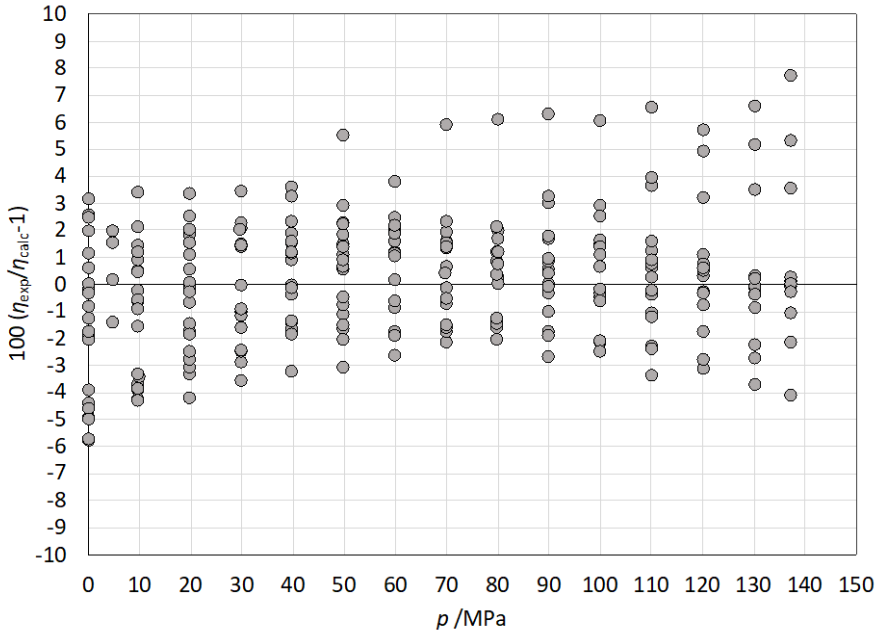

Figure 52: Percentage deviations in viscosity for POE5 as a function of pressure.

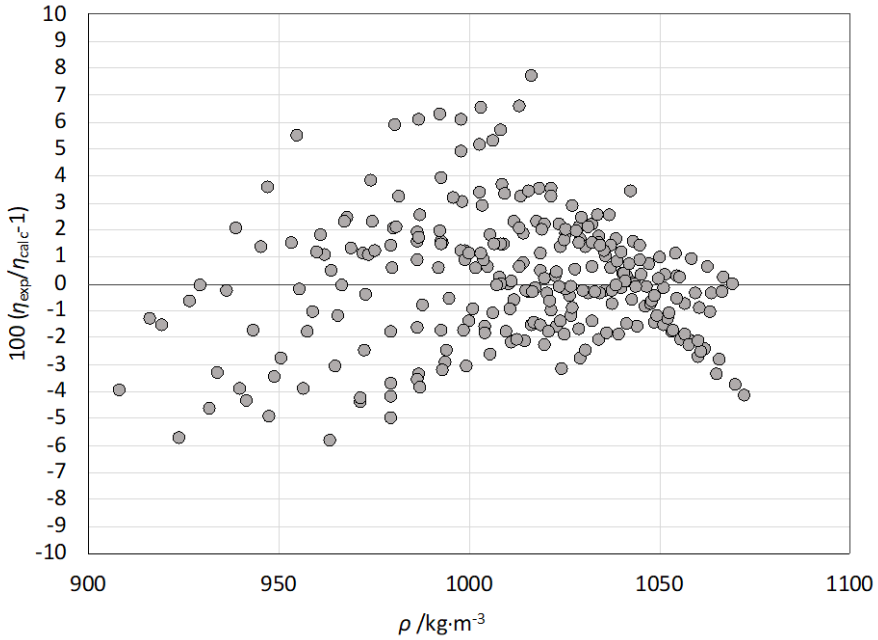

Figure 53: Percentage deviations in viscosity for POE5 as a function of density.

12.3.2.2. POE7

The equation of state for POE7 discussed in section 12.2 has the following values for critical temperature and density, that we adopt here as well: T_c = 940.0 K, ρ_c = 0.412 mol·L^{-1}. The molar mass is 584.835 g·mol^{-1} and the acentric factor is 1.06. Using Eqs. 25 – 26 leads to ε/k = 746.4464 K and F_c = 0.70786. The density scaling factor was found to be γ = 3.43. The equation for residual viscosity obtained from symbolic regression was

$$\Delta\eta(\rho_r, T_r) = (a_1\Gamma^5 + a_2\Gamma^{13} + a_3 T_r^2\Gamma^2)\sqrt{T_r}\rho_r^{2/3}\,, \tag{28}$$

where $\Gamma = \rho_r^{3.43}/T_r$, a_1 = 1.8292961×10^{-9}, a_2 = 2.2667078×10^{-30}, and a_3 = 0.10216630. Eqs. 22 – 26 combined with Eq. 28 are then used to calculate the viscosity. Comparisons with our experimental data in Section 10 resulted in an average absolute deviation of 1.8 %, a bias of 0.0 %, and an uncertainty at the 95 % level of 4.5 %. This is consistent with the estimated experimental uncertainty estimated to be 5 % at the lowest pressures rising to 10 % at the highest pressure nearing 140 MPa. Deviation plots as a function of temperature, pressure and density are shown in Figures 54 – 56. We did not observe any systematic trends in the deviations.

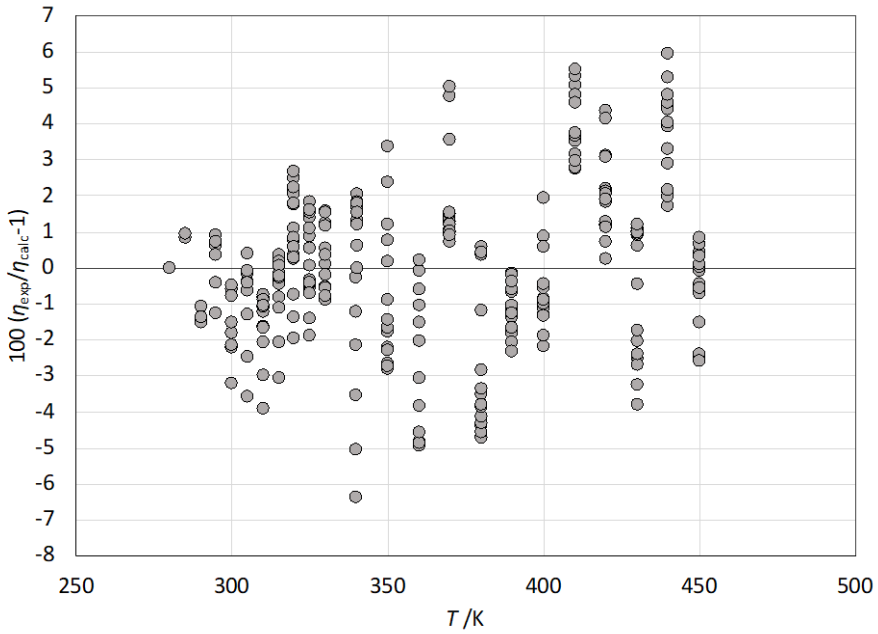

Figure 54: Percentage deviations in viscosity for POE7 as a function of temperature.

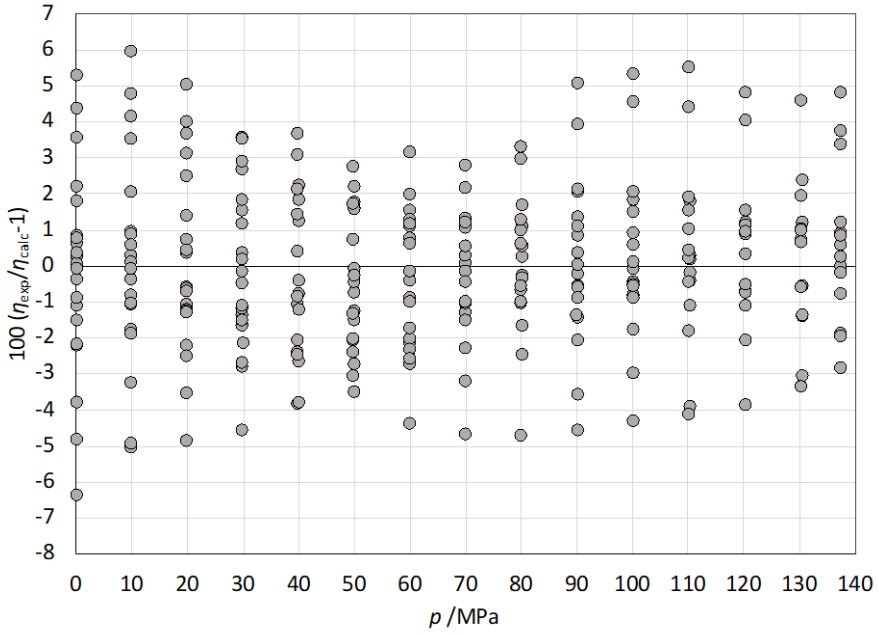

Figure 55: Percentage deviations in viscosity for POE7 as a function of pressure.

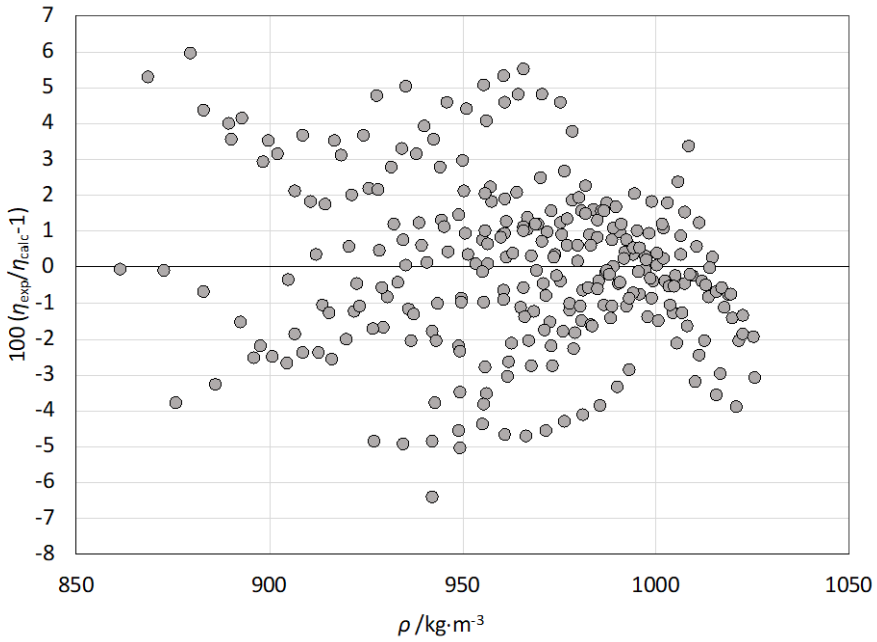

Figure 56: Percentage deviations in viscosity for POE7 as a function of density.

12.3.2.3. POE9

The equation of state for POE9 discussed in Section 12.2 has the following values for critical temperature and density, that we adopt here as well: T_c = 970.0 K and ρ_c = 0.316 mol·L^{-1}. The molar mass is 697.051 g·mol^{-1} and the acentric factor is 0.998. Using Eqs. 25 – 26 leads to ε/k = 770.2692 K, and F_c = 0.72495. The density scaling factor was found to be γ = 3.36. The equation for residual viscosity obtained from symbolic regression was

$$\Delta\eta(\rho_r, T_r) = (a_1\Gamma + a_2\Gamma^2 + a_3\Gamma^3 + a_4\Gamma^{11})\sqrt{T_r}\rho_r^{2/3}, \quad (29)$$

where $\Gamma = \rho_r^{3.36}/T_r$, a_1 = 4.9977918, a_2 = -0.049733553, a_3 = 0.00025851171, and $a_4 = 1.6282415\times10^{-25}$. Eqs. 22 – 26 combined with Eq. 29 are then used to calculate the viscosity. Comparisons with our experimental data in Section 10 resulted in an average absolute deviation of 2.5 %, a bias of -0.8 %, and an uncertainty at the 95 % level of 6.8 %. This is slightly larger than the estimated experimental uncertainty estimated to be 5 % at the lowest pressures rising to 10 % at the highest pressure nearing 140 MPa. Deviation plots as a function of temperature, pressure and density are shown in Figures 57 – 59. We did not observe any trends in the deviations.

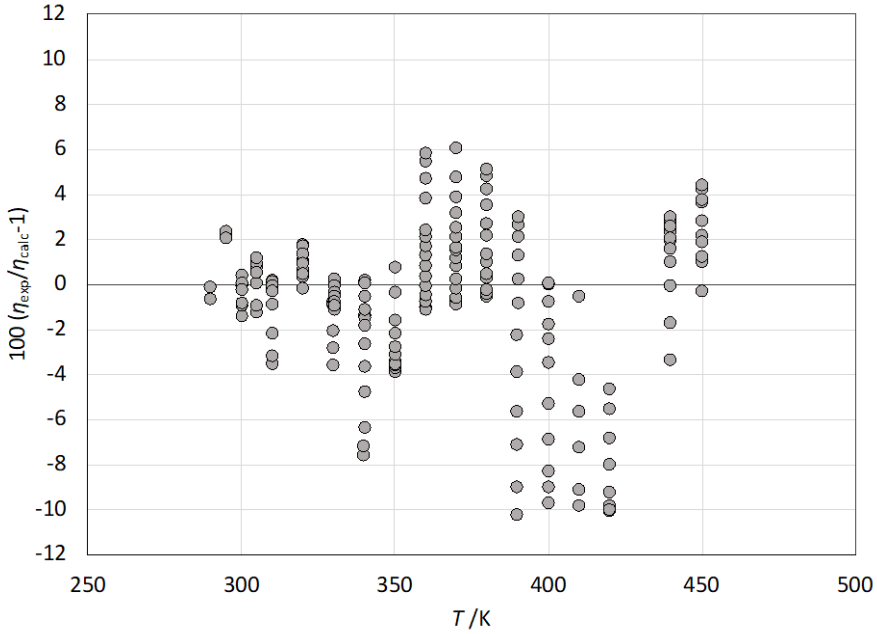

Figure 57: Percentage deviations in viscosity for POE9 as a function of temperature.

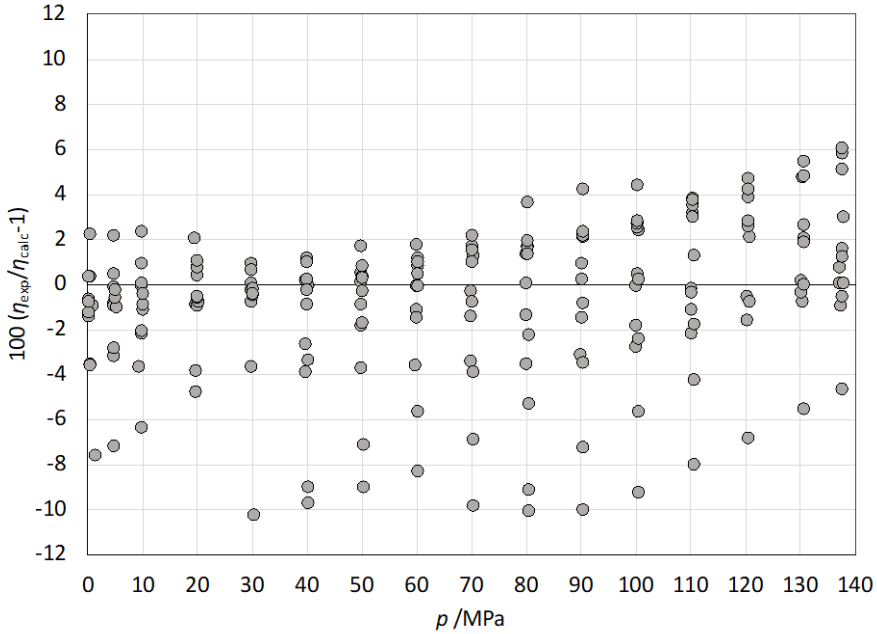

Figure 58: Percentage deviations in viscosity for POE9 as a function of pressure.

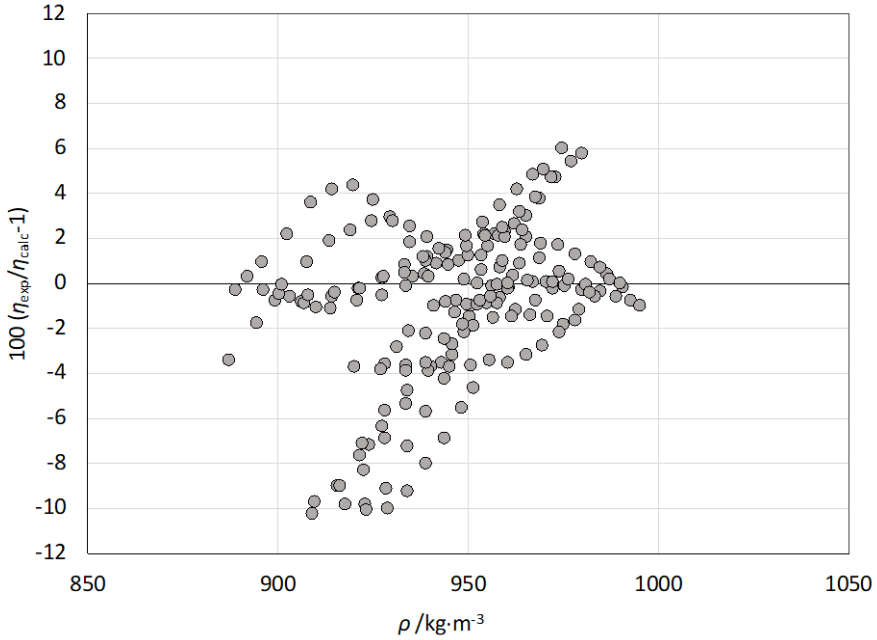

Figure 59: Percentage deviations in viscosity for POE9 as a function of density.

12.4. Thermal Conductivity Modeling

12.4.1. Methodology

Typically, similar to how viscosity is treated, the thermal conductivity is expressed in terms of a dilute gas, residual, and critical enhancement terms:

$$\lambda(T_\mathrm{r}, \rho_\mathrm{r}) = \lambda^0(T_\mathrm{r}) + \Delta\lambda^\mathrm{res}(T_\mathrm{r}, \rho_\mathrm{r}) + \lambda^\mathrm{crit}(T_\mathrm{r}, \rho_\mathrm{r}), \tag{30}$$

where the dilute gas contribution λ_0 is a function of T only. In this work we do not have any experimental data in the gas phase, so we use Chapman-Enskog theory as described in Huber[61] to generate estimates of zero-density thermal conductivity values, which are then fit to a simple polynomial form:

$$\lambda^0(T_\mathrm{r}) = \sum_{k=0}^{n} \alpha_k \, T_\mathrm{r}^k \tag{31}$$

The residual contribution λ^res is written as a polynomial in terms of temperature and density,

$$\Delta\lambda^\mathrm{res}(T, \rho) = \sum_{l=1}^{3} (\beta_{1,l} + \beta_{2,l}(T/T_\mathrm{c}))(\rho/\rho_\mathrm{c})^l \tag{32}$$

and the coefficients are found by fitting experimental data. The critical enhancement contribution is estimated using the generalized method described in Perkins et al.[69] that requires only T_c, ρ_c, p_c, the acentric factor ω and the molar mass of the component.

12.4.2. Results

12.4.2.1. POE5

We fit the liquid-phase thermal conductivity data described in Section 9, incorporating estimated vapor-phase predictions, and obtained the following coefficients for Eq. 31 and Eq. 32. All densities were determined from the EOS described in Section 12.2. The resulting coefficients are given in Table 32. Comparisons with our experimental data (Section 9) resulted in an average absolute deviation of 0.12 %, a bias of 0.0 %, and an uncertainty at the 95 % level of 0.3 %. This is well within the estimated experimental uncertainty estimated to be 0.5 % for the entire range of the experiments that covered 301 K to 502 K at pressures up to 69 MPa. Deviation plots as a function of temperature, pressure and density are shown in Figures 60 – 62.

Table 32: Coefficients for the Thermal Conductivity Equation for POE5.

Coefficients	
α_0	1.847472
α_1	-18.00409
α_2	108.2592
α_3	-80.25605
α_4	26.80722
α_5	-3.439569
$\beta_{1,1}$	0.00804625
$\beta_{1,2}$	0.00500470
$\beta_{1,3}$	-0.000211256
$\beta_{2,1}$	0.0561869
$\beta_{2,2}$	-0.0542289
$\beta_{2,3}$	0.0126351

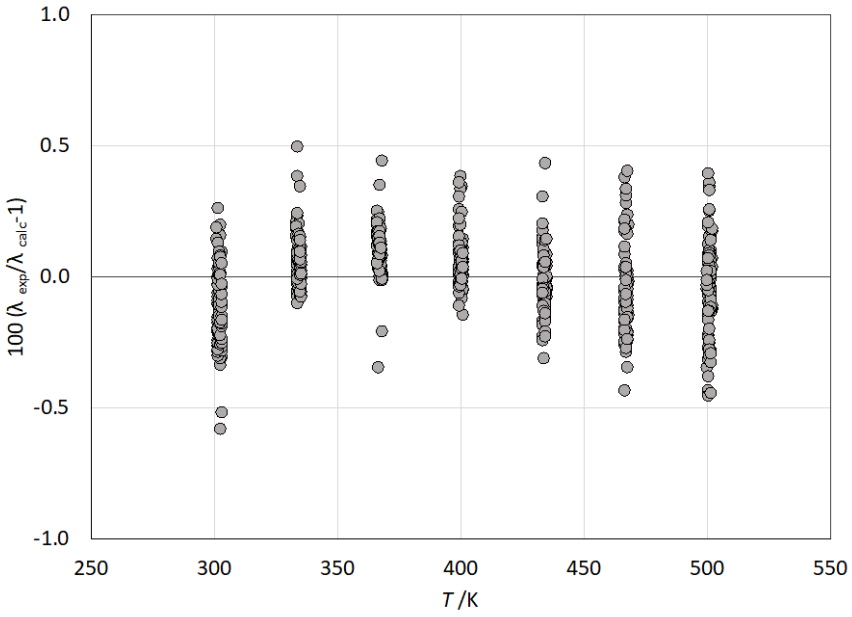

Figure 60: Percentage deviations in thermal conductivity for POE5 as a function of temperature.

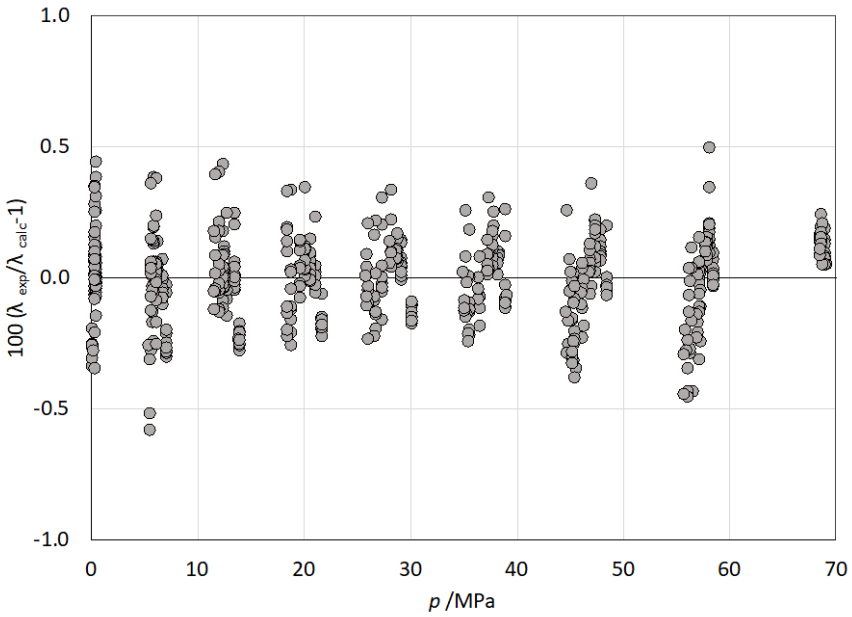

Figure 61: Percentage deviations in thermal conductivity for POE5 as a function of pressure.

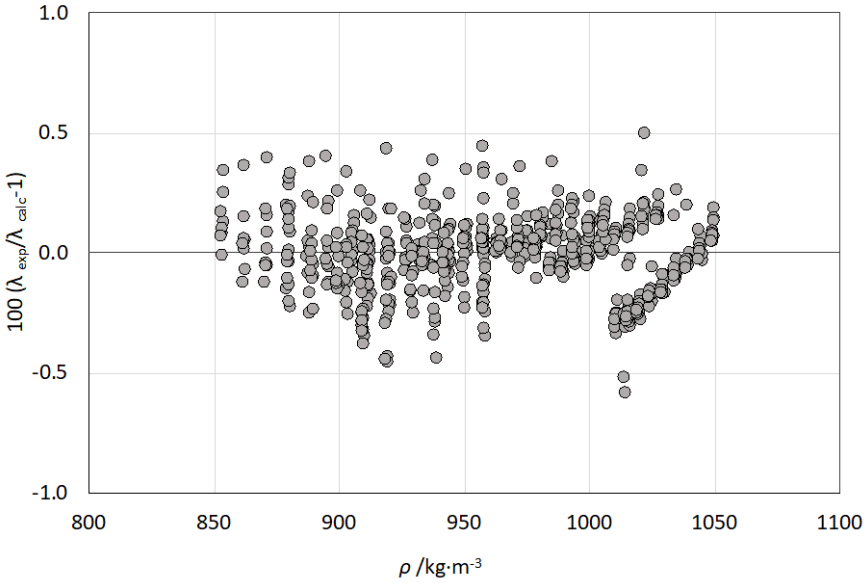

Figure 62: Percentage deviations in thermal conductivity for POE5 as a function of density.

12.4.2.2. POE7

We fit the liquid-phase thermal conductivity data described in Section 9, incorporating estimated vapor-phase predictions, and obtained the following coefficients for Eq. 31 and Eq. 32. All densities were determined from the EOS described in Section 12.2. The resulting coefficients are given in Table 33.

Table 33: Coefficients for the Thermal Conductivity Equation for POE7.

Coefficients	
α_0	5.0156798
α_1	-32.028343
α_2	112.07684
α_3	-52.063516
α_4	7.7818950
α_5	0.16886652
$\beta_{1,1}$	0.0314251
$\beta_{1,2}$	-0.00484656
$\beta_{1,3}$	0.000729462
$\beta_{2,1}$	0.0124139
$\beta_{2,2}$	-0.0359579
$\beta_{2,3}$	0.0105320

Comparisons with our experimental data (Section 9) resulted in an average absolute deviation of 0.24 %, a bias of 0.0 %, and an uncertainty at the 95 % level of 0.7 %. This is slightly above the estimated experimental uncertainty estimated to be 0.5 % for the entire range of the experiments that covered 300 K to 504 K at pressures up to 69 MPa. Deviation plots as a function of temperature, pressure and density are shown in Figures 63 – 65.

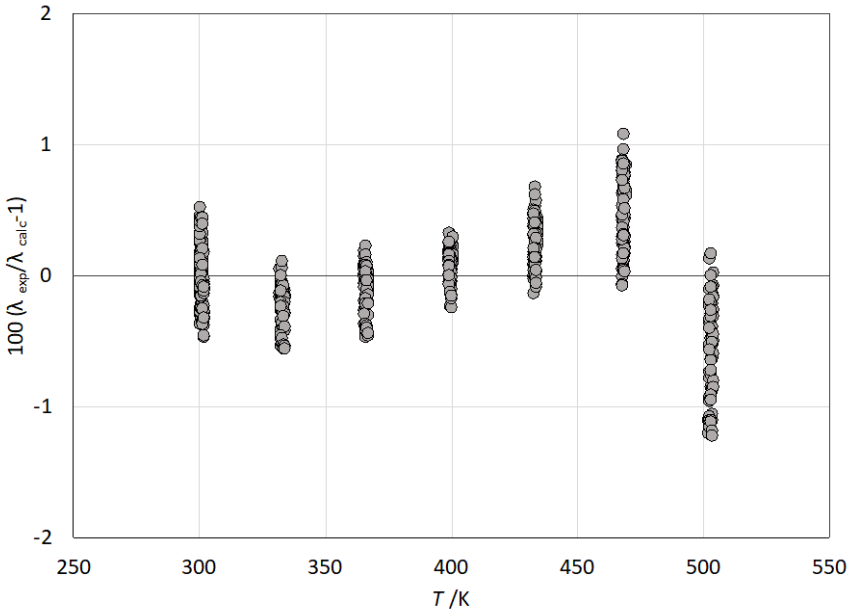

Figure 63: Percentage deviations in thermal conductivity for POE7 as a function of temperature.

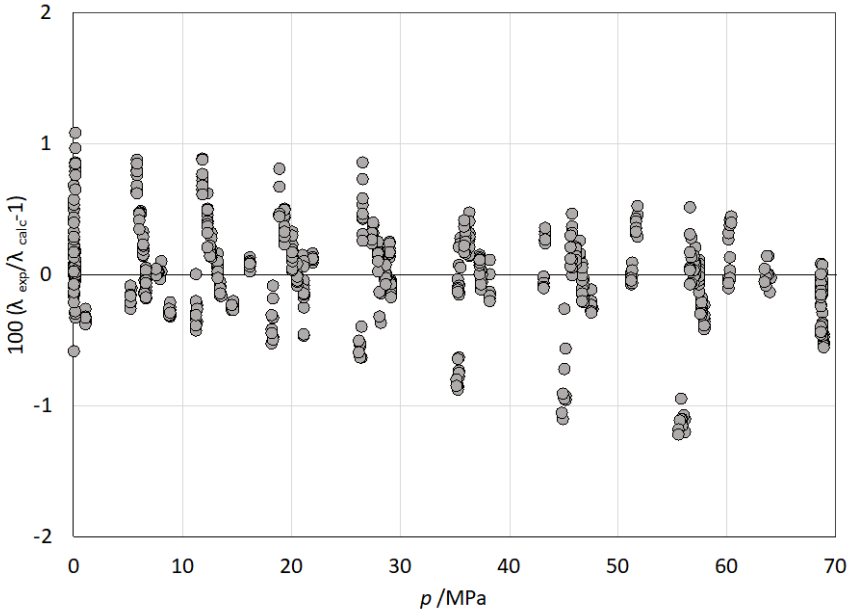

Figure 64: Percentage deviations in thermal conductivity for POE7 as a function of pressure.

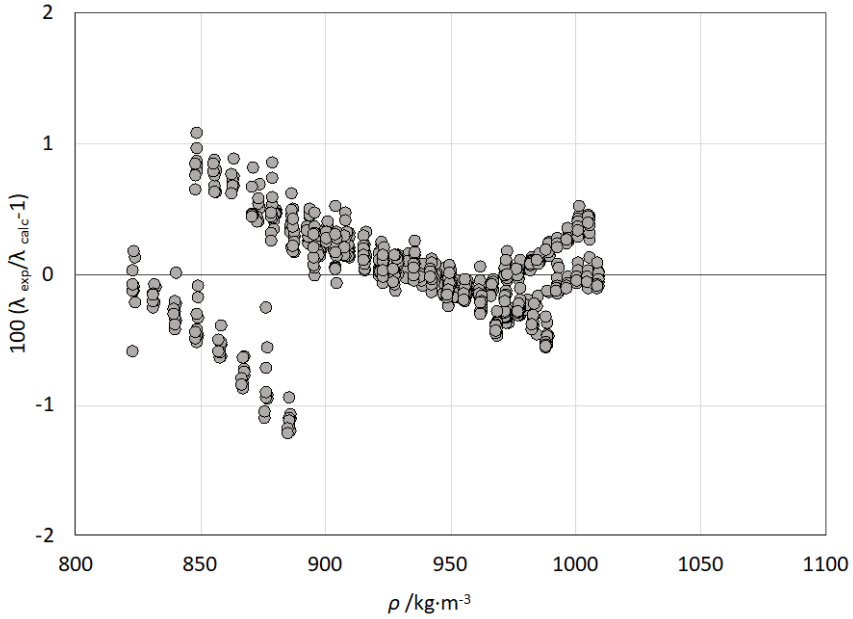

Figure 65: Percentage deviations in thermal conductivity for POE7 as a function of density.

12.4.2.3. POE9

We fit the liquid-phase thermal conductivity data described in Section 9, incorporating estimated vapor-phase predictions, and obtained the following coefficients for Eq. 31 and Eq. 32. All densities were determined from the EOS described in Section 12.2. The resulting coefficients are given in Table 34.

Table 34: Coefficients for the Thermal Conductivity Equation for POE9.

Coefficients	
α_0	-2.617097
α_1	43.187405
α_2	-160.22117
α_3	404.97948
α_4	-339.90316
α_5	99.120658
$\beta_{1,1}$	0.0375194
$\beta_{1,2}$	-0.00967900
$\beta_{1,3}$	0.00151768
$\beta_{2,1}$	0.00348471
$\beta_{2,2}$	-0.0229526
$\beta_{2,3}$	0.00707870

Comparisons with our experimental data (Section 9) resulted in an average absolute deviation of 0.13 %, a bias of 0.0 %, and an uncertainty at the 95 % level of 0.4 %. This is within the estimated experimental uncertainty estimated to be 0.5 % for the entire range of the experiments that covered 301 K to 500 K at pressures up to 69 MPa. Deviation plots as a function of temperature, pressure and density are shown in Figures 66 – 68.

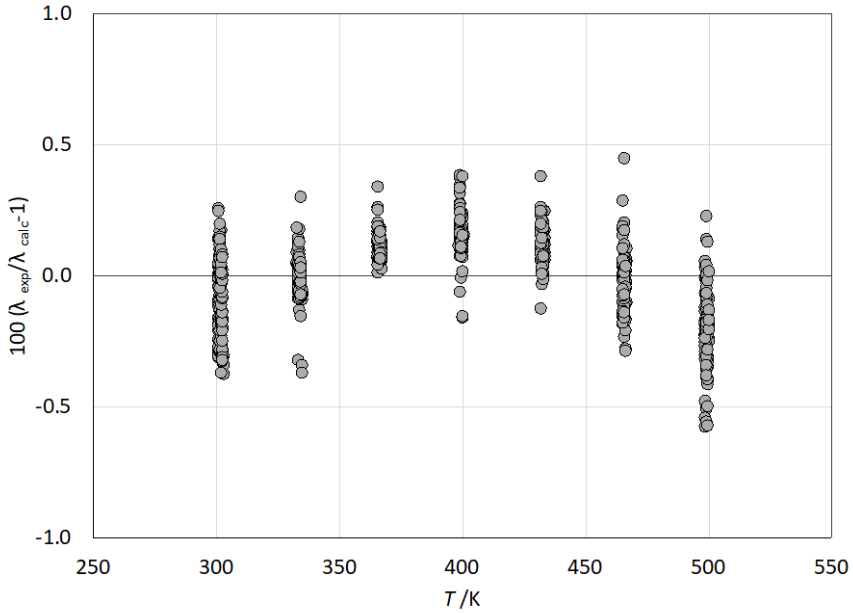

Figure 66: Percentage deviations in thermal conductivity for POE9 as a function of temperature.

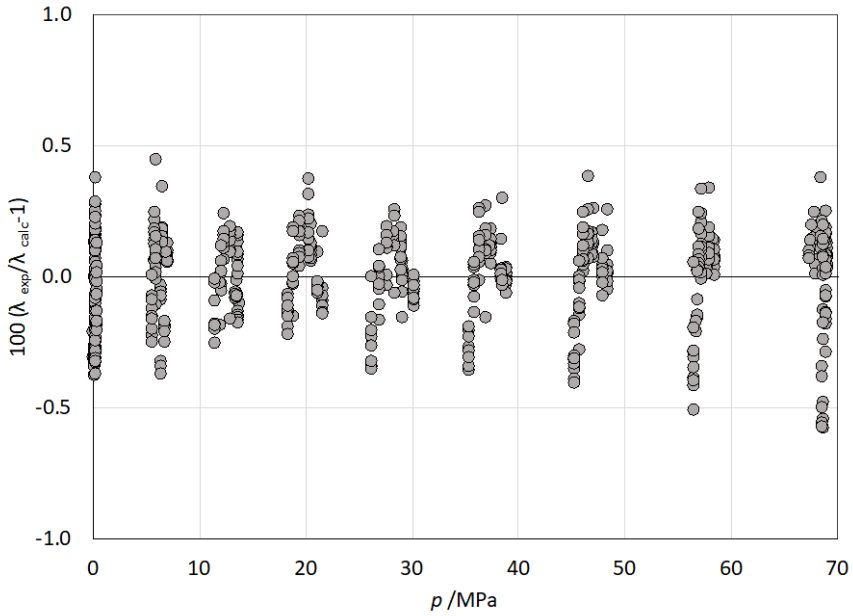

Figure 67: Percentage deviations in thermal conductivity for POE9 as a function of pressure.

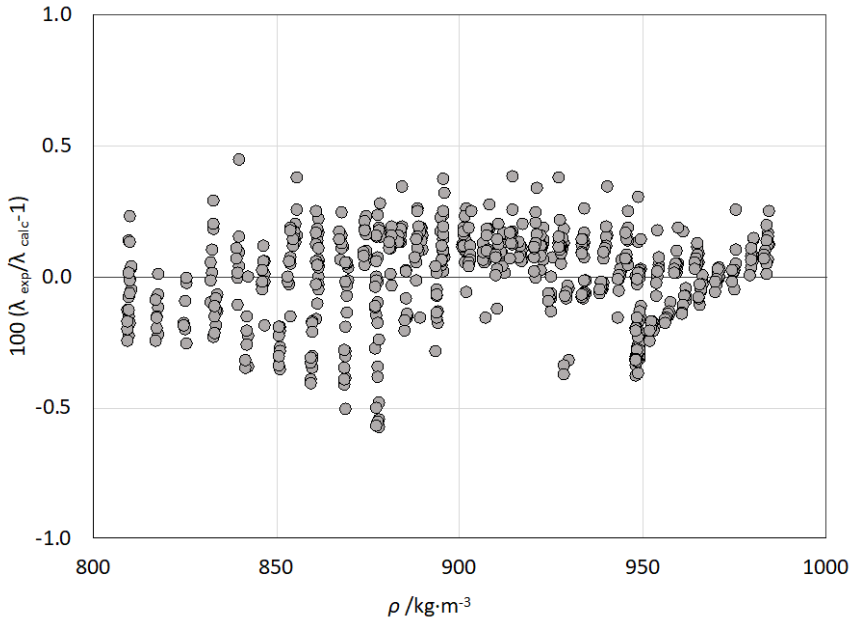

Figure 68: Percentage deviations in thermal conductivity for POE9 as a function of density.

12.5. Mixture Modeling

We have taken two different approaches to modeling the fully qualified lubricant, which is a mixture of numerous components. The first method treats the mixture as a pseudo-pure fluid, and an equation of state, viscosity and thermal conductivity correlations are developed by fitting experimental mixture data. This approach has been used successfully to model mixtures such as air[70], as well as several azeotropic and near-azeotropic refrigerant mixtures such as R404A, R407C, R410A and R507A.[71] Advantages of this approach are that the data can be fit well, as it is treated exactly like a pure fluid. A disadvantage of the pseudo-pure fluid model is that one cannot model the volatility with a distillation curve with this type of model, because a pure fluid distills at a single temperature while a mixture will distill over a range of temperatures beginning with the most volatile component and ending with the least volatile component. An alternative approach, that we also take here, is to approximate the actual lubricant mixture with a surrogate mixture model[72-74]. In this approach, the lubricant is modeled as a defined mixture of components whose composition is determined by finding a best match with the experimental data. The components are selected such that they are chemically similar to the components in the mixture but are not necessarily the actual components in the mixture. For the lubricant mixture considered here, the three pure POE fluids will be combined in such a way as to represent the properties of the actual lubricant.

12.5.1. Pseudo-Pure Fluid Model

12.5.1.1. MIL-PRF-23699 Viscosity Model

The equation of state for MIL-PRF-23699 discussed in Section 12.2 has the following values for critical temperature and density, that we adopt here as well: T_c = 930.0 K and ρ_c = 0.439 mol·L^{-1}. The molar mass is 557.6 g·mol^{-1} and the acentric factor is 0.97. Using Eqs. 25 – 26 leads to ε/k = 738.5055 K, and F_c = 0.73267. The density scaling factor was found to be γ = 3.58. The equation for residual viscosity obtained from symbolic regression was:

$$\Delta\eta(\rho_r, T_r) = (a_1\Gamma + a_2\Gamma^4 + a_3\Gamma^5 + a_4\Gamma^{11} + a_5 T_r + a_6 T_r^2)\sqrt{T_r}\rho_r^{2/3}, \qquad (33)$$

where $\Gamma = \rho_r^{3.35}/T_r$, a_1 = 3.0384588, a_2 = 9.5157314×10^{-07}, a_3 = -3.5296759×10^{-24}, a_4 = -3.5296759×10^{-24}, and a_5 = 0.014280851, and a_6 = 0.014280851. Eqs. 22 – 26 combined with Eq. 33 are then used to calculate the viscosity. Comparisons with our experimental data (Section 10) resulted in an average absolute deviation of 1.9 %, a bias of -0.1 %, and an uncertainty at the 95 % level of 5.0 %. The temperature range covered is 290 K to 450 K at pressures up to 137.4 MPa. This is consistent with the estimated experimental uncertainty, which was estimated to be 5 % at the lowest pressures rising to 10 % at the highest pressure nearing 140 MPa. Deviation plots as a function of temperature, pressure and density are shown in Figures 69 – 71. As shown in Figure 70, we observe only slight systematic trends in the deviations as a function of pressure.

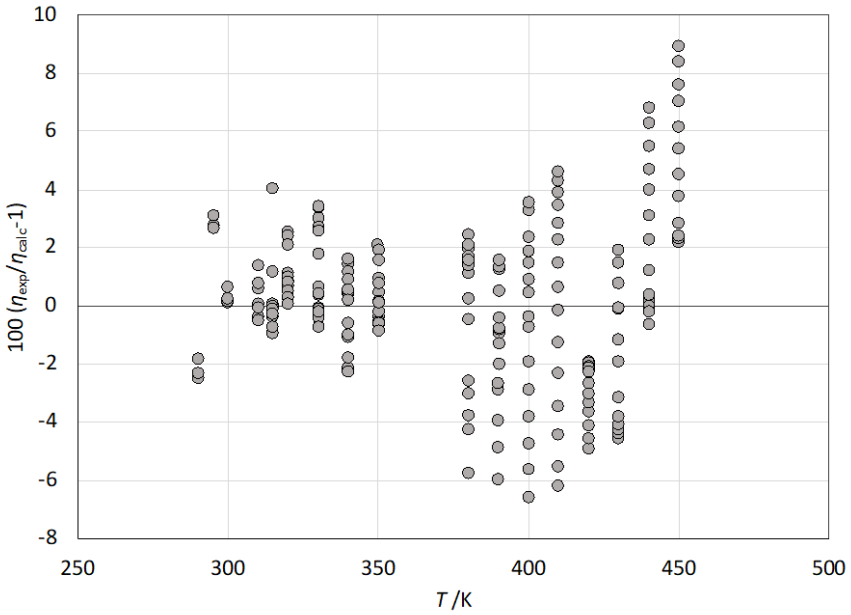

Figure 69: Percentage deviations in viscosity for MIL-PRF-23699 as a function of temperature.

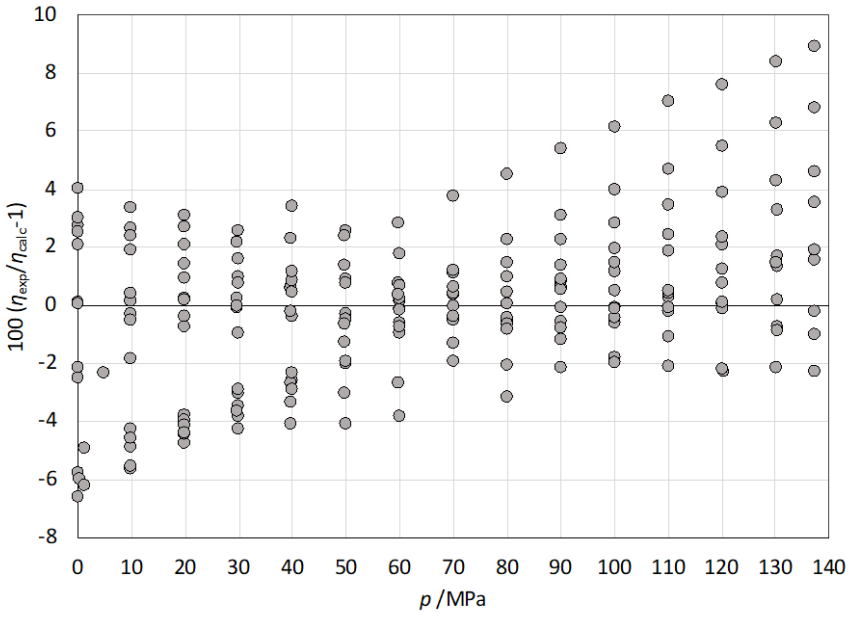

Figure 70: Percentage deviations in viscosity for MIL-PRF-23699 as a function of pressure.

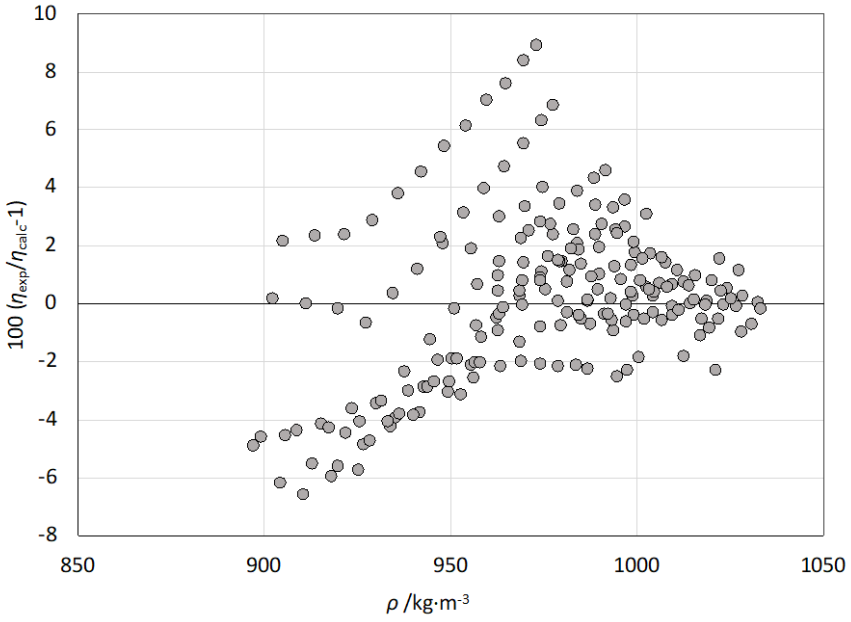

Figure 71: Percentage deviations in viscosity for MIL-PRF-23699 as a function of density.

12.5.1.2. MIL-PRF-23699 Thermal Conductivity Model

We fit the liquid-phase thermal conductivity data described in Section 9, incorporating estimated vapor-phase predictions, and obtained the following coefficients for Eq. 31 and Eq. 32. All densities were determined from the EOS described in Section 12.2. The resulting coefficients are given in Table 35. Comparisons with our experimental data (Section 9) resulted in an average

absolute deviation of 0.19 %, a bias of 0.0 %, and an uncertainty at the 95 % level of 0.5 %. This is consistent with the estimated experimental uncertainty, which was estimated to be 0.5 % for the entire range of the experiments that covered 301 K to 501 K at pressures up to 69 MPa. Deviation plots as a function of temperature, pressure and density are shown in Figures 72 – 74.

Table 35: Coefficients for the Thermal Conductivity Equation for MIL-PRF-23699.

Coefficients	
α_0	2.029847
α_1	-17.66899
α_2	106.7431
α_3	-83.01913
α_4	29.21753
α_5	-3.957349
$\beta_{1,1}$	-0.0717307
$\beta_{1,2}$	0.0411848
$\beta_{1,3}$	-0.00433472
$\beta_{2,1}$	0.1242990
$\beta_{2,2}$	-0.0759461
$\beta_{2,3}$	0.0133060

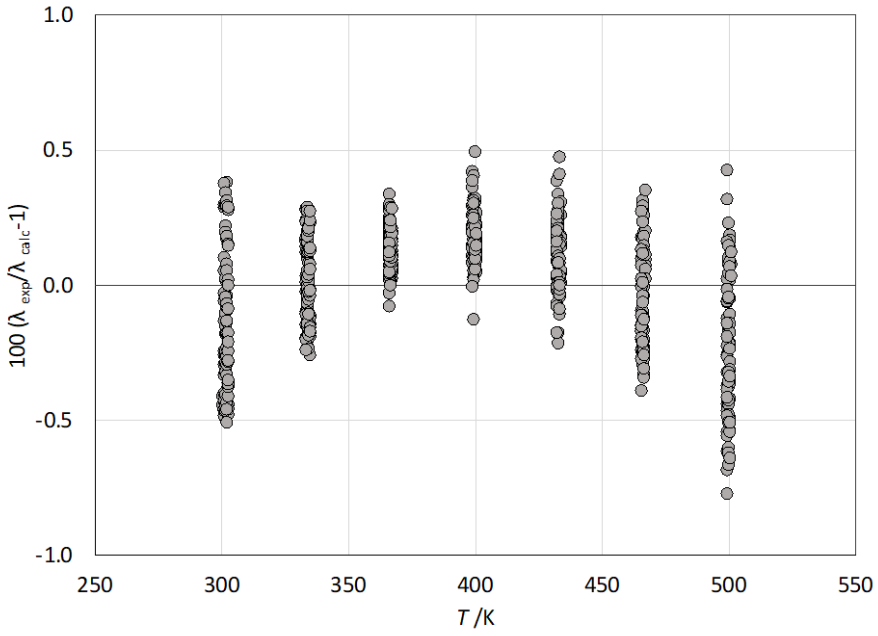

Figure 72: Percentage deviations in thermal conductivity for MIL-PRF-23699 as a function of temperature.

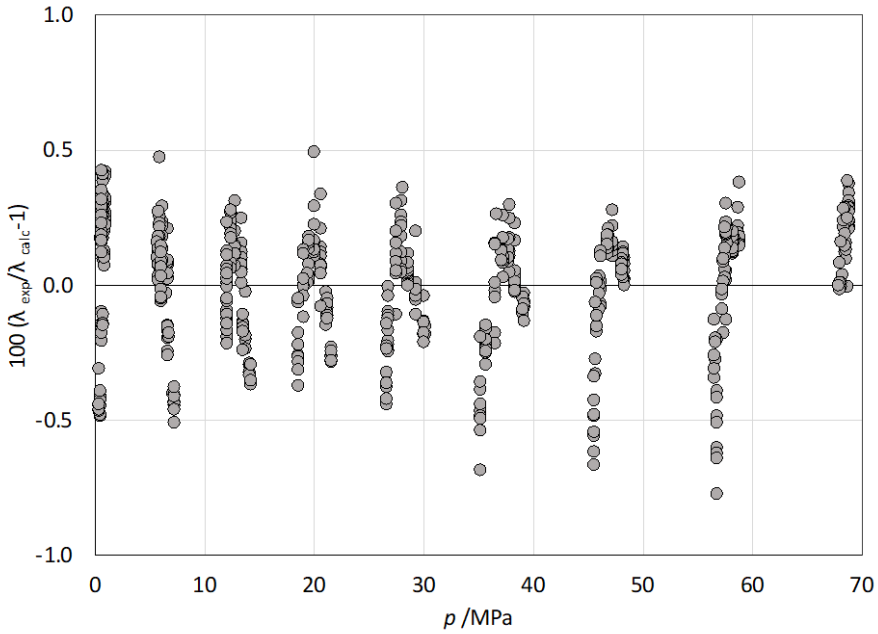

Figure 73: Percentage deviations in thermal conductivity for MIL-PRF-23699 as a function of pressure.

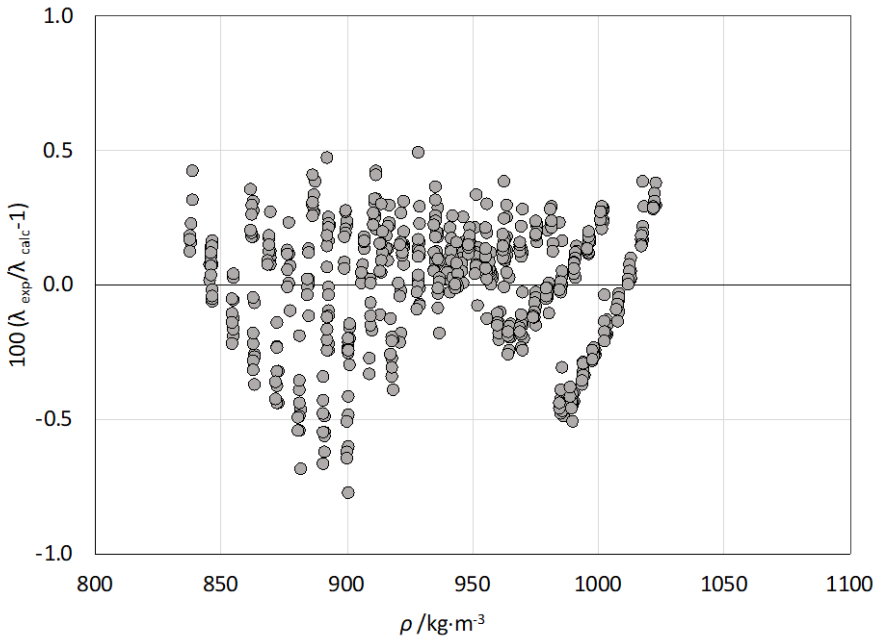

Figure 74: Percentage deviations in thermal conductivity for MIL-PRF-23699 as a function of density.

12.5.2. Surrogate Mixture Models

In order to model a complex fluid mixture, such as jet fuels, diesel fuels or rocket propellants, an approach that has been used successfully is to model the complex fluid as a surrogate mixture[72-74]. The general philosophy is to match desired properties (such as density, viscosity, thermal conductivity, sound speed, heat capacity) of the real mixture by finding compositions of a limited slate of well-characterized fluids that can be mixed together as a surrogate for the real mixture. The exact fluids that are in the actual mixture do not have to be present, but fluids that represent the chemical nature of the constituents should be present. In this project, we have three well-characterized fluids (POE5, POE7, and POE9) that are all polyol esters of the approximate weights of those in the actual mixture and the goal is to combine them in such a way as to represent the properties of the lubricant mixture MIL-PRF-23699.

It is instructive to observe trends among the POE fluids for the properties of interest at standard atmospheric pressure. Figures 75 – 79 show the properties density, sound speed, heat capacity, thermal conductivity, and viscosity at atmospheric pressure as a function of temperature for the three pure POEs, and for the actual lubricant mixture. The curves were generated with the EOS and transport models discussed in earlier sections that represent the experimental data to within, or close to within, the experimental uncertainty. For density, heat capacity, and thermal conductivity there is a clear pattern that the properties of the lubricant mixture fall in between those of POE5 and POE7. For the speed of sound, the lubricant mixture is very close to pure POE7. However, for the viscosity, the properties of the mixture fall in between those of POE7 and POE9, being closest to POE9 at lower temperatures and then becoming closer to POE7 as the temperature approaches 450 K. This presents a significant problem to modeling the lubricant mixture as a surrogate composed of POE5, POE7, and POE9. It just is not possible to combine these three fluids in such a way to capture all properties with a surrogate model approach. That said, we will present here two surrogate model choices. One that focuses more on the representation of the viscosity, and a second that focuses on the equilibrium properties and thermal conductivity. The performance of either of these two models is not as accurate as the pseudo-pure fluid approach discussed earlier but serves as an alternative methodology if a true mixture is required.

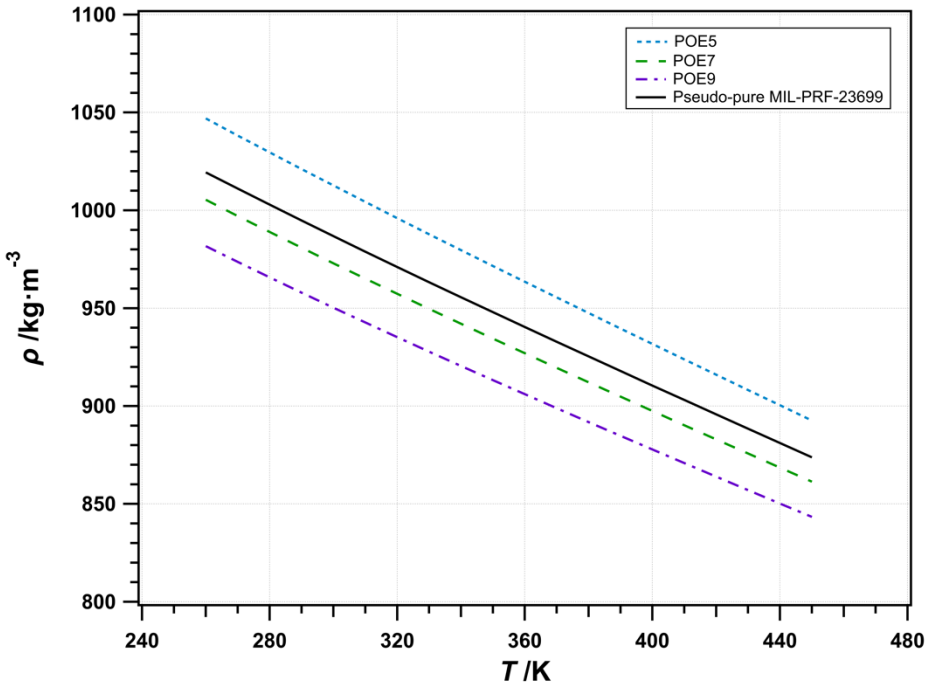

Figure 75: Density at atmospheric pressure as a function of temperature for POE5, POE7, POE9, and MIL-PRF-23699.

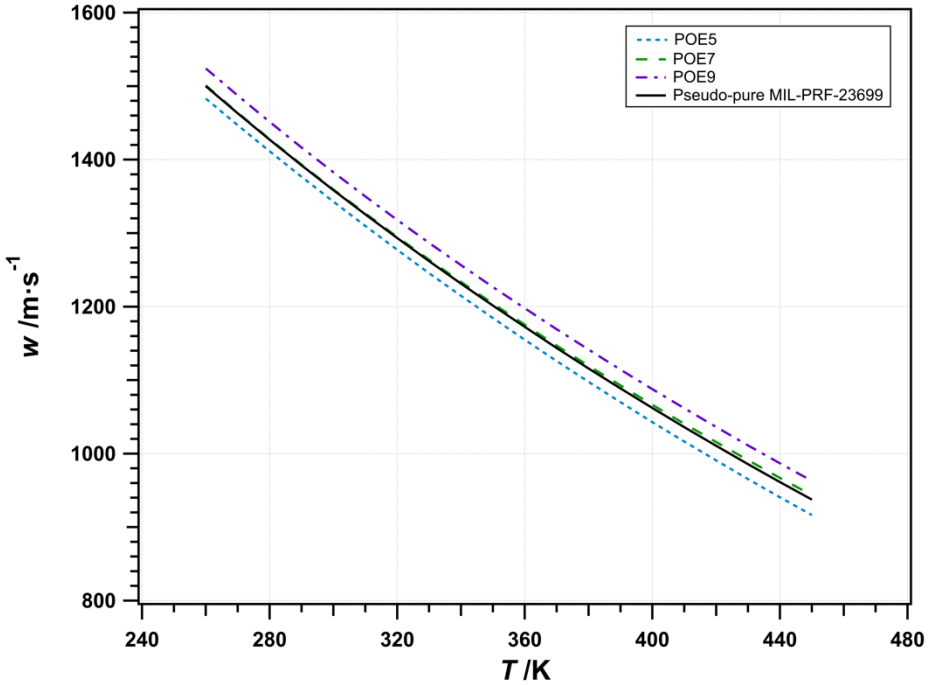

Figure 76: Speed of sound at atmospheric pressure as a function of temperature for POE5, POE7, POE9, and MIL-PRF-23699.

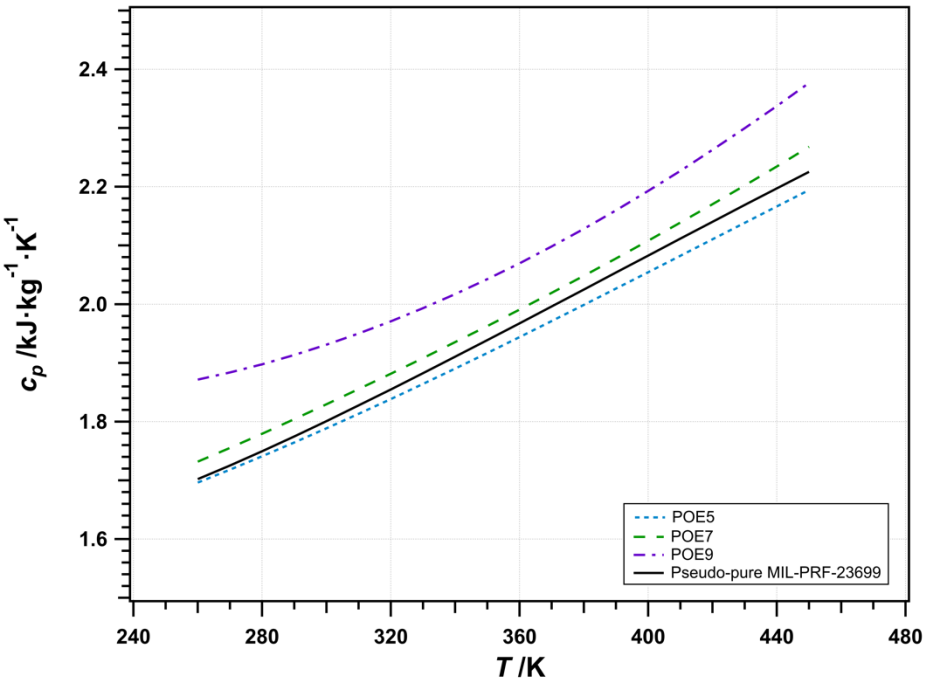

Figure 77: Heat capacity at atmospheric pressure as a function of temperature for POE5, POE7, POE9, and MIL-PRF-23699.

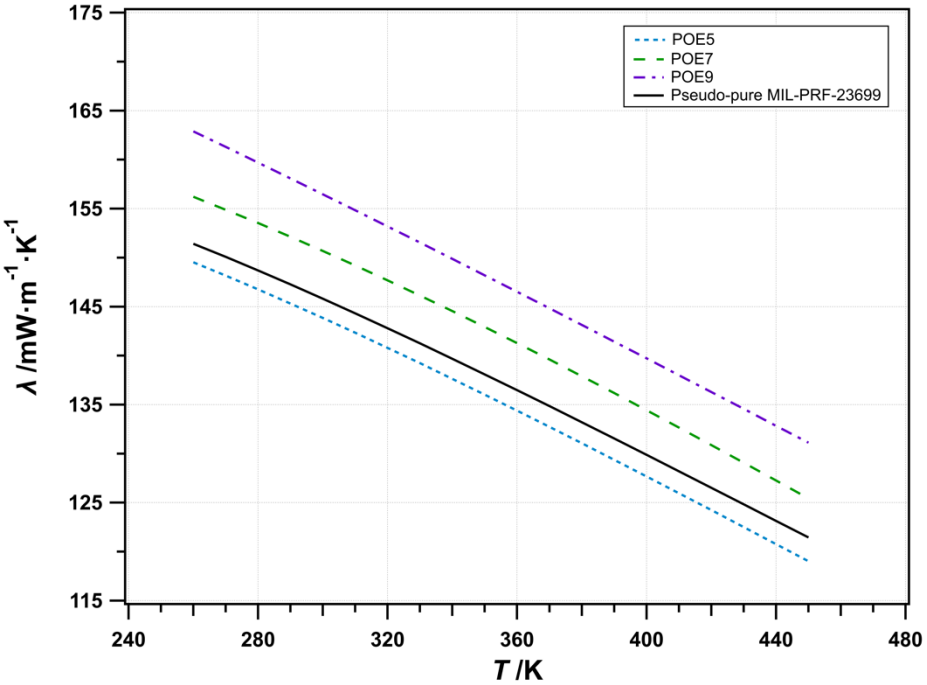

Figure 78: Thermal conductivity at atmospheric pressure as a function of temperature for POE5, POE7, POE9, and MIL-PRF-23699.

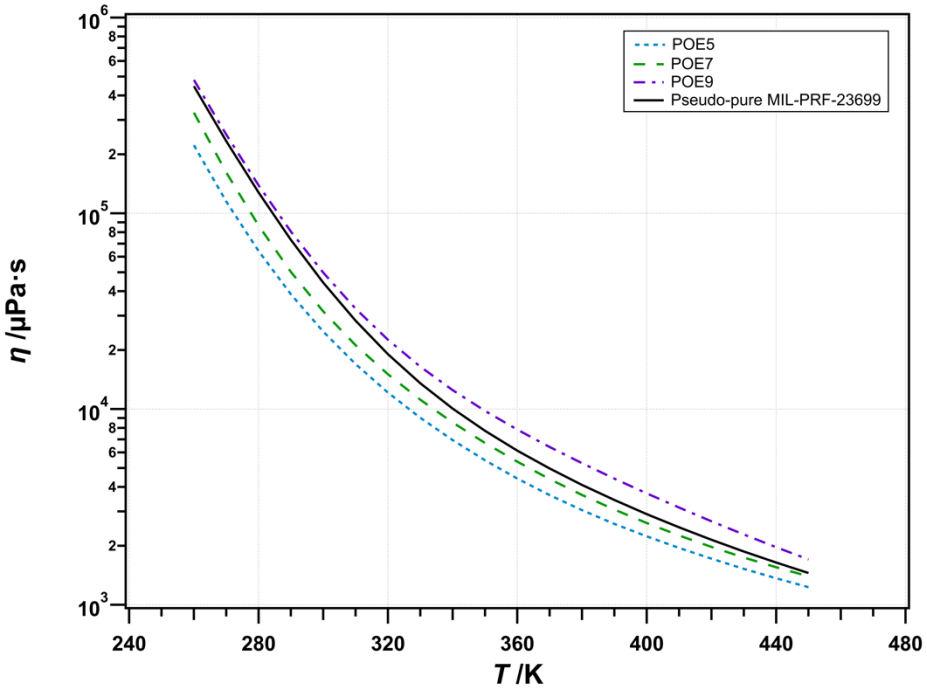

Figure 79: Viscosity at atmospheric pressure as a function of temperature for POE5, POE7, POE9, and MIL-PRF-23699.

The first surrogate model was designed to put more weight on matching the viscosity, resulting in very poor fits for the other properties. The composition of this surrogate, Surrogate 1, is 10 mole % POE5 and 90 mole % POE9. A second surrogate model was developed that weighted the equilibrium properties (density, sound speed, heat capacity), and thermal conductivity much more heavily than viscosity. The composition of this surrogate, Surrogate 2, is 54 mole % POE5 and 46 mole % POE7. The third option, discussed earlier, is to treat the mixture as a pseudo-pure fluid. Deviation plots for the properties as a function of temperature and with pressure for all three models are shown in Figures 80 – 85. The deviations were computed with the experimental data obtained in this work for the lubricant MIL-PRF-23699. The viscosity deviations show that even with an emphasis on fitting viscosity (Surrogate 1, Figures 80 and 83), the results are not within the experimental uncertainty. This can be compared with Figures 82 and 85, which show the deviations with experimental data for the pseudo-pure model. The pseudo-pure fluid model for MIL-PRF-23699 is obviously superior to either of the surrogate models. This is due in part to the fact that the surrogate model lacks any components lighter than POE9 that have a viscosity greater than, or at least close to, that of POE9. A possible solution is found in the work of Pensado et al.[75] who previously observed that the viscosity increases with increasing branching in POEs.

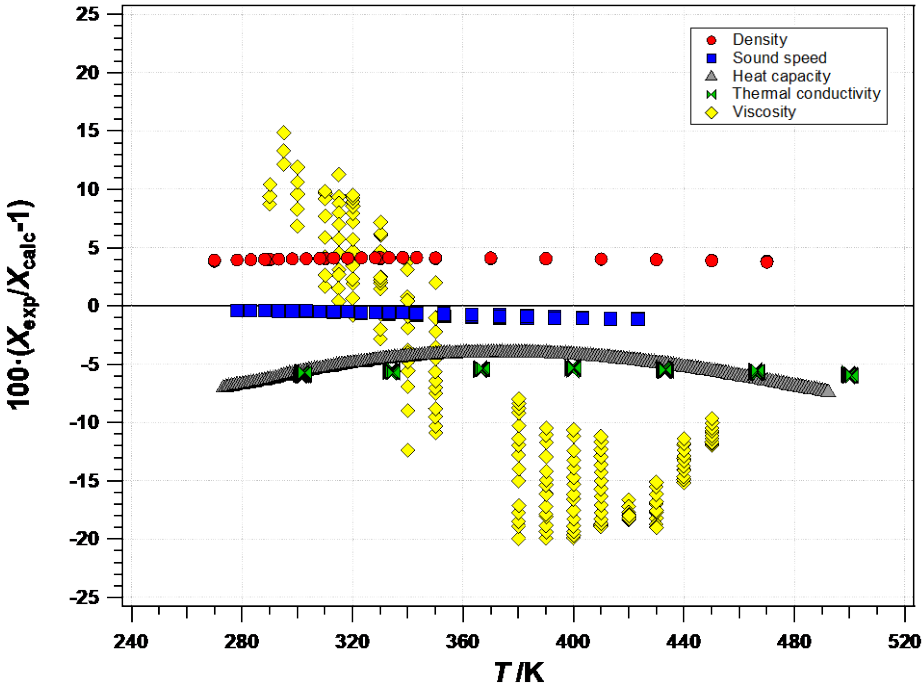

Figure 80: Property deviations of Surrogate 1 model as a function of temperature.

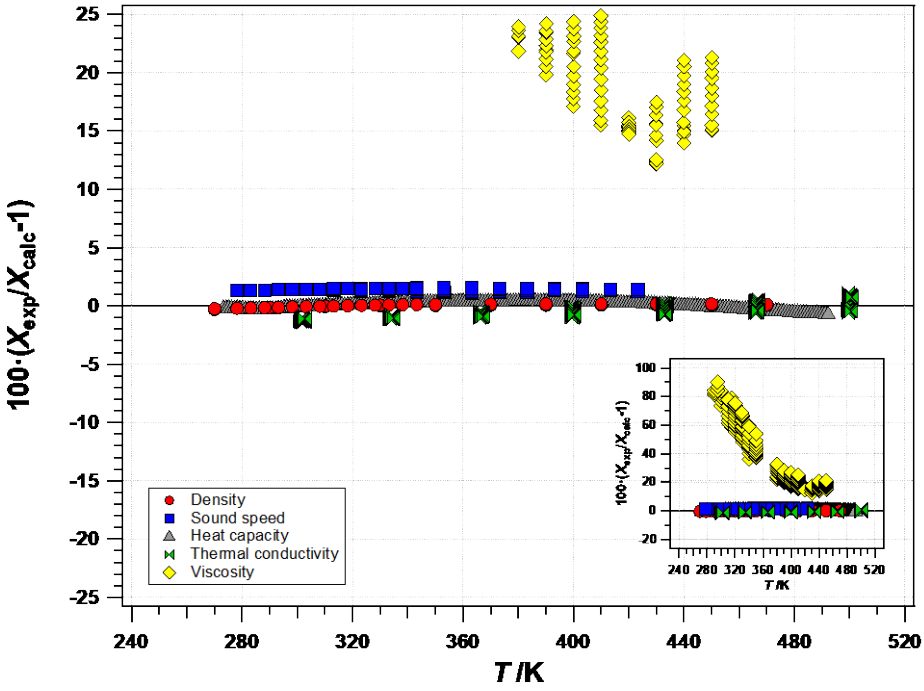

Figure 81: Property deviations of Surrogate 2 model as a function of temperature; the inset shows the large deviations in viscosity at low temperatures.

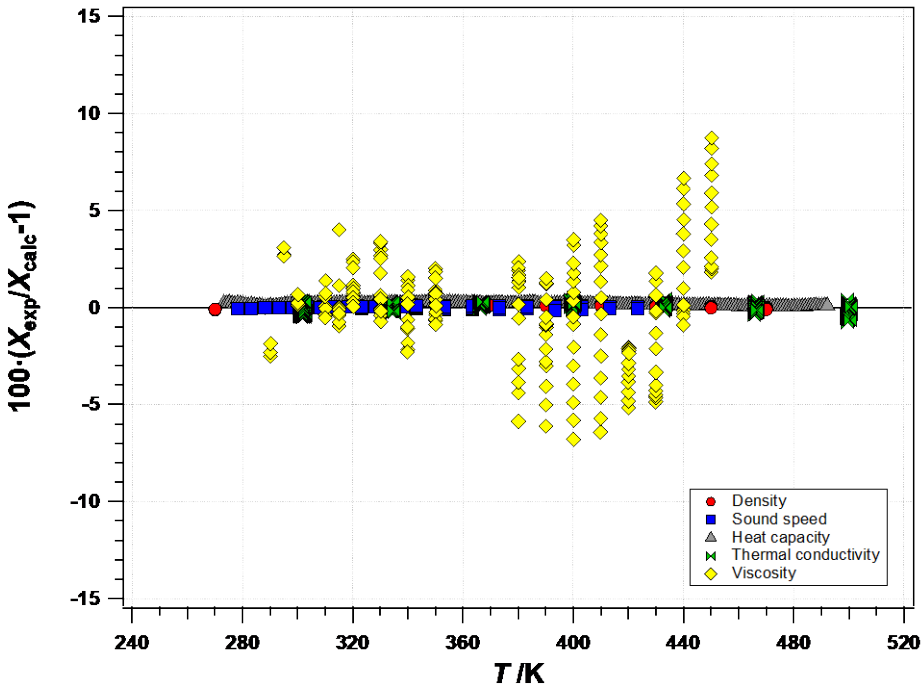

Figure 82: Property deviations of Pseudo-pure fluid model as a function of temperature.

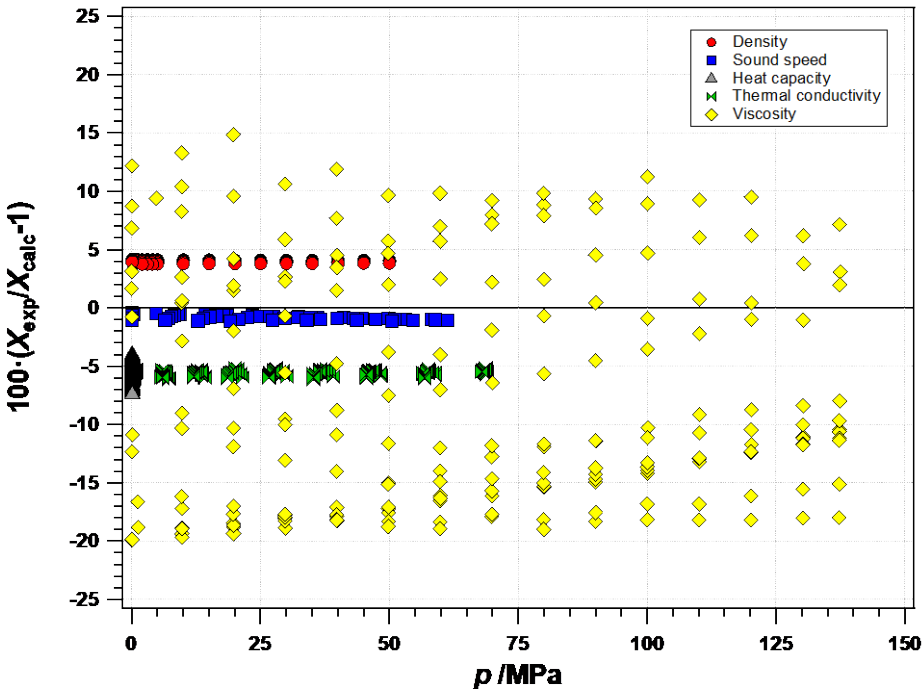

Figure 83: Property deviations of Surrogate 1 model as a function of pressure.

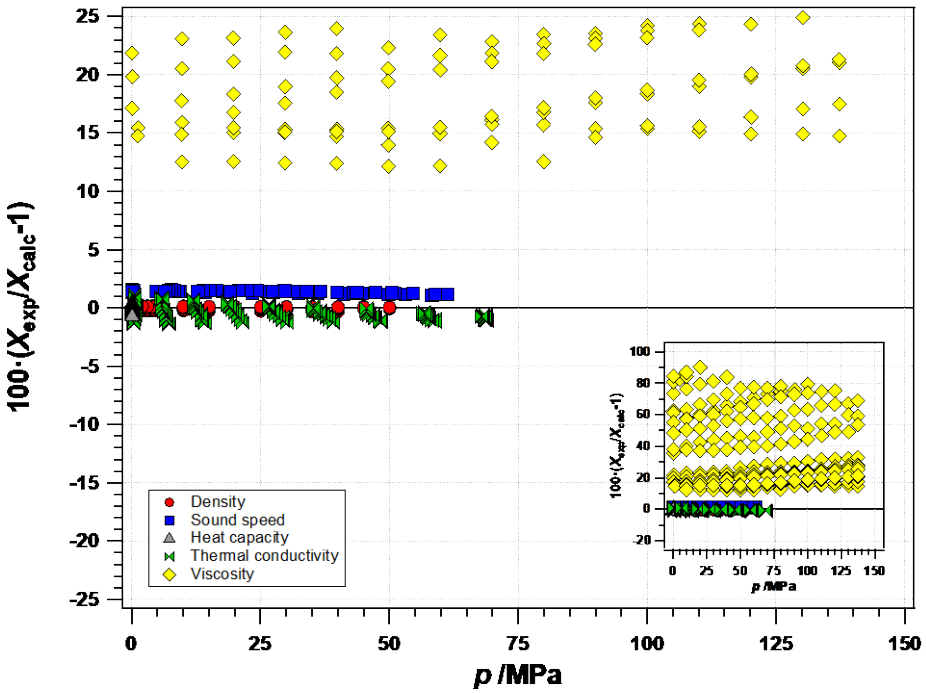

Figure 84: Property deviations of Surrogate 2 model as a function of pressure; the inset shows the large deviations in viscosity.

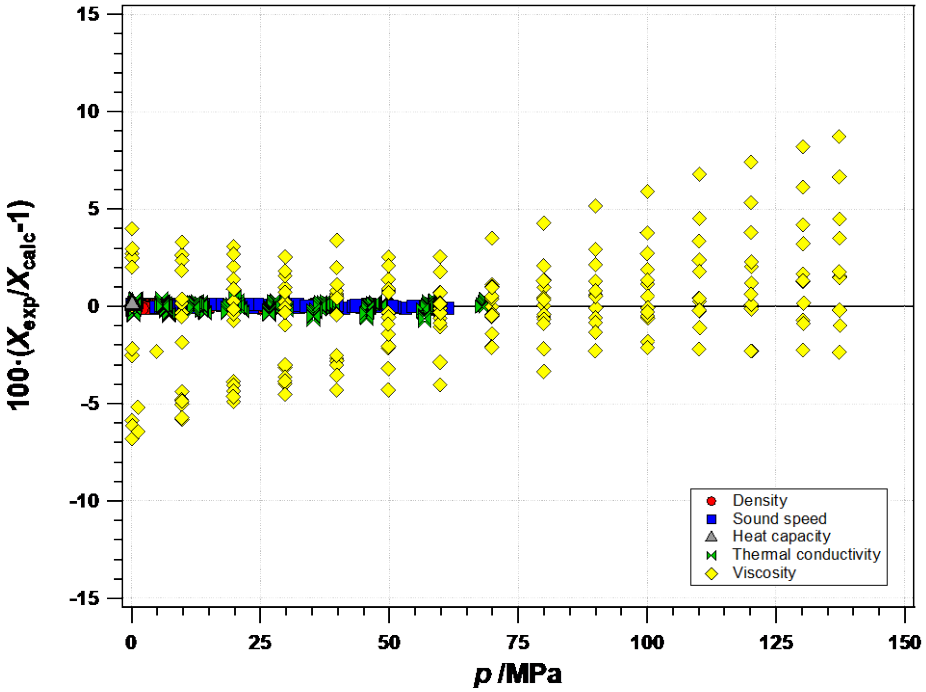

Figure 85: Property deviations of Pseudo-pure fluid model as a function of pressure.

13. Conclusions

An extensive experimental and modeling program was completed that is summarized by the following points:

1. We performed purity and chemical analysis of the fluids pentaerythritol tetrapentanoate (POE5), pentaerythritol tetraheptanoate (POE7), pentaerythritol tetranonanoate (POE9), and MIL-PRF-23699 by gas chromatography with flame ionization detection (GC-FID) and gas chromatography with mass spectrometry (GC-MS).

2. The global thermal decomposition kinetics of the fluids POE5, POE7, POE9, and MIL-PRF-23699 were performed in stainless steel ampule reactors at pressures of approximately 20 MPa with the extent of decomposition determined by GC-FID.

3. We completed thermodynamic (density, heat capacity, speed of sound) and transport (viscosity and thermal conductivity) property measurements of three pure polyol ester lubricants fluids (POE5, POE7, and POE9) and MIL-PRF-23699. Vapor pressure was measured for POE5; however, measurements on lubricant base fluids larger than POE5 were not attempted because their vapor pressures were below the measurable range of our apparatus.

4. The advanced distillation curve methodology was applied at atmospheric pressure, in an argon gas environment, to a sample of MIL-PRF-23699 to establish an initial boiling temperature. Due to decomposition of the heated fluid, the distillation was only carried out to 10 % distillate volume fraction. No initial boiling temperature could be defined under the conditions tested, because the fluid was not thermally stable.

5. Equations of state and transport property models were constructed for the three pure base fluids, and for the fully qualified lubricant (treated as a pseudo-pure fluid). Two surrogate mixture models were developed for MIL-PRF-23699 based on the three pure POEs, one with an emphasis on thermodynamic properties and thermal conductivity, and one with an emphasis on viscosity. Both surrogate models failed to represent the properties to within their experimental uncertainty, and we recommend use of the pseudo-pure-fluid models.

6. Files that are compatible with the REFPROP computer program (version 10) are provided for the three pure fluids and the fully qualified lubricant (see Appendix C).

In conclusion, we provide models for the thermophysical properties of three pure POE base fluids (POE5, POE7, POE9) and a fully qualified lubricant that meets MIL-PRF-23699 that are primarily based upon the comprehensive experimental work described in this document. The models are implemented in files that are compatible with the NIST computer program REFPROP, version 10. The thermophysical properties of the properties measured are predominantly represented by the models to within their experimental uncertainty.

14. Acknowledgements

The authors thank James McDonnell and Dawn Schmidt, both of the Naval Air Systems Command (NAVAIR), for funding (Contract No. N0042115IP00008) and for supplying the four polyol ester lubricant samples. K.N.U. gratefully acknowledges a National Academy of Sciences/National Research Council postdoctoral fellowship. Contribution of the National Institute of Standards and Technology; not subject to U.S. Copyright.

References

1. Cottington, R. L.; Ravner, H. Interactions of Neopentyl Polyol Ester-Tricresyl Phosphate-Iron Systems at 500°F. *ASLE Trans.* **1969**, *12*, 280-286.

2. Zeman, A.; Bartl, P.; Schaaff, A. Mass-Spectrometric Fragmentation of Neopentylpolyol Esters. 1. Pentaerythritol Tetra Esters of Fatty-Acids. *Org. Mass Spectrom.* **1978**, *13*, 248-253.

3. Urness, K. N.; Gough, R. V.; Widegren, J. A.; Bruno, T. J. Thermal Decomposition Kinetics of Polyol Ester Lubricants. *Energy Fuels* **2016**, *30*, 10161-10170.

4. Widegren, J. A.; Bruno, T. J. Thermal Decomposition Kinetics of the Aviation Turbine Fuel Jet A. *Ind. Eng. Chem. Res.* **2008**, *47*, 4342-43448.

5. Widegren, J. A.; Bruno, T. J. Thermal Decomposition Kinetics of Propylcyclohexane. *Ind. Eng. Chem. Res.* **2009**, *48*, 654-659.

6. Razzouk, A.; Mokbel, I.; García, J.; Fernandez, J.; Msakni, N.; Jose, J. Vapor Pressure Measurements in the Range 10^{-5} Pa to 1 Pa of Four Pentaerythritol Esters - Density and Vapor-Liquid Equilibria Modeling of Ester Lubricants. *Fluid Phase Equilibr.* **2007**, *260*, 248-261.

7. Bruno, T. J.; Mayrath, J. E. Concatenated Gas Saturation Vapor Pressure Apparatus. *Rev. Sci. Instrum.* **1997**, *68*, 2864-2870.

8. Carruth, G. F.; Kobayashi, R. Vapor Pressure of Normal Paraffins Ethane through *n*-Decane from Their Triple Points to About 10 mm Hg. *J. Chem. Eng. Data* **1973**, *18*, 115-126.

9. Delle Site, A. The Vapor Pressure of Environmentally Significant Organic Chemicals: A Review of Methods and Data at Ambient Temperature. *J. Phys. Chem. Ref. Data* **1997**, *26*, 157-193.

10. Gerry, H. T.; Gillespie, L. J. The Calculation of Normal Vapor Pressures from the Data of the Gas Current Method, Particularly in the Case of Iodine. *Phys. Rev.* **1932**, *40*, 269-280.

11. Kvande, H.; Wahlbeck, P. G. Theory for Determination of Vapour Pressures by the Transpiration Method. *Acta Chem. Scand. A* **1976**, *30*, 297-302.

12. Macknick, A. B.; Prausnitz, J. M. Vapor-Pressures of High-Molecular-Weight Hydrocarbons. *J. Chem. Eng. Data* **1979**, *24*, 175-178.

13. Mokbel, I.; Razzouk, A.; Hajjaji, A.; Msakni, N.; Jose, J. A Gas Saturation Apparatus for Very Low Vapor or Sublimation Pressure Measurements (10^{-3} Pa): Vapor-Liquid Equilibria of *n*-Alkanes (*n*-C_{10}, *n*-C_{24}, *n*-C_{28}). *J. Chem. Eng. Data* **2007**, *52*, 1720-1725.

14. Razzouk, A.; Abou Naccoul, R.; Mokbel, I.; Saab, J.; Jose, J. Vapor and Sublimation Pressures of Three Normal Alkanes: C-20, C-24, and C-28. *J. Chem. Eng. Data* **2009**, *54*, 1214-1219.

15. Verevkin, S. P.; Emel'yaneriko, V. N. Transpiration Method: Vapor Pressures and Enthalpies of Vaporization of Some Low-Boiling Esters. *Fluid Phase Equilibr.* **2008**, *266*, 64-75.

16. Widegren, J. A.; Beall, C. E.; Tolbert, A. E.; Lovestead, T. M.; Bruno, T. J. The Use of Antioxidants to Improve Vapor Pressure Measurements on Compounds with Oxidative Instability: Methyl Oleate with *tert*-Butylhydroquinone. *J. Chem. Eng. Data* **2017**, *62*, 539-546.

17. Widegren, J. A.; Harvey, A. H.; McLinden, M. O.; Bruno, T. J. Vapor Pressure Measurements by the Gas Saturation Method: The Influence of the Carrier Gas. *J. Chem. Eng. Data* **2015**, *60*, 1173-1180.

18. Merten, U. Diffusion Effects in the Transpiration Method of Vapor Pressure Measurement. *J. Phys. Chem.* **1959**, *63*, 443-445.

19. Frenkel, M.; Chirico, R. D.; Diky, V.; Kroenlein, K.; Muzny, C. D.; Kazakov, A. F.; Magee, J. W.; Abdulagatov, I. M. *Thermodata Engine (TDE)*, Version 8.0; National Institute of Standards and Technology: Gaithersburg, MD, 2013.

20. Span, R.; Lemmon, E. W.; Jacobsen, R. T.; Wagner, W.; Yokozeki, A. A Reference Equation of State for the Thermodynamic Properties of Nitrogen for Temperatures from 63.151 to 1000 K and Pressures to 2200 MPa. *J. Phys. Chem. Ref. Data* **2000**, *29*, 1361-1433.

21. Lemmon, E. W.; Bell, I. H.; Huber, M. L.; McLinden, M. O. *Reference Fluid Thermodynamic and Transport Properties (REFPROP)*, Version 10.0; National Institute of Standards and Technology: Gaithersburg, MD, 2018.

22. Yang, S.; Schultz, A. J.; Kofke, D. A.; Harvey, A. H. Interpreting Gas-Saturation Vapor Pressure Measurements Using Virial Coefficients Derived from Molecular Models. *J. Chem. Eng. Data* **2014**, *59*, 3183-3192.

23. Widegren, J. A.; Bruno, T. J. Gas Saturation Vapor Pressure Measurements of Mononitrotoluene Isomers from (283.15 to 313.15) K. *J. Chem. Eng. Data* **2010**, *55*, 159-164.

24. Lemmon, E. W.; Goodwin, A. R. H. Critical Properties and Vapor Pressure Equation for Alkanes C_nH_{2n+2}: Normal Alkanes with $n \leq 36$ and Isomers for $n = 4$ through $n = 9$. *J. Phys. Chem. Ref. Data* **2000**, *29*, 1-39.

25. Fortin, T. J. Density, Speed of Sound, and Heat Capacity Measurements of Polyol Ester Lubricants. *J. Chem. Eng. Data* **2018**, *63*, 4325-4338.

26. Boerio-Goates, J.; Callanan, J. E. Differential Thermal Methods. In *Physical Methods of Chemistry, Volume VI: Determination of Thermodynamic Properties*; Rossiter, B. W., Baetzold, R. C., Eds.; John Wiley & Sons: New York, NY, 1992; pp 621-717.

27. Reading, M.; Luget, A.; Wilson, R. Modulated Differential Scanning Calorimetry. *Thermochim. Acta* **1994**, *238*, 295-307.

28. Wunderlich, B.; Jin, Y.; Boller, A. Mathematical Description of Differential Scanning Calorimetry Based on Periodic Temperature Modulation. *Thermochim. Acta* **1994**, *238*, 277-293.

29. Höhne, G. W. H.; Hemminger, W.; Flammersheim, H. J. *Differential Scanning Calorimetry: An Introduction for Practitioners*; Springer-Verlag: Berlin, Germany, 1996.

30. Della Gatta, G.; Richardson, M. J.; Sarge, S. M.; Stølen, S. Standards, Calibration, and Guidelines in Microcalorimetry Part 2. Calibration Standards for Differential Scanning Calorimetry. *Pure Appl. Chem.* **2006**, *78*, 1455-1476.

31. Rosasco, G. J.; Whetstone, J. R.; Watters, R. L. *Certificate of Analysis - Standard Reference Material 2232*; National Institute of Standards and Technology: Gaithersburg, MD, 2003.

32. Rasberry, S. D. *Certificate of Analysis - Standard Reference Material 2220*; National Institute of Standards and Technology: Gaithersburg, MD, 1989.

33. Westrum, E. F. The Thermophysical Properties of Three Globular Molecules. *J. Phys. Chem. Solids* **1961**, *18*, 83-85.

34. Archer, D. G. Thermodynamic Properties of Synthetic Sapphire (α-Al_2O_3), Standard Reference Material 720 and the Effect of Temperature-Scale Differences on Thermodynamic Properties. *J. Phys. Chem. Ref. Data* **1993**, *22*, 1441-1453.

35. Harris, G. L.; Torres, J. A. *Selected Laboratory and Measurement Practices and Procedures to Support Basic Mass Calibrations*, NISTIR 6969; National Institute of Standards and Technology: Gaithersburg, MD, 2003.

36. Picard, A.; Davis, R. S.; Glaser, M.; Fujii, K. Revised Formula for the Density of Moist Air (CIPM-2007). *Metrologia* **2008**, *45*, 149-155.

37. Schneider, N.; Fortin, T. J.; Span, R.; Gerber, M. Thermophysical Properties of the Marine Microalgae *Nannochloropsis salina*. *Fuel Process. Technol.* **2016**, *152*, 390-398.

38. *Guide to the Expression of Uncertainty in Measurement*; International Organization for Standardization: Geneva, Switzerland, 1995.

39. Lemmon, E. W.; McLinden, M. O.; Wagner, W. Thermodynamic Properties of Propane. III. A Reference Equation of State for Temperatures from the Melting Line to 650 K and Pressures up to 1000 MPa. *J. Chem. Eng. Data* **2009**, *54*, 3141-3180.

40. Meier, K.; Kabelac, S. Thermodynamic Properties of Propane. IV. Speed of Sound in the Liquid and Supercritical Regions. *J. Chem. Eng. Data* **2012**, *57*, 3391-3398.

41. Outcalt, S. L. Compressed-Liquid Density Measurements of Four Polyol Ester-Based Lubricants. *Energy Fuels* **2018**, *32*, 3775-3782.

42. Outcalt, S. L.; McLinden, M. O. Automated Densimeter for the Rapid Characterization of Industrial Fluids. *Ind. Eng. Chem. Res.* **2007**, *46*, 8264-8269.

43. Wagner, W.; Pruß, A. The IAPWS Formulation 1995 for the Thermodynamic Properties of Ordinary Water Substance for General and Scientific Use. *J. Phys. Chem. Ref. Data* **2002**, *31*, 387-535.

44. Lemmon, E. W.; Span, R. Short Fundamental Equations of State for 20 Industrial Fluids. *J. Chem. Eng. Data* **2006**, *51*, 785-850.

45. May, E. F.; Tay, W. J.; Nania, M.; Aleji, A.; Al-Ghafri, S.; Trusler, J. P. M. Physical Apparatus Parameters and Model for Vibrating Tube Densimeters at Pressures to 140 MPa and Temperatures to 473 K. *Rev. Sci. Instrum.* **2014**, *85*, 095111.

46. Laesecke, A.; Fortin, T. J.; Splett, J. D. Density, Speed of Sound, and Viscosity Measurements of Reference Materials for Biofuels. *Energy Fuels* **2012**, *26*, 1844-1861.

47. Fortin, T. J. Assessment of Variability in the Thermophysical Properties of Rocket Propellant RP-1. *Energy Fuels* **2012**, *26*, 4383-4394.

48. Fortin, T. J.; Laesecke, A.; Freund, M.; Outcalt, S. L. Advanced Calibration, Adjustment, and Operation of a Density and Sound Speed Analyzer. *J. Chem. Thermodyn.* **2013**, *57*, 276-285.

49. Healy, J.; DeGroot, J. J.; Kestin, J. The Theory of the Transient Hot-Wire Method for Measuring the Thermal Conductivity. *Physica* **1976**, *82C*, 392-408.

50. Woodfield, P. L.; Fukai, J.; Fujii, M.; Takata, Y.; Shinzato, K. A Two-Dimensional Analytical Solution for the Transient Short-Hot-Wire Method. *Int. J. Thermophys.* **2008**, *29*, 1278-1298.

51. Laesecke, A.; Junker, C.; Lauria, D. S. Viscosity Measurements of Three Base Oils and One Fully Formulated Lubricant and New Viscosity Correlations for the Calibration Liquid Squalane. *J. Res. NIST* **2019**, *124*, 124002.

52. Mylona, S. K.; Assael, M. J.; Comuñas, M. J. P.; Parades, X.; Gaciño, F. M.; Fernández, J.; Bazile, J. P.; Boned, C.; Daridon, J. L.; Galliero, G.; Pauly, J.; Harris, K. R. Reference Correlations for the Density and Viscosity of Squalane from 273 to 473 K at Pressures to 200 MPa. *J. Phys. Chem. Ref. Data* **2014**, *43*, 013104.

53. Schmidt, K. A.; Pagnutti, D.; Curran, M. D.; Singh, A.; Trusler, J. P. M.; Maitland, G. C.; McBride-Wright, M. New Experimental Data and Reference Models for the Viscosity and Density of Squalane. *J. Chem. Eng. Data* **2015**, *60*, 137-150.

54. Schaschke, C. J.; Abid, S.; Fletcher, I.; Heslop, M. J. Evaluation of a Falling Sinker-Type Viscometer at High Pressure Using Edible Oil. *J. Food. Eng.* **2008**, *87*, 51-58.

55. Laesecke, A.; Bair, S. High Pressure Viscosity Measurements of 1,1,1,2-Tetrafluoroethane. *Int. J. Thermophys.* **2011**, *32*, 925-941.

56. Bair, S.; Laesecke, A. Viscosity Measurements of R32 and R410a to 350 MPa. *Int. J. Refrig.* **2017**, *83*, 157-167.

57. Bruno, T. J.; Ott, L. S.; Smith, B. L.; Lovestead, T. M. Complex Fluid Analysis with the Advanced Distillation Curve Approach. *Anal. Chem.* **2010**, *82*, 777-783.

58. Smith, B. L.; Ott, L. S.; Bruno, T. J. Composition-Explicit Distillation Curves of Commercial Biodiesel Fuels: Comparison of Petroleum-Derived Fuels with B20 and B100. *Ind. Eng. Chem. Res.* **2008**, *47*, 5832-5840.

59. Span, R.; Wagner, W. Equations of State for Technical Applications. II. Results for Nonpolar Fluids. *Int. J. Thermophys.* **2003**, *24*, 41-109.

60. Lemmon, E. W.; Jacobsen, R. T. A New Functional Form and New Fitting Techniques for Equations of State with Application to Pentafluoroethane (HFC-125). *J. Phys. Chem. Ref. Data* **2005**, *34*, 69-108.

61. Huber, M. L. *Models for the Viscosity, Thermal Conductivity, and Surface Tension of Selected Pure Fluids as Implemented in REFPROP V10.0*, NISTIR 8209; National Institute of Standards and Technology: Gaithersburg, MD, 2018.

62. Chung, T.-H.; Ajlan, M.; Lee, L. L.; Starling, K. E. Generalized Multiparameter Correlation for Nonpolar and Polar Fluid Transport Properties. *Ind. Eng. Chem. Res.* **1988**, *27*, 671-679.

63. *Eureqa Formulize*, v.098.1; Nutonian Inc.: Cambridge, MA.

64. Assael, M. J.; Dymond, J. H.; Papadaki, M.; Patterson, P. M. Correlation and Prediction of Dense Fluid Transport Coefficients. I. *n*-Alkanes. *Int. J. Thermophys.* **1992**, *13*, 269-281.

65. Assael, M. J.; Papalas, T. B.; Huber, M. L. Reference Correlations for the Viscosity and Thermal Conductivity of *n*-Undecane. *J. Phys. Chem. Ref. Data* **2017**, *46*, 033103.

66. Tsolakidou, C. M.; Assael, M. J.; Huber, M. L.; Perkins, R. A. Correlations for the Viscosity and Thermal Conductivity of Ethyl Fluoride (R161). *J. Phys. Chem. Ref. Data* **2017**, *46*, 023103.

67. Monogenidou, S. A.; Assael, M. J.; Huber, M. L. Reference Correlation for the Viscosity of Ammonia from the Triple Point to 725 K and up to 50 MPa. *J. Phys. Chem. Ref. Data* **2018**, *47*, 023102.

68. Bair, S.; Casalini, R. A Scaling Parameter and Function for the Accurate Correlation of Viscosity with Temperature and Pressure across Eight Orders of Magnitude of Viscosity. *J. Tribol.* **2008**, *130*, 041802.

69. Perkins, R. A.; Sengers, J. V.; Abdulagatov, I. M.; Huber, M. L. Simplified Model for the Critical Thermal-Conductivity Enhancement in Molecular Fluids. *Int. J. Thermophys.* **2013**, *34*, 191-212.

70. Lemmon, E. W.; Jacobsen, R. T.; Penoncello, S. G.; Friend, D. G. Thermodynamic Properties of Air and Mixtures of Nitrogen, Argon, and Oxygen from 60 to 2000 K at Pressures to 2000 MPa. *J. Phys. Chem. Ref. Data* **2000**, *29*, 331-385.

71. Lemmon, E. W. Pseudo-Pure Fluid Equations of State for the Refrigerant Blends R-410a, R-404a, R-507a, and R-407c. *Int. J. Refrig.* **2003**, *24*, 991-1006.

72. Huber, M. L.; Lemmon, E. W.; Ott, L. S.; Bruno, T. J. Preliminary Surrogate Mixture Models for the Thermophysical Properties of Rocket Propellants RP-1 and RP-2. *Energy Fuels* **2009**, *23*, 3083-3088.

73. Huber, M. L.; Lemmon, E. W.; Bruno, T. J. Surrogate Mixture Models for the Thermophysical Properties of Aviation Fuel Jet-A. *Energy Fuels* **2010**, *24*, 3565-3571.

74. Mueller, C. J.; Cannella, W. J.; Bruno, T. J.; Bunting, B.; Dettman, H. D.; Franz, J. A.; Huber, M. L.; Natarajan, M.; Pitz, W. J.; Ratcliff, M. A.; Wright, K. Methodology for Formulating Diesel Surrogate Fuels with Accurate Compositional, Ignition-Quality, and Volatility Characteristics. *Energy Fuels* **2012**, *26*, 3284-3303.

75. Pensado, A. S.; Comuñas, M. J. P.; Lugo, L.; Fernández, J. High-Pressure Characterization of Dynamic Viscosity and Derived Properties for Squalane and Two

Pentaerythritol Ester Lubricants: Pentaerythritol Tetra-2-ethylhexanoate and Pentaerythritol Tetranonanoate. *Ind. Eng. Chem. Res.* **2006**, *45*, 2394-2404.

Appendix A: Thermal Conductivity Data Tables

Table A1: Thermal Conductivity Data for POE5 at Temperatures from 300 K to 500 K.

T_i[a] /K	p /MPa	T /K	λ /W·m^{-1}K^{-1}	T_i[a] /K	p /MPa	T /K	λ /W·m^{-1}K^{-1}
299.549	0.155	301.436	0.14327	299.590	21.709	301.791	0.14902
299.554	0.161	301.836	0.14323	299.591	21.708	301.795	0.14888
299.549	0.164	301.830	0.14331	299.593	21.701	302.214	0.14879
299.555	0.167	302.275	0.14315	299.592	21.716	302.215	0.14884
299.554	0.170	302.276	0.14317	299.592	21.721	302.676	0.14867
299.552	0.173	302.752	0.14298	299.596	21.708	302.677	0.14876
299.552	0.177	302.750	0.14309	299.590	21.724	303.171	0.14866
299.559	0.180	303.275	0.14294	299.589	21.735	303.166	0.14867
299.561	0.184	303.273	0.14298	299.586	30.144	301.377	0.15101
299.583	5.854	301.456	0.14481	299.578	30.158	301.367	0.15093
299.580	5.646	302.274	0.14459	299.580	30.181	301.742	0.15100
299.580	5.588	302.748	0.14445	299.579	30.153	301.740	0.15098
299.579	5.548	302.747	0.14405	299.579	30.152	302.160	0.15088
299.577	5.495	303.255	0.14406	299.577	30.167	302.156	0.15086
299.575	5.439	303.252	0.14442	299.585	30.160	302.618	0.15077
299.579	7.141	301.449	0.14546	299.578	30.161	302.608	0.15089
299.576	7.127	301.439	0.14505	299.578	30.146	303.099	0.15074
299.576	7.135	301.832	0.14513	299.584	30.154	303.106	0.15072
299.577	7.125	301.828	0.14502	299.596	39.004	301.378	0.15317
299.585	7.122	302.269	0.14497	299.596	39.013	301.379	0.15309
299.585	7.127	302.270	0.14530	299.598	39.016	301.753	0.15357
299.586	7.143	302.744	0.14495	299.591	39.012	301.742	0.15303
299.585	7.142	302.741	0.14502	299.596	39.014	302.161	0.15300
299.585	7.130	303.251	0.14483	299.596	39.013	302.159	0.15296
299.587	7.140	303.250	0.14485	299.595	39.018	302.605	0.15298
299.588	13.947	301.439	0.14698	299.592	39.015	302.604	0.15332
299.587	13.973	301.434	0.14683	299.593	39.012	303.087	0.15284
299.591	13.976	301.819	0.14689	299.591	38.999	303.085	0.15287
299.589	13.946	301.816	0.14682	299.581	48.515	301.325	0.15533
299.587	13.960	302.248	0.14681	299.579	48.501	301.342	0.15533
299.585	13.965	302.240	0.14682	299.580	48.488	301.706	0.15525
299.581	13.946	302.704	0.14669	299.576	48.474	302.111	0.15516
299.582	13.892	302.700	0.14671	299.583	48.475	302.117	0.15519
299.581	13.938	303.211	0.14663	299.582	48.468	302.558	0.15515
299.579	13.937	303.200	0.14665	299.581	48.456	302.551	0.15550
299.593	21.709	301.414	0.14886	299.581	48.454	303.033	0.15508
299.593	21.721	301.413	0.14893	299.583	48.462	303.036	0.15504

[a]Initial cell temperature.

Table A1, continued.

T_i[a] /K	p /MPa	T /K	λ /W·m^{-1}K^{-1}	T_i[a] /K	p /MPa	T /K	λ /W·m^{-1}K^{-1}
299.596	58.504	301.330	0.15742	332.002	6.740	335.405	0.14031
299.596	58.490	301.330	0.15746	332.013	13.507	333.719	0.14266
299.594	58.493	301.689	0.15755	332.009	13.496	333.723	0.14271
299.596	58.487	301.693	0.15749	332.006	13.500	334.074	0.14269
299.591	58.473	302.089	0.15741	332.013	13.490	334.078	0.14256
299.593	58.483	302.089	0.15746	332.010	13.488	334.473	0.14247
299.589	58.463	302.520	0.15738	332.013	13.488	334.474	0.14250
299.587	58.448	302.518	0.15736	332.012	13.499	334.910	0.14246
299.587	58.460	302.989	0.15727	332.010	13.498	334.904	0.14243
299.582	58.473	302.983	0.15746	332.014	13.493	335.377	0.14243
299.574	69.033	301.297	0.15996	332.008	13.498	335.365	0.14241
299.577	69.035	301.299	0.15989	332.016	21.097	333.717	0.14483
299.578	69.039	301.653	0.15984	332.014	21.087	333.708	0.14513
299.574	69.024	301.649	0.15974	332.011	21.089	334.061	0.14471
299.576	69.035	302.046	0.15975	332.012	21.080	334.059	0.14476
299.583	69.059	302.071	0.15968	332.012	21.090	334.455	0.14464
299.581	69.041	302.503	0.15969	332.013	21.086	334.450	0.14465
299.584	69.021	302.505	0.15968	332.014	21.088	334.876	0.14471
299.586	68.999	302.953	0.15959	332.014	21.091	334.874	0.14456
299.588	69.004	302.956	0.15959	332.011	21.079	335.333	0.14458
331.980	0.383	333.737	0.13864	332.015	21.082	335.340	0.14453
331.988	0.413	333.742	0.13867	332.020	29.158	333.689	0.14706
331.981	0.439	334.109	0.13877	332.019	29.155	333.681	0.14720
331.979	0.457	334.107	0.13923	332.023	29.156	334.039	0.14705
331.981	0.473	334.513	0.13861	332.019	29.154	334.031	0.14693
331.983	0.487	334.514	0.13858	332.023	29.144	334.420	0.14697
331.987	0.498	334.960	0.13849	332.021	29.137	334.424	0.14709
331.991	0.507	334.962	0.13852	332.023	29.142	334.844	0.14685
331.987	0.516	335.433	0.13866	332.024	29.144	334.844	0.14689
331.986	0.523	335.431	0.13841	332.020	29.131	335.293	0.14685
331.995	6.770	333.731	0.14057	332.019	29.133	335.289	0.14681
332.000	6.769	333.722	0.14067	332.023	38.323	333.661	0.14952
331.997	6.769	334.080	0.14049	332.024	38.298	333.655	0.14951
332.001	6.765	334.093	0.14063	332.018	38.285	333.992	0.14948
331.996	6.760	334.483	0.14066	332.021	38.304	334.375	0.14942
331.999	6.756	334.493	0.14050	332.025	38.279	334.377	0.14938
331.998	6.731	334.928	0.14041	332.023	38.278	334.793	0.14934
331.996	6.750	334.920	0.14039	332.024	38.265	335.233	0.14920
331.997	6.745	335.396	0.14034	332.019	38.259	335.229	0.14926

[a]Initial cell temperature.

Table A1, continued.

T_i[a] /K	p /MPa	T /K	λ /W·m^{-1}K^{-1}	T_i[a] /K	p /MPa	T /K	λ /W·m^{-1}K^{-1}
332.017	47.909	333.620	0.15206	364.893	6.232	366.861	0.13545
332.016	47.896	333.962	0.15188	364.893	6.204	367.236	0.13534
332.016	47.898	333.960	0.15196	364.891	6.211	367.233	0.13542
332.019	47.881	334.335	0.15188	364.885	6.195	367.642	0.13533
332.015	47.870	334.744	0.15180	364.894	6.188	367.659	0.13532
332.017	47.862	334.742	0.15179	364.892	6.207	368.101	0.13521
332.020	47.853	335.187	0.15172	364.907	13.465	366.514	0.13794
332.014	47.845	335.175	0.15170	364.913	13.471	366.523	0.13816
332.019	58.184	333.585	0.15455	364.910	13.467	366.858	0.13789
332.016	58.174	333.578	0.15458	364.907	13.494	366.843	0.13818
332.017	58.170	333.948	0.15449	364.912	13.493	367.224	0.13777
332.018	58.149	333.946	0.15499	364.907	13.486	367.217	0.13777
332.018	58.135	334.317	0.15449	364.906	13.474	367.624	0.13778
332.016	58.149	334.312	0.15440	364.914	13.490	367.631	0.13779
332.019	58.123	334.716	0.15432	364.911	13.468	368.062	0.13765
332.018	58.118	334.718	0.15428	364.905	13.477	368.056	0.13766
332.022	58.118	335.160	0.15462	364.903	20.645	366.483	0.14026
332.014	58.112	335.143	0.15432	364.899	20.655	366.487	0.14032
332.017	68.637	333.593	0.15693	364.903	20.652	366.820	0.14035
332.013	68.602	333.584	0.15698	364.900	20.664	366.817	0.14023
332.015	68.588	333.916	0.15686	364.899	20.637	367.189	0.14021
332.012	68.585	333.908	0.15702	364.903	20.659	367.184	0.14022
332.012	68.566	334.280	0.15684	364.903	20.641	367.581	0.14008
332.014	68.552	334.278	0.15686	364.900	20.634	367.593	0.14005
332.007	68.541	334.665	0.15680	364.900	20.648	368.011	0.13995
332.008	68.535	334.667	0.15679	364.903	20.650	368.014	0.13996
332.011	68.510	335.097	0.15676	364.906	28.803	366.472	0.14290
332.013	68.504	335.097	0.15674	364.907	28.770	366.475	0.14291
364.917	0.397	367.302	0.13376	364.907	28.793	366.796	0.14273
364.917	0.403	367.722	0.13330	364.907	28.759	367.158	0.14268
364.918	0.406	368.168	0.13287	364.904	28.778	367.158	0.14274
364.919	0.409	368.176	0.13317	364.906	28.762	367.542	0.14269
364.917	0.423	366.586	0.13296	364.906	28.771	367.549	0.14265
364.919	0.431	367.735	0.13322	364.903	28.738	367.978	0.14262
364.919	0.432	367.726	0.13325	364.901	28.740	367.966	0.14258
364.922	0.434	368.185	0.13327	364.906	37.832	366.421	0.14563
364.922	0.435	368.189	0.13375	364.908	37.815	366.419	0.14570
364.889	6.265	366.511	0.13566	364.905	37.806	366.724	0.14552
364.893	6.227	366.512	0.13552	364.906	37.785	366.731	0.14552

[a]Initial cell temperature.

Table A1, continued.

T_i[a] /K	p /MPa	T /K	λ /W·m^{-1}K^{-1}	T_i[a] /K	p /MPa	T /K	λ /W·m^{-1}K^{-1}
364.909	37.769	367.094	0.14540	397.992	0.487	399.893	0.12781
364.903	37.771	367.082	0.14536	397.995	0.489	400.256	0.12781
364.908	37.753	367.482	0.14544	397.990	0.490	400.252	0.12795
364.909	37.761	367.496	0.14537	397.993	0.492	400.668	0.12770
364.907	37.760	367.910	0.14524	397.994	0.494	400.658	0.12776
364.912	37.756	367.912	0.14520	397.993	0.495	401.102	0.12766
364.908	47.403	366.411	0.14834	397.994	0.497	401.093	0.12765
364.908	47.434	366.406	0.14828	397.975	5.940	399.513	0.13026
364.901	47.454	366.720	0.14809	397.979	5.948	399.514	0.13035
364.908	47.455	366.718	0.14808	397.978	5.922	399.827	0.13010
364.907	47.437	367.063	0.14829	397.978	5.902	399.825	0.13029
364.908	47.391	367.069	0.14797	397.980	5.892	400.196	0.13004
364.905	47.409	367.443	0.14802	397.982	5.891	400.212	0.13046
364.907	47.387	367.457	0.14819	397.979	5.878	400.612	0.12982
364.906	47.405	367.853	0.14804	397.980	5.868	400.598	0.13007
364.905	47.362	367.856	0.14812	397.981	5.867	401.047	0.12975
364.918	57.906	366.409	0.15107	397.983	5.859	401.030	0.12975
364.915	57.895	366.406	0.15102	398.003	12.783	400.605	0.13242
364.916	57.868	366.726	0.15099	398.000	12.763	400.601	0.13286
364.916	57.870	366.712	0.15090	398.003	12.767	401.029	0.13227
364.920	57.850	367.059	0.15089	398.003	12.760	401.019	0.13240
364.915	57.833	367.059	0.15093	398.014	20.158	399.523	0.13553
364.916	57.805	367.431	0.15090	398.014	20.137	399.522	0.13537
364.921	57.741	367.423	0.15088	398.010	20.119	399.828	0.13535
364.916	57.755	367.837	0.15085	398.014	20.107	399.833	0.13546
364.914	57.737	367.842	0.15079	398.022	20.111	400.191	0.13534
364.918	68.713	366.375	0.15394	398.013	20.105	400.180	0.13530
364.913	68.686	366.372	0.15369	398.012	20.112	400.566	0.13534
364.913	68.683	366.684	0.15385	398.015	20.107	400.565	0.13567
364.925	68.674	366.688	0.15381	398.014	20.087	400.970	0.13528
364.920	68.656	367.024	0.15381	398.014	20.085	400.973	0.13522
364.919	68.623	367.023	0.15377	398.020	28.213	399.474	0.13845
364.915	68.598	367.389	0.15369	398.023	28.206	399.487	0.13828
364.915	68.560	367.371	0.15362	398.021	28.203	399.797	0.13856
364.913	68.541	367.774	0.15361	398.020	28.189	399.782	0.13816
364.913	68.526	367.775	0.15361	398.017	28.173	400.131	0.13817
397.990	0.479	399.557	0.12823	398.018	28.171	400.131	0.13810
397.990	0.482	399.564	0.12788	398.019	28.140	400.511	0.13806
397.992	0.484	399.883	0.12786	398.019	28.151	400.511	0.13818

[a]Initial cell temperature.

Table A1, continued.

T_i[a] /K	p /MPa	T /K	λ /W·m^{-1}K^{-1}	T_i[a] /K	p /MPa	T /K	λ /W·m^{-1}K^{-1}
398.020	28.156	400.912	0.13801	398.042	12.566	400.629	0.13244
398.020	28.151	400.913	0.13801	398.049	12.561	401.059	0.13250
398.035	37.384	399.474	0.14118	398.050	12.557	401.055	0.13243
398.036	37.376	399.483	0.14157	431.982	0.399	433.510	0.12223
398.038	37.365	399.783	0.14115	431.983	0.401	433.512	0.12219
398.038	37.354	399.777	0.14123	431.981	0.403	433.811	0.12200
398.036	37.350	400.112	0.14118	431.986	0.405	433.818	0.12210
398.041	37.320	400.112	0.14117	431.990	0.406	434.169	0.12183
398.033	37.303	400.473	0.14101	431.986	0.407	434.168	0.12201
398.038	37.294	400.477	0.14106	431.990	0.408	434.572	0.12196
398.035	37.248	400.862	0.14097	431.986	0.409	434.550	0.12182
398.032	37.231	400.859	0.14112	431.990	0.410	434.973	0.12184
398.035	47.003	399.443	0.14409	431.994	0.411	434.984	0.12178
398.034	46.981	399.446	0.14465	431.963	5.844	433.454	0.12471
398.032	46.960	399.744	0.14400	431.964	5.837	433.445	0.12432
398.037	46.946	399.751	0.14415	431.960	5.839	433.758	0.12449
398.027	46.916	400.062	0.14414	431.962	5.835	433.763	0.12444
398.032	46.918	400.078	0.14412	431.962	5.828	434.105	0.12446
398.035	46.882	400.431	0.14414	431.963	5.811	434.105	0.12425
398.034	46.858	400.419	0.14418	431.963	5.820	434.496	0.12429
398.035	46.867	400.827	0.14398	431.963	5.801	434.475	0.12442
398.035	46.839	400.824	0.14396	431.961	5.800	434.883	0.12435
398.048	57.341	399.445	0.14724	431.961	5.793	434.897	0.12421
398.046	57.298	399.438	0.14704	431.983	12.456	433.454	0.12761
398.045	57.270	399.719	0.14721	431.983	12.462	433.461	0.12744
398.046	57.223	399.717	0.14738	431.990	12.448	433.777	0.12738
398.045	57.212	400.044	0.14715	431.985	12.444	434.099	0.12717
398.044	57.187	400.061	0.14709	431.982	12.456	434.110	0.12713
398.046	57.157	400.403	0.14713	431.984	12.450	434.484	0.12719
398.044	57.131	400.406	0.14702	431.981	12.441	434.471	0.12777
398.039	57.109	400.780	0.14709	431.982	12.439	434.881	0.12716
398.043	57.071	400.786	0.14701	431.982	12.441	434.875	0.12727
398.042	12.587	399.456	0.13279	431.996	19.709	433.427	0.13030
398.041	12.577	399.567	0.13256	432.001	19.696	433.455	0.13039
398.042	12.585	399.900	0.13257	432.000	19.695	433.747	0.13034
398.044	12.584	399.888	0.13270	432.004	19.693	433.754	0.13043
398.046	12.588	400.252	0.13247	432.006	19.694	434.085	0.13014
398.041	12.565	400.252	0.13252	432.001	19.692	434.083	0.13021
398.046	12.559	400.635	0.13249	432.008	19.671	434.446	0.13036

[a]Initial cell temperature.

Table A1, continued.

T_i[a] /K	p /MPa	T /K	λ /W·m^{-1}K^{-1}	T_i[a] /K	p /MPa	T /K	λ /W·m^{-1}K^{-1}
432.001	19.676	434.451	0.13014	465.227	0.393	466.727	0.11646
432.002	19.677	434.839	0.13032	465.226	0.407	466.727	0.11637
432.004	19.672	434.851	0.13002	465.220	0.415	467.017	0.11655
432.012	27.422	433.415	0.13372	465.223	0.421	467.031	0.11624
432.008	27.428	433.424	0.13358	465.229	0.426	467.384	0.11653
432.011	27.417	433.704	0.13324	465.227	0.429	467.377	0.11613
432.002	27.408	433.712	0.13333	465.224	0.432	467.743	0.11607
432.008	27.396	434.031	0.13317	465.223	0.434	467.744	0.11610
432.010	27.380	434.396	0.13296	465.225	0.436	468.151	0.11587
432.002	27.371	434.377	0.13317	465.228	0.437	468.165	0.11627
432.006	27.369	434.774	0.13304	465.214	6.186	466.650	0.11929
432.004	27.342	434.755	0.13305	465.222	6.189	466.670	0.11971
432.004	36.556	433.380	0.13640	465.218	6.182	466.958	0.11901
431.999	36.538	433.662	0.13644	465.221	6.181	466.970	0.11891
432.002	36.521	433.643	0.13650	465.223	6.174	467.302	0.11914
432.000	36.507	433.986	0.13666	465.219	6.175	467.310	0.11921
432.000	36.470	434.315	0.13639	465.220	6.168	467.671	0.11937
431.997	36.456	434.316	0.13643	465.226	6.163	467.678	0.11898
432.003	36.436	434.694	0.13644	465.227	6.168	468.076	0.11900
432.001	36.426	434.708	0.13637	465.226	12.106	466.635	0.12198
432.010	46.328	433.354	0.14000	465.224	12.120	466.627	0.12217
432.010	46.275	433.634	0.13970	465.224	12.102	466.942	0.12201
432.008	46.246	433.621	0.13964	465.223	12.093	466.923	0.12234
432.003	46.218	433.936	0.13985	465.225	12.096	467.247	0.12225
432.012	46.193	433.932	0.13995	465.222	12.087	467.250	0.12209
432.006	46.165	434.275	0.13993	465.220	12.080	467.625	0.12180
432.010	46.143	434.290	0.13968	465.227	12.069	467.611	0.12190
432.010	46.120	434.640	0.13966	465.230	12.061	468.021	0.12186
432.010	46.096	434.670	0.13970	465.226	12.060	468.005	0.12239
432.010	57.289	433.326	0.14324	465.247	18.818	466.621	0.12487
432.007	57.250	433.321	0.14351	465.247	18.817	466.912	0.12509
432.008	57.209	433.590	0.14345	465.244	18.809	466.910	0.12499
432.007	57.175	433.591	0.14337	465.247	18.806	467.232	0.12513
432.009	57.134	433.900	0.14303	465.251	18.801	467.239	0.12551
432.010	57.110	433.916	0.14328	465.250	18.797	467.597	0.12507
432.012	57.071	434.235	0.14319	465.251	18.779	467.581	0.12477
432.007	57.015	434.246	0.14311	465.251	18.782	467.978	0.12477
432.006	56.979	434.596	0.14316	465.248	18.771	467.968	0.12483
432.007	56.941	434.588	0.14302	465.257	26.803	466.608	0.12888

[a]Initial cell temperature.

Table A1, continued.

T_i[a] /K	p /MPa	T /K	λ /W·m^{-1}K^{-1}	T_i[a] /K	p /MPa	T /K	λ /W·m^{-1}K^{-1}
465.255	26.774	466.898	0.12837	499.180	0.397	501.311	0.11033
465.260	26.757	466.902	0.12829	499.189	0.402	501.688	0.11029
465.255	26.738	467.216	0.12832	499.196	0.404	501.685	0.11017
465.258	26.722	467.210	0.12851	499.193	0.406	502.089	0.11030
465.257	26.700	467.551	0.12864	499.201	0.407	502.093	0.11019
465.260	26.694	467.566	0.12832	499.135	5.706	500.548	0.11353
465.258	26.669	467.916	0.12828	499.131	5.707	500.529	0.11340
465.261	26.654	467.939	0.12807	499.126	5.702	500.831	0.11335
465.287	35.633	466.610	0.13202	499.124	5.701	501.175	0.11339
465.279	35.618	466.601	0.13239	499.127	5.705	501.166	0.11378
465.290	35.608	466.880	0.13194	499.128	5.705	501.541	0.11338
465.286	35.594	466.895	0.13181	499.128	5.699	501.524	0.11348
465.285	35.562	467.193	0.13179	499.125	5.696	501.920	0.11311
465.287	35.545	467.198	0.13204	499.129	5.691	501.922	0.11328
465.290	35.531	467.540	0.13184	499.173	11.686	500.573	0.11682
465.289	35.499	467.519	0.13200	499.172	11.673	500.566	0.11717
465.292	35.473	467.898	0.13165	499.164	11.667	500.842	0.11669
465.287	35.403	467.903	0.13158	499.162	11.661	501.140	0.11680
465.306	45.511	466.585	0.13578	499.155	11.654	501.168	0.11655
465.305	45.464	466.579	0.13553	499.149	11.649	501.514	0.11651
465.314	45.428	466.847	0.13555	499.156	11.639	501.501	0.11649
465.307	45.357	467.146	0.13579	499.152	11.632	501.887	0.11670
465.308	45.302	467.145	0.13562	499.151	11.623	501.904	0.11634
465.307	45.269	467.466	0.13568	499.222	18.488	500.582	0.12039
465.305	45.237	467.475	0.13546	499.238	18.483	500.608	0.11988
465.309	45.168	467.832	0.13541	499.240	18.479	500.896	0.12051
465.308	56.563	466.563	0.13921	499.245	18.455	501.222	0.11981
465.301	56.500	466.537	0.13985	499.248	18.445	501.225	0.12017
465.305	56.445	466.807	0.13991	499.254	18.435	501.579	0.11983
465.311	56.398	466.812	0.13951	499.258	18.431	501.590	0.12016
465.304	56.341	467.110	0.13929	499.265	18.426	501.967	0.12015
465.302	56.284	467.110	0.13929	499.263	18.435	501.966	0.11981
465.307	56.228	467.414	0.13967	499.183	26.100	500.458	0.12403
465.304	56.184	467.421	0.13951	499.171	26.064	500.419	0.12364
465.308	56.135	467.771	0.13907	499.159	26.042	500.731	0.12365
465.309	56.067	467.761	0.13919	499.154	26.015	500.717	0.12341
499.176	0.382	500.657	0.11049	499.143	25.999	501.043	0.12361
499.178	0.388	500.965	0.11058	499.139	25.967	501.012	0.12369
499.183	0.393	500.977	0.11068	499.140	25.941	501.353	0.12369

[a]Initial cell temperature.

Table A1, continued.

T_i[a] /K	p /MPa	T /K	λ /W·m^{-1}K^{-1}
499.134	25.908	501.314	0.12344
499.134	25.895	501.704	0.12342
499.133	25.864	501.701	0.12351
499.194	35.320	500.490	0.12781
499.186	35.289	500.740	0.12760
499.189	35.246	500.755	0.12757
499.182	35.230	501.024	0.12782
499.178	35.178	501.025	0.12803
499.176	35.142	501.370	0.12753
499.174	35.108	501.325	0.12747
499.179	35.085	501.711	0.12743
499.176	34.992	501.693	0.12757
499.011	45.161	500.153	0.13194
498.996	45.094	500.115	0.13183
498.989	45.049	500.374	0.13148
498.984	44.991	500.362	0.13175
498.978	44.938	500.656	0.13186
498.973	44.874	500.643	0.13152
498.972	44.825	500.958	0.13136
498.969	44.755	500.922	0.13128
498.969	44.723	501.357	0.13194
498.968	44.664	501.325	0.13141
498.975	45.581	500.210	0.13161
498.977	45.522	500.193	0.13201
498.980	45.500	500.500	0.13170
498.981	45.457	500.482	0.13149
498.982	45.404	500.775	0.13152
498.980	45.350	500.770	0.13150
498.983	45.317	501.107	0.13155
498.986	45.268	501.100	0.13145
498.979	45.231	501.452	0.13142
498.982	45.184	501.441	0.13134
499.024	56.282	500.256	0.13616
499.026	56.211	500.507	0.13595
499.027	56.133	500.503	0.13551
499.029	56.059	500.796	0.13542
499.032	55.910	501.078	0.13557
499.040	55.840	501.103	0.13566
499.033	55.753	501.419	0.13546
499.031	55.675	501.423	0.13523

[a]Initial cell temperature.

Table A2: Thermal Conductivity Data for POE7 at Temperatures from 300 K to 500 K.

T_i[a] /K	p /MPa	T /K	λ /W·m^{-1}K^{-1}	T_i[a] /K	p /MPa	T /K	λ /W·m^{-1}K^{-1}
Wire 1				299.327	16.201	301.365	0.15493
299.103	0.220	300.046	0.15072	299.326	16.193	301.368	0.15495
299.107	0.220	300.054	0.15079	299.335	21.992	300.222	0.15662
299.113	0.220	300.311	0.15060	299.337	21.986	300.462	0.15662
299.115	0.220	300.314	0.15065	299.339	21.998	300.465	0.15657
299.119	0.221	300.604	0.15090	299.337	21.992	300.729	0.15664
299.127	0.221	300.612	0.15063	299.339	21.993	301.025	0.15653
299.130	0.221	300.919	0.15065	299.344	22.002	301.031	0.15656
299.138	0.220	300.928	0.15057	299.346	21.992	301.355	0.15651
299.141	0.221	301.273	0.15055	299.344	21.993	301.355	0.15651
299.146	0.221	301.281	0.15058	299.350	29.127	300.211	0.15846
299.257	0.212	300.185	0.15065	299.345	29.136	300.204	0.15852
299.260	0.212	300.186	0.15079	299.346	29.132	300.440	0.15841
299.264	0.212	300.443	0.15075	299.347	29.137	300.440	0.15859
299.263	0.212	300.442	0.15076	299.340	29.120	300.696	0.15848
299.265	0.212	300.724	0.15063	299.341	29.130	300.986	0.15840
299.274	0.212	300.734	0.15069	299.342	29.124	300.986	0.15851
299.276	0.212	301.038	0.15057	299.338	29.110	301.301	0.15837
299.280	0.212	301.044	0.15063	299.343	35.513	300.718	0.15957
299.276	0.211	301.376	0.15059	299.339	35.500	300.715	0.15983
299.280	0.211	301.379	0.15050	299.337	35.480	300.997	0.15945
299.299	8.128	300.198	0.15302	299.340	35.473	300.994	0.16001
299.295	8.060	300.196	0.15288	299.341	35.504	301.315	0.15953
299.294	8.000	300.457	0.15274	299.338	35.534	301.320	0.16000
299.295	7.933	300.458	0.15271	299.334	35.523	300.449	0.15982
299.298	7.885	300.738	0.15274	299.334	35.597	300.996	0.16014
299.296	7.832	300.735	0.15273	299.333	35.552	301.312	0.16001
299.299	7.691	301.035	0.15265	299.331	35.565	301.309	0.16004
299.301	7.648	301.370	0.15256	299.339	43.397	300.177	0.16215
299.298	7.594	301.368	0.15261	299.333	43.373	300.410	0.16209
299.334	16.220	300.238	0.15518	299.339	43.366	300.434	0.16200
299.336	16.218	300.485	0.15511	299.337	43.375	300.691	0.16214
299.332	16.210	300.484	0.15510	299.333	43.310	300.966	0.16193
299.327	16.219	300.750	0.15504	299.337	43.323	300.966	0.16197
299.336	16.204	300.755	0.15505	299.335	43.320	301.283	0.16187
299.332	16.192	301.042	0.15491	299.341	43.306	301.283	0.16192

[a]Initial cell temperature.

Table A2, continued.

T_i[a] /K	p /MPa	T /K	λ /W·m^{-1}K^{-1}	T_i[a] /K	p /MPa	T /K	λ /W·m^{-1}K^{-1}
299.345	51.809	300.219	0.16428	299.317	8.893	300.408	0.15264
299.341	51.802	300.200	0.16439	299.312	8.875	300.686	0.15266
299.340	51.789	300.429	0.16402	299.311	8.882	300.688	0.15250
299.343	51.764	300.686	0.16417	299.313	8.897	301.017	0.15247
299.342	51.788	300.687	0.16415	299.316	8.849	301.009	0.15247
299.344	51.775	300.968	0.16405	299.311	8.866	301.365	0.15249
299.346	51.799	300.973	0.16394	299.314	8.824	301.359	0.15241
299.338	51.770	301.270	0.16397	299.307	8.860	301.754	0.15236
299.352	60.273	300.161	0.16586	299.315	8.877	301.760	0.15239
299.349	60.262	300.154	0.16594	299.307	14.596	300.336	0.15416
299.347	60.303	300.389	0.16603	299.310	14.638	300.359	0.15413
299.348	60.387	300.395	0.16611	299.311	14.539	300.632	0.15413
299.349	60.416	300.650	0.16614	299.303	14.651	300.963	0.15409
299.353	60.426	300.687	0.16614	299.306	14.651	300.973	0.15410
299.347	60.443	300.959	0.16612	299.310	14.673	301.326	0.15413
299.346	60.450	300.957	0.16613	299.307	14.661	301.713	0.15397
299.351	60.459	301.270	0.16609	299.303	14.628	301.699	0.15402
299.349	60.464	301.270	0.16602	299.318	21.057	300.364	0.15644
Wire 2				299.313	21.167	300.656	0.15593
299.323	1.126	300.421	0.15035	299.315	21.150	300.970	0.15627
299.321	1.127	300.419	0.15052	299.314	21.168	301.319	0.15627
299.322	1.138	300.712	0.15039	299.315	21.154	301.316	0.15572
299.322	1.120	301.041	0.15030	299.311	21.170	301.699	0.15534
299.318	1.123	301.032	0.15032	299.315	21.170	301.703	0.15535
299.319	1.052	301.378	0.15024	299.320	28.228	300.340	0.15777
299.316	1.103	301.392	0.15023	299.320	28.195	301.302	0.15766
299.320	1.113	301.793	0.15014	299.322	28.240	301.306	0.15729
299.320	1.120	301.790	0.15021	299.319	28.150	301.669	0.15811
299.303	0.157	300.396	0.15020	299.318	28.193	301.681	0.15732
299.304	0.158	300.398	0.15022	299.323	35.419	300.365	0.15951
299.305	0.158	300.694	0.15016	299.320	35.386	300.632	0.15964
299.310	0.158	301.020	0.15009	299.318	35.421	300.636	0.15956
299.307	0.159	301.021	0.15006	299.319	35.376	300.942	0.15945
299.309	0.160	301.384	0.15001	299.321	35.423	300.950	0.15943
299.305	0.160	301.379	0.15005	299.320	35.428	301.281	0.15996
299.306	0.162	301.777	0.15001	299.317	35.398	301.280	0.15946
299.313	8.897	300.406	0.15261	299.319	35.351	301.653	0.15939

[a]Initial cell temperature.

Table A2, continued.

T_i[a] /K	p /MPa	T /K	λ /W·m^{-1}K^{-1}	T_i[a] /K	p /MPa	T /K	λ /W·m^{-1}K^{-1}
299.320	35.396	301.662	0.15937	299.311	68.747	301.573	0.16694
299.323	43.233	300.351	0.16152	299.314	68.766	301.571	0.16699
299.321	43.232	300.627	0.16149	330.744	0.109	331.790	0.14593
299.317	43.210	300.617	0.16144	330.746	0.109	331.793	0.14561
299.322	43.232	300.934	0.16148	330.745	0.110	332.079	0.14561
299.325	43.208	300.931	0.16139	330.746	0.110	332.073	0.14557
299.322	43.230	301.268	0.16132	330.744	0.111	332.387	0.14553
299.319	43.227	301.637	0.16129	330.744	0.111	332.729	0.14547
299.322	43.204	301.636	0.16126	330.743	0.112	332.726	0.14559
299.318	51.321	300.332	0.16357	330.745	0.112	333.110	0.14544
299.316	51.286	300.324	0.16343	330.757	6.618	332.377	0.14761
299.316	51.312	300.604	0.16341	330.757	6.627	332.382	0.14762
299.318	51.298	300.603	0.16331	330.756	6.618	332.714	0.14771
299.320	51.327	300.913	0.16335	330.758	6.635	332.718	0.14764
299.320	51.333	300.912	0.16342	330.754	6.636	333.087	0.14754
299.315	51.293	301.233	0.16321	330.755	6.648	333.092	0.14746
299.317	51.315	301.240	0.16329	330.756	6.630	333.497	0.14740
299.316	51.321	301.605	0.16319	330.756	6.625	333.494	0.14746
299.318	51.315	301.609	0.16322	330.754	6.624	333.936	0.14738
299.315	60.217	300.325	0.16528	330.759	6.631	333.942	0.14734
299.319	60.290	300.341	0.16562	330.760	13.583	332.356	0.14982
299.318	60.247	300.596	0.16534	330.755	13.573	332.351	0.14975
299.316	60.287	300.605	0.16532	330.762	13.581	332.692	0.14982
299.317	60.235	300.894	0.16526	330.761	13.569	332.686	0.14970
299.316	60.286	300.907	0.16541	330.760	13.580	333.063	0.14962
299.315	60.268	301.226	0.16524	330.762	13.569	333.056	0.14964
299.313	60.243	301.227	0.16514	330.756	13.575	333.455	0.14964
299.317	60.285	301.596	0.16526	330.756	13.581	333.452	0.14956
299.317	60.213	301.590	0.16518	330.763	13.589	333.897	0.14949
299.319	68.743	300.326	0.16708	330.760	13.582	333.893	0.14952
299.317	68.738	300.315	0.16719	330.764	21.235	332.308	0.15207
299.313	68.773	300.590	0.16725	330.762	21.236	332.306	0.15207
299.312	68.781	300.583	0.16724	330.766	21.234	332.638	0.15209
299.318	68.779	300.889	0.16710	330.766	21.237	332.641	0.15225
299.319	68.770	300.885	0.16712	330.765	21.222	333.005	0.15189
299.319	68.775	301.217	0.16704	330.764	21.210	332.999	0.15191
299.316	68.712	301.199	0.16730	330.767	21.224	333.403	0.15180

[a]Initial cell temperature.

Table A2, continued.

T_i[a] /K	p /MPa	T /K	λ /W·m^{-1}K^{-1}	T_i[a] /K	p /MPa	T /K	λ /W·m^{-1}K^{-1}
330.764	21.219	333.393	0.15182	330.781	57.967	333.300	0.16136
330.762	21.233	333.827	0.15182	330.778	57.959	333.289	0.16122
330.760	21.223	333.825	0.15178	330.777	57.963	333.700	0.16115
330.769	29.200	332.313	0.15438	330.782	57.951	333.703	0.16120
330.768	29.201	332.310	0.15435	330.785	68.911	332.240	0.16384
330.766	29.209	332.638	0.15432	330.781	68.913	332.542	0.16371
330.769	29.211	332.639	0.15423	330.778	68.930	332.540	0.16384
330.765	29.203	332.993	0.15418	330.781	68.915	332.891	0.16372
330.767	29.214	332.998	0.15427	330.779	68.898	332.878	0.16378
330.768	29.209	333.390	0.15415	330.779	68.904	333.252	0.16367
330.766	29.204	333.386	0.15420	330.781	68.909	333.255	0.16361
330.767	29.201	333.810	0.15403	330.780	68.910	333.657	0.16361
330.766	29.200	333.811	0.15401	330.786	68.891	333.657	0.16359
330.772	38.294	332.281	0.15693	364.066	0.126	365.625	0.14062
330.775	38.290	332.621	0.15666	364.073	0.127	365.626	0.14056
330.774	38.298	332.640	0.15668	364.073	0.127	365.934	0.14062
330.775	38.286	332.992	0.15659	364.071	0.128	366.279	0.14023
330.773	38.283	332.990	0.15701	364.073	0.128	366.289	0.14026
330.770	38.291	333.372	0.15655	364.071	0.129	366.692	0.14029
330.774	38.280	333.373	0.15651	364.071	0.129	366.685	0.14024
330.773	38.280	333.794	0.15649	364.075	0.129	367.121	0.14015
330.771	38.301	333.789	0.15644	364.071	0.130	367.115	0.14011
330.777	47.667	332.290	0.15895	364.085	0.149	365.640	0.14049
330.776	47.658	332.287	0.15919	364.087	0.151	365.648	0.14046
330.775	47.660	332.599	0.15898	364.088	0.152	365.972	0.14029
330.774	47.660	332.598	0.15902	364.087	0.153	366.002	0.14045
330.779	47.659	332.959	0.15891	364.087	0.154	366.353	0.14023
330.775	47.633	332.947	0.15887	364.091	0.156	366.364	0.14034
330.778	47.633	333.336	0.15881	364.093	0.156	366.759	0.14022
330.776	47.648	333.338	0.15889	364.092	0.156	367.182	0.14009
330.774	47.638	333.743	0.15877	364.091	0.155	367.188	0.14012
330.776	47.644	333.746	0.15876	364.119	6.728	365.669	0.14276
330.783	57.967	332.266	0.16160	364.117	6.738	365.984	0.14279
330.776	57.957	332.571	0.16128	364.118	6.733	365.978	0.14278
330.778	57.966	332.574	0.16139	364.118	6.708	366.331	0.14264
330.780	57.967	332.925	0.16129	364.121	6.707	366.344	0.14271
330.780	57.956	332.917	0.16131	364.120	6.710	366.719	0.14260

[a]Initial cell temperature.

Table A2, continued.

T_i[a] /K	p /MPa	T /K	λ /W·m^{-1}K^{-1}	T_i[a] /K	p /MPa	T /K	λ /W·m^{-1}K^{-1}
364.120	6.711	366.713	0.14263	364.134	37.471	366.992	0.15246
364.117	6.715	367.136	0.14246	364.130	37.418	366.991	0.15250
364.120	6.715	367.159	0.14242	364.122	46.876	365.552	0.15544
364.127	13.279	365.641	0.14514	364.116	46.873	365.557	0.15544
364.125	13.286	365.641	0.14511	364.114	46.853	365.853	0.15523
364.126	13.291	365.965	0.14523	364.113	46.846	365.858	0.15547
364.125	13.294	365.954	0.14511	364.114	46.840	366.195	0.15516
364.124	13.300	366.309	0.14494	364.114	46.830	366.185	0.15524
364.126	13.307	366.316	0.14495	364.108	46.834	366.543	0.15529
364.122	13.300	366.697	0.14486	364.111	46.823	366.545	0.15538
364.128	13.314	366.700	0.14504	364.109	46.828	366.939	0.15517
364.126	13.299	367.107	0.14486	364.110	46.829	366.936	0.15509
364.124	13.295	367.102	0.14479	364.113	57.708	365.481	0.15832
364.128	20.614	365.592	0.14738	364.108	57.707	365.480	0.15822
364.128	20.634	365.601	0.14750	364.111	57.717	365.773	0.15822
364.132	20.636	365.921	0.14759	364.108	57.723	365.774	0.15833
364.127	20.637	365.933	0.14746	364.106	57.711	366.129	0.15811
364.126	20.628	366.276	0.14734	364.106	57.712	366.140	0.15823
364.129	20.620	366.649	0.14736	364.103	57.696	366.489	0.15806
364.132	20.628	366.660	0.14729	364.103	57.709	366.490	0.15804
364.128	20.618	367.064	0.14727	364.102	57.697	366.871	0.15815
364.138	28.765	365.589	0.15014	364.105	57.683	366.880	0.15800
364.130	28.727	365.588	0.15010	364.104	68.798	365.467	0.16104
364.130	28.721	365.898	0.15005	364.105	68.801	365.468	0.16116
364.136	28.706	365.901	0.15007	364.105	68.803	365.762	0.16087
364.134	28.717	366.236	0.14997	364.101	68.782	365.760	0.16099
364.132	28.677	366.231	0.14996	364.100	68.787	366.094	0.16090
364.129	28.679	366.599	0.14996	364.102	68.781	366.097	0.16080
364.136	28.691	366.630	0.15007	364.104	68.778	366.455	0.16091
364.132	28.697	367.032	0.14987	364.103	68.768	366.450	0.16089
364.129	28.705	367.022	0.14981	364.103	68.767	366.823	0.16075
364.134	37.591	365.559	0.15275	364.099	68.753	366.820	0.16079
364.135	37.544	365.875	0.15279	397.623	0.103	399.106	0.13503
364.134	37.517	365.878	0.15282	397.623	0.103	399.101	0.13484
364.136	37.487	366.220	0.15261	397.625	0.107	399.424	0.13472
364.134	37.456	366.579	0.15253	397.622	0.107	399.419	0.13483
364.130	37.462	366.583	0.15260	397.623	0.103	399.762	0.13469

[a]Initial cell temperature.

Table A2, continued.

T_i[a] /K	p /MPa	T /K	λ /W·m^{-1}K^{-1}	T_i[a] /K	p /MPa	T /K	λ /W·m^{-1}K^{-1}
397.628	0.114	399.775	0.13471	397.638	28.020	399.323	0.14564
397.621	0.115	400.153	0.13477	397.637	28.027	399.322	0.14575
397.626	0.126	400.159	0.13480	397.642	28.025	399.657	0.14560
397.626	0.127	400.557	0.13457	397.642	28.040	399.658	0.14538
397.624	0.132	400.558	0.13454	397.644	28.041	400.005	0.14551
397.617	6.475	399.095	0.13771	397.643	28.036	400.012	0.14551
397.617	6.485	399.099	0.13745	397.643	28.038	400.394	0.14548
397.617	6.481	399.414	0.13749	397.644	28.059	400.398	0.14541
397.626	6.486	399.413	0.13761	397.651	37.368	399.021	0.14865
397.623	6.487	399.761	0.13740	397.650	37.365	399.304	0.14880
397.625	6.482	399.757	0.13736	397.650	37.357	399.298	0.14872
397.621	6.483	400.120	0.13735	397.648	37.349	399.616	0.14871
397.629	6.465	400.120	0.13739	397.651	37.354	399.621	0.14879
397.631	6.464	400.531	0.13734	397.654	37.339	399.965	0.14872
397.636	6.453	400.532	0.13733	397.647	37.348	400.340	0.14866
397.646	12.656	399.070	0.14001	397.647	37.344	400.336	0.14865
397.643	12.653	399.065	0.13991	397.646	46.595	398.957	0.15191
397.637	12.651	399.371	0.14012	397.653	46.585	398.964	0.15193
397.643	12.643	399.387	0.14006	397.645	46.581	399.236	0.15177
397.638	12.639	399.710	0.13987	397.649	46.592	399.252	0.15204
397.636	12.642	399.714	0.13983	397.646	46.676	399.570	0.15162
397.633	12.637	400.067	0.13981	397.645	46.715	399.585	0.15176
397.636	12.628	400.065	0.13981	397.645	46.737	399.931	0.15174
397.631	12.629	400.462	0.13981	397.653	46.748	399.936	0.15155
397.634	12.623	400.469	0.13969	397.652	46.758	400.308	0.15157
397.638	20.130	399.054	0.14277	397.657	46.763	400.307	0.15167
397.640	20.133	399.066	0.14303	397.714	57.482	399.041	0.15527
397.640	20.131	399.359	0.14257	397.715	57.482	399.041	0.15522
397.642	20.129	399.355	0.14259	397.711	57.484	399.318	0.15508
397.638	20.119	399.688	0.14261	397.720	57.487	399.326	0.15485
397.640	20.120	399.689	0.14280	397.720	57.489	399.631	0.15491
397.642	20.119	400.055	0.14269	397.724	57.491	399.647	0.15496
397.638	20.111	400.039	0.14261	397.725	57.485	399.976	0.15505
397.641	20.115	400.441	0.14260	397.726	57.483	399.974	0.15502
397.639	20.120	400.430	0.14279	397.725	57.487	400.332	0.15492
397.643	28.026	399.046	0.14569	397.725	57.482	400.333	0.15492
397.638	28.027	399.051	0.14566	397.738	68.861	398.967	0.15860

[a]Initial cell temperature.

Table A2, continued.

T_i[a] /K	p /MPa	T /K	λ /W·m^{-1}K^{-1}	T_i[a] /K	p /MPa	T /K	λ /W·m^{-1}K^{-1}
397.734	68.849	398.969	0.15841	431.347	12.322	433.654	0.13466
397.737	68.847	399.234	0.15838	431.348	12.326	433.673	0.13464
397.738	68.836	399.539	0.15836	431.344	12.324	434.048	0.13455
397.739	68.831	399.546	0.15830	431.343	12.314	434.034	0.13449
397.736	68.828	399.863	0.15823	431.356	19.427	432.729	0.13801
397.743	68.819	399.877	0.15817	431.350	19.433	432.730	0.13792
397.740	68.810	400.222	0.15814	431.354	19.424	433.009	0.13790
397.745	68.735	399.048	0.15834	431.352	19.418	433.009	0.13795
397.748	68.729	399.061	0.15845	431.351	19.414	433.325	0.13757
397.749	68.721	399.325	0.15805	431.353	19.418	433.329	0.13763
397.746	68.710	399.620	0.15818	431.345	19.419	433.664	0.13750
397.741	68.705	399.616	0.15819	431.349	19.417	433.667	0.13756
397.748	68.698	399.950	0.15796	431.349	19.413	434.030	0.13762
397.748	68.686	400.304	0.15803	431.342	19.406	434.018	0.13757
397.744	68.678	400.299	0.15806	431.348	27.520	432.695	0.14114
431.317	0.101	432.783	0.12922	431.357	27.510	432.691	0.14117
431.311	0.106	433.064	0.12940	431.355	27.504	432.971	0.14102
431.318	0.111	433.083	0.12916	431.357	27.495	433.280	0.14088
431.318	0.118	433.421	0.12915	431.356	27.489	433.289	0.14091
431.311	0.119	433.402	0.12898	431.356	27.496	433.616	0.14092
431.319	0.121	433.778	0.12914	431.360	27.492	433.984	0.14076
431.316	0.129	433.779	0.12892	431.359	27.481	433.985	0.14080
431.321	0.133	434.161	0.12890	431.353	36.447	432.643	0.14449
431.318	0.138	434.165	0.12885	431.354	36.427	432.641	0.14450
431.363	6.164	432.763	0.13212	431.351	36.432	432.909	0.14469
431.369	6.166	432.777	0.13208	431.352	36.417	432.904	0.14420
431.375	6.153	433.073	0.13204	431.357	36.423	433.230	0.14455
431.372	6.160	433.392	0.13199	431.355	36.419	433.211	0.14436
431.372	6.150	433.395	0.13198	431.356	36.406	433.557	0.14434
431.374	6.149	433.744	0.13191	431.353	36.414	433.538	0.14413
431.371	6.147	434.149	0.13177	431.355	36.405	433.899	0.14417
431.369	6.141	434.159	0.13168	431.353	36.395	433.891	0.14417
431.353	12.338	432.710	0.13495	431.367	46.217	432.579	0.14780
431.339	12.342	432.999	0.13452	431.357	46.199	432.563	0.14773
431.347	12.343	433.000	0.13485	431.364	46.192	432.841	0.14784
431.342	12.339	433.312	0.13484	431.368	46.193	432.913	0.14781
431.346	12.334	433.320	0.13501	431.365	46.181	433.207	0.14770

[a]Initial cell temperature.

Table A2, continued.

T_i[a] /K	p /MPa	T /K	λ /W·m^{-1}K^{-1}	T_i[a] /K	p /MPa	T /K	λ /W·m^{-1}K^{-1}
431.359	46.184	433.197	0.14782	466.396	5.814	468.345	0.12602
431.368	46.178	433.537	0.14780	466.394	5.820	468.710	0.12589
431.365	46.167	433.528	0.14778	466.397	5.833	468.722	0.12606
431.367	46.156	433.866	0.14765	466.398	5.836	469.095	0.12603
431.365	46.137	433.858	0.14760	466.399	5.829	469.079	0.12611
431.378	57.128	432.639	0.15145	466.440	11.900	467.803	0.12953
431.375	57.124	432.637	0.15168	466.439	11.893	467.799	0.12935
431.374	57.107	432.897	0.15148	466.438	11.896	468.085	0.12921
431.380	57.102	432.897	0.15133	466.446	11.886	468.072	0.12947
431.382	57.085	433.192	0.15146	466.441	11.879	468.391	0.12921
431.380	57.071	433.187	0.15144	466.440	11.875	468.375	0.12913
431.381	57.058	433.506	0.15148	466.438	11.868	468.726	0.12909
431.383	57.039	433.494	0.15115	466.434	11.862	469.078	0.12914
431.389	57.037	433.854	0.15118	466.434	11.874	469.105	0.12896
431.384	57.015	433.836	0.15126	466.413	18.950	467.720	0.13288
431.377	64.069	432.600	0.15364	466.412	18.937	467.986	0.13236
431.372	63.989	432.607	0.15345	466.413	18.950	468.008	0.13237
431.369	63.916	432.870	0.15382	466.414	18.947	468.321	0.13232
431.370	63.851	432.873	0.15359	466.416	18.938	468.298	0.13233
431.367	63.796	433.155	0.15354	466.420	18.940	468.648	0.13226
431.367	63.725	433.140	0.15373	466.422	18.932	469.010	0.13219
431.370	63.668	433.455	0.15344	466.432	18.930	469.022	0.13249
431.368	63.628	433.458	0.15332	466.452	26.665	467.720	0.13631
431.372	63.573	433.784	0.15345	466.452	26.664	467.725	0.13592
431.368	63.527	433.793	0.15329	466.451	26.651	467.982	0.13600
466.376	0.203	467.798	0.12324	466.451	26.653	468.003	0.13586
466.379	0.192	467.796	0.12320	466.445	26.649	468.278	0.13603
466.375	0.196	468.083	0.12346	466.447	26.632	468.274	0.13639
466.374	0.193	468.407	0.12303	466.443	26.648	468.618	0.13578
466.371	0.199	468.400	0.12326	466.441	26.634	468.596	0.13582
466.374	0.198	468.760	0.12293	466.441	26.633	468.968	0.13555
466.377	0.189	469.137	0.12273	466.440	26.634	468.949	0.13549
466.381	0.196	469.151	0.12297	466.452	36.020	467.693	0.13972
466.398	5.823	467.765	0.12627	466.448	36.014	467.695	0.13956
466.399	5.823	467.756	0.12606	466.456	36.011	467.960	0.13963
466.403	5.812	468.039	0.12632	466.451	36.008	467.963	0.13970
466.398	5.825	468.360	0.12597	466.454	36.007	468.263	0.13970

[a]Initial cell temperature.

Table A2, continued.

T_i[a] /K	p /MPa	T /K	λ /W·m^{-1}K^{-1}	T_i[a] /K	p /MPa	T /K	λ /W·m^{-1}K^{-1}
466.456	36.001	468.254	0.13959	500.984	5.326	502.946	0.11871
466.457	35.985	468.566	0.13971	500.990	5.321	503.290	0.11865
466.459	35.977	468.570	0.13978	500.982	5.302	503.665	0.11836
466.453	35.977	468.898	0.13939	500.973	5.319	503.635	0.11844
466.455	35.971	468.907	0.13945	500.971	5.314	504.045	0.11843
466.461	45.826	467.658	0.14395	500.964	5.327	504.032	0.11843
466.471	45.805	467.654	0.14326	500.895	11.398	502.460	0.12199
466.464	45.804	467.921	0.14376	500.887	11.374	502.440	0.12214
466.463	45.789	467.902	0.14330	500.885	11.334	502.743	0.12236
466.470	45.780	468.200	0.14364	500.885	11.284	502.737	0.12197
466.468	45.778	468.203	0.14335	500.879	11.324	503.135	0.12203
466.467	45.770	468.513	0.14324	500.878	11.335	503.138	0.12187
466.473	45.759	468.518	0.14333	500.884	11.338	503.512	0.12170
466.470	45.745	468.835	0.14353	500.880	11.332	503.491	0.12175
466.473	45.736	468.844	0.14340	500.879	11.362	503.882	0.12185
466.463	56.777	467.607	0.14734	500.884	11.340	503.881	0.12178
466.462	56.764	467.622	0.14784	500.884	18.368	502.465	0.12597
466.463	56.750	467.853	0.14760	500.877	18.362	502.459	0.12578
466.464	56.741	467.871	0.14729	500.874	18.344	502.735	0.12604
466.466	56.721	468.132	0.14781	500.863	18.301	502.725	0.12553
466.470	56.706	468.142	0.14743	500.858	18.254	503.027	0.12553
466.466	56.698	468.427	0.14739	500.856	18.214	503.030	0.12565
466.470	56.695	468.449	0.14757	500.857	18.275	503.407	0.12535
466.467	56.675	468.765	0.14732	500.857	18.306	503.403	0.12543
466.465	56.661	468.766	0.14803	500.853	18.307	503.771	0.12535
501.023	0.092	502.705	0.11534	500.855	18.300	503.772	0.12541
501.024	0.099	502.707	0.11574	500.902	26.437	502.434	0.12957
501.021	0.096	503.026	0.11573	500.897	26.459	502.439	0.12977
501.022	0.093	503.035	0.11542	500.896	26.463	502.721	0.12944
501.017	0.097	503.377	0.11537	500.897	26.434	502.704	0.12956
501.012	0.100	503.356	0.11532	500.895	26.413	503.043	0.12936
501.005	0.103	503.721	0.11526	500.890	26.409	503.046	0.12935
500.996	0.097	503.707	0.11472	500.889	26.361	503.360	0.12929
501.000	0.092	504.134	0.11535	500.890	26.294	503.372	0.12930
500.992	0.100	504.128	0.11524	500.890	26.297	503.734	0.12926
500.985	5.344	502.608	0.11877	500.890	26.281	503.730	0.12936
500.990	5.317	502.939	0.11855	500.939	35.510	502.432	0.13351

[a]Initial cell temperature.

Table A2, continued.

T_i[a] /K	p /MPa	T /K	λ /W·m^{-1}K^{-1}
500.943	35.486	502.435	0.13357
500.949	35.445	502.717	0.13348
500.955	35.430	502.735	0.13363
500.956	35.380	503.062	0.13328
500.956	35.361	503.049	0.13355
500.972	35.359	503.402	0.13320
500.975	35.292	503.390	0.13315
500.973	35.242	503.779	0.13319
500.981	35.202	503.784	0.13310
500.930	45.302	502.360	0.13811
500.924	45.254	502.639	0.13754
500.917	45.215	502.634	0.13749
500.909	45.143	502.910	0.13775
500.901	45.103	502.909	0.13837
500.895	45.075	503.212	0.13738
500.878	45.029	503.199	0.13741
500.872	44.966	503.553	0.13707
500.855	44.925	503.547	0.13712
500.769	56.262	502.177	0.14186
500.763	56.188	502.160	0.14169
500.764	56.129	502.441	0.14182
500.761	56.029	502.426	0.14173
500.763	55.948	502.704	0.14160
500.763	55.888	502.716	0.14187
500.763	55.821	503.044	0.14159
500.765	55.775	503.039	0.14155
500.757	55.681	503.369	0.14139
500.754	55.624	503.359	0.14130

[a]Initial cell temperature.

Table A3: Thermal Conductivity Data for POE9 at Temperatures from 300 K to 500 K.

T_i[a] /K	p /MPa	T /K	λ /W·m^{-1}K^{-1}	T_i[a] /K	p /MPa	T /K	λ /W·m^{-1}K^{-1}
299.474	0.117	301.250	0.15582	299.473	0.209	302.439	0.15566
299.471	0.133	301.241	0.15579	299.473	0.230	302.921	0.15554
299.472	0.150	301.610	0.15578	299.469	0.229	302.913	0.15553
299.469	0.091	301.594	0.15576	299.465	0.213	301.220	0.15605
299.469	0.125	302.014	0.15568	299.466	0.214	301.224	0.15612
299.463	0.108	302.000	0.15574	299.464	0.214	301.589	0.15603
299.467	0.122	302.409	0.15563	299.466	0.214	301.590	0.15598
299.465	0.075	302.401	0.15561	299.465	0.214	302.000	0.15590
299.462	0.124	302.885	0.15601	299.467	0.214	301.996	0.15590
299.467	0.115	302.908	0.15549	299.465	0.214	302.440	0.15586
299.465	0.060	301.218	0.15593	299.462	0.215	302.437	0.15580
299.467	0.059	301.234	0.15578	299.465	0.215	302.918	0.15572
299.469	0.108	301.602	0.15575	299.461	0.215	302.910	0.15571
299.468	0.066	301.590	0.15641	299.487	6.767	301.225	0.15786
299.472	0.089	302.009	0.15570	299.488	6.785	301.226	0.15785
299.471	0.076	302.008	0.15570	299.487	6.786	301.587	0.15777
299.472	0.071	302.452	0.15557	299.483	6.778	301.987	0.15774
299.471	0.096	302.450	0.15561	299.485	6.754	301.987	0.15776
299.473	0.091	302.934	0.15540	299.487	6.756	302.427	0.15765
299.473	0.099	302.929	0.15546	299.487	6.754	302.428	0.15769
299.473	0.257	301.232	0.15593	299.488	6.742	302.898	0.15749
299.473	0.240	301.227	0.15593	299.485	6.743	302.898	0.15755
299.472	0.256	301.600	0.15580	299.480	13.701	301.181	0.15989
299.474	0.251	301.594	0.15584	299.485	13.686	301.543	0.15975
299.475	0.256	302.007	0.15573	299.484	13.686	301.540	0.15978
299.475	0.245	302.004	0.15574	299.480	13.687	301.935	0.15970
299.474	0.211	302.440	0.15559	299.479	13.686	302.365	0.15962
299.480	0.231	302.451	0.15568	299.484	13.678	302.371	0.15962
299.477	0.222	302.924	0.15555	299.482	13.659	302.832	0.15953
299.480	0.257	302.936	0.15556	299.480	13.625	302.833	0.15950
299.475	0.207	301.233	0.15604	299.471	21.550	301.140	0.16205
299.475	0.209	301.233	0.15587	299.470	21.578	301.146	0.16198
299.478	0.225	301.604	0.15585	299.471	21.565	301.491	0.16193
299.476	0.210	301.598	0.15580	299.472	21.568	301.496	0.16196
299.474	0.214	302.003	0.15560	299.470	21.555	301.884	0.16190
299.475	0.209	302.003	0.15582	299.467	21.558	301.882	0.16190
299.472	0.220	302.443	0.15565	299.468	21.574	302.309	0.16225

[a]Initial cell temperature.

Table A3, continued.

T_i[a] /K	p /MPa	T /K	λ /W·m^{-1}K^{-1}	T_i[a] /K	p /MPa	T /K	λ /W·m^{-1}K^{-1}
299.469	21.577	302.311	0.16179	299.459	58.425	302.196	0.17099
299.469	21.576	302.770	0.16168	299.455	58.418	302.186	0.17104
299.466	21.573	302.768	0.16167	299.455	58.428	302.630	0.17089
299.463	30.163	301.116	0.16429	299.455	68.112	301.374	0.17339
299.460	30.160	301.115	0.16433	299.456	68.053	301.750	0.17342
299.465	30.158	301.469	0.16422	299.458	68.034	301.750	0.17324
299.460	30.158	301.851	0.16413	299.456	67.990	302.148	0.17316
299.462	30.142	301.857	0.16414	299.458	67.925	302.146	0.17308
299.461	30.139	302.277	0.16411	299.454	67.787	301.045	0.17357
299.460	30.124	302.276	0.16398	299.453	67.730	301.380	0.17336
299.458	30.144	302.733	0.16396	299.454	67.699	301.382	0.17330
299.460	30.142	302.737	0.16397	299.457	67.624	301.742	0.17338
299.458	38.919	301.113	0.16654	299.455	67.420	301.730	0.17323
299.457	38.917	301.112	0.16647	299.456	67.354	302.134	0.17311
299.455	38.909	301.451	0.16646	299.452	67.353	302.153	0.17310
299.451	38.903	301.446	0.16643	299.452	67.355	302.591	0.17303
299.453	38.906	301.834	0.16640	299.454	67.355	302.592	0.17301
299.453	38.875	301.826	0.16643	331.658	0.196	333.293	0.15113
299.454	38.868	302.245	0.16627	331.654	0.197	333.627	0.15084
299.452	38.874	302.247	0.16631	331.655	0.198	333.633	0.15097
299.452	38.863	302.694	0.16617	331.653	0.198	334.007	0.15081
299.450	38.852	302.687	0.16624	331.657	0.199	334.013	0.15071
299.453	48.362	301.073	0.16916	331.656	0.199	334.422	0.15071
299.457	48.352	301.078	0.16881	331.655	0.199	334.415	0.15072
299.455	48.365	301.418	0.16886	331.659	0.199	334.866	0.15066
299.451	48.377	301.790	0.16857	331.659	0.200	334.868	0.15062
299.456	48.369	301.795	0.16869	331.675	6.392	333.276	0.15252
299.456	48.345	302.205	0.16861	331.675	6.392	333.282	0.15294
299.453	48.369	302.202	0.16863	331.674	6.367	333.610	0.15290
299.452	48.367	302.647	0.16859	331.675	6.372	333.993	0.15276
299.450	48.349	302.641	0.16851	331.677	6.364	333.983	0.15280
299.453	58.442	301.057	0.17130	331.674	6.349	334.395	0.15271
299.456	58.341	301.049	0.17128	331.677	6.343	334.839	0.15223
299.460	58.409	301.421	0.17111	331.674	6.372	334.837	0.15219
299.453	58.435	301.411	0.17115	331.680	13.478	333.265	0.15519
299.453	58.425	301.783	0.17110	331.675	13.473	333.261	0.15511
299.454	58.428	301.785	0.17115	331.675	13.449	333.582	0.15535

[a]Initial cell temperature.

Table A3, continued.

T_i[a] /K	p /MPa	T /K	λ /W·m^{-1}K^{-1}	T_i[a] /K	p /MPa	T /K	λ /W·m^{-1}K^{-1}
331.678	13.462	333.594	0.15513	331.699	47.926	333.204	0.16494
331.674	13.472	333.959	0.15500	331.699	47.905	333.512	0.16487
331.677	13.414	333.943	0.15500	331.700	47.918	333.518	0.16495
331.674	13.446	334.360	0.15490	331.698	47.904	333.866	0.16507
331.677	13.458	334.377	0.15493	331.700	47.896	333.861	0.16481
331.682	13.473	334.814	0.15485	331.699	47.910	334.245	0.16474
331.677	13.471	334.809	0.15486	331.703	47.918	334.252	0.16477
331.676	21.127	333.235	0.15745	331.701	47.887	334.651	0.16465
331.679	21.107	333.225	0.15763	331.699	47.899	334.651	0.16457
331.677	21.112	333.564	0.15735	331.704	57.689	333.157	0.16745
331.677	21.103	333.573	0.15737	331.702	57.666	333.146	0.16767
331.676	21.102	333.940	0.15734	331.702	57.673	333.503	0.16741
331.681	21.094	333.941	0.15735	331.700	57.681	333.501	0.16735
331.678	21.102	334.332	0.15725	331.706	57.676	333.853	0.16734
331.674	21.106	334.336	0.15729	331.704	57.672	333.847	0.16745
331.682	21.108	334.769	0.15716	331.705	57.671	334.225	0.16731
331.678	21.108	334.761	0.15718	331.704	57.662	334.222	0.16732
331.679	29.091	333.220	0.15987	331.703	57.629	334.619	0.16724
331.680	29.104	333.225	0.15981	331.702	57.661	334.619	0.16722
331.682	29.118	333.551	0.15978	331.702	69.046	333.130	0.17026
331.683	29.112	333.548	0.15974	331.698	69.058	333.129	0.17032
331.683	29.077	333.902	0.15958	331.698	69.048	333.432	0.17033
331.683	29.108	334.298	0.15961	331.696	69.030	333.430	0.17022
331.681	29.087	334.294	0.15963	331.700	69.036	333.771	0.17032
331.683	29.075	334.717	0.15954	331.698	69.032	333.776	0.17024
331.679	29.087	334.715	0.15932	331.695	69.011	334.136	0.17012
331.695	38.437	333.210	0.16240	331.699	69.003	334.137	0.17018
331.690	38.429	333.207	0.16258	331.695	69.000	334.532	0.17011
331.688	38.432	333.517	0.16231	331.696	68.974	334.530	0.17006
331.688	38.432	333.520	0.16230	364.342	0.232	365.896	0.14573
331.691	38.418	333.875	0.16230	364.341	0.234	366.217	0.14576
331.685	38.433	333.872	0.16228	364.338	0.235	366.205	0.14566
331.694	38.447	334.268	0.16271	364.337	0.236	366.566	0.14554
331.689	38.423	334.257	0.16223	364.337	0.237	366.557	0.14561
331.696	38.441	334.686	0.16211	364.336	0.238	366.951	0.14567
331.693	38.443	334.697	0.16214	364.342	0.239	366.960	0.14564
331.705	47.934	333.206	0.16494	364.339	0.240	367.353	0.14551

[a]Initial cell temperature.

Table A3, continued.

T_i[a] /K	p /MPa	T /K	λ /W·m^{-1}K^{-1}	T_i[a] /K	p /MPa	T /K	λ /W·m^{-1}K^{-1}
364.337	0.241	367.375	0.14548	364.336	28.938	367.136	0.15522
364.336	6.947	365.841	0.14815	364.330	37.437	365.715	0.15818
364.334	6.946	366.139	0.14811	364.330	37.441	365.739	0.15827
364.336	6.933	366.147	0.14806	364.335	37.441	366.065	0.15817
364.331	6.945	366.493	0.14800	364.327	37.380	366.047	0.15809
364.333	6.965	366.500	0.14807	364.335	37.405	366.393	0.15797
364.333	6.948	366.871	0.14805	364.331	37.423	366.388	0.15807
364.334	6.953	366.868	0.14796	364.331	37.368	366.743	0.15801
364.334	6.963	367.292	0.14789	364.333	37.370	366.748	0.15797
364.329	6.936	367.272	0.14793	364.327	37.363	367.130	0.15794
364.337	13.582	365.803	0.15036	364.331	37.318	367.130	0.15796
364.334	13.583	365.804	0.15054	364.331	47.040	365.696	0.16093
364.334	13.595	366.109	0.15054	364.335	47.049	365.709	0.16102
364.336	13.601	366.463	0.15035	364.333	47.011	365.990	0.16119
364.335	13.600	366.455	0.15050	364.331	46.979	365.992	0.16103
364.327	13.614	366.837	0.15032	364.335	46.995	366.324	0.16096
364.335	13.583	366.825	0.15025	364.334	46.989	366.317	0.16091
364.330	13.586	367.235	0.15026	364.336	46.953	366.672	0.16087
364.336	20.492	365.776	0.15296	364.336	46.972	366.680	0.16091
364.335	20.474	365.779	0.15275	364.339	46.949	367.059	0.16078
364.337	20.500	366.090	0.15273	364.339	46.930	367.056	0.16076
364.339	20.491	366.122	0.15277	364.342	57.979	365.726	0.16416
364.337	20.490	366.453	0.15271	364.346	57.981	365.724	0.16446
364.333	20.504	366.456	0.15265	364.345	57.969	366.019	0.16411
364.336	20.501	366.829	0.15264	364.347	57.985	366.013	0.16418
364.336	20.487	366.819	0.15268	364.339	57.989	366.327	0.16403
364.340	20.503	367.238	0.15256	364.344	57.975	366.337	0.16414
364.335	20.499	367.221	0.15265	364.342	57.960	366.677	0.16395
364.337	28.939	365.737	0.15557	364.346	57.926	366.686	0.16396
364.345	28.965	365.766	0.15547	364.346	57.943	367.058	0.16385
364.337	28.956	366.046	0.15562	364.342	57.920	367.052	0.16389
364.341	28.971	366.062	0.15555	364.353	68.874	365.676	0.16692
364.335	28.956	366.378	0.15546	364.353	68.857	365.676	0.16727
364.339	28.969	366.389	0.15547	364.354	68.864	365.965	0.16705
364.337	28.927	366.739	0.15547	364.357	68.864	365.970	0.16713
364.339	28.967	366.760	0.15542	364.355	68.852	366.281	0.16690
364.331	28.975	367.145	0.15531	364.354	68.861	366.278	0.16706

[a]Initial cell temperature.

Table A3, continued.

T_i[a] /K	p /MPa	T /K	λ /W·m^{-1}K^{-1}	T_i[a] /K	p /MPa	T /K	λ /W·m^{-1}K^{-1}
364.353	68.832	366.617	0.16699	397.592	20.257	399.231	0.14799
364.351	68.860	366.624	0.16689	397.590	20.258	399.548	0.14809
364.353	68.858	366.990	0.16700	397.591	20.253	399.552	0.14789
364.355	68.855	367.000	0.16683	397.591	20.246	399.886	0.14794
397.579	0.186	399.052	0.14030	397.591	20.238	399.906	0.14793
397.580	0.187	399.058	0.14016	397.592	20.237	400.268	0.14788
397.582	0.188	399.370	0.14009	397.589	20.246	400.281	0.14796
397.584	0.188	399.365	0.14007	397.595	28.293	398.963	0.15090
397.581	0.189	399.696	0.14007	397.596	28.315	398.967	0.15110
397.585	0.190	399.705	0.14005	397.599	28.326	399.261	0.15058
397.586	0.190	400.078	0.13984	397.591	28.299	399.554	0.15084
397.585	0.191	400.064	0.14007	397.598	28.310	399.571	0.15097
397.586	0.191	400.478	0.13988	397.596	28.298	399.913	0.15081
397.588	0.192	400.481	0.13989	397.597	28.295	400.274	0.15078
397.576	6.488	399.018	0.14302	397.595	28.304	400.290	0.15071
397.583	6.489	399.021	0.14280	397.606	36.962	398.913	0.15408
397.582	6.491	399.327	0.14272	397.596	36.971	398.931	0.15395
397.584	6.488	399.327	0.14267	397.594	36.969	399.196	0.15391
397.581	6.493	399.657	0.14266	397.597	36.960	399.509	0.15373
397.582	6.494	399.655	0.14269	397.596	36.971	399.522	0.15375
397.581	6.485	400.018	0.14255	397.596	36.964	399.843	0.15383
397.575	6.480	400.019	0.14255	397.593	36.967	399.855	0.15370
397.576	6.490	400.400	0.14252	397.597	36.944	400.209	0.15326
397.577	6.484	400.398	0.14249	397.591	36.970	400.208	0.15375
397.583	12.905	398.967	0.14529	397.589	46.634	398.898	0.15742
397.580	12.926	398.951	0.14522	397.594	46.639	398.904	0.15722
397.583	12.911	399.256	0.14529	397.594	46.644	399.179	0.15706
397.580	12.920	399.242	0.14529	397.591	46.628	399.171	0.15697
397.582	12.917	399.577	0.14517	397.596	46.645	399.483	0.15699
397.580	12.908	399.560	0.14517	397.585	46.631	399.472	0.15699
397.586	12.917	399.939	0.14469	397.592	46.641	399.809	0.15697
397.579	12.909	399.917	0.14517	397.592	46.635	399.817	0.15691
397.578	12.918	400.308	0.14514	397.587	46.624	400.157	0.15678
397.583	12.909	400.316	0.14500	397.592	46.635	400.166	0.15693
397.588	20.259	398.934	0.14830	397.588	57.231	398.866	0.16037
397.591	20.243	398.931	0.14793	397.594	57.231	398.867	0.16065
397.586	20.240	399.207	0.14833	397.591	57.230	399.140	0.16041

[a]Initial cell temperature.

Table A3, continued.

T_i[a] /K	p /MPa	T /K	λ /W·m^{-1}K^{-1}	T_i[a] /K	p /MPa	T /K	λ /W·m^{-1}K^{-1}
397.588	57.218	399.128	0.16047	430.690	12.329	432.637	0.13985
397.590	57.218	399.433	0.16004	430.690	12.321	432.629	0.13988
397.593	57.199	399.423	0.16024	430.696	12.322	432.984	0.13973
397.587	57.197	399.757	0.16013	430.694	12.330	433.344	0.13983
397.587	57.197	399.751	0.16018	430.695	12.340	433.348	0.13979
397.584	57.205	400.110	0.16015	430.694	19.391	431.982	0.14300
397.584	57.199	400.109	0.16000	430.693	19.407	431.985	0.14310
397.597	68.575	398.827	0.16367	430.693	19.402	432.248	0.14286
397.593	68.546	399.118	0.16379	430.697	19.391	432.254	0.14287
397.592	68.503	399.422	0.16359	430.692	19.402	432.557	0.14295
397.589	68.480	399.414	0.16360	430.696	19.413	432.578	0.14299
397.594	68.465	399.748	0.16357	430.697	19.412	432.907	0.14271
397.588	68.421	399.733	0.16353	430.696	19.401	432.894	0.14289
397.593	68.425	400.080	0.16394	430.692	19.421	433.273	0.14273
397.597	68.418	400.098	0.16356	430.693	19.426	433.262	0.14271
430.704	0.227	432.115	0.13477	430.697	27.649	431.993	0.14634
430.706	0.228	432.409	0.13455	430.699	27.666	432.265	0.14598
430.708	0.229	432.401	0.13442	430.697	27.654	432.264	0.14625
430.708	0.230	432.724	0.13434	430.698	27.666	432.578	0.14615
430.702	0.230	432.733	0.13443	430.701	27.663	432.576	0.14615
430.708	0.231	433.084	0.13433	430.703	27.670	432.922	0.14595
430.707	0.231	433.087	0.13430	430.700	27.651	433.243	0.14605
430.708	0.232	433.464	0.13419	430.696	27.661	433.244	0.14609
430.707	0.233	433.472	0.13422	430.703	36.356	431.949	0.14974
430.694	5.816	432.054	0.13712	430.700	36.361	431.944	0.14951
430.699	5.822	432.052	0.13698	430.701	36.360	432.234	0.14954
430.703	5.799	432.342	0.13693	430.695	36.352	432.207	0.14968
430.702	5.826	432.349	0.13715	430.699	36.357	432.527	0.14949
430.700	5.818	432.666	0.13704	430.692	36.346	432.840	0.14931
430.698	5.815	432.648	0.13699	430.691	36.360	432.841	0.14922
430.701	5.819	433.009	0.13691	430.690	36.338	433.170	0.14930
430.705	5.799	433.010	0.13696	430.684	46.136	431.957	0.15299
430.699	5.812	433.379	0.13702	430.683	46.140	431.937	0.15323
430.700	5.820	433.404	0.13676	430.684	46.121	432.190	0.15307
430.693	12.302	432.019	0.13994	430.681	46.110	432.193	0.15310
430.692	12.318	432.332	0.13996	430.682	46.109	432.485	0.15293
430.687	12.342	432.317	0.14009	430.683	46.127	432.484	0.15281

[a]Initial cell temperature.

Table A3, continued.

T_i[a] /K	p /MPa	T /K	λ /W·m^{-1}K^{-1}	T_i[a] /K	p /MPa	T /K	λ /W·m^{-1}K^{-1}
430.687	46.107	432.796	0.15281	464.026	5.926	466.268	0.13143
430.683	46.118	432.799	0.15292	464.020	5.940	466.635	0.13150
430.681	46.120	433.138	0.15280	464.016	5.914	466.609	0.13144
430.680	46.107	433.137	0.15280	464.021	11.994	465.310	0.13460
430.686	56.970	431.886	0.15692	464.025	12.008	465.325	0.13434
430.691	56.950	432.150	0.15668	464.020	12.017	465.589	0.13464
430.695	56.962	432.152	0.15663	464.026	12.006	465.590	0.13452
430.698	56.976	432.441	0.15658	464.021	12.018	465.895	0.13459
430.693	56.980	432.749	0.15652	464.033	12.016	465.920	0.13467
430.692	56.972	432.735	0.15653	464.029	12.017	466.232	0.13442
430.690	56.955	433.060	0.15647	464.027	12.014	466.225	0.13449
430.692	56.963	433.077	0.15670	464.026	12.019	466.587	0.13434
430.688	68.654	431.842	0.16051	464.026	12.007	466.585	0.13437
430.695	68.655	431.862	0.16062	464.051	18.864	465.313	0.13807
430.686	68.657	432.096	0.16008	464.047	18.869	465.313	0.13788
430.691	68.636	432.379	0.16030	464.046	18.855	465.560	0.13784
430.690	68.647	432.372	0.16048	464.047	18.865	465.576	0.13801
430.688	68.654	432.688	0.16024	464.049	18.869	465.873	0.13783
430.683	68.647	432.992	0.16032	464.054	18.864	465.876	0.13752
430.688	68.650	432.999	0.16031	464.052	18.870	466.207	0.13765
464.034	0.238	465.413	0.12891	464.058	18.868	466.197	0.13777
464.031	0.239	465.406	0.12877	464.054	18.858	466.549	0.13760
464.034	0.240	465.689	0.12819	464.056	18.859	466.548	0.13763
464.031	0.241	465.694	0.12875	464.058	26.904	465.295	0.14151
464.038	0.240	466.011	0.12857	464.060	26.917	465.296	0.14137
464.031	0.241	466.003	0.12846	464.057	26.915	465.538	0.14140
464.033	0.243	466.354	0.12845	464.061	26.915	465.556	0.14138
464.032	0.243	466.357	0.12836	464.059	26.912	465.844	0.14125
464.031	0.243	466.726	0.12838	464.061	26.915	465.847	0.14123
464.031	0.244	466.716	0.12819	464.062	26.906	466.159	0.14110
464.025	5.933	465.329	0.13177	464.060	26.900	466.151	0.14131
464.023	5.940	465.337	0.13162	464.058	26.876	466.483	0.14116
464.019	5.938	465.618	0.13164	464.063	26.904	466.501	0.14097
464.021	5.935	465.600	0.13212	464.052	35.833	465.269	0.14513
464.020	5.935	465.935	0.13146	464.047	35.811	465.258	0.14505
464.022	5.932	465.924	0.13149	464.046	35.817	465.513	0.14493
464.026	5.926	466.253	0.13128	464.047	35.797	465.502	0.14510

[a]Initial cell temperature.

Table A3, continued.

T_i[a] /K	p /MPa	T /K	λ /W·m^{-1}K^{-1}	T_i[a] /K	p /MPa	T /K	λ /W·m^{-1}K^{-1}
464.052	35.823	465.793	0.14481	497.514	0.246	499.438	0.12287
464.048	35.825	466.117	0.14492	497.526	0.246	499.778	0.12236
464.049	35.804	466.092	0.14504	497.514	0.247	499.784	0.12245
464.047	35.812	466.431	0.14490	497.516	0.248	500.144	0.12228
464.058	45.750	465.233	0.14893	497.519	0.248	500.143	0.12242
464.053	45.733	465.220	0.14881	497.514	5.561	498.828	0.12584
464.053	45.723	465.457	0.14871	497.514	5.569	498.846	0.12571
464.052	45.690	465.451	0.14900	497.509	5.568	499.099	0.12586
464.059	45.707	465.766	0.14888	497.510	5.564	499.102	0.12595
464.048	45.744	465.746	0.14888	497.512	5.555	499.393	0.12564
464.054	45.747	466.076	0.14869	497.517	5.567	499.415	0.12571
464.045	45.749	466.058	0.14870	497.515	5.570	499.734	0.12565
464.055	45.751	466.403	0.14842	497.518	5.569	500.096	0.12568
464.053	45.747	466.384	0.14877	497.517	5.568	500.104	0.12548
464.063	56.877	465.200	0.15283	497.508	11.426	498.766	0.12894
464.073	56.860	465.464	0.15281	497.506	11.432	499.013	0.12921
464.072	56.878	465.473	0.15282	497.499	11.431	499.009	0.12923
464.067	56.842	465.718	0.15305	497.501	11.435	499.323	0.12907
464.060	56.801	465.707	0.15302	497.500	11.420	499.615	0.12888
464.073	56.784	466.021	0.15282	497.507	11.434	499.646	0.12889
464.072	56.729	466.334	0.15258	497.501	11.436	499.974	0.12887
464.067	56.730	466.331	0.15264	497.507	11.437	499.985	0.12886
464.021	68.900	465.143	0.15699	497.510	18.395	498.723	0.13282
464.019	68.902	465.148	0.15706	497.507	18.386	498.730	0.13273
464.022	68.909	465.379	0.15713	497.510	18.385	498.976	0.13262
464.022	68.872	465.381	0.15715	497.501	18.394	499.261	0.13267
464.030	68.898	465.655	0.15724	497.500	18.393	499.262	0.13273
464.028	68.883	465.664	0.15696	497.503	18.388	499.567	0.13250
464.028	68.889	465.941	0.15708	497.504	18.383	499.904	0.13254
464.033	68.867	465.947	0.15696	497.501	18.380	499.910	0.13259
464.031	68.887	466.263	0.15722	497.524	26.223	498.725	0.13642
464.039	68.883	466.272	0.15671	497.521	26.222	498.959	0.13670
497.520	0.244	498.879	0.12278	497.530	26.222	498.977	0.13622
497.519	0.244	498.852	0.12284	497.526	26.205	499.235	0.13629
497.515	0.245	499.153	0.12303	497.528	26.225	499.550	0.13634
497.526	0.246	499.148	0.12267	497.527	26.218	499.552	0.13641
497.520	0.246	499.455	0.12260	497.532	26.205	499.894	0.13609

[a]Initial cell temperature.

Table A3, continued.

T_i[a] /K	p /MPa	T /K	λ /W·m^{-1}K^{-1}	T_i[a] /K	p /MPa	T /K	λ /W·m^{-1}K^{-1}
497.533	26.201	499.889	0.13613	497.635	68.573	499.449	0.15320
497.535	35.370	498.682	0.14063	497.630	68.568	499.739	0.15326
497.531	35.367	498.680	0.14060	497.636	68.555	499.754	0.15315
497.531	35.355	498.923	0.14048	497.767	0.390	499.140	0.12289
497.533	35.349	499.205	0.14042	497.762	0.389	499.130	0.12278
497.534	35.354	499.211	0.14033	497.758	0.389	499.396	0.12258
497.534	35.354	499.512	0.14047	497.763	0.388	499.398	0.12271
497.532	35.339	499.492	0.14052	497.754	0.388	499.702	0.12290
497.541	35.355	499.833	0.14027	497.756	0.390	499.709	0.12272
497.540	35.345	499.828	0.14032	497.754	0.390	500.034	0.12271
497.556	45.239	498.665	0.14485	497.747	0.390	500.035	0.12253
497.551	45.258	498.697	0.14467	497.750	0.391	500.392	0.12238
497.548	45.231	498.900	0.14461	497.753	0.392	500.394	0.12242
497.556	45.257	498.929	0.14482				
497.558	45.258	499.196	0.14454				
497.551	45.267	499.191	0.14475				
497.551	45.265	499.473	0.14445				
497.556	45.240	499.469	0.14453				
497.553	45.241	499.797	0.14453				
497.559	45.222	499.786	0.14438				
497.596	56.482	498.710	0.14967				
497.592	56.472	498.709	0.14915				
497.596	56.472	498.949	0.14927				
497.597	56.471	498.956	0.14910				
497.600	56.460	499.215	0.14877				
497.601	56.466	499.217	0.14895				
497.610	56.455	499.490	0.14888				
497.611	56.455	499.527	0.14891				
497.613	56.424	499.804	0.14904				
497.614	56.432	499.827	0.14894				
497.636	68.666	498.711	0.15327				
497.631	68.646	498.696	0.15341				
497.631	68.634	498.926	0.15329				
497.632	68.628	498.927	0.15376				
497.633	68.623	499.174	0.15383				
497.631	68.606	499.184	0.15357				
497.632	68.594	499.442	0.15348				

[a]Initial cell temperature.

Table A4: Thermal Conductivity Data for MIL-PRF-23699 Lubricant at Temperatures from 300 K to 500 K.

T_i[a] /K	p /MPa	T /K	λ /W·m^{-1}K^{-1}	T_i[a] /K	p /MPa	T /K	λ /W·m^{-1}K^{-1}
299.137	0.421	300.666	0.14515	299.705	14.275	302.821	0.14856
299.158	0.427	300.702	0.14520	299.710	14.267	302.822	0.14855
299.175	0.436	301.038	0.14504	299.743	21.603	301.208	0.15069
299.208	0.447	301.486	0.14508	299.743	21.569	301.204	0.15070
299.223	0.449	301.508	0.14506	299.747	21.579	301.554	0.15063
299.242	0.451	301.968	0.14500	299.748	21.570	301.554	0.15066
299.259	0.468	301.996	0.14505	299.746	21.580	301.933	0.15059
299.273	0.481	302.492	0.14485	299.748	21.544	301.934	0.15063
299.288	0.492	302.515	0.14490	299.748	21.561	302.351	0.15050
299.475	0.348	300.997	0.14505	299.745	21.580	302.349	0.15056
299.479	0.356	301.005	0.14506	299.747	21.587	302.808	0.15045
299.483	0.367	301.371	0.14523	299.743	21.598	302.804	0.15046
299.483	0.374	301.371	0.14504	299.765	30.059	301.200	0.15286
299.493	0.381	301.773	0.14498	299.768	30.071	301.546	0.15274
299.493	0.387	301.774	0.14495	299.768	30.088	301.548	0.15280
299.496	0.393	302.221	0.14491	299.773	30.080	301.926	0.15270
299.500	0.402	302.631	0.14483	299.769	30.073	301.919	0.15271
299.507	0.409	302.638	0.14487	299.768	30.064	302.329	0.15287
299.610	7.170	301.112	0.14692	299.772	30.068	302.336	0.15272
299.613	7.182	301.111	0.14687	299.776	30.074	302.789	0.15261
299.627	7.205	301.486	0.14687	299.777	30.071	302.788	0.15256
299.620	7.235	301.485	0.14682	299.785	39.133	301.188	0.15505
299.622	7.231	301.869	0.14667	299.786	39.128	301.194	0.15500
299.625	7.235	301.873	0.14678	299.785	39.114	301.525	0.15490
299.631	7.253	302.312	0.14673	299.782	39.116	301.534	0.15499
299.632	7.263	302.294	0.14669	299.785	39.129	301.906	0.15481
299.629	7.257	302.760	0.14669	299.783	39.120	301.902	0.15490
299.640	7.250	302.773	0.14674	299.778	39.126	302.305	0.15485
299.677	14.120	301.155	0.14882	299.777	39.124	302.306	0.15487
299.680	14.127	301.159	0.14877	299.773	39.103	302.740	0.15479
299.686	14.137	301.518	0.14879	299.785	48.381	301.183	0.15725
299.689	14.147	301.524	0.14874	299.786	48.368	301.182	0.15717
299.692	14.152	301.911	0.14867	299.784	48.384	301.516	0.15709
299.697	14.190	301.920	0.14874	299.786	48.367	301.519	0.15709
299.700	14.226	302.349	0.14860	299.789	48.333	301.877	0.15713
299.700	14.239	302.351	0.14859	299.789	48.321	302.281	0.15705

[a]Initial cell temperature.

Table A4, continued.

T_i[a] /K	p /MPa	T /K	λ /W·m^{-1}K^{-1}	T_i[a] /K	p /MPa	T /K	λ /W·m^{-1}K^{-1}
299.792	48.314	302.286	0.15705	332.028	6.690	334.104	0.14237
299.792	48.290	302.719	0.15695	332.028	6.692	334.504	0.14237
299.792	48.293	302.721	0.15692	332.030	6.696	334.938	0.14226
299.791	58.660	301.151	0.15968	332.029	6.693	334.935	0.14228
299.788	58.674	301.495	0.15954	332.033	13.746	333.401	0.14454
299.790	58.680	301.499	0.15950	332.035	13.734	334.080	0.14469
299.788	58.776	301.864	0.15945	332.033	13.736	334.470	0.14440
299.792	58.812	301.868	0.15980	332.035	13.736	334.471	0.14433
299.786	58.824	302.259	0.15942	332.029	21.153	333.351	0.14669
299.785	58.825	302.258	0.15944	332.029	21.146	333.353	0.14687
299.785	58.840	302.691	0.15936	332.030	21.173	333.679	0.14676
299.789	58.852	302.694	0.15935	332.031	21.191	333.679	0.14681
299.814	68.848	301.159	0.16172	332.033	21.193	334.028	0.14674
299.824	68.847	301.171	0.16185	332.030	21.196	334.025	0.14666
299.816	68.857	301.488	0.16170	332.028	21.195	334.406	0.14664
299.826	68.857	301.516	0.16177	332.028	21.199	334.407	0.14661
299.822	68.861	301.867	0.16168	332.027	21.209	334.828	0.14657
299.824	68.860	301.868	0.16169	332.024	21.208	334.823	0.14656
299.819	68.869	302.259	0.16163	332.033	29.304	333.366	0.14912
299.827	68.871	302.267	0.16163	332.028	29.303	333.362	0.14895
299.830	68.879	302.697	0.16158	332.024	29.305	333.676	0.14905
299.828	68.879	302.694	0.16159	332.028	29.304	333.678	0.14900
332.027	0.614	333.431	0.14074	332.026	29.297	334.020	0.14932
332.025	0.629	333.761	0.14054	332.029	29.291	334.021	0.14897
332.027	0.643	333.767	0.14064	332.025	29.272	334.399	0.14889
332.030	0.655	334.131	0.14053	332.025	29.280	334.396	0.14889
332.025	0.675	334.526	0.14053	332.027	29.275	334.813	0.14886
332.027	0.684	334.528	0.14058	332.023	29.272	334.810	0.14890
332.027	0.690	334.963	0.14046	332.020	38.358	333.337	0.15169
332.026	0.696	334.966	0.14046	332.029	38.353	333.346	0.15148
332.027	6.684	333.418	0.14247	332.026	38.353	333.655	0.15148
332.030	6.687	333.752	0.14249	332.025	38.353	333.652	0.15140
332.025	6.681	334.101	0.14268	332.022	38.346	333.990	0.15134
332.031	6.689	334.506	0.14235	332.024	38.347	334.368	0.15134
332.031	6.687	334.505	0.14224	332.028	38.343	334.372	0.15128
332.030	6.690	334.933	0.14215	332.021	38.333	334.772	0.15124

[a]Initial cell temperature.

Table A4, continued.

T_i[a] /K	p /MPa	T /K	λ /W·m^{-1}K^{-1}	T_i[a] /K	p /MPa	T /K	λ /W·m^{-1}K^{-1}
332.025	38.335	334.775	0.15162	331.987	13.458	334.845	0.14431
332.036	48.175	333.323	0.15406	331.984	13.456	334.841	0.14429
332.038	48.177	333.326	0.15404	364.655	0.724	365.981	0.13597
332.034	48.166	333.628	0.15398	364.655	0.746	365.986	0.13613
332.027	48.160	333.621	0.15399	364.654	0.764	366.291	0.13583
332.029	48.158	333.954	0.15382	364.655	0.778	366.294	0.13596
332.034	48.153	333.961	0.15392	364.650	0.790	366.629	0.13575
332.035	48.149	334.331	0.15387	364.652	0.799	366.631	0.13580
332.030	48.144	334.324	0.15380	364.648	0.806	367.005	0.13577
332.036	48.134	334.737	0.15381	364.650	0.812	367.009	0.13587
332.031	48.132	334.730	0.15378	364.651	0.818	367.417	0.13568
332.035	58.292	333.303	0.15647	364.656	0.822	367.424	0.13567
332.034	58.289	333.308	0.15649	364.654	6.595	365.972	0.13788
332.036	58.281	333.610	0.15637	364.654	6.595	365.969	0.13792
332.034	58.276	333.606	0.15644	364.656	6.578	366.264	0.13806
332.033	58.267	333.933	0.15634	364.655	6.569	366.275	0.13772
332.032	58.264	333.932	0.15643	364.654	6.593	366.612	0.13783
332.031	58.257	334.298	0.15643	364.658	6.580	366.614	0.13776
332.031	58.251	334.293	0.15631	364.657	6.582	366.985	0.13769
332.032	58.245	334.690	0.15628	364.657	6.587	366.983	0.13777
332.031	58.233	334.686	0.15629	364.659	6.587	367.386	0.13773
332.028	68.853	333.261	0.15904	364.659	6.587	367.390	0.13766
332.027	68.843	333.259	0.15897	364.660	13.411	365.937	0.14030
332.030	68.835	333.560	0.15900	364.663	13.416	365.928	0.14031
332.027	68.825	333.556	0.15893	364.665	13.425	366.240	0.14031
332.024	68.821	333.879	0.15899	364.659	13.421	366.229	0.14044
332.031	68.809	333.883	0.15896	364.660	13.424	366.569	0.14022
332.023	68.801	334.238	0.15885	364.663	13.426	366.566	0.14006
332.024	68.794	334.237	0.15883	364.662	13.424	366.935	0.14013
332.023	68.791	334.647	0.15884	364.664	13.428	366.937	0.14008
332.029	68.780	334.650	0.15889	364.663	13.427	367.333	0.14005
331.982	13.452	333.409	0.14439	364.666	13.430	367.342	0.14001
331.985	13.455	333.669	0.14450	364.677	20.571	365.941	0.14233
331.985	13.458	333.670	0.14449	364.673	20.572	365.932	0.14264
331.982	13.453	334.018	0.14445	364.675	20.570	366.237	0.14257
331.984	13.453	334.021	0.14445	364.678	20.574	366.246	0.14288
331.983	13.454	334.414	0.14444	364.679	20.570	366.565	0.14251

[a]Initial cell temperature.

Table A4, continued.

T_i[a] /K	p /MPa	T /K	λ /W·m^{-1}K^{-1}	T_i[a] /K	p /MPa	T /K	λ /W·m^{-1}K^{-1}
364.679	20.569	366.565	0.14245	364.722	57.651	366.467	0.15320
364.682	20.570	366.932	0.14242	364.722	57.639	366.485	0.15320
364.676	20.567	366.923	0.14241	364.722	57.626	366.825	0.15314
364.678	20.569	367.324	0.14255	364.725	57.617	366.831	0.15322
364.675	20.564	367.320	0.14231	364.721	57.589	367.191	0.15311
364.696	28.628	365.942	0.14494	364.726	68.494	365.896	0.15592
364.694	28.623	365.937	0.14496	364.721	68.477	365.891	0.15587
364.695	28.619	366.236	0.14504	364.721	68.465	366.167	0.15602
364.698	28.621	366.236	0.14493	364.726	68.428	366.474	0.15606
364.698	28.616	366.561	0.14483	364.727	68.415	366.467	0.15596
364.699	28.617	366.559	0.14490	364.724	68.400	366.800	0.15591
364.698	28.623	366.918	0.14487	364.725	68.378	366.800	0.15594
364.699	28.622	366.917	0.14488	364.724	68.349	367.165	0.15597
364.697	28.617	367.296	0.14486	397.909	0.902	399.167	0.13062
364.700	28.618	367.306	0.14486	397.904	0.923	399.163	0.13091
364.701	37.824	365.934	0.14797	397.911	0.938	399.464	0.13074
364.706	37.816	365.934	0.14803	397.907	0.951	399.469	0.13085
364.704	37.809	366.227	0.14763	397.912	0.962	399.788	0.13062
364.705	37.799	366.223	0.14775	397.912	0.972	399.793	0.13068
364.709	37.796	366.547	0.14768	397.912	0.980	400.146	0.13064
364.704	37.799	366.533	0.14778	397.902	0.987	400.143	0.13055
364.702	37.782	366.890	0.14760	397.907	0.993	400.536	0.13052
364.699	37.772	366.891	0.14766	397.906	0.998	400.530	0.13046
364.700	37.775	367.273	0.14758	397.914	6.159	399.153	0.13280
364.700	37.772	367.270	0.14768	397.913	6.158	399.149	0.13290
364.710	47.275	365.903	0.15064	397.915	6.160	399.448	0.13278
364.710	47.266	365.901	0.15040	397.917	6.159	399.446	0.13278
364.709	47.264	366.190	0.15035	397.918	6.162	399.772	0.13260
364.706	47.253	366.185	0.15038	397.914	6.159	399.759	0.13271
364.709	47.247	366.502	0.15048	397.918	6.161	400.128	0.13248
364.711	47.233	366.844	0.15032	397.921	6.162	400.516	0.13248
364.713	47.226	366.849	0.15030	397.921	6.164	400.519	0.13254
364.713	47.216	367.222	0.15028	397.930	12.782	399.136	0.13529
364.715	47.205	367.226	0.15030	397.930	12.782	399.142	0.13528
364.724	57.694	365.887	0.15330	397.932	12.781	399.425	0.13547
364.722	57.684	365.885	0.15321	397.931	12.781	399.428	0.13532
364.719	57.672	366.163	0.15329	397.936	12.784	399.744	0.13519

[a]Initial cell temperature.

Table A4, continued.

T_i[a] /K	p /MPa	T /K	λ /W·m^{-1}K^{-1}	T_i[a] /K	p /MPa	T /K	λ /W·m^{-1}K^{-1}
397.939	12.787	399.757	0.13510	397.957	46.827	399.300	0.14676
397.938	12.788	400.104	0.13515	397.952	46.817	399.590	0.14674
397.936	12.785	400.096	0.13510	397.954	46.809	399.602	0.14676
397.939	12.786	400.471	0.13509	397.953	46.798	399.947	0.14662
397.941	12.784	400.477	0.13505	397.954	46.788	399.955	0.14665
397.953	20.069	399.145	0.13792	397.953	46.775	400.298	0.14660
397.944	20.053	399.415	0.13813	397.956	46.767	400.308	0.14662
397.950	20.051	399.421	0.13803	397.985	57.640	399.097	0.15001
397.950	20.054	399.724	0.13790	397.986	57.620	399.363	0.14977
397.951	20.053	399.732	0.13785	397.982	57.605	399.345	0.15014
397.953	20.057	400.077	0.13832	397.988	57.589	399.648	0.14968
397.951	20.055	400.072	0.13783	397.987	57.575	399.642	0.14946
397.953	20.056	400.448	0.13782	397.993	57.557	399.972	0.14970
397.946	20.049	400.439	0.13777	397.983	57.538	399.955	0.14993
397.955	28.030	399.109	0.14105	397.989	57.524	400.310	0.14973
397.956	28.027	399.114	0.14090	397.990	57.506	400.310	0.14976
397.952	28.021	399.386	0.14094	398.006	68.707	399.104	0.15279
397.953	28.018	399.382	0.14062	398.005	68.682	399.090	0.15338
397.953	28.012	399.689	0.14071	398.005	68.658	399.356	0.15314
397.957	28.007	399.691	0.14079	398.006	68.635	399.351	0.15300
397.957	28.002	400.028	0.14059	398.005	68.609	399.626	0.15297
397.954	27.999	400.028	0.14050	398.010	68.562	399.947	0.15283
397.951	27.995	400.386	0.14068	398.005	68.533	399.943	0.15288
397.954	27.990	400.394	0.14044	398.007	68.513	400.282	0.15286
397.954	37.264	399.082	0.14370	398.002	68.493	400.282	0.15293
397.954	37.255	399.097	0.14372	430.815	0.712	432.322	0.12521
397.953	37.235	399.374	0.14367	430.811	0.722	432.631	0.12503
397.957	37.227	399.381	0.14390	430.813	0.730	432.622	0.12511
397.952	37.212	399.669	0.14353	430.816	0.736	432.979	0.12497
397.948	37.203	399.662	0.14364	430.818	0.746	433.368	0.12509
397.949	37.188	400.004	0.14364	430.814	0.750	433.354	0.12495
397.953	37.190	400.005	0.14370	430.815	0.753	433.754	0.12489
397.958	37.173	400.371	0.14358	430.816	0.756	433.764	0.12483
397.950	37.165	400.366	0.14353	430.818	5.910	432.283	0.12747
397.954	46.868	399.033	0.14687	430.819	5.905	432.586	0.12746
397.952	46.853	399.029	0.14676	430.818	5.901	432.586	0.12735
397.950	46.842	399.297	0.14680	430.811	5.902	432.916	0.12737

[a]Initial cell temperature.

Table A4, continued.

T_i[a] /K	p /MPa	T /K	λ /W·m^{-1}K^{-1}	T_i[a] /K	p /MPa	T /K	λ /W·m^{-1}K^{-1}
430.814	5.899	432.921	0.12735	430.873	36.574	432.512	0.13919
430.808	5.901	433.291	0.12762	430.868	36.566	432.510	0.13966
430.821	5.898	433.292	0.12710	430.866	36.548	432.822	0.13910
430.814	5.897	433.688	0.12714	430.873	36.536	433.171	0.13929
430.816	5.893	433.694	0.12719	430.866	36.527	433.160	0.13956
430.839	12.372	432.283	0.13034	430.870	36.518	433.541	0.13932
430.842	12.371	432.287	0.13036	430.886	46.204	432.200	0.14298
430.839	12.369	432.585	0.13035	430.885	46.188	432.196	0.14270
430.834	12.365	432.578	0.13036	430.885	46.172	432.483	0.14265
430.840	12.366	432.916	0.13022	430.891	46.155	432.484	0.14273
430.838	12.363	432.911	0.13020	430.894	46.133	432.787	0.14273
430.834	12.363	433.273	0.13001	430.892	46.110	432.788	0.14286
430.839	12.366	433.290	0.12998	430.896	46.082	433.124	0.14266
430.838	12.361	433.668	0.13007	430.888	46.081	433.127	0.14271
430.841	12.359	433.672	0.13007	430.894	46.069	433.486	0.14258
430.839	19.491	432.240	0.13320	430.889	46.045	433.492	0.14248
430.839	19.488	432.244	0.13326	430.899	57.479	432.189	0.14649
430.839	19.487	432.537	0.13319	430.899	57.424	432.455	0.14615
430.840	19.481	432.540	0.13319	430.892	57.399	432.455	0.14653
430.841	19.475	432.867	0.13303	430.897	57.376	432.765	0.14639
430.842	19.472	432.871	0.13294	430.898	57.357	432.764	0.14649
430.838	19.471	433.228	0.13293	430.898	57.331	433.086	0.14646
430.841	19.470	433.222	0.13292	430.896	57.306	433.085	0.14626
430.837	19.464	433.602	0.13283	430.901	57.283	433.441	0.14614
430.834	19.462	433.609	0.13288	430.896	57.256	433.435	0.14624
430.852	27.523	432.231	0.13632	430.904	68.198	432.175	0.14979
430.851	27.516	432.238	0.13642	430.900	68.132	432.429	0.14968
430.848	27.513	432.521	0.13653	430.900	68.100	432.421	0.14992
430.849	27.508	432.526	0.13617	430.900	68.069	432.717	0.14965
430.851	27.496	432.845	0.13619	430.896	68.036	432.709	0.14975
430.852	27.497	432.850	0.13628	430.905	67.973	433.040	0.14960
430.860	27.487	433.188	0.13587	430.898	67.941	433.378	0.14953
430.851	27.487	433.184	0.13609	430.898	67.908	433.375	0.14954
430.854	27.482	433.562	0.13618	464.206	0.519	465.673	0.11924
430.857	27.477	433.574	0.13604	464.210	0.539	465.678	0.11925
430.865	36.593	432.225	0.13985	464.210	0.554	465.974	0.11937
430.874	36.578	432.228	0.13945	464.210	0.569	465.987	0.11934

[a]Initial cell temperature.

Table A4, continued.

T_i[a] /K	p /MPa	T /K	λ /W·m^{-1}K^{-1}	T_i[a] /K	p /MPa	T /K	λ /W·m^{-1}K^{-1}
464.210	0.584	466.319	0.11931	464.249	26.784	465.861	0.13150
464.214	0.593	466.318	0.11917	464.249	26.782	466.173	0.13130
464.210	0.602	466.683	0.11914	464.254	26.786	466.168	0.13144
464.209	0.609	466.681	0.11922	464.255	26.768	466.508	0.13122
464.216	0.615	467.086	0.11927	464.247	26.769	466.489	0.13127
464.213	0.623	467.089	0.11909	464.248	26.750	466.867	0.13127
464.216	5.813	465.632	0.12200	464.247	26.754	466.863	0.13133
464.218	5.817	465.622	0.12222	464.259	35.732	465.560	0.13509
464.218	5.810	465.928	0.12192	464.262	35.735	465.562	0.13504
464.220	5.814	465.939	0.12199	464.266	35.714	465.829	0.13507
464.218	5.810	466.262	0.12199	464.274	35.703	465.836	0.13486
464.221	5.807	466.258	0.12193	464.271	35.700	466.142	0.13494
464.218	5.806	466.616	0.12194	464.275	35.707	466.148	0.13489
464.225	5.807	466.619	0.12190	464.274	35.686	466.466	0.13488
464.224	5.807	467.028	0.12177	464.280	35.682	466.479	0.13486
464.223	5.808	467.022	0.12175	464.278	35.651	466.828	0.13480
464.222	12.061	465.592	0.12490	464.272	35.634	466.828	0.13485
464.225	12.039	465.596	0.12510	464.291	45.827	465.512	0.13891
464.222	12.051	465.881	0.12498	464.292	45.816	465.527	0.13893
464.216	12.051	465.886	0.12526	464.291	45.780	465.782	0.13894
464.223	12.062	466.203	0.12507	464.288	45.774	465.766	0.13913
464.221	12.052	466.191	0.12494	464.292	45.758	466.078	0.13907
464.217	12.041	466.539	0.12503	464.290	45.745	466.076	0.13897
464.214	12.044	466.551	0.12486	464.289	45.722	466.397	0.13856
464.215	12.047	466.935	0.12489	464.289	45.684	466.390	0.13854
464.214	12.049	466.922	0.12496	464.290	45.654	466.728	0.13858
464.236	19.060	465.580	0.12832	464.307	56.764	465.561	0.14246
464.238	19.082	465.585	0.12847	464.308	56.745	465.533	0.14273
464.238	19.082	465.877	0.12841	464.305	56.684	465.789	0.14269
464.242	19.067	466.193	0.12806	464.309	56.670	465.797	0.14258
464.242	19.051	466.196	0.12821	464.305	56.628	466.079	0.14263
464.246	19.068	466.541	0.12816	464.306	56.592	466.400	0.14239
464.247	19.072	466.542	0.12812	464.296	56.588	466.392	0.14244
464.245	19.031	466.900	0.12813	464.300	56.555	466.715	0.14247
464.250	26.810	465.587	0.13166	464.302	56.503	466.716	0.14264
464.246	26.809	465.578	0.13135	498.013	0.622	499.455	0.11381
464.255	26.779	465.862	0.13157	498.015	0.628	499.443	0.11393

[a]Initial cell temperature.

Table A4, continued.

T_i[a] /K	p /MPa	T /K	λ /W·m^{-1}K^{-1}	T_i[a] /K	p /MPa	T /K	λ /W·m^{-1}K^{-1}
498.014	0.633	499.756	0.11366	498.020	26.693	499.597	0.12725
498.015	0.636	500.083	0.11353	498.013	26.698	499.870	0.12684
498.020	0.638	500.090	0.11361	498.012	26.699	499.875	0.12692
498.021	0.641	500.464	0.11350	498.007	26.688	500.201	0.12706
498.021	0.641	500.453	0.11348	498.005	26.671	500.189	0.12694
498.024	0.646	500.852	0.11337	498.015	26.675	500.545	0.12685
498.017	5.724	499.408	0.11676	498.018	26.649	500.544	0.12676
498.004	5.737	499.684	0.11663	498.044	35.247	499.299	0.13039
498.011	5.751	499.692	0.11666	498.050	35.239	499.309	0.13068
498.003	5.726	499.994	0.11660	498.051	35.251	499.564	0.13076
498.004	5.730	500.353	0.11647	498.053	35.238	499.564	0.13101
498.004	5.732	500.340	0.11659	498.049	35.241	499.858	0.13059
498.003	5.731	500.728	0.11646	498.048	35.218	499.839	0.13051
497.997	5.740	500.709	0.11640	498.043	35.229	500.165	0.13072
498.001	12.033	499.367	0.12006	498.048	35.234	500.170	0.13061
497.996	12.031	499.366	0.11998	498.041	35.231	500.500	0.13044
497.995	12.033	499.637	0.12012	498.040	35.251	500.508	0.13051
497.998	12.041	499.650	0.11986	498.035	45.556	499.246	0.13474
497.987	12.019	499.935	0.12009	498.028	45.559	499.231	0.13484
497.988	12.005	499.938	0.11983	498.033	45.551	499.497	0.13479
497.987	12.029	500.300	0.11974	498.029	45.562	499.501	0.13489
497.978	12.035	500.269	0.11987	498.027	45.547	499.778	0.13462
497.981	12.036	500.660	0.11978	498.030	45.572	500.090	0.13485
497.980	12.040	500.643	0.11989	498.027	45.567	500.079	0.13492
498.009	18.615	499.316	0.12349	498.027	45.523	500.398	0.13471
498.005	18.597	499.301	0.12324	498.028	45.526	500.397	0.13499
498.007	18.605	499.617	0.12319	498.044	56.816	499.231	0.13933
498.007	18.617	499.601	0.12307	498.047	56.817	499.481	0.13921
498.011	18.617	499.927	0.12327	498.045	56.816	499.487	0.13881
498.007	18.596	499.905	0.12342	498.047	56.817	499.779	0.13902
498.005	18.589	500.244	0.12316	498.045	56.794	500.063	0.13911
498.004	18.601	500.241	0.12309	498.045	56.809	500.068	0.13896
498.008	18.605	500.602	0.12317	498.047	56.787	500.374	0.13908
498.010	18.596	500.603	0.12300	498.045	56.808	500.400	0.13890
498.022	26.629	499.312	0.12703	498.054	5.995	499.472	0.11665
498.018	26.629	499.303	0.12688	498.049	5.991	499.459	0.11670
498.018	26.678	499.595	0.12714	498.049	5.993	499.753	0.11684

[a]Initial cell temperature.

Table A4, continued.

T_i[a] /K	p /MPa	T /K	λ /W·m^{-1}K^{-1}
498.048	5.995	499.736	0.11662
498.054	5.991	500.068	0.11671
498.053	5.990	500.083	0.11657
498.053	5.988	500.431	0.11667
498.049	5.992	500.427	0.11665
498.054	5.993	500.795	0.11665
498.049	5.994	500.795	0.11655

[a]Initial cell temperature.

Appendix B: Viscosity Data Tables

Table B1: Viscosity of POE5 at Temperatures from 275 K to 430 K with Pressures to 137 MPa.

T /K	p /MPa	η /mPa·s	T /K	p /MPa	η /mPa·s
350.03	19.828	6.740	380.02	9.816	3.278
350.03	29.842	7.603	380.02	19.814	3.691
350.04	39.859	8.632	380.02	29.814	4.124
350.04	49.893	9.649	380.03	39.838	4.594
350.04	59.928	10.78	380.03	49.874	5.067
350.05	69.986	12.00	380.04	59.913	5.558
350.05	80.043	13.32	380.03	69.958	6.088
350.05	90.090	14.74	380.04	79.990	6.657
350.06	100.160	16.24	380.04	90.044	7.242
350.06	110.223	17.85	380.05	100.123	7.846
350.06	120.297	19.55	380.05	110.186	8.507
360.04	0.154	4.156	380.00	120.265	9.148
360.05	9.822	4.756	379.97	130.367	9.950
360.05	19.817	5.347	389.95	0.142	2.494
360.06	29.820	6.020	389.97	9.812	2.835
360.07	39.838	6.727	389.97	19.818	3.162
360.07	49.865	7.475	389.98	29.821	3.532
360.07	59.911	8.306	389.99	39.842	3.926
360.07	69.946	9.205	390.00	49.876	4.353
360.07	79.989	10.19	390.01	59.915	4.812
360.07	90.042	11.26	390.00	69.967	5.239
360.08	100.115	12.40	390.02	90.075	6.168
360.08	110.191	13.59	390.02	100.138	6.726
360.09	120.245	14.86	390.03	110.205	7.228
360.08	130.316	16.23	390.03	120.273	7.786
360.08	137.352	17.27	390.03	130.341	8.350
369.98	0.131	3.629	390.04	137.389	8.797
369.98	9.798	4.102	390.01	70.073	5.257
369.99	19.800	4.623	390.00	19.872	3.171
370.00	29.803	5.165	390.01	9.864	2.799
370.00	39.827	5.702	399.93	0.151	2.136
370.00	49.861	6.342	399.93	9.831	2.390
370.01	59.906	6.967	399.92	19.832	2.699
370.01	69.949	7.612	399.93	29.832	3.034
370.02	79.999	8.290	399.93	39.851	3.370
370.02	90.058	9.037	399.94	49.882	3.732
370.03	100.140	9.862	399.95	59.932	4.113
370.04	110.197	10.76	399.94	69.965	4.471
370.04	120.266	11.70	399.94	80.016	4.857
370.04	130.336	12.70	399.94	90.074	5.315
370.04	137.395	13.46	399.95	100.134	5.738
380.01	0.139	2.896	399.96	110.208	6.235

Table B1, continued.

T /K	p /MPa	η /mPa·s	T /K	p /MPa	η /mPa·s
399.96	120.267	6.687	410.01	120.267	5.802
399.97	130.345	7.212	410.01	130.324	6.275
399.97	137.390	7.585	410.03	137.369	6.653
419.97	0.131	1.698	310.02	0.111	16.65
419.96	9.807	1.903	310.02	9.781	19.43
419.96	19.810	2.116	310.02	19.790	22.36
419.96	29.807	2.367	310.00	29.803	25.75
419.97	39.831	2.594	309.99	39.826	29.57
419.96	49.859	2.838	310.02	49.838	33.69
419.95	59.908	3.102	310.02	59.889	38.56
419.95	69.950	3.354	310.03	69.928	44.05
419.96	79.988	3.616	310.03	79.984	50.18
419.96	90.057	3.881	310.04	90.024	56.75
419.96	100.121	4.164	310.04	100.092	64.09
419.98	110.197	4.459	310.04	110.149	72.22
419.98	120.262	4.773	310.01	120.246	81.36
419.98	130.326	5.062	309.97	130.335	91.00
419.98	137.362	5.296	309.96	137.408	98.51
430.04	0.172	1.467	300.03	0.120	24.33
430.02	9.821	1.674	300.04	9.797	28.53
430.03	19.810	1.880	300.04	19.791	33.22
430.03	29.819	2.111	300.05	29.795	38.41
430.04	39.839	2.341	300.04	39.803	44.84
430.03	49.850	2.595	300.04	49.837	52.04
430.04	59.890	2.694	300.03	59.890	60.44
430.03	69.936	2.920	300.03	69.933	69.05
430.02	79.987	3.143	300.03	79.980	78.80
430.03	90.042	3.448	300.02	90.042	89.67
430.04	100.109	3.674	305.03	0.117	20.39
430.04	110.163	3.987	305.03	9.797	23.63
430.05	120.225	4.304	305.02	19.798	27.36
430.06	130.297	4.605	305.03	29.802	31.49
430.07	137.350	4.823	305.03	39.827	36.28
410.03	0.144	1.839	305.03	49.849	42.01
410.03	9.822	2.101	305.03	59.901	48.29
410.00	19.822	2.369	305.03	69.942	55.22
410.00	39.849	2.950	305.03	79.982	62.73
410.00	49.872	3.259	305.02	90.041	71.10
410.00	59.914	3.601	305.02	100.117	80.39
410.01	69.960	3.987	305.03	110.175	90.42
410.01	80.008	4.326	340.05	0.129	6.58
410.02	90.064	4.681	340.03	9.808	7.56
410.02	100.132	5.036	340.02	19.809	8.70
410.02	110.200	5.444	340.01	29.813	9.97

Table B1, continued.

T /K	p /MPa	η /mPa·s	T /K	p /MPa	η /mPa·s
340.01	39.830	11.31	315.08	29.762	22.10
340.01	49.873	12.76	315.08	39.783	25.17
340.01	59.921	14.32	315.07	49.805	28.64
340.01	69.965	16.00	315.08	59.848	32.46
340.02	80.018	17.83	315.08	69.898	36.60
340.02	90.083	19.81	315.09	79.942	41.40
340.02	100.138	21.92	315.09	89.995	47.08
340.01	110.210	24.23	315.08	100.072	53.23
340.01	120.288	26.55	315.09	110.138	59.82
340.02	130.348	29.16	315.09	120.185	67.07
340.01	137.399	31.21	315.08	130.257	75.04
325.01	0.125	10.49	315.09	137.303	81.09
324.97	9.798	12.05	320.02	0.135	12.53
324.97	19.792	13.90	320.03	9.815	14.40
324.96	29.794	15.90	320.03	19.819	16.52
324.96	39.817	18.05	320.04	29.820	18.88
324.96	49.841	20.39	320.05	39.838	21.45
324.97	59.886	22.98	320.05	49.874	24.28
324.95	69.930	25.74	320.05	59.913	27.31
324.96	79.968	28.70	320.06	69.966	30.62
324.96	90.030	31.91	320.06	80.017	34.29
324.96	100.096	35.51	320.07	90.073	38.28
324.96	110.176	39.52	320.07	100.143	42.97
324.96	120.235	44.25	320.07	110.217	48.43
324.96	130.297	49.25	320.07	120.293	53.94
324.97	137.355	53.00	320.07	130.358	60.32
330.00	0.158	8.965	320.07	137.402	65.25
330.01	9.831	10.25	275.06	0.107	86.85
330.01	19.834	11.81	279.97	0.116	65.78
330.01	29.845	13.52	279.98	4.793	71.02
330.02	39.868	15.35	279.98	9.781	77.48
330.02	49.896	17.35	279.97	19.788	91.56
330.02	59.935	19.45	285.06	0.094	50.09
330.02	69.987	21.70	285.08	4.776	54.38
330.03	80.034	24.24	285.07	9.777	59.49
330.02	90.083	26.87	285.07	19.776	70.94
330.03	100.146	30.25	285.07	29.795	84.65
330.03	110.224	32.82	290.02	0.106	37.87
330.04	120.301	36.30	290.02	4.794	41.20
330.04	130.355	40.10	290.02	9.790	45.07
330.05	137.405	43.16	290.01	19.794	53.59
315.06	0.101	14.41	290.01	29.797	63.18
315.07	9.768	16.64	290.01	39.813	74.00
315.07	19.766	19.28	290.02	49.841	86.08

Table B1, continued.

T /K	*p* /MPa	*η* /mPa·s
295.07	0.120	30.55
295.08	4.802	33.17
295.08	9.798	36.10
295.07	19.794	42.88
295.07	29.795	50.09
295.07	39.808	58.26
295.07	49.848	67.51
295.07	59.886	77.67
295.07	69.939	89.12

Table B2: Viscosity of POE7 at Temperatures from 280 K to 450 K with Pressures to 137 MPa.

T /K	*p* /MPa	*η* /mPa·s	*T* /K	*p* /MPa	*η* /mPa·s
290.01	19.939	70.87	309.99	9.917	24.53
290.01	29.938	83.96	309.99	19.921	28.43
295.01	0.247	39.75	309.99	29.931	32.84
295.03	9.927	47.19	309.99	39.947	38.17
295.03	19.934	55.88	310.00	49.980	44.15
295.02	29.944	65.78	309.99	60.019	50.72
295.02	39.968	76.83	310.00	70.071	58.09
295.03	49.996	89.27	310.00	80.111	66.12
300.04	0.259	30.87	310.00	90.179	75.26
300.04	9.918	36.47	310.01	100.222	84.96
300.04	19.927	43.50	310.01	110.281	95.79
300.02	29.934	51.17	280.04	0.266	86.54
300.02	39.958	59.69	284.96	0.251	66.09
300.02	49.996	69.11	284.96	9.935	79.44
300.02	60.040	79.87	315.03	0.282	17.84
300.01	70.097	91.65	315.03	9.952	20.65
305.03	0.234	25.66	315.04	19.954	23.91
305.03	9.929	29.94	315.03	29.964	27.54
305.03	19.927	34.96	315.04	39.988	31.46
305.03	29.935	40.98	315.03	50.017	36.08
305.03	39.953	47.92	315.03	60.061	41.40
305.03	49.983	55.31	315.03	70.118	47.36
305.03	60.025	63.75	315.03	80.168	53.78
305.03	70.082	72.91	315.03	90.228	61.17
305.03	80.144	82.91	315.03	100.283	69.02
305.03	90.202	94.13	315.03	110.358	78.01
309.98	0.246	21.03	315.04	120.424	87.38

Table B2, continued.

T /K	p /MPa	η /mPa·s	T /K	p /MPa	η /mPa·s
315.04	130.486	97.66	330.03	100.280	37.99
320.03	0.262	15.41	330.03	110.341	42.61
320.03	9.935	17.74	330.03	120.413	47.42
320.03	19.928	20.52	330.03	130.485	52.87
320.03	29.941	23.60	330.03	137.529	56.91
320.03	39.959	26.88	339.96	0.274	8.022
320.03	49.982	30.51	339.98	9.961	9.284
320.04	60.030	34.36	339.98	19.967	10.74
320.04	70.070	38.84	339.99	29.978	12.33
320.04	80.122	44.00	340.00	39.993	14.01
320.05	90.176	49.83	340.01	50.023	15.88
325.04	0.263	12.93	340.02	60.068	17.93
325.05	9.942	14.97	340.02	70.113	20.15
325.05	19.944	17.26	340.02	80.176	22.53
325.05	29.954	19.75	340.02	90.233	25.14
325.06	39.979	22.55	340.02	100.290	27.84
325.06	50.001	25.53	340.03	110.362	30.85
325.06	60.043	28.76	340.03	120.422	34.07
325.06	70.099	32.33	340.04	130.497	37.57
325.05	80.154	36.17	340.03	137.545	39.81
325.04	90.219	40.66	340.00	0.341	8.026
325.04	100.281	45.77	349.97	0.266	6.777
325.05	110.355	51.41	350.00	9.959	7.521
325.04	120.430	57.51	350.01	19.962	8.498
325.03	130.502	63.99	350.02	29.965	9.524
325.03	137.543	68.89	350.03	39.985	10.70
325.00	0.331	13.14	350.04	50.022	11.94
319.99	0.269	15.37	350.05	60.053	13.28
320.01	80.160	44.45	350.05	70.103	14.81
320.03	90.220	50.14	350.06	80.169	16.49
320.03	100.281	56.49	350.05	90.225	18.26
320.04	110.347	63.52	350.06	100.284	20.24
320.04	120.417	70.83	350.07	110.348	22.51
320.05	130.479	79.14	350.07	120.415	25.00
320.04	137.533	85.39	350.08	130.499	27.76
329.99	0.275	11.09	350.07	137.549	29.92
330.00	9.955	12.83	360.02	0.178	5.120
330.00	19.958	14.71	360.03	9.854	5.822
330.01	29.961	16.88	360.04	19.860	6.601
330.01	39.977	19.15	360.03	29.863	7.451
330.01	50.017	21.72	360.04	39.875	8.398
330.01	60.064	24.48	360.04	49.903	9.425
330.01	70.110	27.44	360.05	59.942	10.56
330.02	80.158	30.61	360.05	69.986	11.72
330.03	90.216	34.24	360.05	80.037	12.98

Table B2, continued.

T /K	p /MPa	η /mPa·s	T /K	p /MPa	η /mPa·s
360.06	90.100	14.33	390.01	19.861	3.907
360.07	100.150	15.78	390.01	29.872	4.365
360.08	110.220	17.33	390.02	39.885	4.843
369.99	9.843	5.241	390.03	49.909	5.363
370.00	19.836	5.948	390.03	59.950	5.894
370.00	29.844	6.589	400.01	0.216	2.562
370.00	39.864	7.207	399.98	9.885	2.930
369.99	49.900	7.952	399.96	19.876	3.337
369.99	59.931	8.839	399.97	29.879	3.749
369.98	69.974	9.717	399.97	39.898	4.186
369.98	80.019	10.66	399.99	49.921	4.607
369.98	90.082	11.71	399.99	59.963	5.088
369.99	100.151	12.81	400.00	70.002	5.575
369.99	110.216	13.97	400.00	80.054	6.085
370.00	120.291	15.14	400.01	90.106	6.624
370.00	130.361	16.42	400.01	100.153	7.205
370.00	137.397	17.36	400.02	110.215	7.800
380.00	0.195	3.660	400.00	120.294	8.531
380.01	9.874	4.175	399.99	130.353	9.280
380.01	19.886	4.720	399.98	137.408	9.635
380.02	29.888	5.213	399.96	0.188	2.591
380.01	39.917	5.744	410.02	0.151	2.342
380.02	49.946	6.295	410.02	9.821	2.669
380.02	59.995	6.883	410.01	19.837	3.026
380.03	70.033	7.539	410.02	29.846	3.388
380.03	80.088	8.255	410.03	39.861	3.776
380.04	90.142	9.025	410.03	49.885	4.138
380.05	100.200	9.850	410.03	59.921	4.568
380.05	110.268	10.72	410.04	69.971	4.980
380.05	120.338	11.65	410.03	80.029	5.441
380.06	130.406	12.67	410.04	90.091	6.030
380.06	137.466	13.45	410.04	100.152	6.545
380.02	40.035	5.667	410.03	110.208	7.079
390.04	0.139	3.094	410.04	120.277	7.572
390.04	69.958	6.609	410.05	130.341	8.120
390.04	80.008	7.186	410.05	137.393	8.461
390.04	90.064	7.773	420.01	0.201	2.064
390.05	100.115	8.408	420.02	9.893	2.351
390.05	110.189	9.109	420.03	19.891	2.635
390.06	120.249	9.915	420.02	29.907	2.917
390.06	130.331	10.75	420.02	39.921	3.284
390.06	137.377	11.37	420.03	49.936	3.596
390.01	0.176	3.057	420.03	59.971	3.912
390.00	9.845	3.459	420.02	70.021	4.279

Table B2, continued.

T /K	p /MPa	η /mPa·s	T /K	p /MPa	η /mPa·s
419.98	80.068	4.666	450.10	49.909	2.433
419.97	90.122	5.105	450.11	59.946	2.663
420.03	100.177	5.512	450.10	69.994	2.968
420.07	110.236	5.931	450.11	80.042	3.218
420.06	120.315	6.331	450.10	90.100	3.503
420.07	130.382	6.764	450.11	100.146	3.778
420.08	137.431	7.064	450.11	110.212	4.073
430.00	9.841	2.039	450.11	120.281	4.361
430.02	19.850	2.297	450.11	130.350	4.677
430.01	29.861	2.504	450.12	137.400	4.904
429.98	39.886	2.788			
429.96	49.931	3.056			
429.95	59.972	3.328			
430.14	70.030	3.642			
430.04	0.190	1.680			
430.03	9.858	1.929			
430.03	19.869	2.202			
430.02	29.875	2.464			
430.02	39.894	2.747			
430.02	49.929	3.045			
430.03	59.967	3.352			
430.03	70.016	3.710			
430.03	80.067	4.079			
430.04	90.123	4.441			
430.04	100.181	4.789			
430.03	110.240	5.163			
430.04	120.318	5.541			
430.04	130.396	5.942			
430.05	137.451	6.240			
440.07	19.855	2.097			
440.07	29.869	2.325			
440.06	39.882	2.564			
440.08	49.908	2.818			
440.09	59.945	3.099			
440.11	69.997	3.387			
440.11	80.034	3.722			
440.10	90.083	4.054			
440.09	100.143	4.402			
440.10	110.208	4.728			
440.09	120.272	5.056			
440.09	130.352	5.440			
440.09	137.415	5.710			
450.10	29.851	2.004			
450.10	39.875	2.205			

Table B3: Viscosity of POE9 at Temperatures from 290 K to 450 K with Pressures to 137 MPa.

T /K	p /MPa	η /mPa·s	T /K	p /MPa	η /mPa·s
300.11	0.025	48.73	320.10	69.999	60.44
300.11	0.839	49.65	320.10	80.053	68.41
300.12	4.823	53.24	320.11	90.112	77.19
300.12	9.810	58.37	320.10	100.180	86.85
300.13	19.819	69.18	320.10	110.255	97.30
300.12	29.860	81.03	330.11	0.344	15.87
300.12	39.886	94.35	330.10	4.805	17.04
289.89	0.181	80.78	330.10	9.814	18.40
289.94	4.824	88.09	330.12	19.817	21.30
295.07	0.317	64.31	330.14	29.836	24.34
295.09	4.819	69.57	330.17	39.836	27.62
295.10	9.819	75.97	330.19	49.849	31.33
295.10	19.375	89.09	330.20	59.876	35.36
305.03	0.150	39.43	330.20	70.179	40.23
305.04	4.820	42.77	330.21	79.996	45.58
305.06	9.813	46.85	330.22	90.052	51.35
305.08	19.822	55.39	330.23	100.117	57.48
305.10	29.825	64.80	330.23	110.184	64.23
305.10	39.849	75.62	330.23	120.265	71.72
305.09	49.881	87.16	330.24	130.340	79.87
309.97	0.446	31.64	330.23	137.405	86.05
310.00	4.788	34.03	330.21	0.396	16.16
310.02	9.777	37.20	340.06	1.367	11.72
310.03	19.788	44.05	340.08	4.748	12.31
310.04	29.801	51.60	340.10	9.759	13.25
310.05	39.811	60.01	340.10	19.772	15.30
310.06	49.841	69.26	340.11	29.782	17.50
310.06	49.888	69.29	340.12	39.806	19.94
310.06	59.913	79.60	340.13	49.829	22.61
310.06	69.950	91.10	340.13	59.878	25.48
320.05	0.313	22.69	340.14	69.918	28.55
320.07	4.806	24.29	340.14	79.978	31.96
320.08	9.798	26.28	340.14	90.031	35.65
320.08	19.810	30.44	340.15	100.102	39.59
320.09	29.826	34.93	340.15	110.176	44.38
320.09	39.856	40.28	340.16	120.240	49.61
320.10	49.892	46.45	340.16	130.311	55.47
320.10	59.935	53.08	340.16	137.153	59.40

Table B3, continued.

T /K	p /MPa	η /mPa·s	T /K	p /MPa	η /mPa·s
340.12	2.365	11.85	370.06	70.168	13.55
350.16	9.421	10.56	370.07	80.227	14.87
350.17	19.732	11.94	370.08	90.283	16.34
350.18	29.736	13.43	370.08	100.332	17.92
350.18	39.750	15.00	370.08	110.402	19.677
350.19	49.781	16.77	370.09	120.476	21.591
350.20	59.825	18.69	370.10	130.555	23.703
350.20	69.874	20.82	370.10	137.602	25.454
350.20	79.934	23.08	379.98	0.151	5.306
350.20	89.999	25.68	379.99	5.018	5.61
350.20	100.059	28.53	379.99	10.024	5.94
350.20	110.139	31.73	380.00	20.014	6.65
350.21	120.220	35.22	380.02	30.030	7.41
350.20	130.234	39.32	380.01	40.047	8.21
350.20	137.274	42.54	380.02	50.061	9.09
350.18	0.333	9.40	380.03	60.116	9.99
359.99	0.220	7.79	380.03	70.169	10.99
360.02	5.114	8.26	380.03	80.220	12.04
360.03	10.114	8.76	380.05	90.285	13.21
360.04	20.125	9.88	380.05	100.335	14.44
360.05	30.135	11.07	380.06	110.410	15.803
360.06	40.142	12.37	380.07	120.483	17.242
360.06	50.170	13.78	380.07	130.567	18.789
360.08	60.216	15.32	380.08	137.599	19.899
360.08	70.268	16.99	440.03	40.107	3.081
360.09	80.317	18.80	440.03	50.129	3.454
360.10	90.374	20.77	440.03	60.172	3.85
360.10	100.429	22.89	440.02	70.227	4.24
360.10	110.503	25.48	440.02	80.274	4.64
360.11	120.584	28.184	440.01	90.335	5.04
360.12	130.664	31.076	440.02	100.384	5.45
360.12	137.703	33.22	440.02	110.468	5.86
369.83	0.123	6.37	440.02	120.548	6.250
369.89	5.015	6.77	440.02	130.625	6.644
369.93	10.012	7.16	440.03	137.675	6.915
369.97	20.023	8.05	450.12	50.112	3.060
370.00	30.029	9.00	450.13	60.151	3.398
370.02	40.055	10.02	450.12	70.204	3.751
370.04	50.084	11.13	450.12	80.262	4.130
370.04	60.120	12.30	450.11	90.320	4.49

Table B3, continued.

T /K	*p* /MPa	*η* /mPa·s
450.11	100.380	4.84
450.11	110.450	5.17
450.11	120.533	5.48
450.11	130.613	5.80
450.12	137.677	6.03

Table B4: Viscosity of Generic MIL-PRF-23699 Oil at Temperatures from 290 K to 450 K with Pressures to 137 MPa.

T /K	*p* /MPa	*η* /mPa·s	*T* /K	*p* /MPa	*η* /mPa·s
315.02	79.941	75.61	320.08	49.798	40.60
315.02	69.898	66.05	320.09	59.836	46.59
315.01	59.865	57.49	320.09	69.885	53.59
315.00	49.827	49.78	320.09	79.958	61.08
315.01	39.787	42.94	320.09	90.010	69.36
315.01	29.759	36.72	320.09	100.067	78.43
315.02	19.733	31.49	320.08	110.145	88.50
300.01	0.051	44.20	320.09	120.214	99.51
300.02	9.732	52.58	330.06	0.088	13.92
300.03	19.737	62.48	330.07	9.767	16.15
300.04	29.740	73.69	330.07	19.758	18.57
300.04	39.759	86.81	330.08	29.760	21.36
310.09	0.030	28.13	330.09	39.782	24.71
310.08	9.717	33.00	330.08	49.811	28.05
310.08	19.721	38.97	330.09	59.853	31.75
310.07	29.725	45.85	330.09	69.897	35.62
310.07	39.748	53.83	330.10	79.942	40.06
310.08	49.776	63.00	330.10	89.996	45.79
310.07	59.807	72.39	330.10	100.062	51.31
310.08	69.868	82.28	330.11	110.129	58.02
310.08	79.917	94.34	330.10	120.210	64.82
290.04	0.064	71.13	330.11	130.265	72.13
290.05	4.748	77.76	330.11	137.310	78.39
290.04	9.747	85.65	339.96	0.087	9.846
295.06	0.056	57.81	339.97	9.758	11.58
295.07	9.736	68.88	339.98	19.763	13.41
295.06	19.747	82.45	339.98	29.763	15.34
320.09	0.075	19.48	339.98	39.775	17.38
320.07	9.753	22.74	339.96	49.808	19.68
320.07	19.742	26.48	339.96	59.843	21.94
320.07	29.753	30.47	339.95	69.896	25.03
320.07	39.776	35.22	339.96	79.938	28.20

Table B4, continued.

T /K	p /MPa	η /mPa·s	T /K	p /MPa	η /mPa·s
339.96	89.993	31.72	390.10	79.923	7.635
339.95	100.061	34.76	390.11	89.978	8.325
339.89	110.161	39.28	390.11	100.046	9.092
339.86	120.259	43.41	390.12	110.109	9.966
339.83	130.343	49.68	390.13	120.174	10.89
339.83	137.402	52.93	390.13	130.250	11.81
349.99	0.076	7.893	390.14	137.313	12.51
350.01	9.755	8.969	400.00	0.088	2.709
350.02	19.762	10.11	400.01	9.758	3.079
350.03	29.770	11.43	400.02	19.756	3.479
350.03	39.799	12.86	400.02	29.765	3.904
350.04	49.816	14.51	400.03	39.789	4.355
350.05	59.857	16.19	400.04	49.804	4.836
350.05	69.913	18.05	400.05	59.833	5.360
350.05	79.959	20.12	400.05	69.890	5.875
350.06	90.003	22.46	400.06	79.936	6.448
350.06	100.071	25.01	400.07	89.981	7.034
350.07	110.144	27.91	400.08	100.051	7.667
350.07	120.213	31.09	400.08	110.114	8.331
350.06	130.275	34.13	400.10	120.183	9.043
350.06	137.337	37.55	400.10	130.249	9.846
380.10	0.072	3.849	400.11	137.281	10.40
380.10	9.752	4.404	409.88	1.271	2.367
380.10	19.745	4.970	409.90	9.753	2.643
380.11	29.752	5.585	409.92	19.744	2.990
380.11	39.770	6.233	409.93	29.748	3.354
380.11	49.804	7.043	409.94	39.769	3.743
380.12	59.853	7.822	409.95	49.785	4.154
380.13	69.902	8.673	409.96	59.826	4.591
380.13	79.954	9.549	409.97	69.861	5.042
380.14	90.003	10.45	409.98	79.900	5.518
380.14	100.064	11.49	409.98	89.947	6.025
380.15	110.128	12.59	409.99	100.016	6.548
380.16	120.187	13.68	409.99	110.068	7.106
380.17	130.255	14.84	409.99	120.141	7.686
380.18	137.317	15.72	410.00	130.205	8.296
390.03	0.204	3.223	410.01	137.266	8.746
390.04	9.747	3.662	420.01	1.215	2.067
390.05	19.752	4.145	420.02	9.730	2.302
390.05	29.751	4.663	420.01	19.732	2.588
390.07	39.760	5.171	420.02	29.736	2.887
390.08	49.796	5.739	420.03	39.749	3.192
390.09	59.837	6.374	420.03	49.775	3.512
390.09	69.870	6.954	420.04	59.817	3.847

Table B4, continued.

T /K	p /MPa	η /mPa·s	T /K	p /MPa	η /mPa·s
420.05	69.864	4.216	450.11	120.147	4.435
420.05	79.904	4.564	450.13	130.209	4.763
420.07	89.945	4.926	450.13	137.252	5.001
420.07	100.016	5.321	380.06	0.048	3.856
420.08	110.074	5.719	380.06	9.742	4.372
420.08	120.137	6.136	380.07	19.740	4.950
420.09	130.199	6.583	380.06	29.748	5.550
420.09	137.243	6.897	380.08	39.764	6.205
429.94	9.742	2.008	380.08	49.803	6.886
429.93	19.738	2.253	380.08	59.835	7.594
429.93	29.749	2.502	380.08	69.882	8.371
429.93	39.765	2.763	380.08	79.927	9.268
429.94	49.798	3.027	380.10	89.991	10.21
429.95	59.824	3.309	380.10	100.055	11.23
429.96	69.862	3.665	380.11	110.119	12.28
429.96	79.913	3.917	380.11	120.181	13.40
429.96	89.956	4.313	380.11	130.250	14.61
429.97	100.021	4.691	380.12	137.307	15.49
429.98	110.086	5.041			
429.99	120.141	5.446			
429.99	130.208	5.868			
429.99	137.260	6.173			
439.97	19.717	2.071			
439.97	29.716	2.293			
439.96	39.731	2.523			
439.96	49.763	2.749			
439.97	59.814	3.027			
439.97	69.867	3.312			
439.97	79.917	3.619			
439.98	89.958	3.932			
439.98	100.025	4.262			
439.99	110.087	4.601			
440.00	120.142	4.959			
440.00	130.198	5.336			
440.00	137.254	5.610			
450.11	29.738	2.070			
450.11	39.747	2.283			
450.11	49.776	2.501			
450.11	59.820	2.736			
450.10	69.855	2.993			
450.11	79.907	3.257			
450.11	89.955	3.536			
450.11	100.022	3.822			
450.11	110.091	4.128			

Appendix C: REFPROP Fluid Files

C.1. POE5.FLD

```
POE5                 !Short name
15834-04-5           !CAS number
pentaerythritol tetrapentanoate !Full name
C25H44O8             !Chemical formula
POE5                 !Synonym
472.612              !Molar mass [g/mol]
250.                 !Triple point temperature [K]
707.618              !Normal boiling point [K]
890.0                !Critical temperature [K]
1270.0               !Critical pressure [kPa]
0.556                !Critical density [mol/L]
0.89                 !Acentric factor
-1.                  !Dipole moment [Debye]
NBP                  !Default reference state
10.0                 !Version number

! compiled by E.W. Lemmon, NIST Physical and Chemical Properties Division, Boulder,
Colorado
! 12-01-17 EWL, Original version.
! 08-09-18 EWL, Add final equation of state.
! 08-29-18 MLH, Add viscosity correlation.
! 09-06-18 MLH, Add thermal conductivity correlation.

_____________________________________________________________________________

#EOS   !---Equation of state---
FEQ    !Helmholtz equation of state for POE5 of Lemmon and Eckermann (2018).
?
?```````````````````````````````````````````````````````````````````````````````
?Lemmon, E.W. and Eckermann, T.
?
?The uncertainty of calculated values in the liquid phase is 0.2 % in density and
? speed of sound between 260 K and 450 K with pressures to 70 MPa. For speed of
? sound, the uncertainty may increase to 0.3 % above 380 K. Outside of these
? ranges, the uncertainties will slowly increase as a function of the distance
? from the upper or lower bounds given above.  Values could be as small as 0.4 % at
? 220 K (assuming the oil is still fluid) or, for density, at temperatures up to
? 600 K. The uncertainties in the critical region and vapor phase are unknown, but
? not expected to exceed 1 % for density at temperatures up to 600 K in the vapor
? phase.  The uncertainty in vapor-phase speed of sound is unknown due to the lack
? of information pertaining to the ideal-gas isobaric heat capacity (at very low
? pressures).
?
?The uncertainty in heat capacities in the liquid phase is 0.5 % from 250 K to
? 450 K. The uncertainties for vapor pressures are difficult to quantify due to
? the extremely low vapor pressures below 500 K. An approximate value would be one
? order of magnitude; for example, at a temperature where the calculated value of
? the vapor pressure is 1 Pa, the true value could be between 0.1 Pa to 10 Pa.
? For vapor pressures above 1 atmosphere, the same may be true, but it is
? estimated that the values would be less than 50 %.
?
!```````````````````````````````````````````````````````````````````````````````
250.0              !Lower temperature limit [K]
1000.0             !Upper temperature limit [K]
100000.0           !Upper pressure limit [kPa]
2.24               !Maximum density [mol/L]
CPP                                !Pointer to Cp0 model
472.612                            !Molar mass [g/mol]
```

```
250.0                                   !Triple point temperature [K]
0.000000000000001                       !Pressure at triple point [kPa]
2.23                                    !Density at triple point [mol/L]
707.618                                 !Normal boiling point temperature [K]
0.89                                    !Acentric factor
890.0          1270.0        0.556      !Tc [K], pc [kPa], rhoc [mol/L]
890.0                        0.556      !Reducing parameters [K, mol/L]
8.3144598                               !Gas constant [J/mol-K]
  10   4    4 12    0 0     0 0  0 0  0 0  !# terms and # coefs/term for normal terms,
Gaussian terms, and Gao terms
  0.0106971    1.0     5.  0.          !a(i),t(i),d(i),l(i)
  1.510321     0.08    1.  0.
 -2.596894     1.2     1.  0.
 -2.311273     1.162   2.  0.
  0.3332414    0.54    3.  0.
  2.500028     1.08    2.  1.
  7.527764     1.56    3.  1.
 -5.405529     1.78    3.  1.
  0.94954      1.42    4.  1.
  0.3303842    1.62    5.  1.
 -0.0234605    2.0     1.  2. 2.   -1.0    -0.36     1.57     1.7       0. 0. 0.
  0.0156448    1.0     2.  2. 2.   -1.31   -0.35     1.45     0.55      0. 0. 0.
 -0.0092188    1.0     4.  2. 2.   -0.46   -0.55     1.63     0.95      0. 0. 0.
 -0.5415831    1.0     3.  2. 2.   -20.0  -1000.0    1.09     0.91      0. 0. 0.

#AUX   !---Auxiliary function for Cp0
CPP    !Ideal gas heat capacity function for POE5 of Lemmon and Eckermann (2018).
?
?```````````````````````````````````````````````````````````````````````````````
?Lemmon, E.W. and Eckermann, T.
?
!```````````````````````````````````````````````````````````````````````````````
0.                !
10000.            !
0.                !
0.                !
1.0     8.3144598  !Reducing parameters for T, Cp0
1 2   0 0   0 0 0  !Nterms:  polynomial, exponential, cosh, sinh
 30.0     0.0
 69.0   850.0
 98.0  2000.0

^^^^^^^^^^^^^^^^^^^^^^^^^^^^^^^^^^^^^^^^^^^^^^^^^^^^^^^^^^^^^^^^^^^^^^^^^^^^^^^^

#ETA   !---Viscosity---
VS7    !Pure fluid viscosity model for POE5 of Huber (2018).
?
?```````````````````````````````````````````````````````````````````````````````
? Estimated uncertainty is 5 % for the liquid over the temperature range 275 K to 430 K
at pressures to 140 MPa.
? Larger uncertainties in the gas phase; data unavailable for comparisons.
?
!```````````````````````````````````````````````````````````````````````````````
250.              !Lower temperature limit [K]
1000.             !Upper temperature limit [K]
150000.           !Upper pressure limit [kPa]
3.                !Maximum density [mol/L]
CI0               !Pointer to reduced effective collision cross-section model
0.9838            !Lennard-Jones coefficient sigma [nm]
706.7418          !Lennard-Jones coefficient epsilon/kappa [K]
1.0    1.0        !Reducing parameters for eta, T, rho
1.0    0.5        !Chapman-Enskog term
!
```

```
!Dilute gas
$DG CNST CNST CNST TEMP * SQRT * * DC THRD2 POWR * OMEGAS /
!
!Residual function odrfit1 may16
$RF RED DR CNST POWR TR / =DEL SUMDEL:4 DR THRD2 POWR *
!
!Coefficients
$CF
0.040785               0.   0.    0.  0
0.75472                0.   0.    0.  0
472.612                0.   0.    0.  0
1.                   890.   0.556 0.  0
3.58                   0.   0.    0.  0
 1.43071132871263      0.5  1.0   0.  0
 0.0190909592490056    0.5  2.0   0.  0
 4.09041797712726e-12  0.5  6.0   0.  0
 1.38884778119428e-30  0.5  13.0  0.  0
NUL                  !Pointer to the viscosity critical enhancement auxiliary function
(none used)

================================================================================

#TCX   !---Thermal conductivity---
TC1    !Pure fluid thermal conductivity model for POE5 of Huber and Perkins (2018).
?
?```````````````````````````````````````````````````````````````````````````````
? Estimated uncertainty is 0.5 % for the liquid at pressures to 70 MPa for 300 K to 500
K.
? Larger uncertainties in the critical region and in the gas phase; data unavailable for
comparisons.
?
!```````````````````````````````````````````````````````````````````````````````
250.0              !Lower temperature limit [K]
1000.0             !Upper temperature limit [K]
100000.0           !Upper pressure limit [kPa]
3.                 !Maximum density [mol/L]
6   0              !# terms for dilute gas function:  numerator, denominator
 890.0       0.001 !Reducing parameters for T, tcx
 1.847472    0.
-18.00409    1.
 108.2592    2.
-80.25605    3.
 26.80722    4.
-3.439569    5.
 10  0             !# terms for background gas function:  numerator, denominator
 890.0  0.556  1.  !Reducing parameters for T, rho, tcx
 0.00804625    0.  1.  0.
 0.0050047     0.  2.  0.
-0.000211256   0.  3.  0.
 0.0           0.  4.  0.
 0.0           0.  5.  0.
 0.0561869     1.  1.  0.
-0.0542289     1.  2.  0.
 0.0126351     1.  3.  0.
 0.0           1.  4.  0.
 0.0           1.  5.  0.
TK3                !Pointer to critical enhancement auxiliary function

#AUX   !---Auxiliary function for the thermal conductivity critical enhancement
TK3    !Simplified thermal conductivity critical enhancement for POE5 of Perkins et al.
(2013).
?
?```````````````````````````````````````````````````````````````````````````````
```

```
?Perkins, R.A., Sengers, J.V., Abdulagatov, I.M., and Huber, M.L.,
? "Simplified model for the critical thermal-conductivity enhancement in molecular
fluids"
? Int. J. Thermophysics, 34(2):191-212, 2013. doi: 10.1007/s10765-013-1409-z
?
!```````````````````````````````````````````````````````````````````````````````
0.                !
10000.            !
0.                !
0.                !
9 0 0 0           !# terms:  CO2-terms, spare, spare, spare
1.0  1.0  1.0     !Reducing parameters for T, rho, tcx [mW/(m-K)]
0.63              !Nu (universal exponent)
1.239             !Gamma (universal exponent)
1.02              !R0 (universal amplitude)
0.063             !Z (universal exponent--not used for t.c., only viscosity)
1.0               !C (constant in viscosity eqn = 1/[2 - (alpha + gamma)/(2*nu)], but
often set to 1)
0.343e-9          !Xi0 (amplitude) [m]
0.082             !Gam0 (amplitude) [-]
1.218e-9          !Qd_inverse (modified effective cutoff parameter) [m]
1335.0            !Tref (reference temperature)=1.5*Tc [K]

++++++++++++++++++++++++++++++++++++++++++++++++++++++++++++++++++++++++++++++++

@TRN    !---ECS Transport---
ECS     !Extended Corresponding States model (N2 reference); predictive mode for POE5.
          ?

?```````````````````````````````````````````````````````````````````````````````
          ?*** ESTIMATION METHOD *** NOT STANDARD REFERENCE QUALITY ***
          ?Unpublished; uses method described in the following reference:
          ?Huber, M.L., Laesecke, A., and Perkins, R.A.
          ? "Model for the Viscosity and Thermal Conductivity of Refrigerants, Including
          ? a New Correlation for the Viscosity of R134a,"
          ? Ind. Eng. Chem. Res., 42(13):3163-3178, 2003. doi: 10.1021/ie0300880.
          ?
          ?Estimated uncertainty 3 % for liquid in range 293 K to 350 K at pressures
<180 MPa
          ?
          ?The Lennard-Jones parameters were taken from Reid, R.C., Prausnitz, J.M., and
Poling, B.E., "The Properties of Gases and Liquids," 4th edition, New York, McGraw-Hill
Book Company, 1987.
          ?

!```````````````````````````````````````````````````````````````````````````````
          250.               !Lower temperature limit [K]
          1000.              !Upper temperature limit [K]
          100000.            !Upper pressure limit [kPa]
          10.                !Maximum density [mol/L]
          FEQ NITROGEN.FLD
          VS1                !Model for reference fluid viscosity
          TC1                !Model for reference fluid thermal conductivity
          BIG                !Large molecule identifier
          0.75472 0. 0. 0.   !Large molecule parameters
          1                  !Lennard-Jones flag (0 or 1) (0 => use estimates)
          0.9838             !Lennard-Jones coefficient sigma [nm]
          706.7418          !Lennard-Jones coefficient epsilon/kappa [K] for ECS method
          1  0  0                !Number of terms in f_int term in Eucken correlation,
spare1, spare2
           0.00132       0. 0. 0.  !Coefficient, power of T, spare1, spare2
          3   0   0                     !Number of terms in psi (visc shape factor):
poly,spare1,spare2
```

```
           1.09271       0. 0. 0.  !Coefficient, power of Tr, power of Dr, spare
          -0.161324      0. 1. 0.  !Coefficient, power of Tr, power of Dr, spare
           0.0486596     0. 2. 0.  !Coefficient, power of Tr, power of Dr, spare
          1   0   0                    !Number of terms in chi (t.c. shape factor):
poly,spare1,spare2
           1.0           0. 0. 0.  !Coefficient, power of Tr, power of Dr, spare
          TK3               !Pointer to critical enhancement auxiliary function

~~~~~~~~~~~~~~~~~~~~~~~~~~~~~~~~~~~~~~~~~~~~~~~~~~~~~~~~~~~~~~~~~~~~~~~~~~~~~~~~

#PS    !---Vapor pressure---
PS5    !Vapor pressure equation for POE5 of Lemmon and Eckermann (2018).
?
?```````````````````````````````````````````````````````````````````````````````
?Functional Form:  P=Pc*EXP[SUM(Ni*Theta^ti)*Tc/T] where Theta=1-T/Tc, Tc and Pc
? are the reducing parameters below, which are followed by rows containing Ni and ti.
?
!```````````````````````````````````````````````````````````````````````````````
0.                 !
10000.             !
0.                 !
0.                 !
890.0   1270.0     !Reducing parameters
5 0 0 0 0 0        !Number of terms in equation
-11.0745   1.0
 7.7727    1.5
-7.8638    1.85
-9.9844    3.44
-10.450   10.00

#DL    !---Saturated liquid density---
DL1    !Saturated liquid density equation for POE5 of Lemmon and Eckermann (2018).
?
?```````````````````````````````````````````````````````````````````````````````
?Functional Form:  D=Dc*[1+SUM(Ni*Theta^ti)] where Theta=1-T/Tc, Tc and Dc are
? the reducing parameters below, which are followed by rows containing Ni and ti.
?
!```````````````````````````````````````````````````````````````````````````````
0.                 !
10000.             !
0.                 !
0.                 !
890.0  0.556       !Reducing parameters
5 0 0 0 0 0        !Number of terms in equation
 3.5330   0.44
-1.8646   0.9
 3.3949   1.4
-3.2549   2.0
 2.1666   2.7

#DV    !---Saturated vapor density---
DV3    !Saturated vapor density equation for POE5 of Lemmon and Eckermann (2018).
?
?```````````````````````````````````````````````````````````````````````````````
?Functional Form:  D=Dc*EXP[SUM(Ni*Theta^ti)] where Theta=1-T/Tc, Tc and Dc are
? the reducing parameters below, which are followed by rows containing Ni and ti.
?
!```````````````````````````````````````````````````````````````````````````````
0.                 !
10000.             !
0.                 !
0.                 !
890.0  0.556       !Reducing parameters
```

```
5 0 0 0 0 0        !Number of terms in equation
-4.8478   0.483
-9.9537   1.5
-28.962   3.08
-81.61    5.5
-280.12  12.0

@END
c        1         2         3         4         5         6         7         8
c2345678901234567890123456789012345678901234567890123456789012345678901234567890
```

C.2. POE7.FLD

```
POE7                 !Short name
25811-35-2           !CAS number
pentaerythritol tetraheptanoate !Full name
C33H60O8             !Chemical formula
POE7                 !Synonym
584.835              !Molar mass [g/mol]
250.                 !Triple point temperature [K]
770.561              !Normal boiling point [K]
940.0                !Critical temperature [K]
1030.0               !Critical pressure [kPa]
0.412                !Critical density [mol/L]
1.06                 !Acentric factor
-1.                  !Dipole moment [Debye]
NBP                  !Default reference state
10.0                 !Version number

! compiled by E.W. Lemmon, NIST Physical and Chemical Properties Division, Boulder,
Colorado
! 12-01-17 EWL, Original version.
! 08-09-18 EWL, Add final equation of state.
! 09-08-18 MLH, Add viscosity correlation.
! 09-09-18 MLH, Add thermal conductivity correlation.
```

```
#EOS   !---Equation of state---
FEQ    !Helmholtz equation of state for POE7 of Lemmon and Eckermann (2018).
?
?```````````````````````````````````````````````````````````````````````````````
?Lemmon, E.W. and Eckermann, T.
?
?The uncertainty of calculated values in the liquid phase is 0.2 % in density and
? speed of sound between 260 K and 450 K with pressures to 70 MPa. For speed of
? sound, the uncertainty may increase to 0.3 % above 380 K. Outside of these
? ranges, the uncertainties will slowly increase as a function of the distance
? from the upper or lower bounds given above.  Values could be as small as 0.4 % at
? 220 K (assuming the oil is still fluid) or, for density, at temperatures up to
? 600 K. The uncertainties in the critical region and vapor phase are unknown, but
? not expected to exceed 1 % for density at temperatures up to 600 K in the vapor
? phase.  The uncertainty in vapor-phase speed of sound is unknown due to the lack
? of information pertaining to the ideal-gas isobaric heat capacity (at very low
? pressures).
?
?The uncertainty in heat capacities in the liquid phase is 0.5 % from 250 K to
? 450 K. The uncertainties for vapor pressures are difficult to quantify due to
? the extremely low vapor pressures below 500 K. An approximate value would be one
? order of magnitude; for example, at a temperature where the calculated value of
? the vapor pressure is 1 Pa, the true value could be between 0.1 Pa to 10 Pa.
```

```
? For vapor pressures above 1 atmosphere, the same may be true, but it is
? estimated that the values would be less than 50 %.
?
!```````````````````````````````````````````````````````````````````````````
250.0              !Lower temperature limit [K]
1000.0             !Upper temperature limit [K]
100000.0           !Upper pressure limit [kPa]
1.74               !Maximum density [mol/L]
CPP                                !Pointer to Cp0 model
584.835                            !Molar mass [g/mol]
250.0                              !Triple point temperature [K]
0.000000000000001                  !Pressure at triple point [kPa]
1.73                               !Density at triple point [mol/L]
770.561                            !Normal boiling point temperature [K]
1.06                               !Acentric factor
940.0          1030.0        0.412     !Tc [K], pc [kPa], rhoc [mol/L]
940.0                        0.412     !Reducing parameters [K, mol/L]
8.3144598                          !Gas constant [J/mol-K]
  10  4   4 12   0 0    0 0  0 0  0 0  !# terms and # coefs/term for normal terms,
Gaussian terms, and Gao terms
  0.00996664   1.0     5.  0.          !a(i),t(i),d(i),l(i)
  1.801441     0.08    1.  0.
 -2.872737     1.2     1.  0.
 -2.347331     1.162   2.  0.
  0.3403607    0.54    3.  0.
  2.550799     1.08    2.  1.
  7.625433     1.56    3.  1.
 -5.44993      1.78    3.  1.
  0.8612612    1.42    4.  1.
  0.3734221    1.62    5.  1.
 -0.00711446   2.0     1.  2. 2.   -1.0    -0.36     1.57     1.7       0. 0. 0.
  0.02289254   1.0     2.  2. 2.   -1.31   -0.35     1.45     0.55      0. 0. 0.
 -0.00893703   1.0     4.  2. 2.   -0.46   -0.55     1.63     0.95      0. 0. 0.
 -0.75359521   1.0     3.  2. 2.   -20.0  -1000.0    1.09     0.91      0. 0. 0.

#AUX   !---Auxiliary function for Cp0
CPP    !Ideal gas heat capacity function for POE7 of Lemmon and Eckermann (2018).
?
?```````````````````````````````````````````````````````````````````````````
?Lemmon, E.W. and Eckermann, T.
?
!```````````````````````````````````````````````````````````````````````````
0.                 !
10000.             !
0.                 !
0.                 !
1.0     8.3144598  !Reducing parameters for T, Cp0
1 2   0 0   0 0 0  !Nterms:  polynomial, exponential, cosh, sinh
 55.00     0.0
 109.0  1100.0
 240.5  3000.0

^^^^^^^^^^^^^^^^^^^^^^^^^^^^^^^^^^^^^^^^^^^^^^^^^^^^^^^^^^^^^^^^^^^^^^^^^^^^^^^

#ETA   !---Viscosity---
VS7    !Pure fluid viscosity model for POE7 of Huber (2018).
?
?```````````````````````````````````````````````````````````````````````````
? Estimated uncertainty is 5 % for the liquid over the temperature range 280 K to 450
K at pressures to 140 MPa.
? Larger uncertainties in the gas phase; data unavailable for comparisons.
?
!```````````````````````````````````````````````````````````````````````````
```

```
250.0              !Lower temperature limit [K]
1000.0             !Upper temperature limit [K]
150000.0           !Upper pressure limit [kPa]
3.                 !Maximum density [mol/L]
CI0                !Pointer to reduced effective collision cross-section model
1.087188           !Lennard-Jones coefficient sigma [nm]
746.4464           !Lennard-Jones coefficient epsilon/kappa [K]
1.0    1.0         !Reducing parameters for eta, T, rho
1.0    0.5         !Chapman-Enskog term
!
!Dilute gas
$DG CNST CNST CNST TEMP * SQRT * * DC THRD2 POWR * OMEGAS /
!
!Residual function odrfit sep 2018
$RF RED DR CNST POWR TR / =DEL SUMDEL:3 DR THRD2 POWR *
!
!Coefficients
$CF
0.040785               0.   0.    0.  0
0.70786                0.   0.    0.  0
584.835                0.   0.    0.  0
1.                   940.   0.412 0.  0
3.43                   0.   0.    0.  0
 1.82929606864369e-09  0.5  5.0   0.  0
 2.26670776452313e-30  0.5  13.0  0.  0
 0.102166296616783     2.5  2.0   0.  0
NUL                !Pointer to the viscosity critical enhancement auxiliary function
(none used)

================================================================================

#TCX   !---Thermal conductivity---
TC1    !Pure fluid thermal conductivity model for POE7 of Huber and Perkins (2018).
?
?```````````````````````````````````````````````````````````````````````````````
? Estimated uncertainty is 0.5 % for the liquid at pressures to 70 MPa for 300 K to
504 K.
? Larger uncertainties in the critical region and in the gas phase; data unavailable
for comparisons.
?
!```````````````````````````````````````````````````````````````````````````````
250.0              !Lower temperature limit [K]
1000.0             !Upper temperature limit [K]
100000.0           !Upper pressure limit [kPa]
3.                 !Maximum density [mol/L]
6   0              !# terms for dilute gas function:  numerator, denominator
 940.0       0.001 !Reducing parameters for T, tcx
 5.0156798   0.
-32.028343   1.
 112.07684   2.
-52.063516   3.
 7.7818950   4.
 0.16886652  5.
 10  0             !# terms for background gas function:  numerator, denominator
 940.0  0.412  1.  !Reducing parameters for T, rho, tcx
 0.0314251     0.  1.  0.
-0.00484656    0.  2.  0.
 0.000729462   0.  3.  0.
 0.0           0.  4.  0.
 0.0           0.  5.  0.
 0.0124139     1.  1.  0.
-0.0359579     1.  2.  0.
 0.010532      1.  3.  0.
```

```
 0.0           1.  4.  0.
 0.0           1.  5.  0.
TK3               !Pointer to critical enhancement auxiliary function

#AUX   !---Auxiliary function for the thermal conductivity critical enhancement
TK3    !Simplified thermal conductivity critical enhancement for POE7 of Perkins et
al. (2013).
?
?```````````````````````````````````````````````````````````````````````````````
?Perkins, R.A., Sengers, J.V., Abdulagatov, I.M., and Huber, M.L.,
? "Simplified model for the critical thermal-conductivity enhancement in molecular
fluids"
? Int. J. Thermophysics, 34(2):191-212, 2013. doi: 10.1007/s10765-013-1409-z
?
!```````````````````````````````````````````````````````````````````````````````
0.                !
10000.            !
0.                !
0.                !
9 0 0 0           !# terms:  CO2-terms, spare, spare, spare
1.0  1.0  1.0     !Reducing parameters for T, rho, tcx [mW/(m-K)]
0.63              !Nu (universal exponent)
1.239             !Gamma (universal exponent)
1.02              !R0 (universal amplitude)
0.063             !Z (universal exponent--not used for t.c., only viscosity)
1.0               !C (constant in viscosity eqn = 1/[2 - (alpha + gamma)/(2*nu)], but
often set to 1)
0.367e-9          !Xi0 (amplitude) [m]
0.090             !Gam0 (amplitude) [-]
1.349e-9          !Qd_inverse (modified effective cutoff parameter) [m]
1410.0            !Tref (reference temperature)=1.5*Tc [K]

++++++++++++++++++++++++++++++++++++++++++++++++++++++++++++++++++++++++++++++++++++

@TRN    !---ECS Transport---
ECS     !Extended Corresponding States model (N2 reference); predictive mode for POE7.
          ?

?```````````````````````````````````````````````````````````````````````````````
          ?*** ESTIMATION METHOD *** NOT STANDARD REFERENCE QUALITY ***
          ?Unpublished; uses method described in the following reference:
          ?Huber, M.L., Laesecke, A., and Perkins, R.A.
          ? "Model for the Viscosity and Thermal Conductivity of Refrigerants,
Including
          ? a New Correlation for the Viscosity of R134a,"
          ? Ind. Eng. Chem. Res., 42(13):3163-3178, 2003. doi: 10.1021/ie0300880.
          ?
          ?The Lennard-Jones parameters were estimated with the method of Chung
          ?

!```````````````````````````````````````````````````````````````````````````````
          250.              !Lower temperature limit [K]
          1000.             !Upper temperature limit [K]
          100000.           !Upper pressure limit [kPa]
          10.               !Maximum density [mol/L]
          FEQ NITROGEN.FLD
          VS1               !Model for reference fluid viscosity
          TC1               !Model for reference fluid thermal conductivity
          BIG               !Large molecule identifier
          0.70786 0. 0. 0.  !Large molecule parameters
          1                 !Lennard-Jones flag (0 or 1) (0 => use estimates)
          1.087188          !Lennard-Jones coefficient sigma [nm]
```

```
          746.4464           !Lennard-Jones coefficient epsilon/kappa [K] for ECS
method
          1  0  0                 !Number of terms in f_int term in Eucken
correlation, spare1, spare2
           0.00132       0. 0. 0.  !Coefficient, power of T, spare1, spare2
          3  0  0                 !Number of terms in psi (visc shape factor):
poly,spare1,spare2
           1.09271       0. 0. 0.  !Coefficient, power of Tr, power of Dr, spare
          -0.161324      0. 1. 0.  !Coefficient, power of Tr, power of Dr, spare
           0.0486596     0. 2. 0.  !Coefficient, power of Tr, power of Dr, spare
          1  0  0                 !Number of terms in chi (t.c. shape factor):
poly,spare1,spare2
           1.0           0. 0. 0.  !Coefficient, power of Tr, power of Dr, spare
          TK3               !Pointer to critical enhancement auxiliary function

~~~~~~~~~~~~~~~~~~~~~~~~~~~~~~~~~~~~~~~~~~~~~~~~~~~~~~~~~~~~~~~~~~~~~~~~~~~~~~~~~~~

#PS    !---Vapor pressure---
PS5    !Vapor pressure equation for POE7 of Lemmon and Eckermann (2018).
?
?``````````````````````````````````````````````````````````````````````````````
?Functional Form:  P=Pc*EXP[SUM(Ni*Theta^ti)*Tc/T] where Theta=1-T/Tc, Tc and Pc
? are the reducing parameters below, which are followed by rows containing Ni and ti.
?
!``````````````````````````````````````````````````````````````````````````````
0.                 !
10000.             !
0.                 !
0.                 !
940.0   1030.0     !Reducing parameters
5 0 0 0 0 0        !Number of terms in equation
-11.582   1.0
 5.9741   1.5
-5.7551   1.9
-11.617   3.2
-10.450   9.4

#DL    !---Saturated liquid density---
DL1    !Saturated liquid density equation for POE7 of Lemmon and Eckermann (2018).
?
?``````````````````````````````````````````````````````````````````````````````
?Functional Form:  D=Dc*[1+SUM(Ni*Theta^ti)] where Theta=1-T/Tc, Tc and Dc are
? the reducing parameters below, which are followed by rows containing Ni and ti.
?
!``````````````````````````````````````````````````````````````````````````````
0.                 !
10000.             !
0.                 !
0.                 !
940.0  0.412       !Reducing parameters
4 0 0 0 0 0        !Number of terms in equation
 3.0882    0.43
 0.61105   1.08
-1.4658    1.85
 1.9244    2.5

#DV    !---Saturated vapor density---
DV3    !Saturated vapor density equation for POE7 of Lemmon and Eckermann (2018).
?
?``````````````````````````````````````````````````````````````````````````````
?Functional Form:  D=Dc*EXP[SUM(Ni*Theta^ti)] where Theta=1-T/Tc, Tc and Dc are
? the reducing parameters below, which are followed by rows containing Ni and ti.
?
```

```
!``````````````````````````````````````````````````````````````````````````````
0.                  !
10000.              !
0.                  !
0.                  !
940.0  0.412        !Reducing parameters
5 0 0 0 0 0         !Number of terms in equation
-5.0595   0.5
-11.784   1.5
-52.705   3.5
-97.681   6.6
-318.67  13.0

@END
c        1         2         3         4         5         6         7         8
c2345678901234567890123456789012345678901234567890123456789012345678901234567890

                    #ETA   !---Viscosity---
                    VS7    !Pure fluid viscosity model for POE7 of Huber (2018).
                    :DOI:
                    ?

!``````````````````````````````````````````````````````````````````````````````
                    0.                  !Lower temperature limit [K]
                    10000.              !Upper temperature limit [K]
                    100000000.          !Upper pressure limit [kPa]
                    100.                !Maximum density [mol/L]
                    CI0                 !Pointer to reduced effective collision cross-
section model
                    1.087188            !Lennard-Jones coefficient sigma [nm]
                    746.4464            !Lennard-Jones coefficient epsilon/kappa [K]
                    1.0    1.0          !Reducing parameters for eta, T, rho
                    1.0    0.5          !Chapman-Enskog term
                    !
                    !Dilute gas
                    $DG CNST CNST CNST TEMP * SQRT * * DC THRD2 POWR * OMEGAS /
                    !
                    !Residual function odrfit1 may16
                    $RF RED DR CNST POWR TR / =DEL SUMDEL:2 SUM:1 + DR 2 3 / POWR *
                    !
                    !Coefficients
                    $CF
                    4.0785e-2       0.   0.   0.  0
                    0.70786         0.   0.   0.  0
                    584.835         0.   0.   0.  0
                    1.            940.   0.412 0.  0
                    3.43            0.   0.   0.  0
                     1.82929606864369D-09      0.5   5.0     0.  0
                     2.26670776452313D-30      0.5   13.0    0.  0
                     0.102166296616783         2.5   2.0    0.  0
                    NUL                 !Pointer to the viscosity critical enhancement
auxiliary function (none used)

                    #ETA   !---Viscosity---
                    VS7    !Pure fluid viscosity model for POE7 of Huber (2018).
aug20.4 fit
                    :DOI:
                    ?

!``````````````````````````````````````````````````````````````````````````````
                    0.                  !Lower temperature limit [K]
                    10000.              !Upper temperature limit [K]
                    100000000.          !Upper pressure limit [kPa]
```

```
                    100.               !Maximum density [mol/L]
                    CI0                !Pointer to reduced effective collision cross-
section model
                    1.087188           !Lennard-Jones coefficient sigma [nm]
                    746.4464           !Lennard-Jones coefficient epsilon/kappa [K]
                    1.0    1.0         !Reducing parameters for eta, T, rho
                    1.0    0.5         !Chapman-Enskog term
                    !
                    !Dilute gas
                    $DG CNST CNST CNST TEMP * SQRT * * DC THRD2 POWR * OMEGAS /
                    !
                    !Residual function odrfit1 may16
                    $RF RED DR CNST POWR TR / =DEL SUMDEL:4 SUM:1 + DR 2 3 / POWR *
                    !
                    !Coefficients
                    $CF
                    4.0785e-2       0.   0.   0.  0
                    0.70786         0.   0.   0.  0
                    584.835         0.   0.   0.  0
                    1.            940.   0.412 0.  0
                    3.43            0.   0.   0.  0
                     0.000212774089055934      0.5   1.0     0.  0
                    -0.0863685877011118        0.5   2.0     0.  0
                     0.000347206660020975      0.5   3.0     0.  0
                     5.23640129648801D-25      0.5   11.0    0.  0
                     0.769337343185798        -0.5   5.43    0.  0
                    NUL                !Pointer to the viscosity critical enhancement
auxiliary function (none used)
```

C.3. POE9.FLD

```
POE9                !Short name
14450-05-6          !CAS number
pentaerythritol tetranonanoate !Full name
C41H76O8            !Chemical formula
POE9                !Synonym
697.051             !Molar mass [g/mol]
250.                !Triple point temperature [K]
796.639             !Normal boiling point [K]
970.0               !Critical temperature [K]
885.0               !Critical pressure [kPa]
0.316               !Critical density [mol/L]
0.998               !Acentric factor
-1.                 !Dipole moment [Debye]
NBP                 !Default reference state
10.0                !Version number

! compiled by E.W. Lemmon, NIST Physical and Chemical Properties Division, Boulder,
Colorado
! 12-01-17 EWL, Original version.
! 08-21-18 EWL, Add final equation of state.
! 09-12-18 MLH, Add thermal conductivity and viscosity.

_____________________________________________________________________________

#EOS   !---Equation of state---
FEQ    !Helmholtz equation of state for POE9 of Lemmon and Eckermann (2018).
?
?```````````````````````````````````````````````````````````````````````````````
?Lemmon, E.W. and Eckermann, T.
?
?The uncertainty of calculated values in the liquid phase is 0.2 % in density and
```

```
? speed of sound between 260 K and 450 K with pressures to 70 MPa. For speed of
? sound, the uncertainty may increase to 0.3 % above 380 K. Outside of these
? ranges, the uncertainties will slowly increase as a function of the distance
? from the upper or lower bounds given above.  Values could be as small as 0.4 % at
? 220 K (assuming the oil is still fluid) or, for density, at temperatures up to
? 600 K. The uncertainties in the critical region and vapor phase are unknown, but
? not expected to exceed 1 % for density at temperatures up to 600 K in the vapor
? phase.  The uncertainty in vapor-phase speed of sound is unknown due to the lack
? of information pertaining to the ideal-gas isobaric heat capacity (at very low
? pressures).
?
?The uncertainty in heat capacities in the liquid phase are 0.5 % from 250 K to
? 450 K, and increases to 1 % or more below 330 K. The uncertainties for vapor
? pressures are difficult to quantify due to the extremely low vapor pressures
? below 500 K. An approximate value would be one order of magnitude; for example,
? at a temperature where the calculated value of the vapor pressure is 1 Pa, the
? true value could be between 0.1 Pa to 10 Pa.  For vapor pressures above 1
? atmosphere, the same may be true, but it is estimated that the values would be
? less than 50 %.
?
!```````````````````````````````````````````````````````````````````````````````
250.0              !Lower temperature limit [K]
1000.0             !Upper temperature limit [K]
100000.0           !Upper pressure limit [kPa]
1.43               !Maximum density [mol/L]
CPP                                !Pointer to Cp0 model
697.051                            !Molar mass [g/mol]
250.0                              !Triple point temperature [K]
0.000000000000001                  !Pressure at triple point [kPa]
1.42                               !Density at triple point [mol/L]
796.639                            !Normal boiling point temperature [K]
0.998                              !Acentric factor
970.0          885.0       0.316   !Tc [K], pc [kPa], rhoc [mol/L]
970.0                      0.316   !Reducing parameters [K, mol/L]
8.3144598                          !Gas constant [J/mol-K]
  10   4    4 12    0 0     0 0  0 0  0 0  !# terms and # coefs/term for normal terms,
Gaussian terms, and Gao terms
  0.00811      1.0     5.  0.          !a(i),t(i),d(i),l(i)
  1.446665     0.08    1.  0.
 -2.303871     1.2     1.  0.
 -2.320483     1.162   2.  0.
  0.336244     0.54    3.  0.
  2.383751     1.08    2.  1.
  8.210469     1.56    3.  1.
 -6.200227     1.78    3.  1.
  0.813201     1.42    4.  1.
  0.377317     1.62    5.  1.
  0.0023328    2.0     1.  2. 2.   -1.0    -0.36     1.57     1.7       0. 0. 0.
  0.0217847    1.0     2.  2. 2.   -1.31   -0.35     1.45     0.55      0. 0. 0.
 -0.009014     1.0     4.  2. 2.   -0.46   -0.55     1.63     0.95      0. 0. 0.
 -1.54251      1.0     3.  2. 2.   -20.0  -1000.0    1.09     0.91      0. 0. 0.

#AUX   !---Auxiliary function for Cp0
CPP    !Ideal gas heat capacity function for POE9 of Lemmon and Eckermann (2018).
?
?```````````````````````````````````````````````````````````````````````````````
?Lemmon, E.W. and Eckermann, T.
?
!```````````````````````````````````````````````````````````````````````````````
0.                 !
10000.             !
0.                 !
0.                 !
```

```
1.0     8.3144598  !Reducing parameters for T, Cp0
1 2   0 0   0 0 0  !Nterms:  polynomial, exponential, cosh, sinh
 75.0     0.0
 93.0  1000.0
 360.0 2700.0

^^^^^^^^^^^^^^^^^^^^^^^^^^^^^^^^^^^^^^^^^^^^^^^^^^^^^^^^^^^^^^^^^^^^^^^^^^^^^^^^

#ETA   !---Viscosity---
VS7    !Pure fluid viscosity model for POE9 of Huber (2018).
?
?``````````````````````````````````````````````````````````````````````````````
? Estimated uncertainty for the liquid phase from 290 K to 450 K at pressures to 140 MPa
is 6.8 %
? Larger uncertainties in the gas phase; data unavailable for comparisons.
?
!``````````````````````````````````````````````````````````````````````````````
250.0              !Lower temperature limit [K]
1000.0             !Upper temperature limit [K]
150000.0           !Upper pressure limit [kPa]
3.                 !Maximum density [mol/L]
CI0                !Pointer to reduced effective collision cross-section model
1.187703           !Lennard-Jones coefficient sigma [nm]
770.2692           !Lennard-Jones coefficient epsilon/kappa [K]
1.0    1.0         !Reducing parameters for eta, T, rho
1.0    0.5         !Chapman-Enskog term
!
!Dilute gas
$DG CNST CNST CNST TEMP * SQRT * * DC THRD2 POWR * OMEGAS /
!
!Residual function odrfit1 may16
$RF RED DR CNST POWR TR / =DEL SUMDEL:4 DR THRD2 POWR *
!
!Coefficients
$CF
0.040785               0.   0.    0.  0
0.72495                0.   0.    0.  0
697.051                0.   0.    0.  0
1.                   970.   0.316 0.  0
3.36                   0.   0.    0.  0
 4.99779178923251      0.5  1.0   0.  0
-0.0497335534006545    0.5  2.0   0.  0
 0.00025851170571577   0.5  3.0   0.  0
 1.62824150564936e-25  0.5  11.0  0.  0
NUL                !Pointer to the viscosity critical enhancement auxiliary function
(none used)

================================================================================

#TCX   !---Thermal conductivity---
TC1    !Pure fluid thermal conductivity model for POE9 of Huber and Perkins (2018).
?
?``````````````````````````````````````````````````````````````````````````````
? Estimated uncertainty for the liquid phase from 301 K to 500 K at pressures to 69 MPa
is 0.5 %
? Larger uncertainties in the critical region and in the gas phase; data unavailable for
comparisons.
?
!``````````````````````````````````````````````````````````````````````````````
250.0              !Lower temperature limit [K]
1000.0             !Upper temperature limit [K]
100000.0           !Upper pressure limit [kPa]
3.                 !Maximum density [mol/L]
```

```
6   0              !# terms for dilute gas function:  numerator, denominator
 970.0       0.001 !Reducing parameters for T, tcx
-2.617097    0.
 43.187405   1.
-160.22117   2.
 404.97948   3.
-339.90316   4.
 99.120658   5.
 10  0             !# terms for background gas function:  numerator, denominator
 970.0  0.316  1.  !Reducing parameters for T, rho, tcx
 0.0375194     0.  1.  0.
-0.009679      0.  2.  0.
 0.00151768    0.  3.  0.
 0.0           0.  4.  0.
 0.0           0.  5.  0.
 0.00348471    1.  1.  0.
-0.0229526     1.  2.  0.
 0.0070787     1.  3.  0.
 0.0           1.  4.  0.
 0.0           1.  5.  0.
TK3               !Pointer to critical enhancement auxiliary function

#AUX   !---Auxiliary function for the thermal conductivity critical enhancement
TK3    !Simplified thermal conductivity critical enhancement for POE9 of Perkins et al.
(2013).
?
?```````````````````````````````````````````````````````````````````````````````
?Perkins, R.A., Sengers, J.V., Abdulagatov, I.M., and Huber, M.L.,
? "Simplified model for the critical thermal-conductivity enhancement in molecular
fluids"
? Int. J. Thermophysics, 34(2):191-212, 2013. doi: 10.1007/s10765-013-1409-z
?
!```````````````````````````````````````````````````````````````````````````````
0.                !
10000.            !
0.                !
0.                !
9 0 0 0           !# terms:  CO2-terms, spare, spare, spare
1.0  1.0  1.0     !Reducing parameters for T, rho, tcx [mW/(m-K)]
0.63              !Nu (universal exponent)
1.239             !Gamma (universal exponent)
1.02              !R0 (universal amplitude)
0.063             !Z (universal exponent--not used for t.c., only viscosity)
1.0               !C (constant in viscosity eqn = 1/[2 - (alpha + gamma)/(2*nu)], but
often set to 1)
0.405e-9          !Xi0 (amplitude) [m]
0.096             !Gam0 (amplitude) [-]
1.476e-9          !Qd_inverse (modified effective cutoff parameter) [m]
1455.0            !Tref (reference temperature)=1.5*Tc [K]

++++++++++++++++++++++++++++++++++++++++++++++++++++++++++++++++++++++++++++++++++

@TRN    !---ECS Transport---
ECS     !Extended Corresponding States model (N2 reference); predictive mode for POE9.
          ?

?```````````````````````````````````````````````````````````````````````````````
          ?*** ESTIMATION METHOD *** NOT STANDARD REFERENCE QUALITY ***
          ?Unpublished; uses method described in the following reference:
          ?Huber, M.L., Laesecke, A., and Perkins, R.A.
          ? "Model for the Viscosity and Thermal Conductivity of Refrigerants, Including
          ? a New Correlation for the Viscosity of R134a,"
          ? Ind. Eng. Chem. Res., 42(13):3163-3178, 2003. doi: 10.1021/ie0300880.
```

```
          ?
          ?The Lennard-Jones parameters were estimated with the method of Chung
          ?

!````````````````````````````````````````````````````````````````````````````
          250.               !Lower temperature limit [K]
          1000.              !Upper temperature limit [K]
          100000.            !Upper pressure limit [kPa]
          10.                !Maximum density [mol/L]
          FEQ NITROGEN.FLD
          VS1                !Model for reference fluid viscosity
          TC1                !Model for reference fluid thermal conductivity
          BIG                !Large molecule identifier
          0.72495 0. 0. 0.   !Large molecule parameters
          1                  !Lennard-Jones flag (0 or 1) (0 => use estimates)
          1.187703           !Lennard-Jones coefficient sigma [nm]
          770.2692          !Lennard-Jones coefficient epsilon/kappa [K] for ECS method
          1  0  0                !Number of terms in f_int term in Eucken correlation,
spare1, spare2
           0.00132       0. 0. 0.  !Coefficient, power of T, spare1, spare2
          3   0   0                    !Number of terms in psi (visc shape factor):
poly,spare1,spare2
           1.09271       0. 0. 0.  !Coefficient, power of Tr, power of Dr, spare
          -0.161324      0. 1. 0.  !Coefficient, power of Tr, power of Dr, spare
           0.0486596     0. 2. 0.  !Coefficient, power of Tr, power of Dr, spare
          1   0   0                    !Number of terms in chi (t.c. shape factor):
poly,spare1,spare2
           1.0           0. 0. 0.  !Coefficient, power of Tr, power of Dr, spare
          TK3                !Pointer to critical enhancement auxiliary function

~~~~~~~~~~~~~~~~~~~~~~~~~~~~~~~~~~~~~~~~~~~~~~~~~~~~~~~~~~~~~~~~~~~~~~~~~~~~~~~~

#PS    !---Vapor pressure---
PS5    !Vapor pressure equation for POE5 of Lemmon and Eckermann (2018).
?
?````````````````````````````````````````````````````````````````````````````
?Functional Form:  P=Pc*EXP[SUM(Ni*Theta^ti)*Tc/T] where Theta=1-T/Tc, Tc and Pc
? are the reducing parameters below, which are followed by rows containing Ni and ti.
?
!````````````````````````````````````````````````````````````````````````````
0.                 !
10000.             !
0.                 !
0.                 !
970.0    885.0     !Reducing parameters
5 0 0 0 0 0        !Number of terms in equation
-9.7122  1.0
 1.239   1.5
-2.604   1.94
-14.757  3.36
-13.73   9.7

#DL    !---Saturated liquid density---
DL1    !Saturated liquid density equation for POE5 of Lemmon and Eckermann (2018).
?
?````````````````````````````````````````````````````````````````````````````
?Functional Form:  D=Dc*[1+SUM(Ni*Theta^ti)] where Theta=1-T/Tc, Tc and Dc are
? the reducing parameters below, which are followed by rows containing Ni and ti.
?
!````````````````````````````````````````````````````````````````````````````
0.                 !
10000.             !
0.                 !
```

```
0.                !
970.0  0.316       !Reducing parameters
5 0 0 0 0 0        !Number of terms in equation
 0.8426   0.23
 7.992    0.8
-10.95    1.25
 6.562    1.7
-0.02654  2.5

#DV    !---Saturated vapor density---
DV3    !Saturated vapor density equation for POE5 of Lemmon and Eckermann (2018).
?
?```````````````````````````````````````````````````````````````````````````````
?Functional Form:  D=Dc*EXP[SUM(Ni*Theta^ti)] where Theta=1-T/Tc, Tc and Dc are
? the reducing parameters below, which are followed by rows containing Ni and ti.
?
!```````````````````````````````````````````````````````````````````````````````
0.                !
10000.            !
0.                !
0.                !
970.0  0.316       !Reducing parameters
5 0 0 0 0 0        !Number of terms in equation
-2.7213   0.4
-9.231    1.12
-41.30    3.0
-109.8    5.83
-368.9   12.5

@END
c        1         2         3         4         5         6         7         8
c2345678901234567890123456789012345678901234567890123456789012345678901234567890
```

C.4. MILPRF23699.FLD

```
MIL-PRF-23699        !Short name
1-1-1                !CAS number
MIL-PRF-23699        !Full name
MIL-PRF-23699        !Chemical formula
MIL-PRF-23699        !Synonym
557.6                !Molar mass [g/mol]
250.                 !Triple point temperature [K]
753.335              !Normal boiling point [K]
930.0                !Critical temperature [K]
1080.0               !Critical pressure [kPa]
0.439                !Critical density [mol/L]
0.97                 !Acentric factor
-1.                  !Dipole moment [Debye]
NBP                  !Default reference state
10.0                 !Version number

! compiled by E.W. Lemmon, NIST Physical and Chemical Properties Division, Boulder,
Colorado
! 12-01-17 EWL, Original version.
! 08-29-18 EWL, Add final equation of state.
! 09-12-18 MLH, Add transport.
```

```
#EOS   !---Equation of state---
FEQ    !Helmholtz equation of state for MIL-PRF-23699 of Lemmon (2018).
?
```

```
?```````````````````````````````````````````````````````````````````````````````
?Lemmon, E.W.
?
?The uncertainty of calculated values in the liquid phase is 0.2 % in density and
? speed of sound between 260 K and 450 K with pressures to 70 MPa. For speed of
? sound, the uncertainty may increase to 0.3 % above 380 K. Outside of these
? ranges, the uncertainties will slowly increase as a function of the distance
? from the upper or lower bounds given above.  Values could be as small as 0.4 % at
? 220 K (assuming the oil is still fluid) or, for density, at temperatures up to
? 600 K. The uncertainties in the critical region and vapor phase are unknown, but
? not expected to exceed 1 % for density at temperatures up to 600 K in the vapor
? phase.  The uncertainty in vapor-phase speed of sound is unknown due to the lack
? of information pertaining to the ideal-gas isobaric heat capacity (at very low
? pressures).
?
?The uncertainty in heat capacities in the liquid phase is 0.5 % from 250 K to
? 450 K. The uncertainties for vapor pressures are difficult to quantify due to
? the extremely low vapor pressures below 500 K. An approximate value would be one
? order of magnitude; for example, at a temperature where the calculated value of
? the vapor pressure is 1 Pa, the true value could be between 0.1 Pa to 10 Pa.
? For vapor pressures above 1 atmosphere, the same may be true, but it is
? estimated that the values would be less than 50 %.
?
!```````````````````````````````````````````````````````````````````````````````
250.0              !Lower temperature limit [K]
1000.0             !Upper temperature limit [K]
100000.0           !Upper pressure limit [kPa]
1.85               !Maximum density [mol/L]
CPP                                !Pointer to Cp0 model
557.6                              !Molar mass [g/mol]
250.0                              !Triple point temperature [K]
0.000000000000001                  !Pressure at triple point [kPa]
1.84                               !Density at triple point [mol/L]
753.335                            !Normal boiling point temperature [K]
0.97                               !Acentric factor
930.0          1080.0        0.439     !Tc [K], pc [kPa], rhoc [mol/L]
930.0                        0.439     !Reducing parameters [K, mol/L]
8.3144598                          !Gas constant [J/mol-K]
  10  4    4 12    0 0     0 0  0 0  0 0  !# terms and # coefs/term for normal terms,
Gaussian terms, and Gao terms
  0.00990044   1.0     5.  0.          !a(i),t(i),d(i),l(i)
  1.633544     0.08    1.  0.
 -2.6606       1.2     1.  0.
 -2.328001     1.162   2.  0.
  0.3281252    0.54    3.  0.
  2.4664585    1.08    2.  1.
  7.657825     1.56    3.  1.
 -5.569829     1.78    3.  1.
  0.914727     1.42    4.  1.
  0.3668741    1.62    5.  1.
 -0.007457     2.0     1.  2. 2.   -1.0    -0.36     1.57     1.7       0. 0. 0.
  0.028916     1.0     2.  2. 2.   -1.31   -0.35     1.45     0.55      0. 0. 0.
 -0.0103879    1.0     4.  2. 2.   -0.46   -0.55     1.63     0.95      0. 0. 0.
 -0.645008     1.0     3.  2. 2.   -20.0  -1000.0    1.09     0.91      0. 0. 0.

#AUX   !---Auxiliary function for Cp0
CPP    !Ideal gas heat capacity function for MIL-PRF-23699 of Lemmon (2018).
?
?```````````````````````````````````````````````````````````````````````````````
?Lemmon, E.W.
?
!```````````````````````````````````````````````````````````````````````````````
0.                 !
```

```
10000.             !
0.                 !
0.                 !
1.0     8.3144598  !Reducing parameters for T, Cp0
1 2   0 0   0 0 0  !Nterms:  polynomial, exponential, cosh, sinh
 50.0     0.0
 78.0  1000.0
 105.0 2000.0

^^^^^^^^^^^^^^^^^^^^^^^^^^^^^^^^^^^^^^^^^^^^^^^^^^^^^^^^^^^^^^^^^^^^^^^^^^^^^^^^

#ETA   !---Viscosity---
VS7    !Pure fluid viscosity model for full lubricant MIL-PRF-23699 of Huber (2018).
?
?````````````````````````````````````````````````````````````````````````````````
? Estimated uncertainty for the liquid phase from 290 K to 450 K at pressures to 140 MPa
is 5 %
? Larger uncertainties in the gas phase; data unavailable for comparisons.
?
!````````````````````````````````````````````````````````````````````````````````
250.0              !Lower temperature limit [K]
1000.0             !Upper temperature limit [K]
150000.0           !Upper pressure limit [kPa]
3.                 !Maximum density [mol/L]
CI0                !Pointer to reduced effective collision cross-section model
1.064437           !Lennard-Jones coefficient sigma [nm]
738.5055           !Lennard-Jones coefficient epsilon/kappa [K]
1.0    1.0         !Reducing parameters for eta, T, rho
1.0    0.5         !Chapman-Enskog term
!
!Dilute gas
$DG CNST CNST CNST TEMP * SQRT * * DC THRD2 POWR * OMEGAS /
!
!Residual function odrfit1 may16
$RF RED DR CNST POWR TR / =DEL SUMDEL:4 SUM:2 + DR THRD2 POWR *
!
!Coefficients
$CF
0.040785               0.   0.    0.  0
0.73267                0.   0.    0.  0
557.6                  0.   0.    0.  0
1.                   930.   0.439 0.  0
3.35                   0.   0.    0.  0
 3.03845876244641      0.5  1.0   0.  0
 9.51573140029214e-07  0.5  4.0   0.  0
-3.52967591410229e-24  0.5  5.0   0.  0
 3.52967591410229e-24  0.5  11.0  0.  0
 0.0142808510636033    0.5  3.35  0.  0
 0.0142808510636033    1.5  3.35  0.  0
NUL                  !Pointer to the viscosity critical enhancement auxiliary function
(none used)

================================================================================

#TCX   !---Thermal conductivity---
TC1    !Pure fluid thermal conductivity model for full lubricant MIL-PRF-23699 of Huber
and Perkins (2018).
?
?````````````````````````````````````````````````````````````````````````````````
? Estimated uncertainty for the liquid phase from 301 K to 500 K at pressures to 69 MPa
is 0.5 %
? Larger uncertainties in the critical region and in the gas phase; data unavailable for
comparisons.
```

```
?
!```````````````````````````````````````````````````````````````````````````````
250.0              !Lower temperature limit [K]
1000.0             !Upper temperature limit [K]
100000.0           !Upper pressure limit [kPa]
3.                 !Maximum density [mol/L]
6   0              !# terms for dilute gas function:  numerator, denominator
 930.0       0.001 !Reducing parameters for T, tcx
 2.029847    0.
-17.66899    1.
 106.7431    2.
-83.01913    3.
 29.21753    4.
-3.957349    5.
 10  0             !# terms for background gas function:  numerator, denominator
 930.0  0.439  1.  !Reducing parameters for T, rho, tcx
-0.0717307     0.  1.  0.
 0.0411848     0.  2.  0.
-0.00433472    0.  3.  0.
 0.0           0.  4.  0.
 0.0           0.  5.  0.
 0.124299      1.  1.  0.
-0.0759461     1.  2.  0.
 0.013306      1.  3.  0.
 0.0           1.  4.  0.
 0.0           1.  5.  0.
TK3                !Pointer to critical enhancement auxiliary function

#AUX   !---Auxiliary function for the thermal conductivity critical enhancement
TK3     !Simplified thermal conductivity critical enhancement for full lubricant MIL-
PRF-23699 from model of Perkins et al. (2013).
?
?```````````````````````````````````````````````````````````````````````````````
?Perkins, R.A., Sengers, J.V., Abdulagatov, I.M., and Huber, M.L.,
? "Simplified model for the critical thermal-conductivity enhancement in molecular
fluids"
? Int. J. Thermophysics, 34(2):191-212, 2013. doi: 10.1007/s10765-013-1409-z
?
!```````````````````````````````````````````````````````````````````````````````
0.                 !
10000.             !
0.                 !
0.                 !
9 0 0 0            !# terms:  CO2-terms, spare, spare, spare
1.0  1.0  1.0      !Reducing parameters for T, rho, tcx [mW/(m-K)]
0.63               !Nu (universal exponent)
1.239              !Gamma (universal exponent)
1.02               !R0 (universal amplitude)
0.063              !Z (universal exponent--not used for t.c., only viscosity)
1.0                !C (constant in viscosity eqn = 1/[2 - (alpha + gamma)/(2*nu)], but
often set to 1)
0.365e-9           !Xi0 (amplitude) [m]
0.087              !Gam0 (amplitude) [-]
1.320e-9           !Qd_inverse (modified effective cutoff parameter) [m]
1395.0             !Tref (reference temperature)=1.5*Tc [K]

++++++++++++++++++++++++++++++++++++++++++++++++++++++++++++++++++++++++++++++++++++

@TRN    !---ECS Transport---
ECS     !Extended Corresponding States model (N2 reference); predictive mode for full
lubricant MIL-PRF-23699.
          ?
```

```
?```````````````````````````````````````````````````````````````````````````````
          ?*** ESTIMATION METHOD *** NOT STANDARD REFERENCE QUALITY ***
          ?Unpublished; uses method described in the following reference:
          ?Huber, M.L., Laesecke, A., and Perkins, R.A.
          ? "Model for the Viscosity and Thermal Conductivity of Refrigerants, Including
          ? a New Correlation for the Viscosity of R134a,"
          ? Ind. Eng. Chem. Res., 42(13):3163-3178, 2003. doi: 10.1021/ie0300880.
          ?
          ?Estimated uncertainty 3 % for liquid in range 293 K to 350 K at pressures
<180 MPa
          ?
          ?The Lennard-Jones parameters were taken from Reid, R.C., Prausnitz, J.M., and
Poling, B.E., "The Properties of Gases and Liquids," 4th edition, New York, McGraw-Hill
Book Company, 1987.
          ?

!```````````````````````````````````````````````````````````````````````````````
          250.               !Lower temperature limit [K]
          1000.              !Upper temperature limit [K]
          100000.            !Upper pressure limit [kPa]
          10.                !Maximum density [mol/L]
          FEQ NITROGEN.FLD
          VS1                !Model for reference fluid viscosity
          TC1                !Model for reference fluid thermal conductivity
          BIG                !Large molecule identifier
          0.73267 0. 0. 0.   !Large molecule parameters
          1                  !Lennard-Jones flag (0 or 1) (0 => use estimates)
          1.064427           !Lennard-Jones coefficient sigma [nm]
          738.5055          !Lennard-Jones coefficient epsilon/kappa [K] for ECS method
          1  0  0                 !Number of terms in f_int term in Eucken correlation,
spare1, spare2
           0.00132       0. 0. 0.  !Coefficient, power of T, spare1, spare2
          3   0   0                    !Number of terms in psi (visc shape factor):
poly,spare1,spare2
           1.09271       0. 0. 0.  !Coefficient, power of Tr, power of Dr, spare
          -0.161324      0. 1. 0.  !Coefficient, power of Tr, power of Dr, spare
           0.0486596     0. 2. 0.  !Coefficient, power of Tr, power of Dr, spare
          1   0   0                    !Number of terms in chi (t.c. shape factor):
poly,spare1,spare2
           1.0           0. 0. 0.  !Coefficient, power of Tr, power of Dr, spare
          TK3               !Pointer to critical enhancement auxiliary function

~~~~~~~~~~~~~~~~~~~~~~~~~~~~~~~~~~~~~~~~~~~~~~~~~~~~~~~~~~~~~~~~~~~~~~~~~~~~~~~~~~~~

#PS    !---Vapor pressure---
PS5    !Vapor pressure equation for MIL-PRF-23699 of Lemmon (2018).
?
?```````````````````````````````````````````````````````````````````````````````
?Functional Form:  P=Pc*EXP[SUM(Ni*Theta^ti)*Tc/T] where Theta=1-T/Tc, Tc and Pc
? are the reducing parameters below, which are followed by rows containing Ni and ti.
?
!```````````````````````````````````````````````````````````````````````````````
0.                 !
10000.             !
0.                 !
0.                 !
930.0   1080.0     !Reducing parameters
5 0 0 0 0 0        !Number of terms in equation
-11.111   1.0
 7.2815   1.5
-7.7491   1.83
-10.767   3.4
```

```
-10.545  10.0

#DL    !---Saturated liquid density---
DL1    !Saturated liquid density equation for MIL-PRF-23699 of Lemmon (2018).
?
?```````````````````````````````````````````````````````````````````````````````
?Functional Form:  D=Dc*[1+SUM(Ni*Theta^ti)] where Theta=1-T/Tc, Tc and Dc are
? the reducing parameters below, which are followed by rows containing Ni and ti.
?
!```````````````````````````````````````````````````````````````````````````````
0.                 !
10000.             !
0.                 !
0.                 !
930.0  0.439       !Reducing parameters
4 0 0 0 0 0        !Number of terms in equation
 2.9491   0.42
 1.1681   1.03
-1.9815   1.65
 2.003    2.4

#DV    !---Saturated vapor density---
DV3    !Saturated vapor density equation for MIL-PRF-23699 of Lemmon (2018).
?
?```````````````````````````````````````````````````````````````````````````````
?Functional Form:  D=Dc*EXP[SUM(Ni*Theta^ti)] where Theta=1-T/Tc, Tc and Dc are
? the reducing parameters below, which are followed by rows containing Ni and ti.
?
!```````````````````````````````````````````````````````````````````````````````
0.                 !
10000.             !
0.                 !
0.                 !
930.0  0.439       !Reducing parameters
5 0 0 0 0 0        !Number of terms in equation
-4.971    0.493
-13.796   1.62
-61.443   3.86
-109.33   7.6
-306.06  14.0

@END
c        1         2         3         4         5         6         7         8
c234567890123456789012345678901234567890123456789012345678901234567890123456789
```